52250

National Library of Canada / Bibliothèque nationale du Canada

CANADIAN THESES ON MICROFICHE / *THÈSES CANADIENNES SUR MICROFICHE*

NAME OF AUTHOR/*NOM DE L'AUTEUR* Vedavyasa Joshi

TITLE OF THESIS/*TITRE DE LA THÈSE* Aseismic Analysis of Underground Openings

UNIVERSITY/*UNIVERSITÉ* McMaster

DEGREE FOR WHICH THESIS WAS PRESENTED/ *GRADE POUR LEQUEL CETTE THÈSE FUT PRÉSENTÉE* Ph.D.

YEAR THIS DEGREE CONFERRED/*ANNÉE D'OBTENTION DE CE DEGRÉ* 1981

NAME OF SUPERVISOR/*NOM DU DIRECTEUR DE THÈSE* Dr. J.J. Emery

Permission is hereby granted to the NATIONAL LIBRARY OF CANADA to microfilm this thesis and to lend or sell copies of the film.

The author reserves other publication rights, and neither the thesis nor extensive extracts from it may be printed or otherwise reproduced without the author's written permission.

L'autorisation est, par la présente, accordée à la BIBLIOTHÈQUE NATIONALE DU CANADA de microfilmer cette thèse et de prêter ou de vendre des exemplaires du film.

L'auteur se réserve les autres droits de publication, ni la thèse ni de longs extraits de celle-ci ne doivent être imprimés ou autrement reproduits sans l'autorisation écrite de l'auteur.

DATED/*DATÉ* November 4, 1980 SIGNED/*SIGNÉ* [signature]

PERMANENT ADDRESS/*RÉSIDENCE FIXÉ*

C/o Dr K.H. JOSHI
NO 366, JUNIPETH,
RAMDURG; DT. BELGAUM
KARNATAKA STATE
INDIA

NL-91 (11-79)

NOTICE

The quality of this microfiche is heavily dependent upon the quality of the original thesis submitted for microfilming. Every effort has been made to ensure the highest quality of reproduction possible.

If pages are missing, contact the university which granted the degree.

Some pages may have indistinct print especially if the original pages were typed with a poor typewriter ribbon or if the university sent us a poor photocopy.

Previously copyrighted materials (journal articles, published tests, etc.) are not filmed.

Reproduction in full or in part of this film is governed by the Canadian Copyright Act, R.S.C. 1970, c. C-30. Please read the authorization forms which accompany this thesis.

THIS DISSERTATION
HAS BEEN MICROFILMED
EXACTLY AS RECEIVED.

AVIS

La qualité de cette microfiche dépend grandement de la qualité de la thèse soumise au microfilmage. Nous avons tout fait pour assurer une qualité supérieure de reproduction.

S'il manque des pages, veuillez communiquer avec l'université qui a conféré le grade.

La qualité d'impression de certaines pages peut laisser à désirer, surtout si les pages originales ont été dactylographiées à l'aide d'un ruban usé ou si l'université nous a fait parvenir une photocopie de mauvaise qualité.

Les documents qui font déjà l'objet d'un droit d'auteur (articles de revue, examens publiés, etc.) ne sont pas microfilmés.

La reproduction, même partielle, de ce microfilm est soumise à la Loi canadienne sur le droit d'auteur, SRC 1970, c. C-30. Veuillez prendre connaissance des formules d'autorisation qui accompagnent cette thèse.

LA THÈSE A ÉTÉ
MICROFILMÉE TELLE QUE
NOUS L'AVONS REÇUE

ASEISMIC ANALYSES OF UNDERGROUND OPENINGS

By

© VEDAVYASA H. JOSHI, M.E.

A Thesis

Submitted to the School of Graduate Studies

in Partial Fulfilment of the Requirements

for the Degree

Doctor of Philosophy

McMaster University

September 1980

DOCTOR OF PHILOSOPHY (1980)

TITLE: Aseismic Analyses of Underground Openings

AUTHOR: Vedavyasa H. Joshi, B.E. (Mysore University, India)
M.E. (University of Roorkee, India)

SUPERVISOR: Dr. J.J. Emery

NUMBER OF PAGES: 258

ACKNOWLEDGEMENTS

The author wishes to express his appreciation to the Association of Universities and Colleges of Canada for the Commonwealth Fellowship that provided financial support for much of this research work; and to McMaster University for providing computing facilities.

The author also wishes to thank the following individuals:

- His Supervisor, Dr. J.J. Emery, for his continued encouragement and guidance throughout the study.
- Dr. A.C. Heidebrecht, Dr. W.K. Tso, Dr. Y.P. Vaid, and Dr. F.A. Mirza for their valuable suggestions and comments.
- Dinah Lindsay Emery for typing the manuscript.
- Robert Sheppard of the Computing Centre for granting special priority to many non-standard jobs.
- Marianne Bayley and Allen Chan of the Computing Centre for their help in programming.
- The author's employer - The University of Roorkee, Roorkee (India) - for granting the study leave to complete this study.
- Finally, his wife Vijaya and daughter Anjali for their understanding and other adjustments throughout.

ABSTRACT

Facilities such as pipelines, tunnels, shafts and some power plant components require safe underground construction and operation. Many of these facilities are also critical from an overall safety viewpoint and/or the provision of relief services after earthquakes. For this reason, such underground structures require reliable and economic procedures for their aseismic analysis and design: a subject which has not received much attention until recently.

The aseismic analysis work described herein may be divided into two major parts: the spatial distribution of seismic ground motions; and the dynamic analysis of the structure-medium system. For the first part, a method of computing component responses at the base rock level due to upward and downward propagating shear waves was developed. An improved method for determination of period and phase velocity of R-waves and their contribution to seismic ground motions was also adopted. The size of the problems involved is often too large for efficient computing or design office computers. To overcome this difficulty, methods for substantially reducing the size of the problem and cost of the analysis were applied. For underground structures of considerable length, analysis of a typical portion is often satisfactory. A method for such analysis, with due consideration of the continuity of the system in the axial direction at the transverse ends, was selected from a number of approaches and verified.

Parametric studies using a simple, single layer system with a horizontal tunnel were carried out for a number of soil and tunnel properties. The results of these analyses were reasonable and consistent with the behaviour of such structures observed during past earthquakes and field tests. It is considered that the investigation has both contributed to a better understanding of the seismic response of underground structure-medium systems, and provides the necessary methods for the detailed aseismic design of such systems.

TABLE OF CONTENTS

LIST OF TABLES

LIST OF FIGURES

CHAPTER 1

ASEISMIC ANALYSIS OF UNDERGROUND OPENINGS

1.1 INTRODUCTION

Many facilities such as water, sewer, oil and gas pipelines, transmission cable conduits, irrigation, power and transportation tunnels, mining shafts and some components of power plants involve safe underground construction and operation. Many of these facilities are so important in providing post disaster relief to potentially earthquake-affected communities that they are termed lifeline systems. Some of these facilities such as nuclear power plant components are critical to overall safety. Underground construction is very expensive and a growing component of civil engineering construction. For these reasons, reliable and economic procedures for the aseismic analysis and design of such structures are very important.

The dynamic analysis may be divided into two major parts: the spatial distribution of ground motions along the boundary chosen for the system that includes the structure and the surrounding medium; and the dynamic analysis of the system. Recent seismic ground motion records indicate that spatial variations in ground motions can be significant, especially when the structure has a considerable length (Haskell, 1953; Nair, 1974). In general, the seismic wave propagates upwards through the ground with direction of propagation at some angle with the

vertical. As such, the response should be treated as a three dimensional quantity (Suzuki, 1932). Previous research carried out at McMaster University by Nair provided considerable information on obtaining the spatial distribution of ground motions, as well as in the dynamic analysis of axisymmetric structures (Nair, 1974).

Unfortunately, the topic has still not received enough attention, although more research has been initiated recently. As such, the present state-of-the-art is not well developed. The few available methods for determining the dynamic response at underground openings often make over simplifying assumptions, and at times fail to predict some important response aspects required for the aseismic design of such structures.

This study mainly considers horizontal tunnels of considerable axial length, but the findings are also useful for the aseismic analysis of other underground structures such as pipelines and mining shafts, for instance.

1.2 STUDY OF EARTHQUAKE DAMAGE TO LONG UNDERGROUND STRUCTURES

Most of the available literature on this topic is qualitative and for pipelines. However, there are some reports about the performance of tunnels during strong ground shaking. A brief review of this topic is given in Appendix A, and the following important observations can be made:

1. The underground structures closely follow the movements of the surrounding medium;
2. Axial stresses and strains predominate, though, other strains may be significant too, especially for structures of large diameters;
3. Stress concentrations occur near bends, ventilation towers, manholes and other special fixtures on the structure;
4. Damage is severe at places where the structure passes through the interface of two media of appreciably different dynamic properties; and
5. Due to the considerable length of the structure, the spatial distribution of the ground motions along the length has to be considered in dynamic analyses.

1.3 AVAILABLE METHODS OF ASEISMIC ANALYSIS

There are a number of publications dealing with field and laboratory tests on buried structures, and the design and analysis of long underground openings subjected to seismic ground motions (Akoi and Hayashi, 1973; Duke and Moran, 1975; Goto et al, 1973; Hamada et al, 1977; Hindy and Noval, 1979; Iwan, 1975; Iwasaki and Tatsuoka, 1977; Katayama et al, 1975; Kubo, 1973; Nasu et al, 1973; Okamoto, 1973; Okamoto et al, 1973; Parmelee, 1975; Sakurai and Takahashi, 1969).

The method suggested by Sakurai and Takahashi (1969) uses the beam on elastic foundation analogy. Response of the medium is assumed

to be a sinusoidal acceleration function, and the response of the structure is the same as that of medium before relative slip between medium and structure takes place. The method suggested by Akoi and Hayashi (1973) also uses the beam on elastic foundation analogy and a sinusoidal seismic ground response not influenced by the presence of the structure. A bending equation is used to evaluate the relative displacements between the medium and the structure at various positions along the length of the structure. The analysis reported by Hamada et al (1977) also uses the beam on elastic foundation analogy, but the medium is represented as a single spring and a single concentrated mass at regular intervals along the length of the structure. The studies reported by Goto et al (1973) and Parmelee (1975) analyze the system in a transverse plane with plane strain conditions; the medium being represented by finite elements in the former, where as in the latter the resistance of the medium is obtained by using Mindlin's equations. In the studies reported by Goto et al (1973), the finite element method of analysis involved two media of different elastic moduli with their interface being transverse to the axis. The studies reported by Okamoto et al (1973) represent the structure by a series of segments with lumped masses interconnected to each other and to the medium by a series of compression and shear springs. The ground vibrations are assumed to be due to shear wave propagation. In the study reported by Hindy and Novac (1979), the soil resistance function is evaluated by using Mindlin's equation. The structure is represented by a series of lumped masses. Media of different elastic modulii with interface transvere to the axis are included in the analysis.

Studies based on field tests are reported by Sakurai and Takahashi (1969), Nasu et al (1973) and Kubo (1973). Laboratory model studies are reported by Goto et al (1973). The design of structures subjected to large seismic displacements is reported by Newmark and Hall (1975). More complete details are available in the sources indicated.

Many of these studies neglect the structure-medium interaction. The computed response of the structure is close to that of the surrounding medium. Computed stresses show stress concentrations at the joints, abrupt changes in cross sections and at media interfaces. The constants representing soil resistance in methods suggested by Sakurai and Takahashi (1969), and by Akoi and Hayashi (1973), are based on costly and time-consuming field tests. The numerous spring constants used in the studies reported by Okamoto et al (1973) and Hamada et al (1977) are not easily obtained. In the analysis using a lumped mass representation of the structure at regular intervals along the axial length (Okamoto et al, 1973; Hindy and Novac, 1979; Hamada et al, 1977); and many others), the variation of response of the structure along the rim of the structure is not obtained. In the methods employing the plane strain analysis, the response in the axial direction is not obtained, which has been indicated to be significant from the behaviour of structures during past earthquakes, as well as by laboratory and field tests on such structures.

The observation that the response of the buried structure is close to that of the surrounding medium does not necessarily mean that

the stresses and strains induced in the structure are not influenced by the medium-structure interaction, since even small strains can cause significant stresses depending upon the stiffness of the system in that direction. It is therefore important to consider the medium-structure interaction in such analyses.

It is clear from this discussion that there is no recognized method at present that accounts for the three-dimensional character of the problem and the influence of the structure medium interaction on the dynamic response of the structure.

1.4 SPATIAL DISTRIBUTION OF GROUND MOTIONS

The three-dimensional spatial distribution of seismic ground motions has to be considered in realistic aseismic analyses. For all practical purposes, the propagation of shear and Rayleigh waves are the important aspects to be considered. It should be noted that the principles of shear wave propagation at the base rock level are not accounted for correctly in most analyses (Haskell, 1973; Tsai, 1969). The usual assumption that the total base rock response is the component response of the base rock due to upward propagating seismic wave is incorrect, and can lead to errors in the computed response of the system.

Our knowledge of R-waves is inadequate in many aspects and suggests that the entire range of R-waves needs to be considered at regular intervals (Oliver and Ewing, 1957; Haskell, 1953). However, for most cases, only a narrow range of velocities will enable the

R-waves to reach the site together with the shear waves, which is really of interest to engineers. Presently, there are no known methods for choosing the phase velocity of R-waves. Another difficulty is to find the wave number for the chosen phase velocity, which involves trial and error solution using approximate trial values from charts presented by Oliver and Ewing (1957) or by Sezawa (1927). Since a number of wave numbers can satisfy the conditions for a given phase velocity, and the trial values are only approximate, finding the wave numbers is a significant problem. Yet another difficulty is the quantitative estimation of the R-wave contribution to the seismic ground response. For instance, Nair (1974) arbitrarily suggested this to be 25 per cent for nearby sites, zero for distant sites and of intermediate value for other sites. Any further refinements in the computation of ground response due to R-waves is meaningless without a more precise method for the quantitative estimation of the R-wave contribution to seismc ground response.

1.5 DYNAMIC ANALYSIS OF FHE INTERACTIVE SYSTEM

The finite element method of analysis is often used in dynamic analyses because of its versatility in accounting for different loading conditions, various types of materials and structural arrangements. In this study, the finite element method of analysis is adopted.

The lining of most underground structures (tunnels) is quite thin compared to its axial dimension. This leads to a large number of elements, nodes, displacement degrees of freedom and matrices in the

dynamic analysis. Conventional dynamic analysis methods will result in problems that are too large for most computers and too expensive for regular design use. For economic analysis, and to reduce the size of the problem, significant improvements are necessary in the technique of assembling the stiffness matrix of the system, and for the solution of the equations of motion.

1.6 SUITABILITY OF AXISYMMETRIC ANALYSIS

Many underground structures such as pipelines, power tunnels and mining shafts are axisymmetric. In situations where the ground formations are homogeneous or run transverse to the axis of symmetry, an axisymmetric analysis is quite appropriate. For most rock and some soils (saturated clays, for instance) the moduli do not depend significantly on the confining pressure variations within the boundaries of the interactive system being analyzed. An axisymmetric analysis may be considered acceptable in such situations as well.

If the axis of symmetry runs parallel to, or at an angle to, the formations, but not quite transverse, the use of an axisymmetric analysis is questionable. For soils, if the depth of cover is large compared to the lateral dimension of the structure, the moduli of the medium may not vary appreciably within the boundaries of the problem. In such situations, an axisymmetric analysis may also be considered useful.

In many other situations the system may not be axisymmetric. Even for such cases, with some simplifying assumptions, the axisymmetric

analysis may still be the best option in the absence of better alternatives. However, the results of such analyses should be interpreted in the light of the simplifying assumptions made.

1.7 CONTINUITY OF INTERACTIVE SYSTEMS AT TRANSVERSE BOUNDARIES

Figures 1.7.1 and 1.7.2 show a simple example of the interactive systems being considered. For the aseismic analysis, the response of the system along the boundary ABCD needs to be known. It is possible to establish the minimum radial distance of the boundary BC from the axis of symmetry by trial and error analysis, such that free field motions occur along BC. However, the responses along the boundaries AB and CD are unknown at the beginnning of the analysis for any time station, and without knowing the response along these boundaries, the dynamic analysis cannot be conducted for any time station. This is a typical indeterminate problem.

A method of considering energy dissipating boundaries has been proposed (Kaussel et al, 1975; Kuhlmeyer et al, 1973; Lysmer et al, 1969), but is applicable to analyses in the frequency domain only. Moreover, the energy dissipating boundary is a curved cylindrical surface. It cannot account for such a boundary on a transverse plane. As such, this approach will not be useful for the problems under consideration.

The conventional approach suggests that the boundaries AB and CD be chosen at an appropriate distance from the zone of interest EFGH, so that the effects of any assumed boundary conditions are

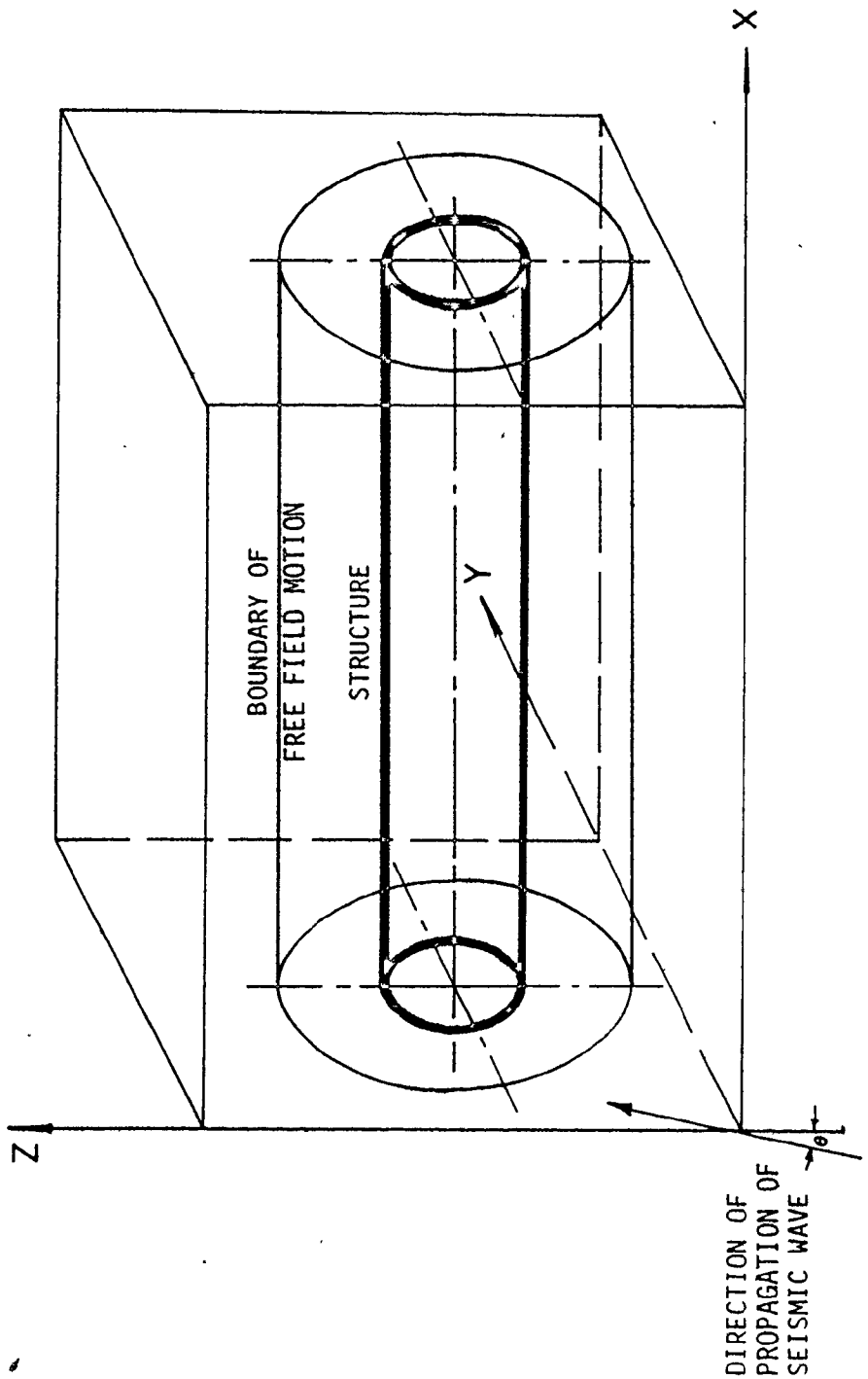

FIGURE 1.7.1 THREE DIMENSIONAL VIEW OF AN AXISYMMETRIC SYSTEM

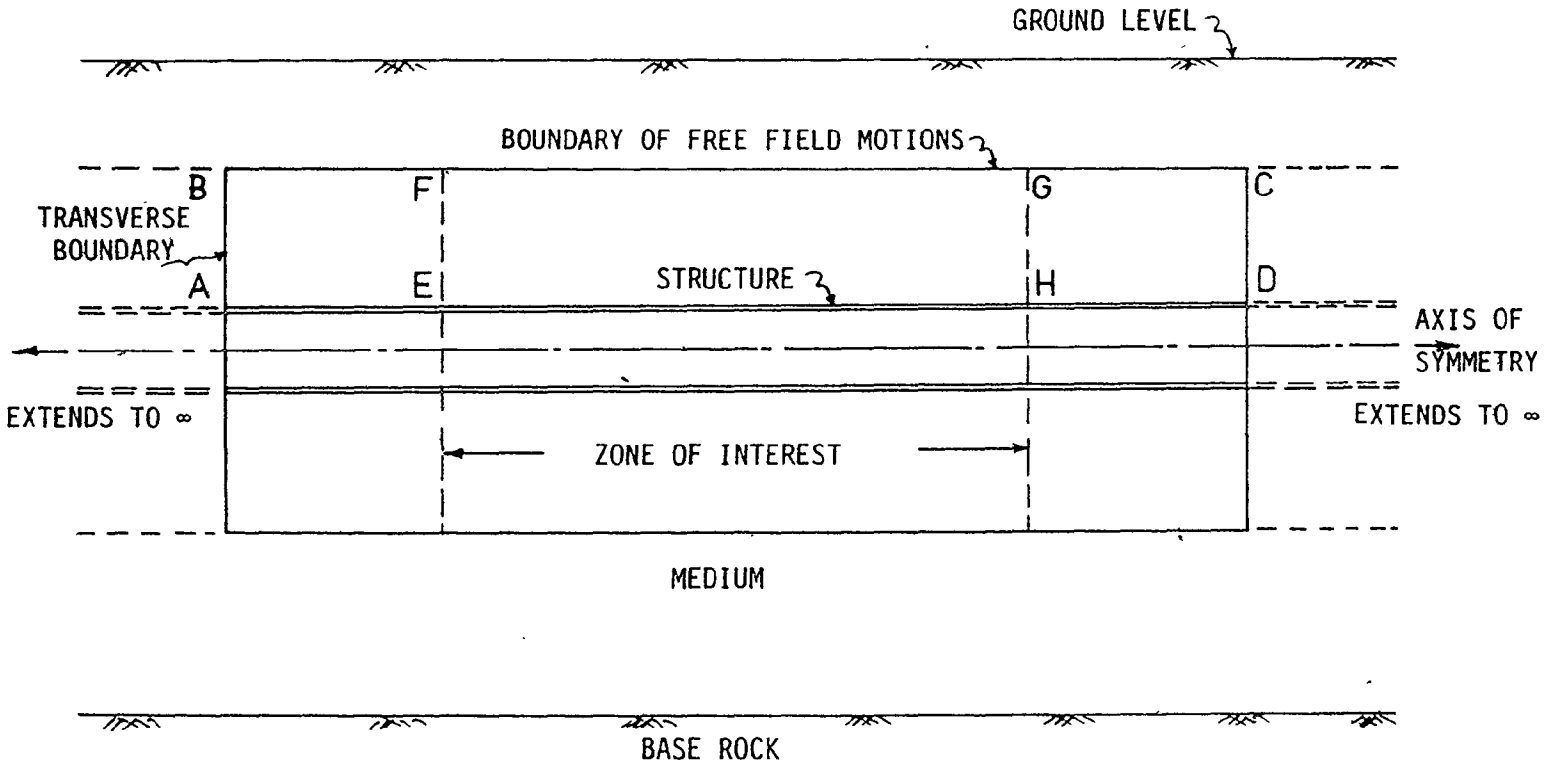

FIGURE 1.7.2 A FINITE PORTION OF A LONG AXISYMMETRIC INTERACTIVE SYSTEM

minimized. However, such an approach will result in a further increase in the size of the problem, which is already large to handle. A reasonable method of accounting for the continuity of the system at these transverse boundaries would be of great help in aseismic analyses.

1.8 PURPOSE AND SCOPE OF THE STUDY

The purpose and scope of this study is to develop a reliable and economic finite element method of aseismic analysis for axisymmetric underground structures, that may permit simplified dynamic piping analysis programs to be adopted in the future.

The finite element method of analysis is used because it offers the versatility to consider different materials and structural arrangemenets of the interactive system. A straightforward three-dimensional analysis, though simple, would be too large for general use and very expensive. (Such analyses could not be handled on the McMaster computing system, for instance.) Fortunately, acceptable three-dimensional analysis can generally be formulated using axisymmetric finite elements subjected to symmetric and/or antisymmetric loads and/or displacements. The loads, displacements, stresses and strains can be expanded in Fourier series for symmetric and/or antisymmetric components. By considering an adequate number of harmonics, satisfactory estimates of these quantities may be obtained. The details of the technique have been well explained by Wilson (1965) for symmetric components and by Nair (1974) for antisymmetric components.

In Chapter 2, a method of obtaining the component response at the base rock level due to upward propagating shear wave is explained. A method for obtaining the phase velocity and period of R-waves, and the contribution of R-waves to the seismic ground motion, is also developed in this Chapter. Economic methods to use quadrilateral elements in the finite element analysis, to assemble the stiffness matrix of the system, and to solve the resulting equations of motion are outlined in Chapter 3. The method by which the continuity of the system at the transverse boundaries may be considered is described and verified in Chapter 4. Chapter 5 summarizes the parametric studies completed using the methods previously described, and provides a discussion of the results obtained. The last chapter covers the conclusions, and provides suggestions for further research.

CHAPTER 2

RESPONSE OF LAYERED MEDIA DURING EARTHQUAKES

2.1 INTRODUCTION - SEISMIC WAVES

It is generally accepted that tectonic earthquakes are caused by slip along geologic faults resulting in the release of energy through the propagation of body waves. After travelling a series of paths within the earth's crust, these waves reach the site where seismic ground motions are felt. When body waves are incident at the interface of two layers, or at the ground surface, they cause surface waves. Rayleigh and Love waves are of this type. Studies of seismic ground motion records indicate that a significant portion of the ground response can be caused by the surface waves (Housner, 1965; Trifunac, 1971; Trifunac and Brune, 1970). The arrival time of any of these waves, due to a given earthquake for any particular site, depends on the focal depth of the earthquake, epicentral distance of the site and multiple reflections, refractions and dispersions of various waves along the paths of travel.

Because of the non uniform nature of the materials making up the earth's crust, and the waves themselves, simplifying assumptions are necessary in choosing a representative system (Tsai, 1959). Figure 2.1.1 gives a highly idealized system for near-by sites with epicentral distances less than 2.25 d (d being the focal depth) where the seismic ground response is due to shear as well as surface waves (Okamoto, 1973).

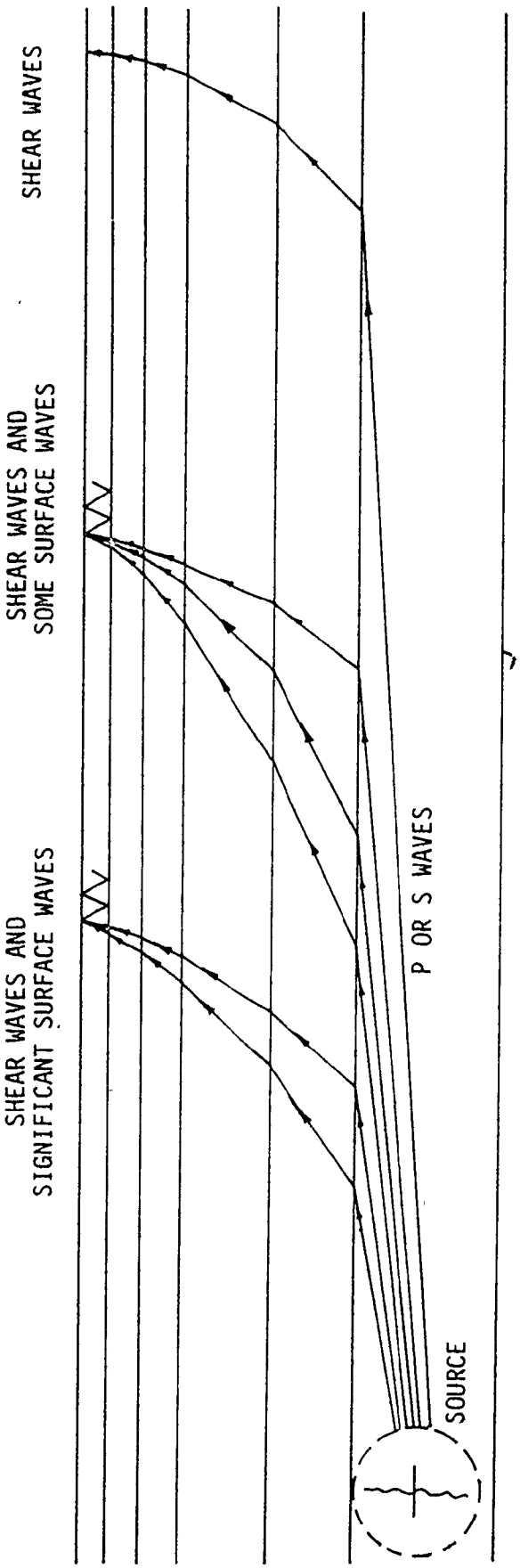

FIGURE 2.1.1 IDEALIZED SYSTEM SHOWING FOCAL DEPTH, EPICENTRAL DISTANCE AND WAVE PATHS (NAIR, 1974)

At distant sites, the difference between arrival times of shear and surface waves is so large that there is no possibility of their combined effect. For intermediate sites, surface waves are often masked by shear waves. As such, a portion of the seismic ground response is actually due to surface waves. Love waves are possible only when the shear wave velocity for the surface layer is less than that for any underlying layer. However, Love waves are not considered in this study as they are generally not important to engineering structures.

2.2 VERTICAL PROPAGATION OF SHEAR WAVES

When a shear wave is refracted from a medium of lower rigidity into a medium of higher rigidity, the direction of propagation moves away from the normal to the interface. If the shear wave is refracted from a medium of lower rigidity, the direction of propagation moves closer to the normal to the interface. Because of a series of such reflections and refractions through the formations of the earth's crust, the shear waves propagate in a nearly vertical direction through surface layers for distant sites.

2.3 EQUATION OF MOTION FOR SHEAR WAVE PROPAGATION

This topic is discussed in greater detail by Okamoto (1973). The following assumptions are made in developing the equation of motion for shear wave propagation:

1. Linear elastic medium.
2. Layers and the interfaces are horizontal, and extend to

infinity.

3. Propagation of plane shear waves in the vertical plane of propagation.

As such, the particles of the medium are subjected to movements within the plane of propagation in the direction perpendicular to the direction of propagation. If x and z are the horizontal and vertical co-ordinate axes, t is the time, ρ, β and G the mass density, shear wave velocity and the rigidity modulus of the medium (Figure 2.3.1), the shear stress differential $d\tau$ and the shear stress τ are obtained as:

$$d\tau = \frac{\partial \tau}{\partial z} \cdot dz = \frac{\partial x^2}{\partial t^2} \cdot \rho \cdot dz \qquad (2.3.1)$$

$$\tau = G \cdot \frac{\partial x}{\partial z} \qquad (2.3.2)$$

From these relationships:

$$\rho \cdot \frac{\partial^2 x}{\partial t^2} - G \cdot \frac{\partial^2 x}{\partial z^2} = 0 \qquad (2.3.3)$$

i.e. $$\frac{\partial^2 x}{\partial t^2} - \beta^2 \cdot \frac{\partial^2 x}{\partial z^2} = 0 \qquad (2.3.4)$$

wgere $$\beta^2 = G/\rho \qquad (2.3.5)$$

The solutions for equation (2.3.4) are:

$$Xu = U(t-z/\beta) \qquad (2.3.6)$$

$$Xd = D(t+z/\beta) \qquad (2.3.7)$$

where Xu is the displacement at depth z due to the upward propagating shear wave, and Xd is that at depth z due to the downward propagating shear wave, at time t. The net displacement at any instant t is the sum

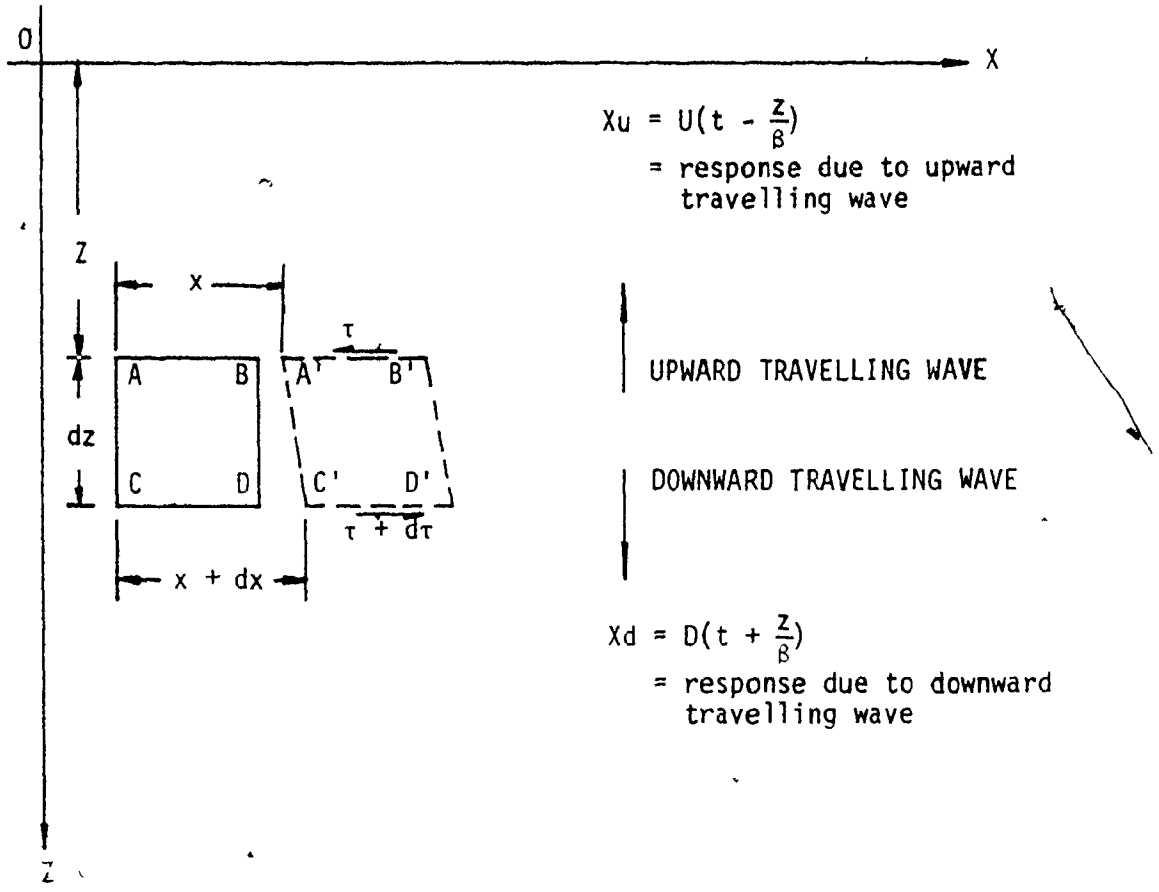

FIGURE 2.3.1 VERTICAL PROPAGATION OF SHEAR WAVE

of Xu and Xd:

$$X = Xu + Xd = U(t+z/\beta) + D(t-z/\beta) \qquad (2.3.8)$$

The corresponding shear strain γ is given by:

$$\gamma = \frac{dx}{dz} = \frac{1}{\beta}\dot{U}(t+\frac{z}{\beta}) - \frac{1}{\beta}\cdot\dot{D}(t-\frac{z}{\beta}) \qquad (2.3.9)$$

where $\dot{U}$ and $\dot{D}$ are first derivatives of U and D with respect to $(t-\frac{z}{\beta})$. The shear stress at any time at the ground surface is zero. Substituting this condition into Equation (2.3.9) leads to:

$$\dot{D}(t) = \dot{U}(t) \qquad (2.3.10)$$

and $$X(t) = U(t) + D(t) = 2U(t) \qquad (2.3.11)$$

where X(t) = displacement at ground level.

Consider the system of n layers shown in Figure 2.3.2. If ρ_k and β_k are the mass density and shear wave velocity for layer k, and ρ_{k-1} and β_{k-1} those for the $(k-1)^{th}$ layer of the system, the impedences of these layers are expressed as:

$$i_k = \rho_k \cdot \beta_k \qquad (2.3.12)$$

$$i_{k-1} = \rho_{k-1} \cdot \beta_{k-1} \qquad (2.3.13)$$

The impedence ratio μ_{k-1} for the $(k-1)^{th}$ interface between the layers (k-1) and k is given by:

$$\mu_{k-1} = \frac{i_{k-1}}{i_k} = \frac{\rho_{k-1}\cdot\beta_{k-1}}{\rho_k\cdot\beta_k} \qquad (2.3.14)$$

When an upward propagating shear wave is incident at the interface k, it is partially reflected downwards and partially transmitted

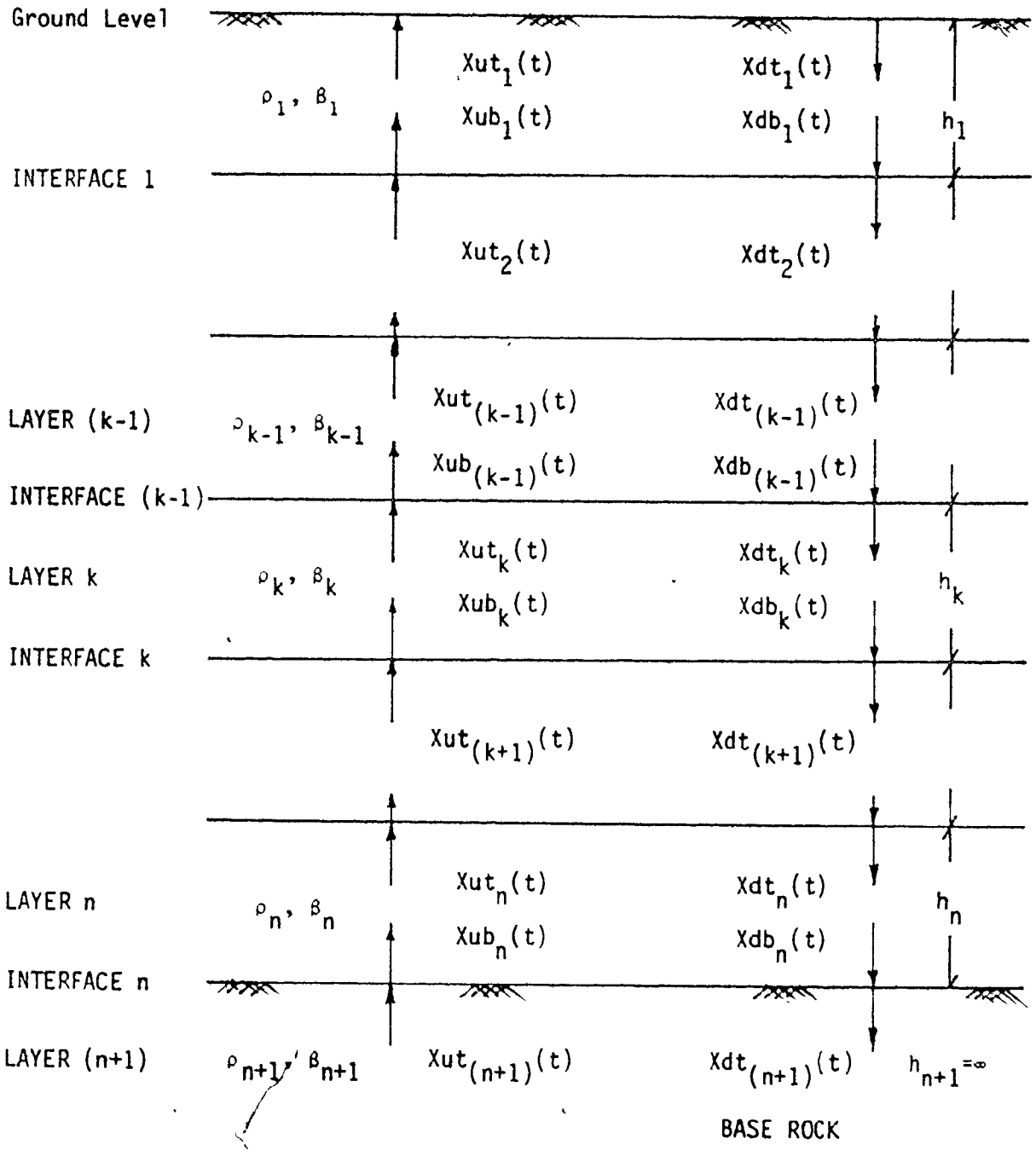

FIGURE 2.3.2 COMPONENT RESPONSES OF A MULTILAYER SYSTEM

upwards. Similarly, a downward propagating wave is partially reflected upwards and partially transmitted downwards. The coefficients for upward reflection Ru_k, downard reflection Rd_k, upward transmission Tu_k and downward transmission Td_k for interface k between layer (k-1) and k are:

$$\begin{aligned} Rd_k &= (1-u_k)/(1+u_k) \\ Ru_k &= -Rd_k \\ Tu_k &= 1 + Rd_k \\ Td_k &= 1 - Rd_k \end{aligned} \tag{2.3.15}$$

Let $Xub_k(t)$ and $Xut_k(t)$ represent the response at the bottom and top of the layer k due to upward propagating wave, and $Xdb_k(t)$ and $Xdt_k(t)$ those due to the downward propagating wave. The expressions for these quantities are:

$$\begin{aligned} Xub_k(t) &= Xut_{(k+1)}(t) \cdot Tu_k + Xdb_k(t) \cdot Ru_k \\ Xdt_k(t) &= Xdb_{(k-1)}(t) \cdot Td_{(k-1)} + Xut_k(t) \cdot Rd_{(k-1)} \\ Xut_k(t) &= Xub_k(t-t_k) \\ Xdb_k(t) &= Xdt_k(t-t_k) \end{aligned} \tag{2.3.16}$$

where t_k is the time of travel for the seismic wave to cover the depth of the layer k. Similar expressions may be obtained for other layers. For the topmost layer:

$$Xut_1(t) = Xdt_1(t) = X_1(t)/2 \tag{2.3.17}$$

Thus, if the surface response is known for a given system, it is possible

to compute the component responses and hence the net response at any interface for any time station may be obtained by using Equations (2.3.16) and (2.3.17).

However, if the base rock response is known at all time stations, it is not possible to obtain component responses at various interfaces with these two equations since the expressions for obtaining component responses at base rock are required. No rational approach for obtaining these component responses was available. To overcome this difficulty, it is usually assumed that the total response is due to the upward propagating wave and that there is no downward transmission due to the downward propagating wave from the layer over the base rock (Tsai, 1959; Nair, 1974). This is not in conformity with the principles of shear wave propagation when applied to the interface at the base rock level. It may also result in overestimation of the response at other levels by 30 to 50%. It is obvious that a rational approach for obtaining the component responses at the base rock level in conformity with the principles of wave propagation is very important to determining the seismic response of systems for which the response at base rock level is known.

2.4 RESPONSE COMPONENTS FOR BASE ROCK LEVEL

For engineering purposes, it is reasonable to assume that the base rock formation extends to infinite depth below the base rock level. As such, a downward propagating wave entering into the base rock from above has no chance of being reflected upwards. Denoting the base rock as the $(n+1)^{th}$ layer, then for any time t the response of the base rock

$Xt_n(t)$ is:

$$Xt_n(t) = Xut_{(n+1)}(t) + Xdt_{(n+1)}(t)$$

i.e. $$Xdt_{(n+1)}(t) = Xt_n(t) - Xut_{(n+1)}(t)$$

i.e. $$Xut_{(n+1)}(t) \cdot Rd_n + Xdb_n \cdot Td_n = Xt_n(t) - Xut_{(n+1)}(t)$$

i.e. $$Xut_{(n+1)}(t) = \frac{Xt_n(t) - Xdb_n(t) \cdot Td_n}{1 + Rd_n} \qquad (2.4.1)$$

and $$Xdt_{(n+1)}(t) = Xt_n(t) - Xut_{(n+1)}(t) \qquad (2.4.2)$$

The quantity of $Xdb_n(t)$ is absent when the downward reflected wave of the upward propagating wave at the top of the n^{th} layer reaches the base rock level. For any other time stations, this is also a known quantity. Using this information and Equations (2.4.1) and (2.4.2) the component responses of the base rock may be obtained from the known base rock response.

2.5 RESPONSE OF A SINGLE LAYER SYSTEM

The differences in the response of the system obtained by Nair's method, Kobayashi's method and the proposed method in Section 2.4 (referred to as first, second and third methods throughout) may be clearly shown by considering a single layer system subjected to a sinusoidal base rock excitation of acceleration (single) amplitude 1 m/s^2. The depth of the layer and frequency of base rock excitation were varied, but the material properties of the layer and the base rock were kept constant (Figure 2.5.1). The magnification factor obtained is defined as

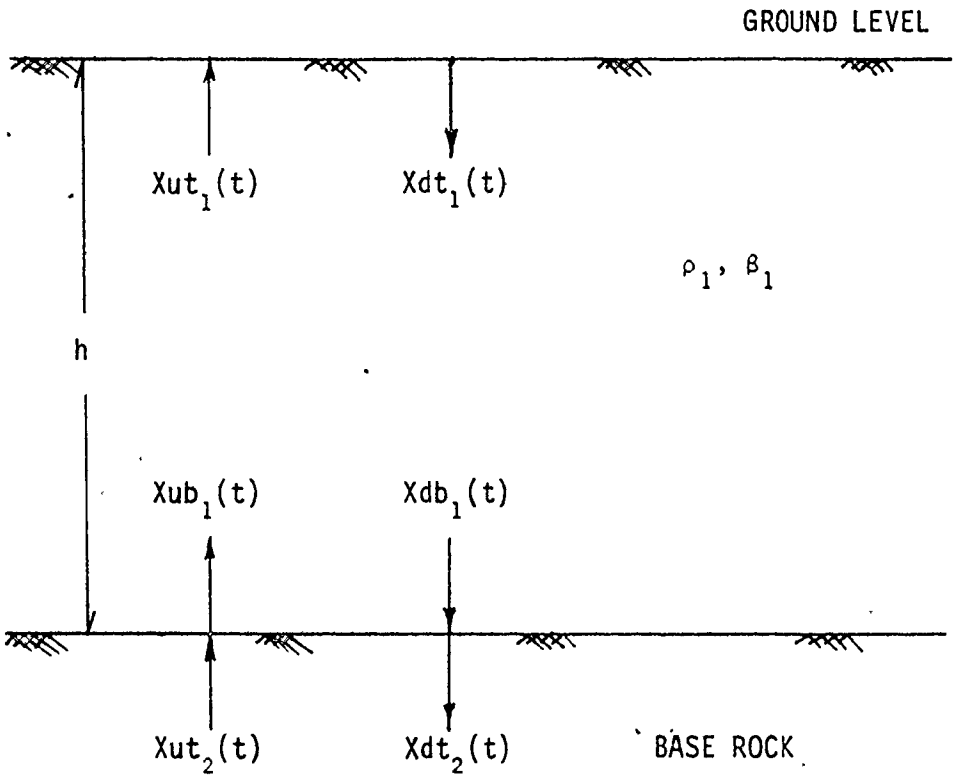

FIGURE 2.5.1 SINGLE LAYER SYSTEM

the ratio of the maximum amplitude of the ground surface to the amplitude of base rock response. These magnification factors were also compared with those obtained by using the expression suggested by Kanai (1965):

$$G_T = 1 + \frac{1.0}{\sqrt{\left[\left\{\frac{1+k}{1-k}\right\}\left\{1 - \frac{T^2}{T_G^2}\right\}\right]^2 + \left\{\frac{0.3}{\sqrt{T_G}} \cdot \frac{T}{T_G}\right\}^2}} \qquad (2.5.1)$$

where $k = \rho_1 \cdot \beta_1 / \rho_2 \cdot \beta_2$

T = Period of component vibration of seismic wave

T_G = Predominant period of surface layer

It should be noted that in the first method the upward reflection, downward transmission and downward reflection are neglected, and the total base rock response is considered as the component response due to the upward propagating wave. The second method is similar to the first one except that the upward reflection at the base rock level is accounted for. In the third method, the reflection and refraction in the upward as well as the downward direction are considered at the base rock level in accordance with the principles of shear wave propagation. Table 2.5.1 gives the magnification factors obtained from these methods. The magnification factor obtained by the first method remains constant for all the frequencies and depths considered for the top layer, which is not realistic. The reason for this is clear, as method one does not account for the influence of the depth of the layer at all by neglecting the contribution of downward propagating shear wave to the base rock response. The second method partially accounts for the influence of the depth of

TABLE 2.5.1

MAGNIFICATION FACTORS FOR THE SURFACE RESPONSE OF A SINGLE LAYER SYSTEM

Frequency of excitation	Details of the System		Magnification Factors			
	h_1	β_1	First	Second	Third	Kanai Method
Hz	m	m/s	Method	Method	Method	(Okamoto, 1973)
1.00	80.0	500.0	3.26	2.6	1.88	1.4158
1.56	80.0	500.0	3.26	8.28	5.17	3.6667
2.00	80.0	500.0	3.26	3.17	2.45	2.4380
4.00	80.0	500.0	3.26	2.50	1.73	1.7252
2.00	80.0	750.0	3.26	2.44	-	-
1.56	30.0	500.0	3.26	-	-	-
1.56	100.0	500.0	3.26	-	-	-

Depth of the top layer = h_1

Shear wave velocity in top layer = β_1

Shear wave velocity in base rock = 2000 m/s

Mass density of top layer = ρ_1

Mass density of base rock = 2330 kg/m^3

Type of base excitation = Sinusoidal

Single amplitude of excitation = $\pm$ 1.0 m/s^2

the layer by considering the upward reflection at the base rock. However, if the impedence of the upper layer is not appreciably different from that for the base rock, the coefficient of downward transmission could be significant enough to cause errors, along with errors already introduced by the assumption of the component base rock response due to the upward propagating shear wave. These two methods may lead to under-estimation or over-estimation of the computed response at any point depending upon the depth of the layer, ratio of impedence of the two layers and the frequency of excitation.

The surface response and the component response of the base rock due to the upward propagating wave for the case of a 80 m deep layer of shear wave velocity 50 m/s, base rock shear wave velocity of 2000 m/s and excitation frequency of 1 Hz obtained by the three methods are shown in Figures 2.5.2 and 2.5.3. Similar plots were obtained for other cases showing the difference between the results obtained by these methods.

The influence of the material properties of the upper layer and base rock on the component response of the base rock due to upward propagating shear wave may be further highlighted by considering the expression for this component response:

$$Xut_{(n+1)}(t) = \frac{Xt_{(n+1)}(t) - Xdb_n(t)Td_n}{Tu_n} \qquad (2.5.2)$$

If this component response is examined for the duration of $2t_1$, t_1 being the shear wave time of travel through the thickness of the

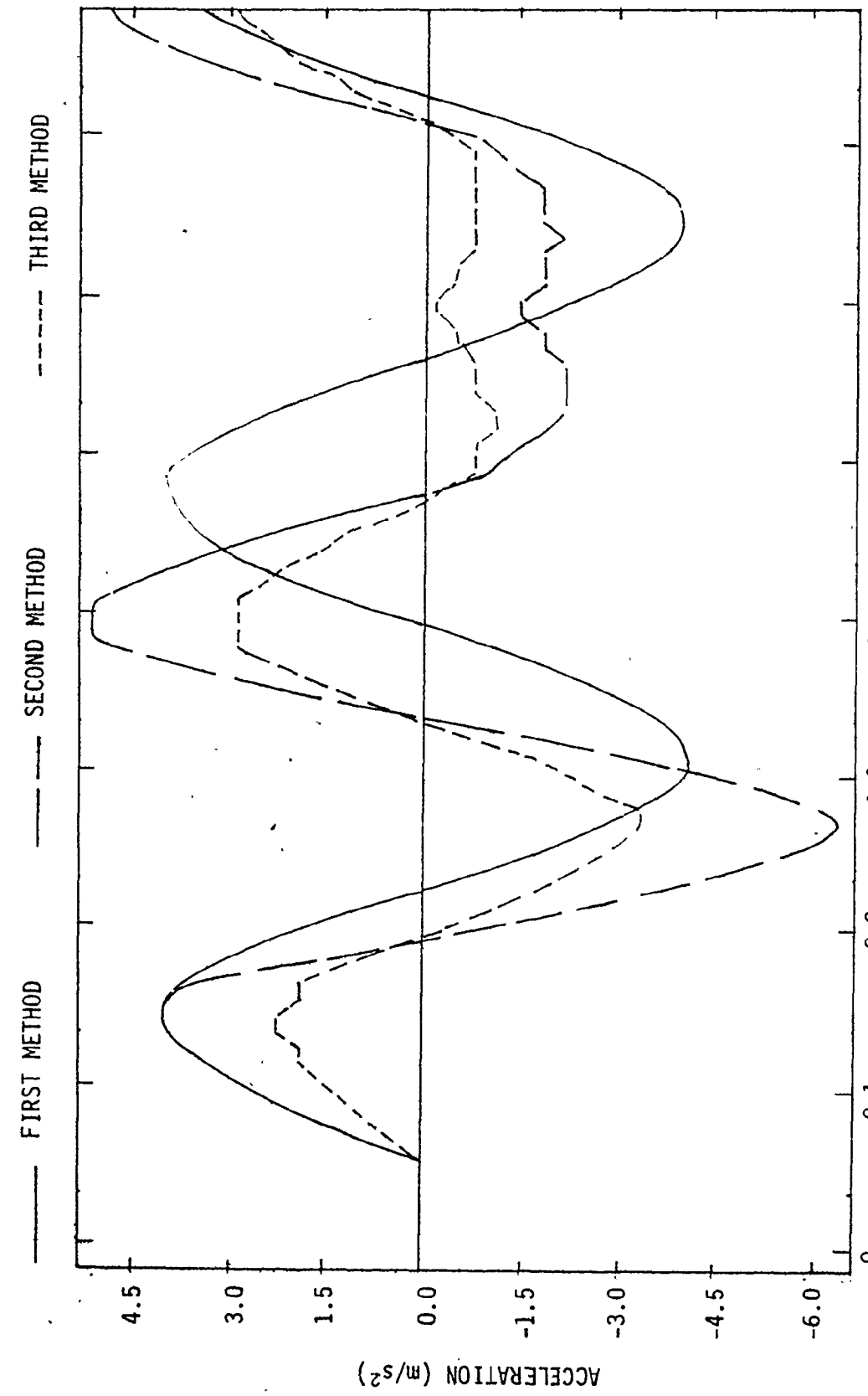

FIGURE 2.5.2 SURFACE RESPONSE FOR THE ONE LAYER SYSTEM

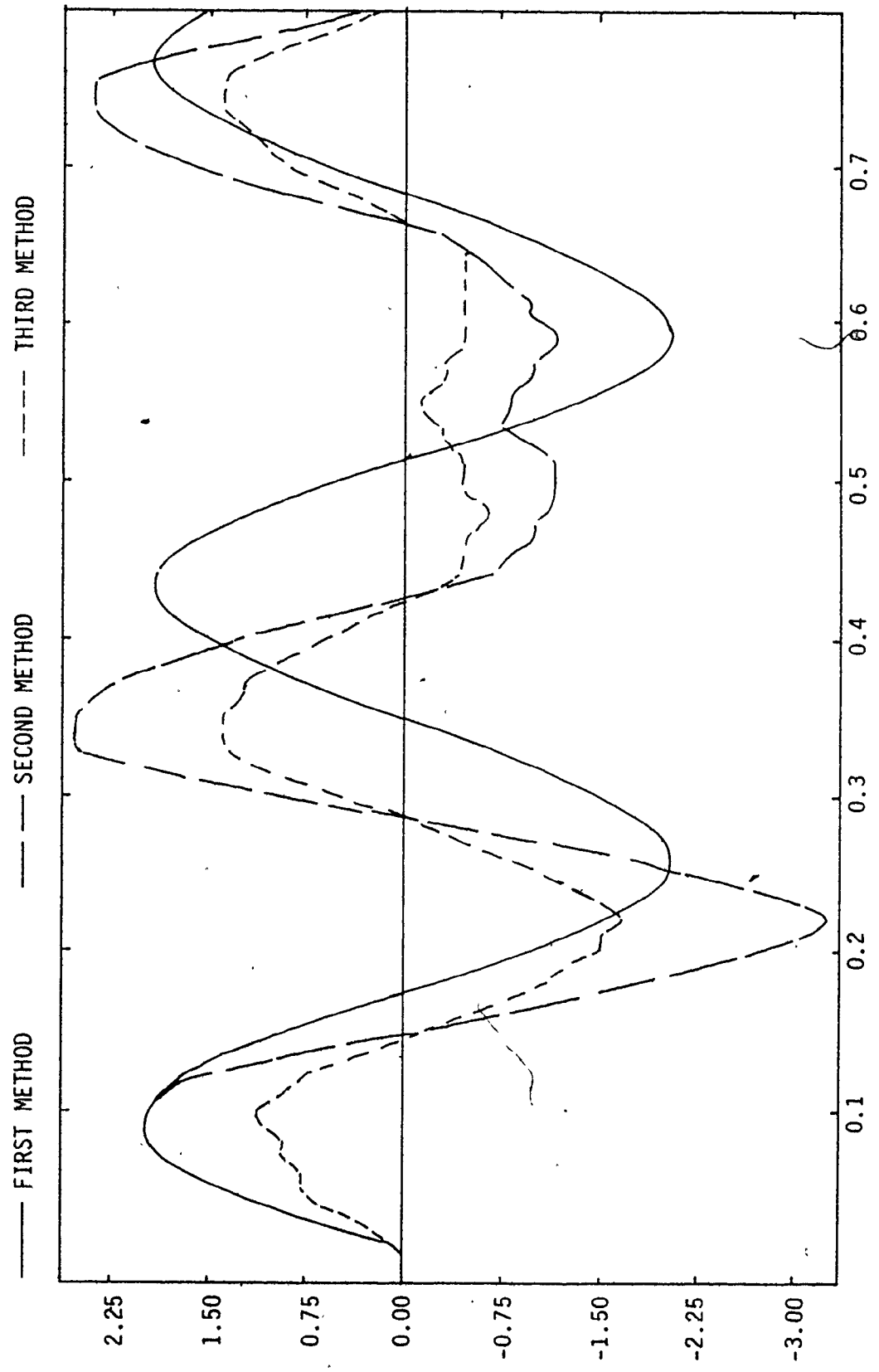

FIGURE 2.5.3 UPWARD COMPONENT RESPONSE AT BASE ROCK LEVEL OF THE SINGLE LAYER SYSTEM

layer, the component response $Xdb_n(t)$ does not exist during this period. Hence the expression for the component response $Xut_{(n+1)}(t)$ is given by:

$$Xut_{(n+1)}(t) = \frac{Xt_{(n+1)}(t)}{Tu_{(n+1)}} = c \cdot Xt_{(n+1)}(t) \qquad (2.5.3)$$

This expression is independent of the excitation frequency. Table 2.5.2 shows the value of c, which represents the fraction of the total response that constitutes the upward component response at base rock level. The impedence ratio μ was varied through the entire range from unity to zero. Obviously, when the top layer properties are identical to the base rock, the total response is the same as the upward component response since all of the response is transmitted through. At the other extreme, if the impedence of the top layer is zero (impedence ratio is zero, i.e. the base rock level is also the ground level) c is equal to 0.5 (upward component response is half the total response) which is in accordance with the principles of wave propagation discussed in Section 2.3, Equation (2.3.11). For impedence ratio values between these limits, the value of c varies linearly from 1.0 to 0.5. Thus, it is clear that the closer the impedence of the top layer is to that of the bottom layer, the greater is the upward component response for a given response of the interface. For most cases, the value of c lies between 0.65 to 0.75, which is much less than the value of c = 1.0 for all cases as suggested by previous methods.

TABLE 2.5.2

CONTRIBUTION OF TOTAL RESPONSE TO UPWARD COMPONENT RESPONSE AT BASE ROCK LEVEL

Impedence Ratio (μ)	Constant $c = \frac{1}{T\mu_n} = \frac{\mu+1}{2}$
1.0	1.0
0.9	0.95
0.8	0.90
0.7	0.85
0.6	0.80
0.5	0.75
0.4	0.70
0.3	0.65
0.2	0.60
0.1	0.55
0.0	0.50

2.6 RESPONSE OF A FOUR LAYER SYSTEM

A single layer system is a rather highly idealized soil system. A more realistic situation would be a four-layer system such as that shown in Figure 2.6.1. The magnification factors obtained by the three methods and Equation (2.5.1) for all the interfaces are given in Table 2.6.1. It can be observed that the magnification factors obtained by the proposed method, are in general much smaller than those obtained by the other two methods for all frequencies considered.

For this system and a sinusoidal base excitation of 2 Hz frequency and ± 1.0 m/s amplitude, the ground response and upward component response at the base rock level are given in Figures 2.62 and 2.63. The differences in the results obtained by these methods is obvious.

The response computed by the proposed method tends to be smaller in magnitude than that obtained by the other two methods. This is because present methods equate the total base rock response to the upward component response at that level, while in most realistic cases it should be between 65 to 75% of the total base rock response. In other words, by assuming the energy reflected downwards at the base rock level to be travelling into the upper layers, present methods tend to over-estimate the response of the system. This point is further highlighted by the Figure 2.6.3 plot of the upward component response of the base rock using the three methods. It should also be noted that actual monitored responses tend to be less than those that might be predicted by methods one and two.

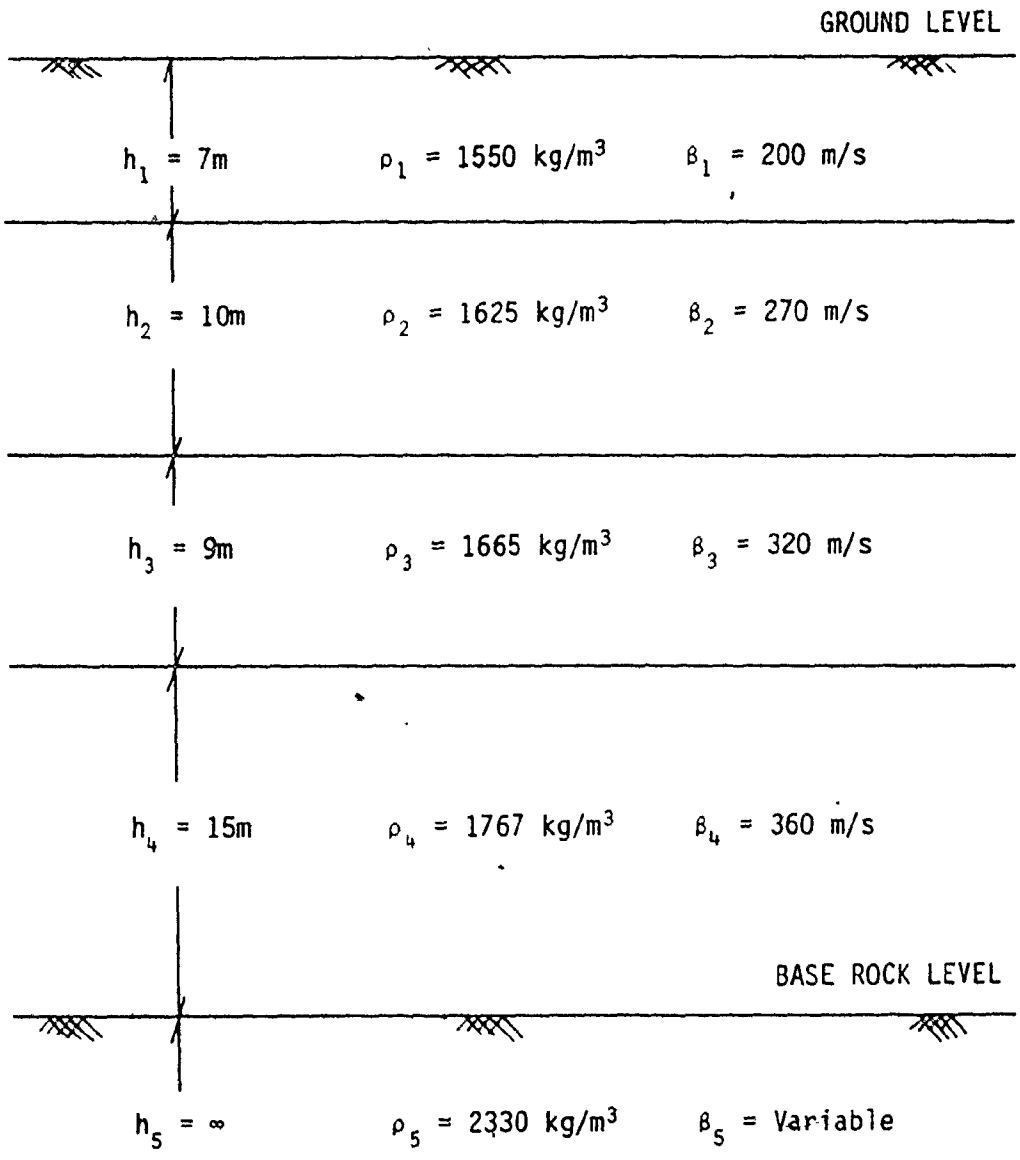

FIGURE 2.6.1 FOUR LAYER SYSTEM

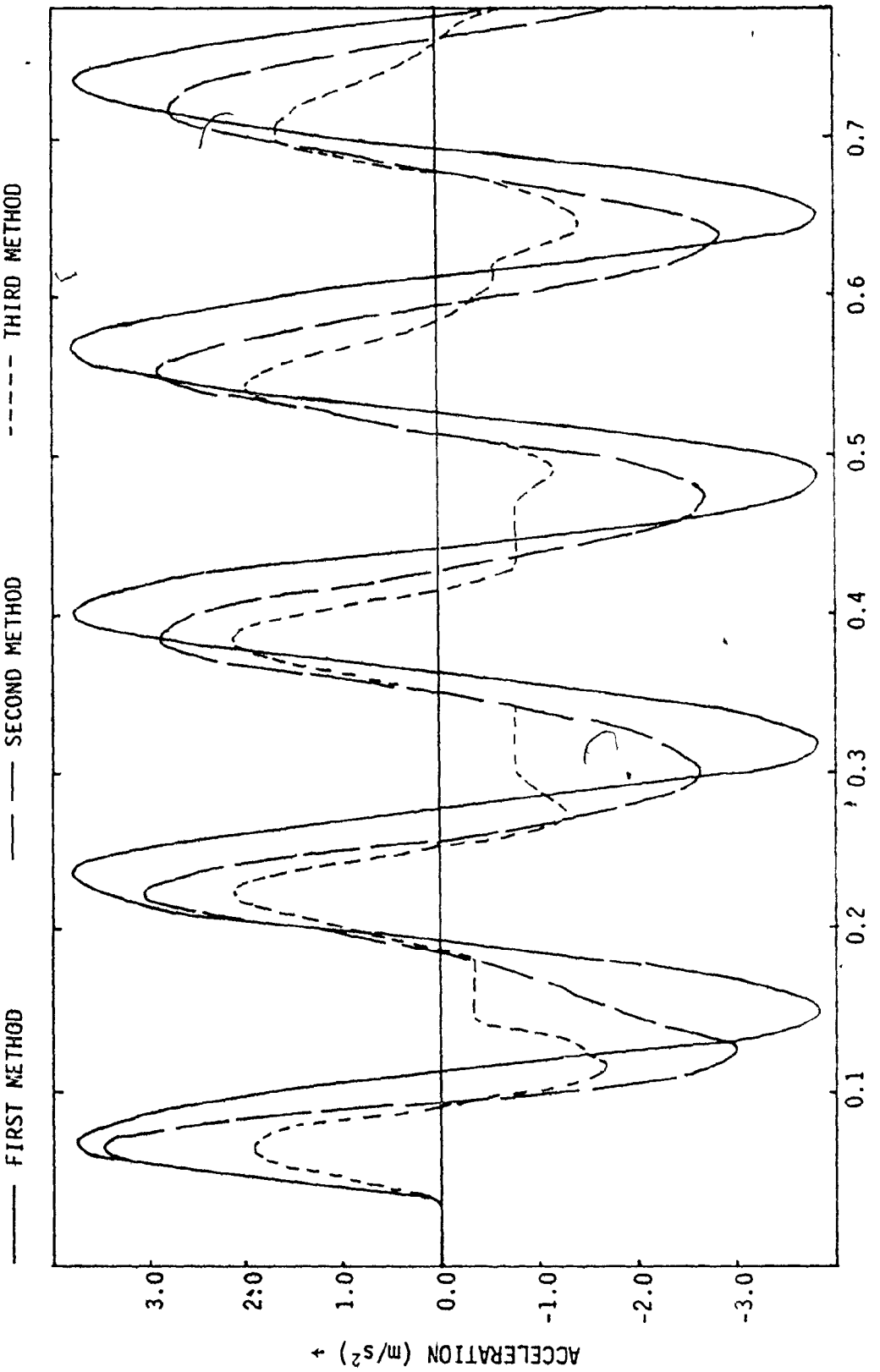

FIGURE 2.6.2 SURFACE RESPONSE FOR THE FOUR LAYER SYSTEM

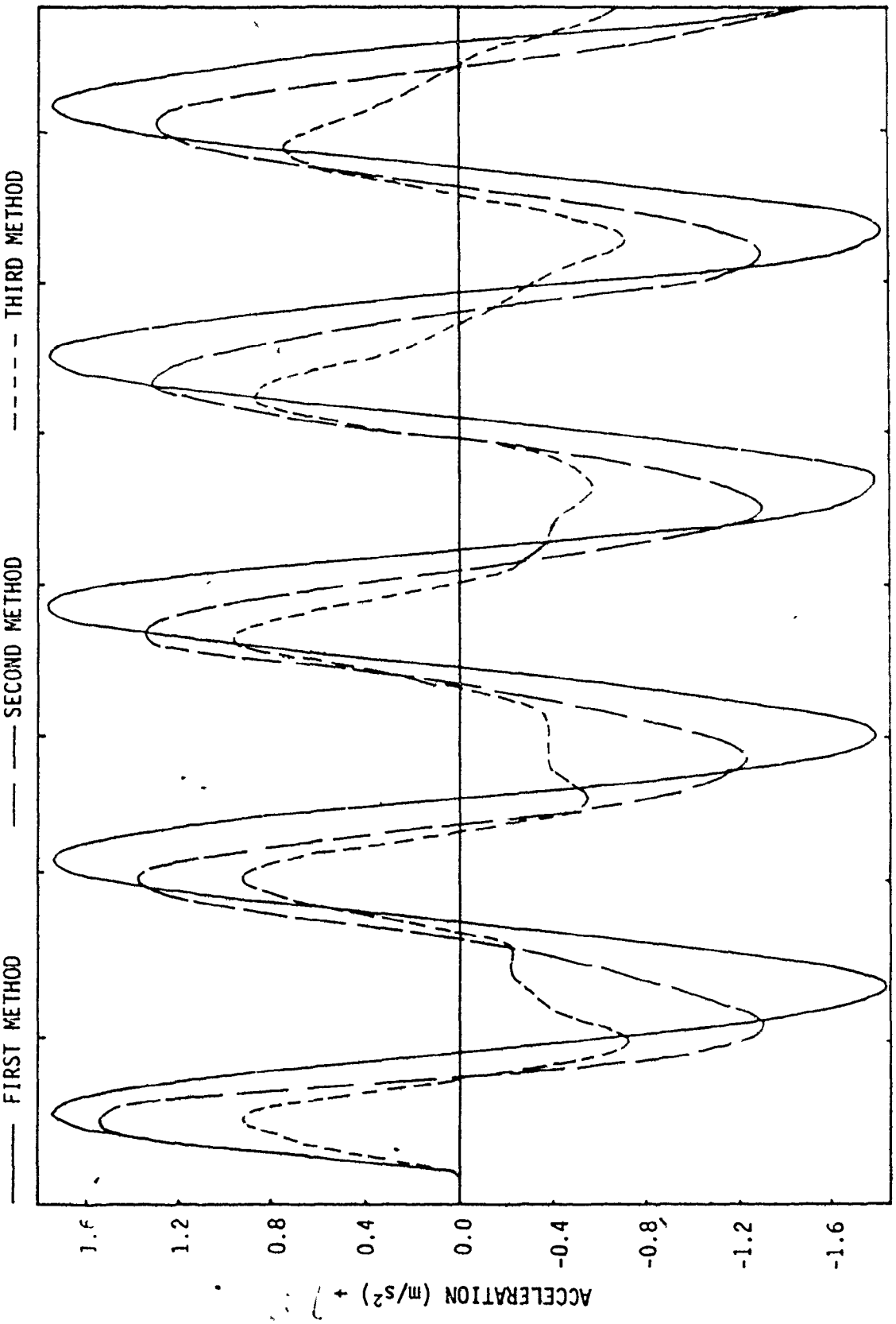

FIGURE 2.6.3 UPWARD COMPONENT RESPONSE AT THE BASEROCK LEVEL FOR THE FOUR LAYER SYSTEM

TABLE 2.6.1

MAGNIFICATION FACTORS FOR THE FOUR LAYER SYSTEM

Frequency of excitation Hz	Magnification Factors				Interface
	First Method	Second Method	Third Method	Kanai Method (Okamoto, 1973)	
1.0	3.764	3.459	1.099	1.369	Ground Level
	3.718	3.331	1.060		1
	3.467	3.012	0.930		2
	3.190	2.634	0.828		3
	1.000	1.000	1.000		Base Rock
3.0	5.466	6.531	2.341	2.438	Ground Level
	4.327	5.347	1.873		1
	2.172	2.908	1.039		2
	2.018	1.993	0.644		3
	1.000	1.000	1.000		Base Rock
4.5	5.534	6.679	2.363	2.162	Ground Level
	3.133	3.886	1.372		1
	2.097	2.571	0.913		2
	3.282	3.540	1.399		3
	1.000	1.000	1.000		Base Rock
6.0	5.735	8.912	3.293	2.086	Ground Level
	2.450	3.859	1.415		1
	3.457	5.312	2.017		2
	3.178	5.320	1.989		3
	1.000	1.000	1.000		Base Rock
8.0	5.929	7.942	2.708	2.047	Ground Level
	2.439	3.012	0.998		1
	3.668	5.031	1.769		2
	2.007	2.943	1.122		3
	1.000	1.000	1.000		Base Rock

Amplitude of sinusoidal base excitation = $\pm$ 1.0 m/s^2

2.7 ANGLE OF INCIDENCE OF SEISMIC WAVES

The angle of incidence of the seismic shear wave at the ground level depends on the epicentral distance of the site, shear wave velocity of the surface layer and the focal depth. The angles of incidence for a surface layer with shear wave velocity of 3400 m/s have been computed and are available as a set of tables for epicentral distances greater than 2172 km (Chandra, 1972). These tables are based on a theoretical model of the earth and are not really suitable for sites in the epicentral region. At 2172 km the angles of incidence are given as 36.21, 35.67 and 34.67 degrees for focal depths of 0, 40 and 104 km, respectively. This indicates that the focal depth has relatively little influence on the angle of incidence.

The angle of incidence in any layer is proportional to the shear wave velocity of the layer. By allowing a model adjustment factor of 1.5, the angle of incidence may be considered for this case to be 54 degrees. Based on this finding, Nair (1974) suggested that the surface layer angle of incidence for near sites can be approximated as:

$$\theta \text{ (degrees)} = \frac{\text{Shear Wave Velocity in the layer (m/s)}}{73.15} \quad (2.7.1)$$

For distant sites, θ is zero.

However, seismologists generally neglect the soil and other weak and soft rock formations near the top of the earth's crust. For most engineering problems, what a seismologist refers to as the angle of incidence at the ground level is actually the angle of incidence at the

base rock level, or in many cases much below the formations generally referred to as bedrock in engineering problems. The shear wave velocity of surface rock formations in general are of the order of 2 km/s. Using the laws of refraction for the angle of incidence i and the angle of refraction r:

$$\text{Sin}(r) = \frac{\beta_r}{\beta_i} \cdot \text{Sin}(i)$$

where β_r = shear wave velocity of the layer into which the wave is refracted

β_i = shear wave velocity of the layer through which it is incident at the interface.

If β_r = 2.0 km/s, β_i = 3.5 km/s and i = 36^0, r = 20^0. The largest possible angle of incidence is 90^0, and even for this case, the value of r works out to be only 35^0. Thus, for engineering problems, the largest angle of incidence at the base rock level would be of the order of 30 to 35 degrees, and much less in many cases.

It should be noted that when a shear wave is incident at an interface, it is partially reflected and partially refracted as S-wave; and partially reflected and refracted as P-wave. The contribution to P-wave form of reflection and refraction is zero at zero angle of incidence and increases rather gradually as the angle of incidence increases up to 30^0. However, in the range of interest (Figure 2.7.1) most of the incident S-wave is transmitted or reflected. For the smaller angles of incidence, the principles of vertical propagation of shear waves may well be considered justifiable.

$$\frac{\text{Sin } \theta_1}{\beta_1} = \frac{\text{Sin } \theta_2}{\beta_2} = \frac{\text{Sin } \theta_3}{\alpha_1} = \frac{\text{Sin } \theta_4}{\alpha_2}$$

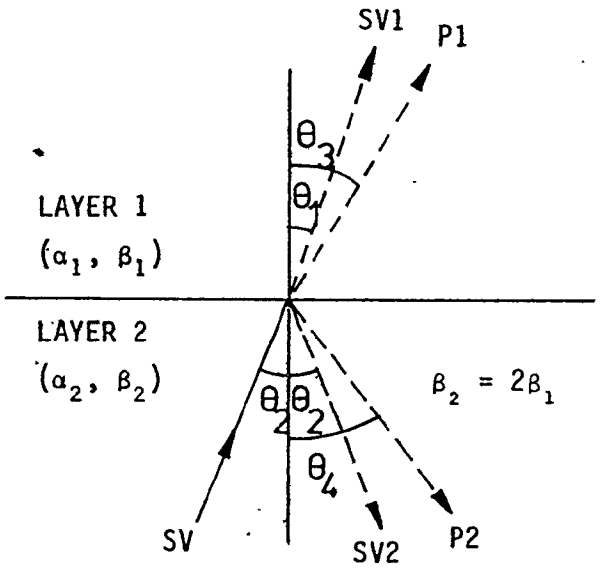

a. DECOMPOSITION OF SHEAR WAVE AT INTERFACE BETWEEN TWO ELASTIC MEDIA

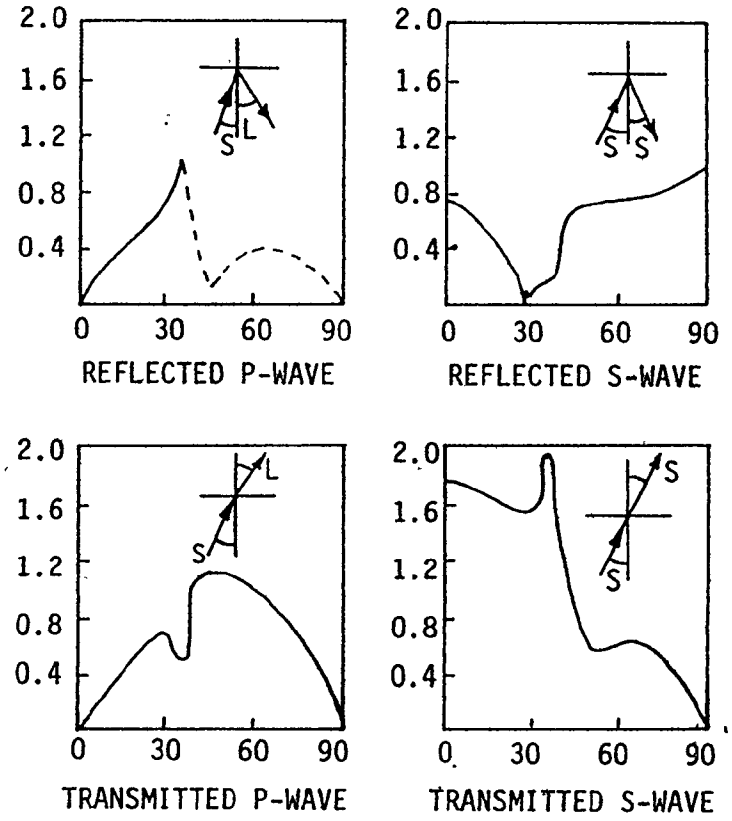

b. RELATION BETWEEN AMPLITUDE RATIO OF EMITTED WAVES AND INCIDENT ANGLE

FIGURE 2.7.1 DECOMPOSITION OF SHEAR WAVES WITH INCIDENT ANGLE (RICHARTS, WOODS AND HALL, 1970)

It should also be noted that the angle of propagation of the seismic waves should be determined for the base rock first, and based on this quantity values for other layers may be computed. Doing it the other way round can sometimes result in angles of incidence of greater than 90^0 in the lower layers, which is obviously incorrect.

2.8 PROPAGATION OF SHEAR WAVES

Shear waves are considered to be planar. This means the propagation in mutually perpendicular horizontal directions is independent so that S-waves in the x-z plane cause shear strains in the x-z plane only, and those in the y-z plane cause shear strains in the y-z plane only.

For vertical propagation of shear waves, only vertical distances introduce time lags. For this case, all points in a horizontal plane have the same response. However, if the wave propagation is at an angle to the vertical, horizontal distances also contribute to the time lags. For this case, the responses at two points on the same horizontal level, but separated by a horizontal distance, will be different. For the reasons explained in section 2.7 and above, the use of vertical propagation of shear waves for the horizontal component of the shear wave (propagating at an angle to the vertical) is justified for engineering purposes. The details of the procedures have been well documented by Nair (1974), and are not repeated here.

2.9 CONTRIBUTION OF RAYLEIGH WAVES TO SEISMIC GROUND MOTIONS

When body waves are incident at interfaces, surface waves are generated. Rayleigh waves are of this type. The equation of motion governing the propagation of R-waves is well documented and is not repeated here (Haskell, 1953; Richart et al, 1970; Nair, 1974).

However, present methods are not adequate to determine the frequency and wave length of R-waves for a given phase velocity, since many frequencies can satisfy the equation of motion and compatibility conditions. To avoid this difficulty, curves presented by Sezawa (1927), Figure 2.9.1, or those presented by Oliver and Ewing (1957), Figure 2.9.2 and 2.9.3, are used to obtain a reasonable estimate of the wave length and frequency for a given phase velocity of the system. In many cases, it is difficult to read these curves even for obtaining approximate values because of the logarithmic scale and the narrow range of material properties represented. Since the transfer functions used to obtain the response of the ground due to R-waves at any depth below the surface are quite sensitive to the wave number, the determination of the wave number with adequate accuracy is very important.

The phase velocity of R-waves can range from 0.93 times the shear wave velocity of the weakest layer of the system to the shear wave velocity of the stiffest layer of the system, usually the base rock. Present methods suggest consideration of this entire range at regular intervals, and then averaging the values for use in analysis. However, for a given earthquake and site, R-waves of only a narrow range of phase

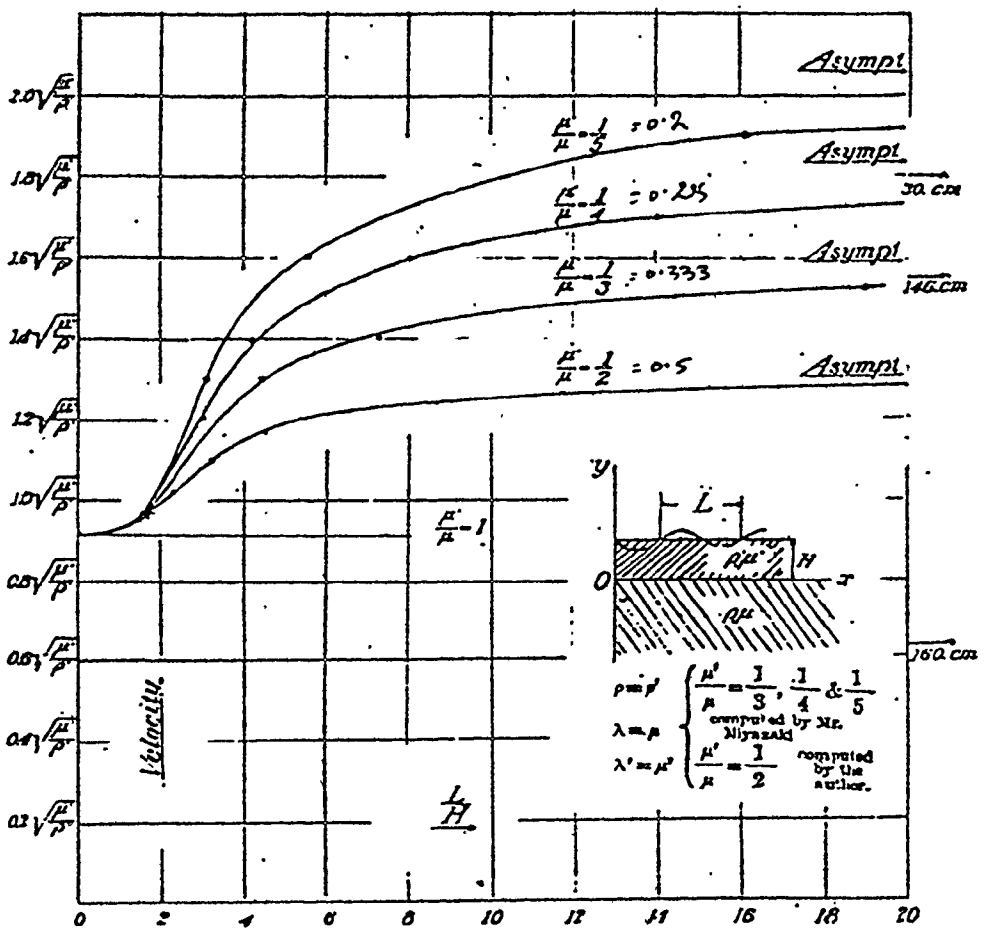

FIGURE 2.9.1 DISPERSION OF ELASTIC WAVES OVER STRATIFIED SURFACES (SEZAWA, 1927)

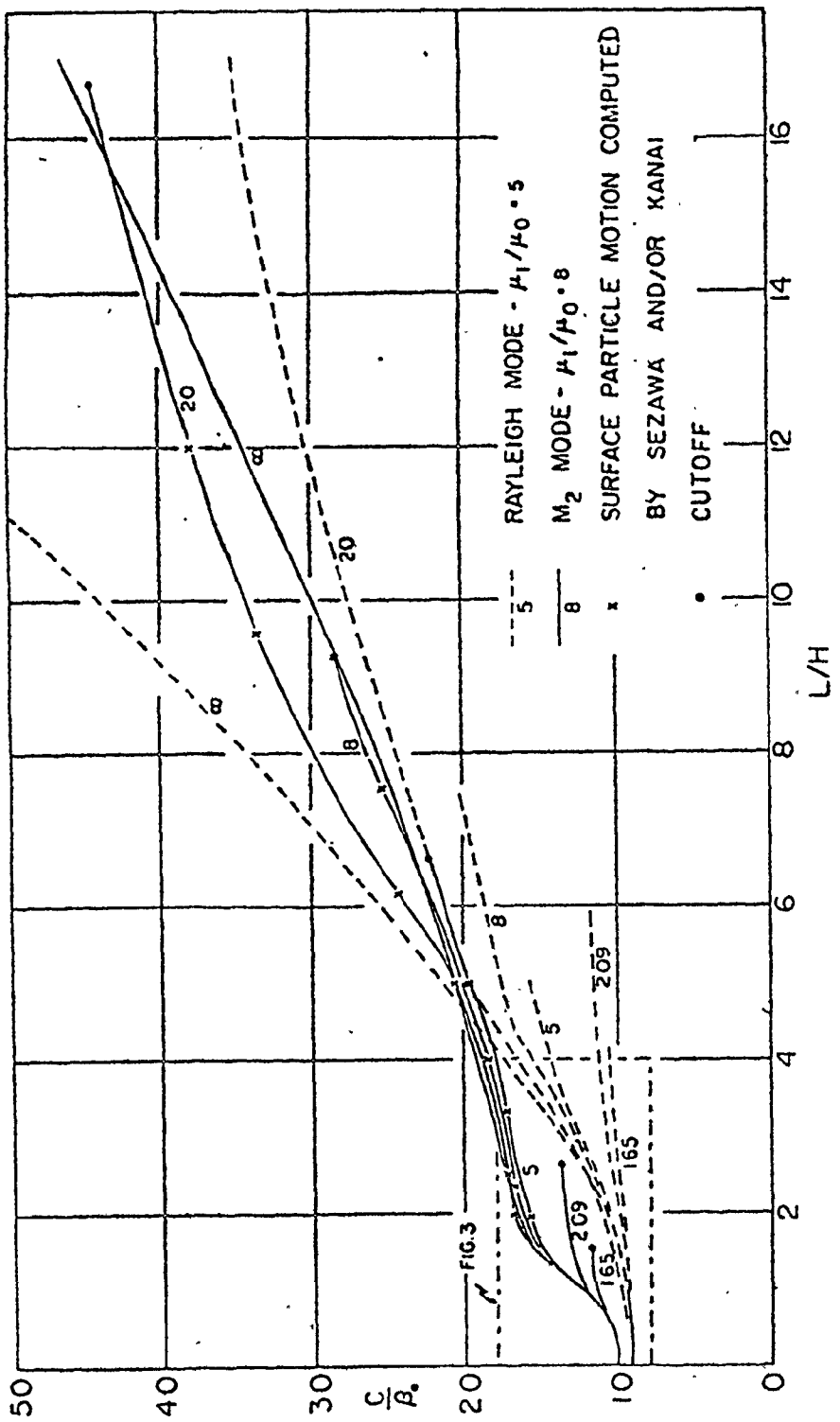

FIGURE 2.9.2 THEORETICAL DISPERSION CURVES FOR RAYLEIGH AND m_2 MODES (OLIVER AND EWING, 1957)

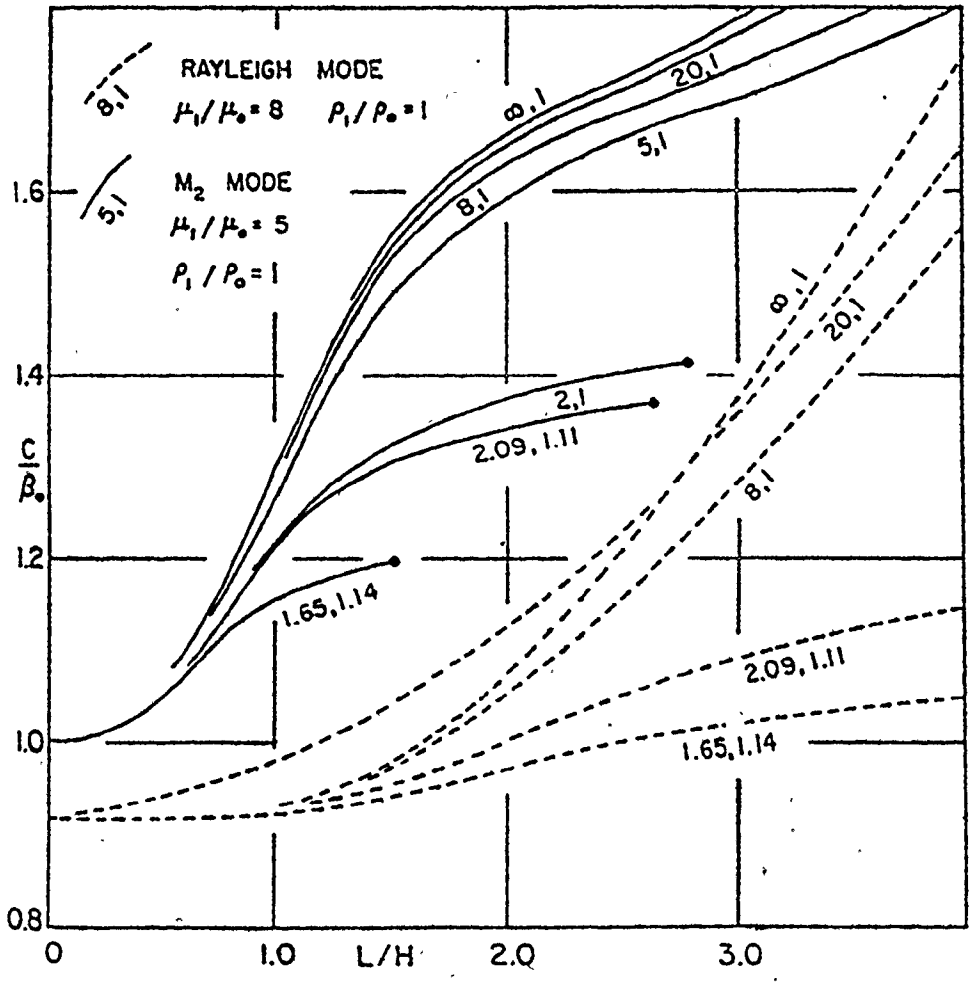

FIGURE 2.9.3 OBSERVED DATA AND THEORETICAL DISPERSION CURVES FOR RAYLEIGH AND m_2 MODES (OLIVER AND EWING, 1957)

velocities can reach the site along with the shear waves. Hence, it is important to consider the appropriate phase velocity of the R-waves in the analysis.

Another aspect of the R-waves not well investigated is the contribution of the R-waves to the seismic ground response. It is suggested that the contribution of R-waves is about 25% of the total response for near sites, zero for distant sites and in this range for intermediate epicentral distances (Nair, 1974). These approximations may lead to considerable error in the computed ground response.

It is clear that improved handling of the difficulties cited above is required to obtain reasonable estimates of R-wave contributions to seismic ground motions. In following sections, an attempt is made to provide the necessary improvements.

2.10 OBSERVATIONS FROM PAST EARTHQUAKE RECORDS

Earthquake records, even though the seismic response appears to be a random variable, reveal the presence of two regular frequencies dominating the record at various stages. It is also possible to recognize the instant of arrival of primary, shear and Rayleigh waves and their respective frequencies. The wave velocities may be obtained from the knowledge of the epicentral distance and the time of travel.

Figure 2.10.1 shows the plot of phase velocities and periods of the R-waves obtained from the analysis of many earthquake records

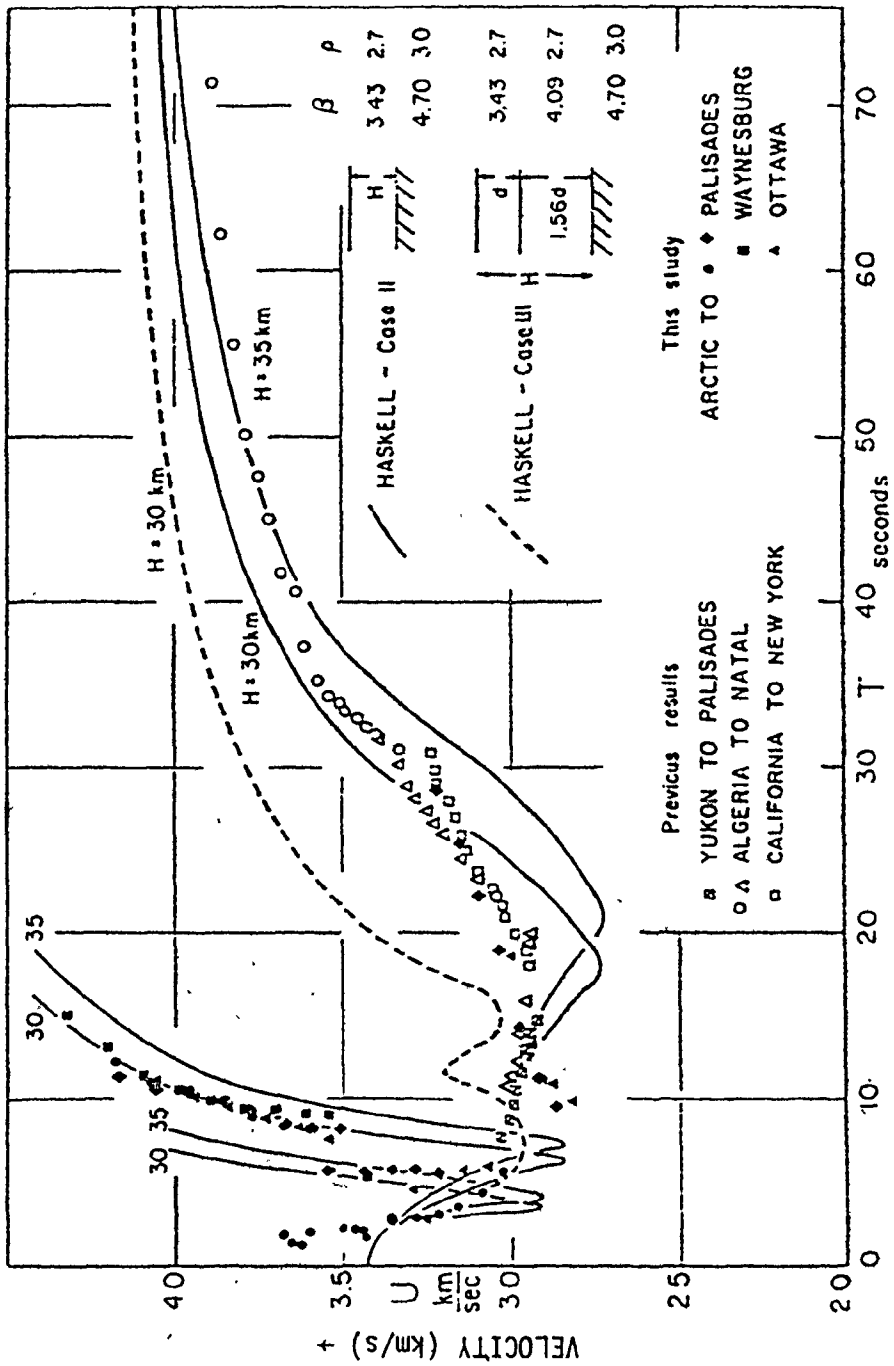

FIGURE 2.10.1 OBSERVED DATA AND THEORETICAL DISPERSION CURVES FOR RAYLEIGH AND m_2 MODES (OLIVER AND EWING, 1957)

(Oliver and Ewing, 1957). The dispersion curve takes the shape of a flat trough in the range of periods from 10 to 20 s. The point density in this range is greatest. For phase velocities greater than 3.5 km/s, the density of recorded points decreases considerably. The suggested velocity of shear wave propagation for the top mantle of the earth's crust as suggested by various investigators is about 3.5 km/s. It can be observed from Figure 2.10.1 that the point density is greatest for the range of phase velocities approximately 0.93 times the suggested shear wave velocity.

The surface waves may propagate in higher modes as well. The higher mdoes are associated with much smaller periods, and the energy and amplitudes of such waves are too small to make a positive identification (Oliver and Ewing, 1957). They are not of much significance from an engineering point of view, and are not accounted for in this study.

2.11 NATURAL PERIOD OF COMPRESSION VIBRATIONS OF THE TOP MANTLE

It has been suggested by many investigators that the depth of the top mantle H is about 30 km and the velocity of shear wave β_0 is about 3.5 km/s. Assuming a poisson's ratio of 0.35, the compression wave velocity α_0 for the layer is 7.3 km/s. The natural period of compression vibrations can be obtained from:

$$Tgv = 4H/\alpha_0 \qquad (2.11.1)$$

Using this expression, Tgv for a uniform top mantle is 16.4 s, which is well within the range of periods for the trough-shaped region of Figure 2.10.1 where the point density is greatest.

2.12 THEORETICAL DISPERSION CURVES FOR R-WAVES PRESENTED BY OLIVER AND EWING

Many investigations concerning the propagation of R-waves in the top mantle have been reported (Haskell, 1953; Oliver and Ewing, 1957). Oliver and Ewing (1957) have compiled this data along with their investigations and presented a set of curves relating the dimensionless phase velocity c/β_0 to the dimensionless wave length L/H, where c is the phase velocity and L is the wave length of the R-wave, and H is the depth of the layer (single layer system) as shown in Figures 2.9.2 and 2.9.3. For any assumed phase velocity c, c/β_0 is computed and the corresponding c/H value is read from the appropriate curve. The curves are presented for various rigidity ratios μ_1/μ_0 where μ_1 and μ_0 represent the rigidity moduli of the top mantle and the formation below it. Knowing L/H and the wave length L, the wave number k is obtained. This value of k is taken as a good approximation for the trial and error evaluation of the wave number.

Difficulties in Using the Curves.

1. For systems with very low shear wave velocities, the range of c/β_0 is inadequate.
2. Curves are presented for only a small range of rigidity

ratios μ_1/μ_0, especially for the lower rigidity ratios where it is difficult to obtain reasonable interpolation of the curves.

3. When these curves are nearly parallel to the L/H axis, the L/H values are very sensitive to small changes in c/β_0, which makes it difficult to read these curves.

2.13 WAVE NUMBERS FOR SINGLE LAYER SYSTEM FROM OLIVER AND EWING CURVES

The wave numbers were obtained by using the Oliver and Ewing curves for the single layer system of Figure 2.5.1 with a 30 m deep layer. The material properties used and the results of the analysis are given in Table 2.13.1, from which the following observations can be made:

1. For high rigidity ratios (greater than 20), the periods of the waves at various phase velocities very nearly remain the same (column 7 of Table 2.13.1).
2. As the phase velocity increases from 0.93 β_0 to β_r, the periods of these waves also increase.
3. Such an increase in period is more pronounced for low rigidity ratios, and less pronounced for high rigidity ratios.
4. For all rigidity ratios, for phase velocities close to β_0, the period of the wave is comparable to the natural period of compression vibrations of the system.

TABLE 2.13.1

WAVE NUMBERS FOR SINGLE LAYER SYSTEMS

Set No.	(L/H) from Oliver-Ewing Curves				L from Tgv	
	c/β_0	L/H	K	T (s)	L (m)	K
Set E1	0.93	-	-	-	139.7	3.730
E = 50 mPa	3.46	8.00	0.785	1.734	519.0	0.908
ρ = 1875 kg/m³	5.99	13.20	0.476	1.652	898.5	0.524
β_0 = 199.1 m/s	8.52	18.24	0.345	1.606	1278.0	0.369
ν = 0.33	11.05	23.30	0.270	1.581	1657.5	0.284
GR = 573	13.58	28.36	0.222	1.566	2037.0	0.231
Tgv = 1.5 s	16.11	33.42	0.188	1.556	2416.5	0.195
	18.64	38.48	0.163	1.548	2796.0	0.169
	21.00	43.20	0.145	1.542	3150.0	0.150
				Average T = 1.598		
Set E2	0.93	-	-	-	139.5	3.378
E = 500 mPa	1.94	4.50	1.396	0.572	290.9	1.610
ρ = 2000 kg/m³	2.95	6.90	0.911	0.576	442.9	1.060
β_0 = 304 m/s	3.95	9.15	0.688	0.570	593.7	0.794
ν = 9,33	4.96	11.00	0.571	0.546	745.0	0.632
GR = 57.8	5.97	13.14	0.478	0.542	1896.0	0.526
Tgv = 0.493 s	6.90	15.00	0.420	0.536	1036.0	0.455
				Average T = 0.475		
Set E3	0.93	-	-	-	139.5	3.378
E = 5 gPa	1.17	2.10	2.992	0.150	175.1	2.692
ρ = 2275 kg/m³	1.40	3.85	1.632	0.149	210.7	2.237
β_0 = 902.2 m/s	1.64	5.50	1.142	0.279	246.2	1.194
ν = 0.35	1.88	7.50	0.839	0.332	282.0	1.671
GR = 5.79	2.38	14.00	0.449	0.500	349.1	1.350
Tgv = 0.167 s				Average T = 0.282		
Set E4	0.93	-	-	-	139.5	3.378
E = 50 gPa	0.96	2.25	2.957	0.083	144.7	3.257
ρ = 2350 kg/m³	0.98	3.00	2.094	0.115	147.3	3.199
β_0 = 1985 m/s	1.04	4.00	1.571	0.146	155.2	3.036
ν = 0.4	1.06	5.00	1.257	0.179	158.7	2.970
GR = 1.157				Average T = 0.1308		
Tgv = 0.075 s						

Depth of the top layer H = 75 m Wave length L

Dimensionless Wave Number K = $2\pi H/L$ Period of R-wave T

2.14 WAVE NUMBERS FOR R-WAVES BY TRIAL AND ERROR ANALYSIS

The wave numbers for the single layer system of Section 2.13 were obtained for various phase velocities of R-waves by a trial and error process. Material properties indicated for set E1 and E3 of Table 2.13.1 were employed. Trial values of wave numbers were obtained by using the natural period of vertical vibrations for the top layer. Figure 2.14.1 gives the plots of dimensionless period T/Tgv versus dimensionless phase velocity c/β_0, from which the following observations can be made:

1. For a high rigidity ratio of 573 ($\beta_r/\beta_0 = 21.21$), the dimensionless period remains the same (close to 1.0) for dimensionless phase velocities from 1.0 to 2.0.
2. For a low rigidity ratio of 5.8 ($\beta_r/\beta_0 = 0.425$), the dimensionless period increases quite sharply for dimensionless phase velocities up to 1.0. It increases rather gradually for most of the remaining range of dimensionless phase velocities.
3. For dimensionless phase velocities close to 1.0, the dimensionless period is close to 1.0 in both sets.

2.15 TRANSFER FUNCTIONS FOR SINGLE LAYER SYSTEMS

The vertical and horizontal response due to R-waves at any depth is obtained by multiplying the respective response at the ground level by the respective transfer function at that instant of time. The

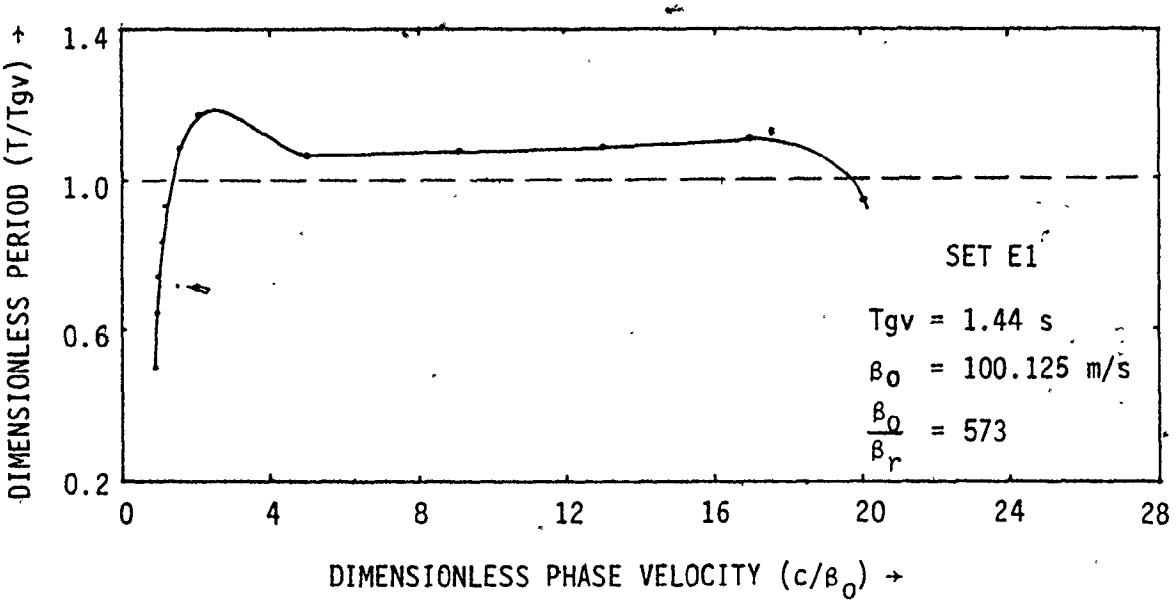

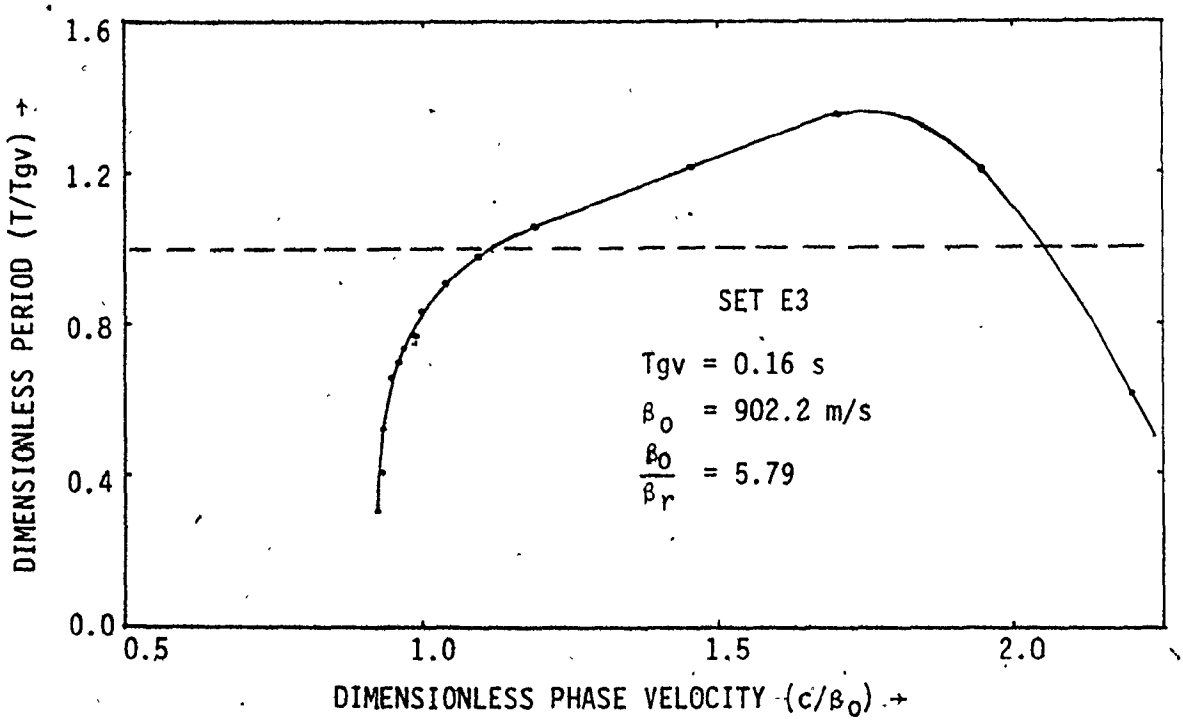

FIGURE 2.14.1 DIMENSIONLESS PHASE VELOCITIES AND DIMENSIONLESS PERIODS FOR R-WAVES

transfer functions for the single layer systems of Section 2.14 are used for the respective natural periods of vertical vibrations. The transfer functions at various phase velocities for these systems are shown in Figures 2.15.1 to 2.15.4. From these results the following observations can be made:

1. For the system with a high rigidity ratio, the vertical transfer function curves for all phase velocities are nearly identical, and the value is nearly zero for all phase velocities at the base rock level. The curves of horizontal transfer functions for most of the range of phase velocities are very close to each other, and again close to zero at the base rock level.
2. For the system with low rigidity ratio, the curves of horizontal and vertical transfer functions are very different for various phase velocities. The horizontal transfer function is less than 0.2 over most of the phase velocity range.
3. For dimensionless phase velocities close to unity, the curves of vertical transfer functions are close to each other, and tend to values close to zero at base rock level. For this range of phase velocities, the curves of horizontal transfer functions also tend to values close to zero at base rock level, and the curves vary sharply and almost linearly with depth from a value of unity at ground level to a negative maximum. This variation is much sharper for

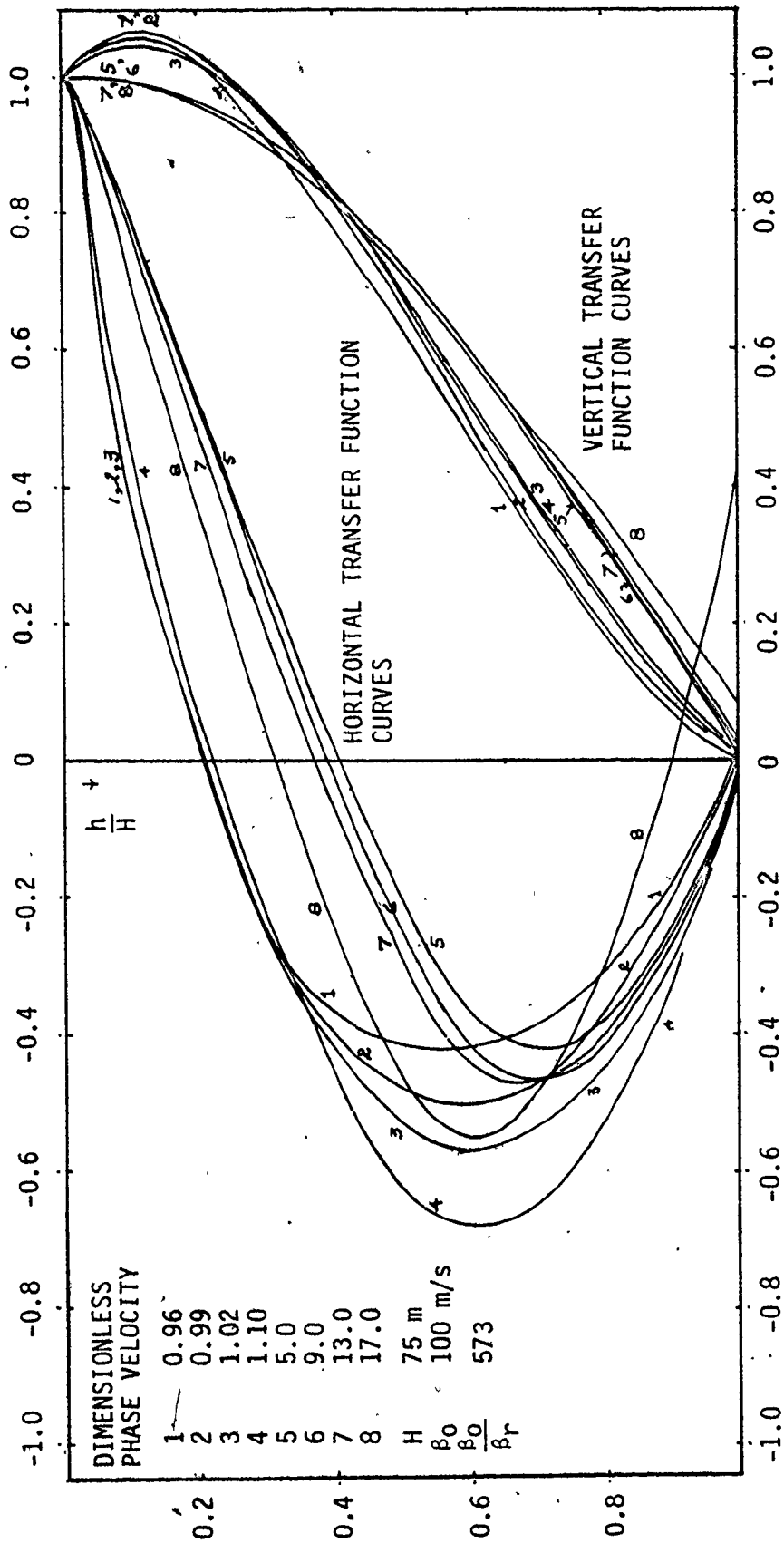

FIGURE 2.15.1 TRANSFER FUNCTIONS FOR SINGLE LAYER SYSTEM (E1)

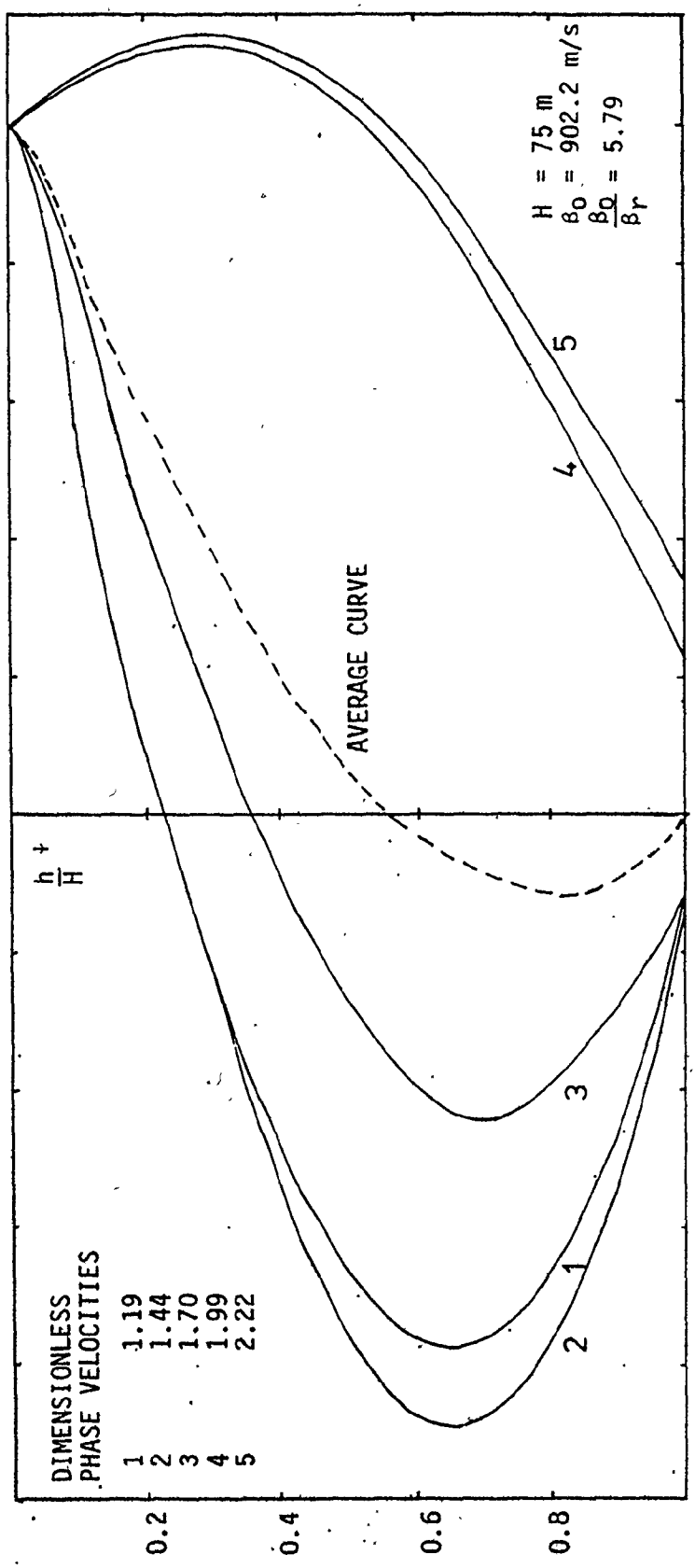

FIGURE 2.15.2 HORIZONTAL TRANSFER FUNCTIONS FOR SINGLE LAYER SYSTEM (E3)

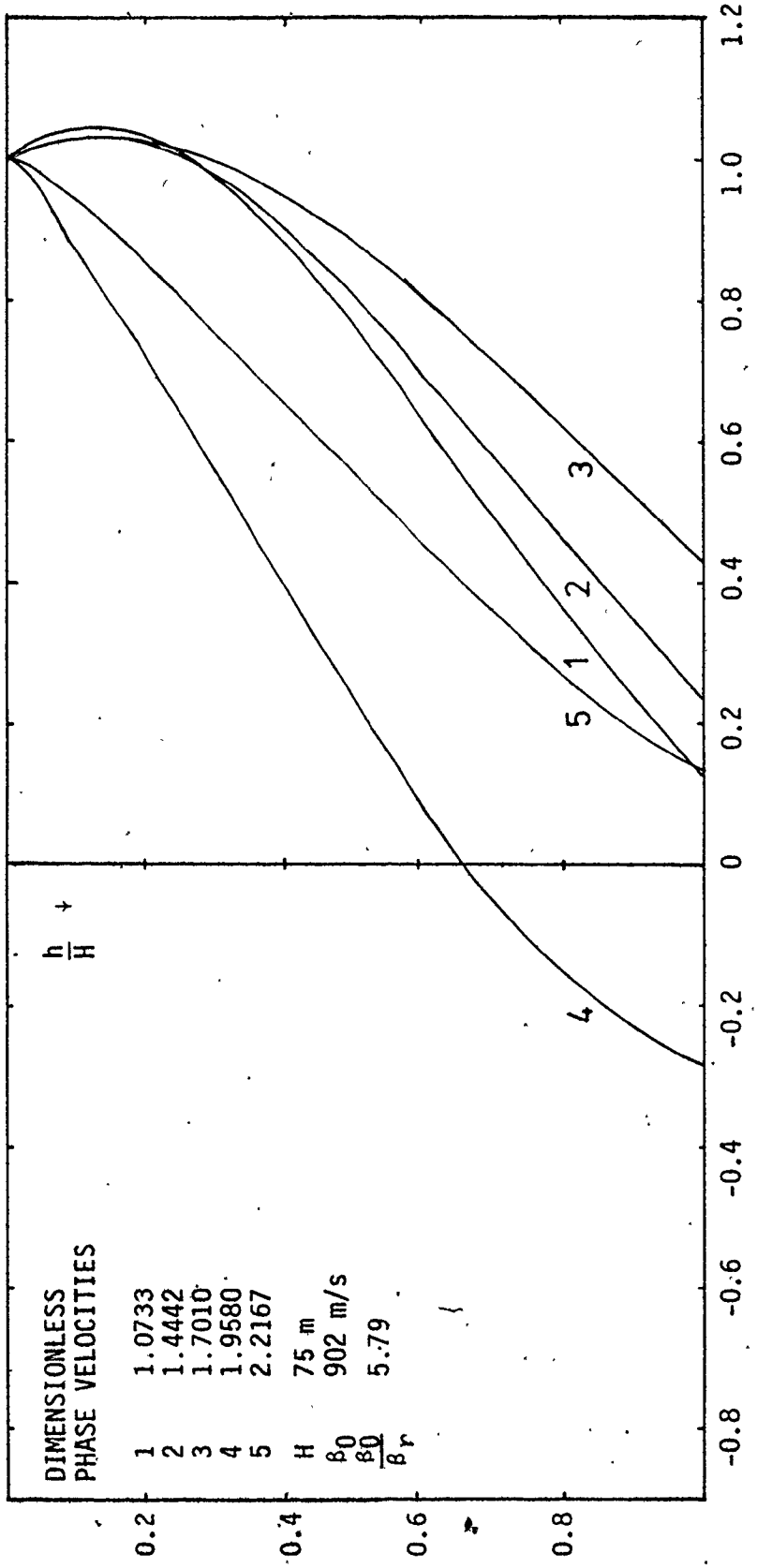

FIGURE 2.15.3 VERTICAL TRANSFER FUNCTIONS FOR SINGLE LAYER SYSTEM (E3)

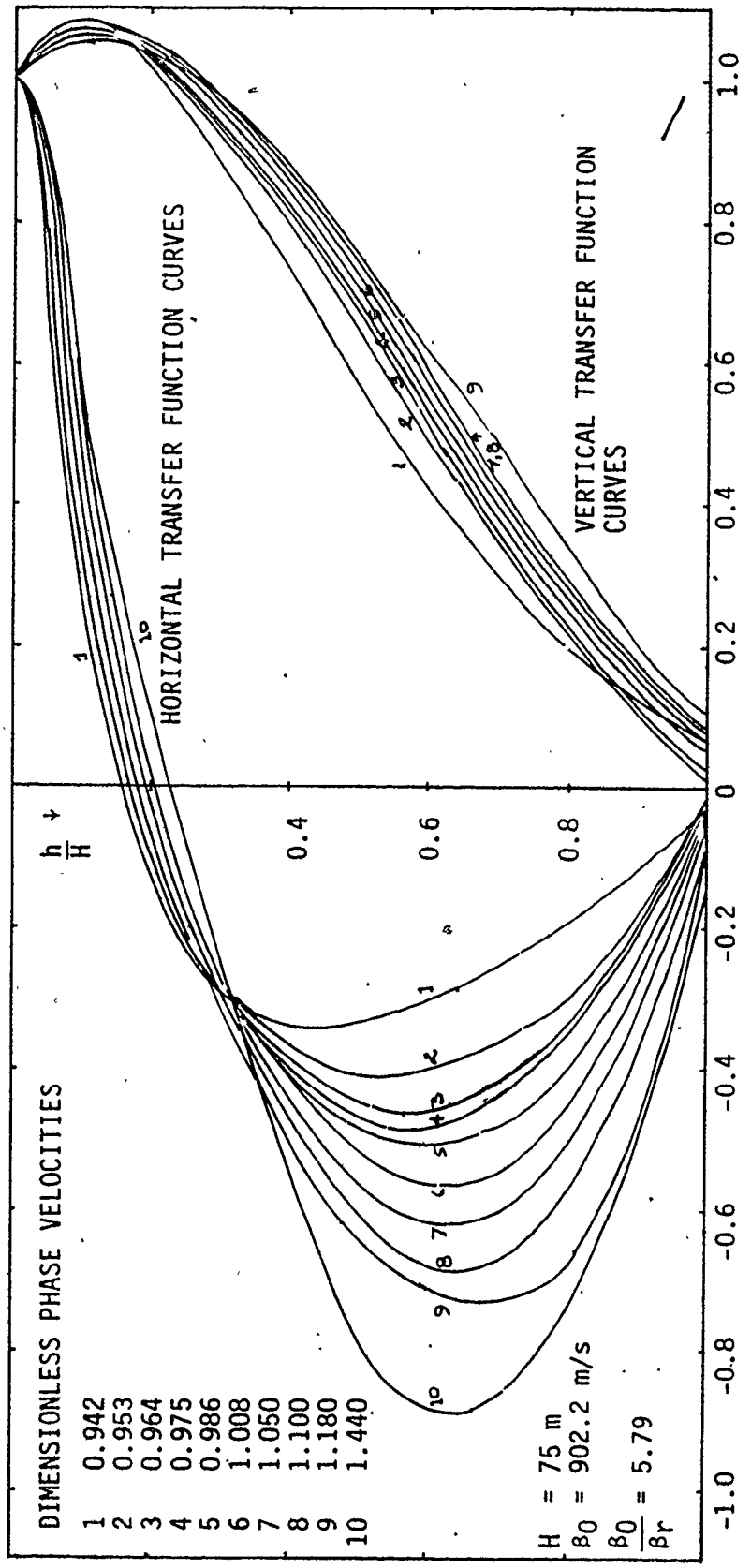

FIGURE 2.15.4 TRANSFER FUNCTIONS FOR THE SINGLE LAYER SYSTEM (E3)

the case of lower rigidity ratio.

The R-waves with phase velocity close to the shear wave velocity of the base rock are of special interest, and are discussed in the next section. For the phase velocity of 0.93 β_r and top layer of 75 m depth, the vertical transfer function remains constant at almost unity for periods greater than 10 s when β_0 = 100.125 m/s (E1) or 902.2 m/s (E2). For this range of periods, the horizontal transfer functions show somewhat larger variations over the depth for β_0 = 902.2 m/s, but still remain close to unity as shown in Figure 2.15.5. For β_0 = 100.125 m/s, this variation is much greater, but decreases with increasing period.

The ratio of the vertical response to horizontal response for these two cases at ground level and base rock level for various periods is given in Figure 2.15.6. The ratio at ground level does not vary appreciably for either case for periods greater than 10 s. For this range of periods, the ratio at base rock level for both cases remains practically constant. This indicates that for phase velocities comparable to the shear wave velocity of the base rock, and for periods greater than 10 seconds, any error in the assumed value of periods of R-wave does not lead to appreciable error in the computed values of vertical and horizontal transfer functions, or the ratio of vertical response to horizontal response at ground and base rock levels.

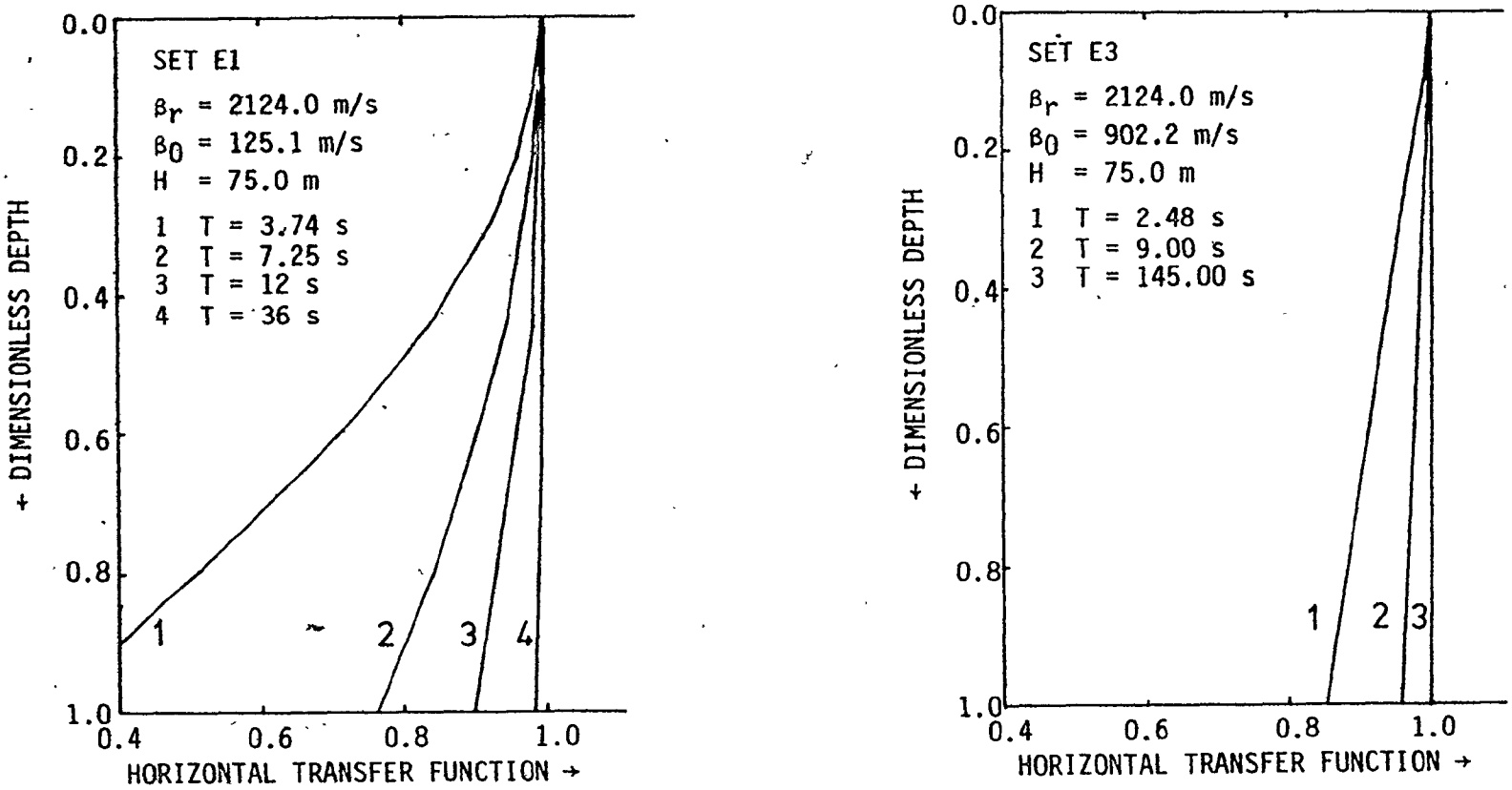

FIGURE 2.15.5 HORIZONTAL TRANSFER FUNCTIONS FOR DIFFERENT PERIODS

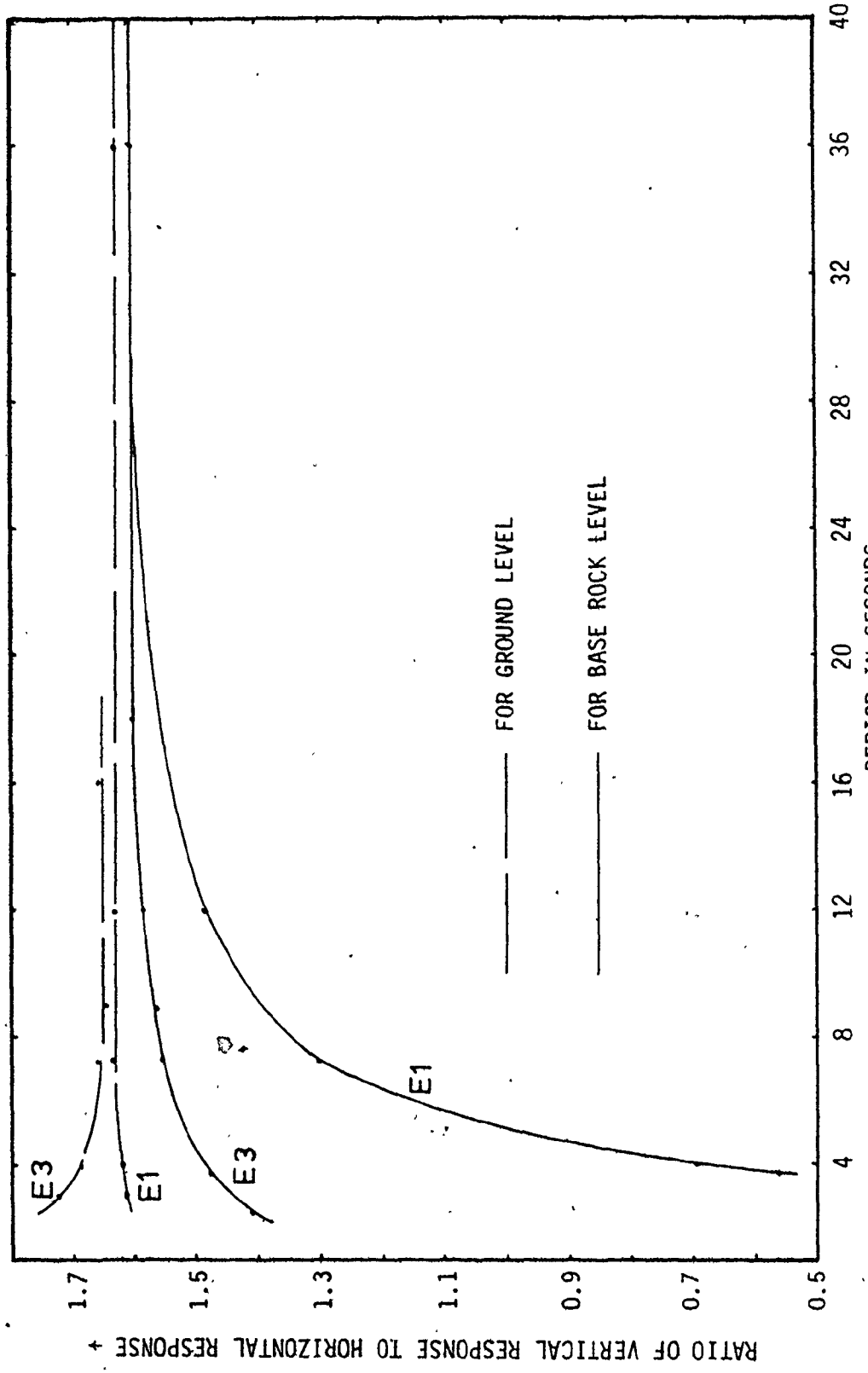

FIGURE 2.15.6 RATIO OF VERTICAL RESPONSE TO HORIZONTAL RESPONSE FOR SINGLE LAYER SYSTEMS

2.16 DETERMINATION OF WAVE NUMBER AND PHASE VELOCITY OF R-WAVES

As discussed in Section 2.10, the study of earthquake records indicates that only the Rayleigh waves with phase velocities close to the shear wave velocities of the top layers have a chance of reaching the site together with the shear waves. Since shear waves generally constitute the most important phase of the earthquake responsible for damage, in most cases it is satisfactory to only consider those R-waves that reach the site together with the shear waves. Thus, it appears that only R-waves with phase velocities comparable to the shear wave velocity of the base rock need be considered in the analysis of most engineering problems. The study also indicates that the period of these R-waves ranges from 10 to 20 s. If an earthquake record is available for a location close to the site under investigation, the period of R-waves from that record can be adopted during determination of the wave number of R-waves. In the absence of such a record, as indicated by Figure 2.10.1, a mean value of 15 s would be the best estimate for the period of R-waves.

For the subsurface layers of engineering importance, the natural period of vertical vibrations would be of the order of 0.25 to 1 s. Since the records of past earthquakes do not indicate the presence of significant R-waves of such periods, it is reasonable to assume that the R-waves generated by the incidence of shear waves at the interfaces of layers close to ground level are insignificant.

The advantages of the proposed method described in the next

section can be summarized as:

1. It is based on the study of many records of past earthquakes.
2. Since the phase velocity and period of the R-wave are determined explicity, there is no need to carry out the trial and error analysis for determination of wave number for R-waves.
3. The method is general, simple, straightforward and applicable to any site. It is free from the need for numerous curves and charts, and the errors associated with reading such charts to determine wave numbers.
4. If transfer functions obtained from averaging the values yielded by various phase velocities are adopted, as suggested by present methods, the transfer functions would be quite unrealistic since earthquake records do not indicate the presence of R-waves of all these phase velocities. To this extent, the predicted seismic response will also be incorrect.
5. For periods greater than 10 s, vertical and horizontal transfer functions are not very sensitive to changes in periods. This is also true for the ratio of vertical response to horizontal response at the ground or base rock level as shown in Section 2.5 and Figures 2.15.5 and 2.15.6. Any value of period in the 10 to 20 s range should be adequate for all engineering purposes.

2.17 DETERMINATION OF R-WAVE CONTRIBUTION TO SEISMIC GROUND RESPONSE

By using the principles of vertical propagation of shear waves, it is possible to obtain the response of the ground at any point in the medium if the response due to the earthquake is known at either ground or base rock level. For the base rock level, let θ be the angle of shear wave propagation with respect to vertical. Let U_r, U_{rr} and U_{rs} be the total response, response due to R-waves and response due to S-waves in the horizontal direction, respectively; and V_r, V_{rr} and V_{rs} those for the response in the vertical direction, all being referred to at base rock level. From the principles of R-wave propagation, it is possible to determine the ratio of the R-wave response in the vertical direction to that in the horizontal direction at the surface (Haskell, 1957; Nair, 1974). Knowing this ratio, and the vertical and horizontal transfer functions, it is possible to define a similar ratio R_r for the base rock level. From earthquake records in the vertical and horizontal direction, it is possible to obtain the ratio of the net vertical response to net horizontal response k at any instant of time. The contribution of R-waves to the seismic response is then defined by the factor F, such that:

$$U_{rr} = F \cdot U_{rs} \tag{2.17.1}$$

From this information, the following relationships are established:

$$T = \tan\theta$$

$$V_{rr} = R_r \cdot U_{rr}$$

$$V_{rs} = T \cdot U_{rs}$$

$$V_r = V_{rr} + V_{rs} = k \cdot U_r$$

$$U_r = U_{rr} + U_{rs}$$

$$\text{or, } k \cdot U_{rr} + k \cdot U_{rs} = R_r \cdot U_{rr} + T \cdot U_{rs}$$

$$\text{or, } F = \frac{T - k}{k + R_r} \qquad (2.17.2)$$

Thus, it is possible to obtain the factor F at any instant of time and to separate the response due to R and s-waves from the bedrock response. From a knowledge of the base rock response due to R-waves only, and the vertical and horizontal transfer functions for the base rock level, the vertical and horizontal responses at the ground surface due to R-waves can be determined for any instant of time. Then the response at any point below the ground surface due to R-waves can be computed. Using the response due to s-waves only at the base rock and the principles of shear wave propagation, the response at any point due to shear waves can be obtained. The net response at any point and instant of time is then obtained by adding the shear and Rayleigh wave responses in that direction.

If the seismic response at the ground surface is available instead of at base rock level, similar relationships can be established for this case. In fact, it is possible to establish such relationships for any point at which the seismic records are available for vertical

and horizontal responses.

When the seismic response records are available in the vertical and two orthogonal horizontal directions, additional assumptions are required to break up the total vertical response into those due to the R and s wave responses for each horizontal direction. Since R_r and T remain the same for either direction due to the assumptions of plane waves, it is logical and reasonable to attribute the vertical response for the two horizontal directions in proportion to the horizontal responses in the respective directions at that instant of time.

From Equation (2.17.2), it is difficult to make an overall assessment of the contribution of R-waves as it depends on the values of T and R_r, whic remain constant with respect to time, and on k, which varies with time. However, it is quite evident from Equation (2.17.2) that the contribution of R-waves increases as the angle of incidence of earthquake increases. This is logical and consistent with observations that R-wave contributions are significant for near sites.

It should also be noted that Equation (2.17.2) is valid when angle θ is zero, or when R-waves are totally absent. If $\theta = 0$ and R-waves are absent, T and k are both equal to zero, thus giving F = 0, which is correct. If $\theta = 0$ but k is not, then naturally all of the vertical response will be due to R-waves, and as such, a non-zero value of F is obtained for this case. There is no need to arbitrarily fix the R-wave contributions for any site as done in the past.

The determination of shear wave angle of incidence with respect to the vertical direction was discussed in Section 2.7. It is possible to get a reasonable estimate of the angle of incidence from the seismic records for the site. In any case, the precision with which the angle θ can be determined is certainly better than the precision with which present methods suggest for fixing the contribution of R-waves to seismic ground motions.

2.18 CONCLUDING REMARKS

It is very important to obtain as precisely as possible the spatial distribution of ground motions since this is the basic input to any aseismic analysis and design.

Present methods do not completely account for the principles of shear wave propagation at the base rock level. To overcome this difficulty, the entire base rock response is assumed to be the upward component response. This assumption leads to conditions not compatible with realistic situations at the base rock level. It also leads to serious errors in the computed spatial distribution of ground motions. A method of accounting for the component responses due to the upward and downward travelling shear waves at the base rock levels was outlined in this Chapter. This new method is in accordance with the principles of shear wave propagation, and which eliminates the errors due to the assumptions cited above.

Even though the mathematical formulation of R-wave propagation

is well developed, present methods are inadequate in determining the appropriate phase velocity and the corresponding wave number for the R-waves. To overcome this difficulty, the entire range of phase velocities for R-waves is covered at regular intervals, and the average of the transfer functions is used in the analysis. Trial and error procedures are used to evalute the wave number for any phase velocity, by using the approximate values of wave numbers from curves suggested by Sezawa, or Oliver and Ewing. However, it is obvious that only a narrow range of phase velocities will enable the R-waves to reach the site along with the s-waves. As such, the proposition of including the entire range of phase velocities is erroneous. Present methods do not suggest a quantitative way to estimate the contribution of R-waves to the seismic ground response. The contribution is usually arbitrarily fixed for nearby and distant sites. Without better estimates of R-wave contributions to seismic ground motions, a very refined inclusion of R-waves loses much of its importance.

A method of fixing the phase velocity of R-waves and corresponding wave number was suggested in this Chapter. The method is based upon the data obtained from numerous earthquake records. This eliminates the need for trial and error estimates of wave number, and also the numerous curves required in present methods. Moreover, a method of estimating the R-wave contribution to seismic ground response was formulated, which is based upon data that can be obtained for any system with reasonable accuracy.

The findings of this Chapter are not only important in giving a more precise estimation of seismic ground motions, but also a better understanding of the shear wave and Rayleigh wave propagation through layered media.

CHAPTER 3

DYNAMIC ANALYSIS OF AXISYMMETRIC INTERACTIVE SYSTEMS

3.1. INTRODUCTION

Until the early 1950's, the dynamic response of structures was generally computed using the seismic coefficient method in which the response at all points of the structure is the same. This assumption of rigid body response is difficult to justify for many engineering structures given their flexibility and important ductility. The lumped parameter idealization of structures was developed to introduce a realistic response, and the resulting ordinary differential equations are solved to obtain the dynamic response of the system. The use of consistent mass matrices in this idealization increases the computational requirements with generally no significant improvement in solution accuracy. On the other hand, lumped mass matrices result in considerable computational savings and generally yield satisfactory results (Clough, 1971; Desai and Abel, 1972; Dibaj and Penzien, 1971; Faddev and Faddeeva, 1963; Nair, 1974).

The dynamic analysis may be carried out by either the modal super position method or by a time-step method. The first method involves the solution of the eigenvalue problem and uncouples the response of the system, so that for each mode the response may be computed independently (Desai and Abel, 1972; Zienkiewicz, 1979). In

the second method the equilibrium equations are numerically integrated at each time station.

The modal analysis is suitable for linear structural behaviour only, and gives the required accuracy, but solution of the eigenvalue problem and transformation of co-ordinates presents major computation efforts. The step-by-step method automatically accounts for all modes and can also incorporate non-linear material behaviour. As such, it is more versatile, and is used throughout this study.

3.2 FINITE ELEMENT METHOD ANALYSIS OF AXISYMMETRIC BODIES

The finite element method analysis of axisymmetric systems was proposed by Clough et al (1965) and Zienkiewicz (1979). It was developed for antisymmetric loadings with one plane of symmetry by Wilson (1965), and for general antisymmetric loadings by Nair (1974). Figure 3.2.1 shows a typical axisymmetric body with ring elements. The material properties and the geometry of the problem do not vary with the θ-coordinate by definition, but the displacement components in the R, θ or Z direction can vary with θ. Some of these patterns are shown in Figure 3.2.2. The method may be summarized as follows:

1. Divide the system in the R-Z plane at the $\theta = 0$ position into a number of quadrilateral, triangular and/or linkage elements to properly represent the system.
2. Evaluate the stiffness matrix for each element, and then generate the global stiffness matrix for the system.

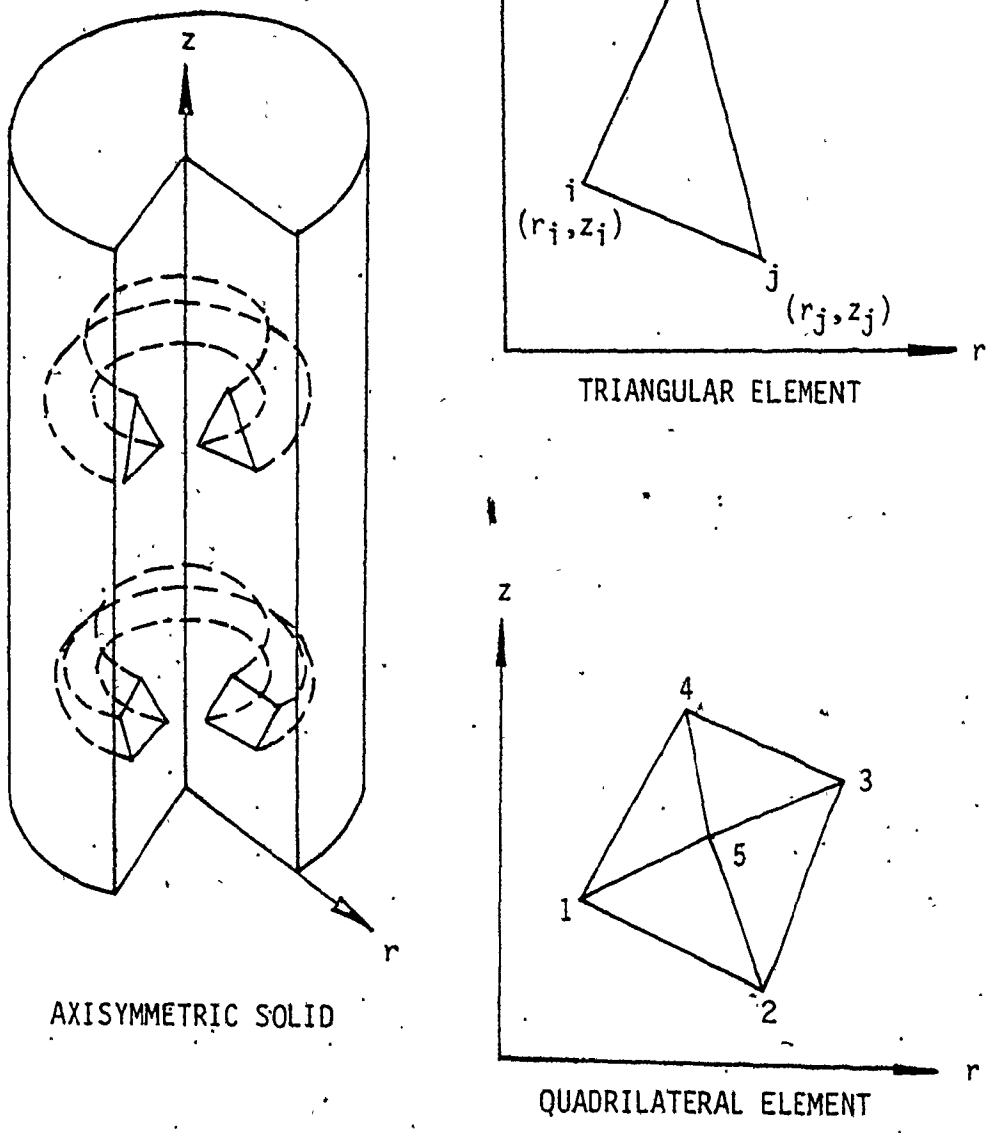

FIGURE 3.2.1 TYPICAL AXISYMMETRIC BODY

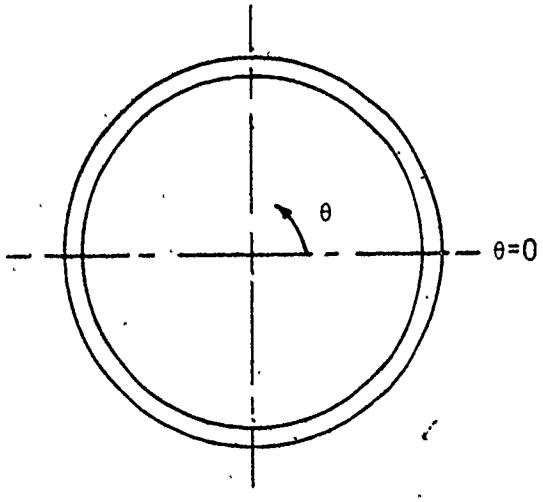

AXISYMMETRIC HARMONIC (n=0)

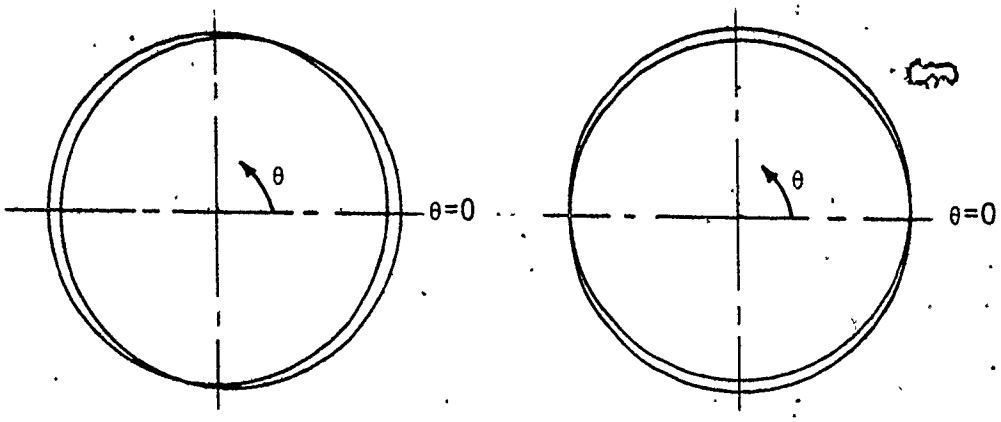

(SYMMETRIC) (ANTISYMMETRIC)

FIRST HARMONIC (n=1)

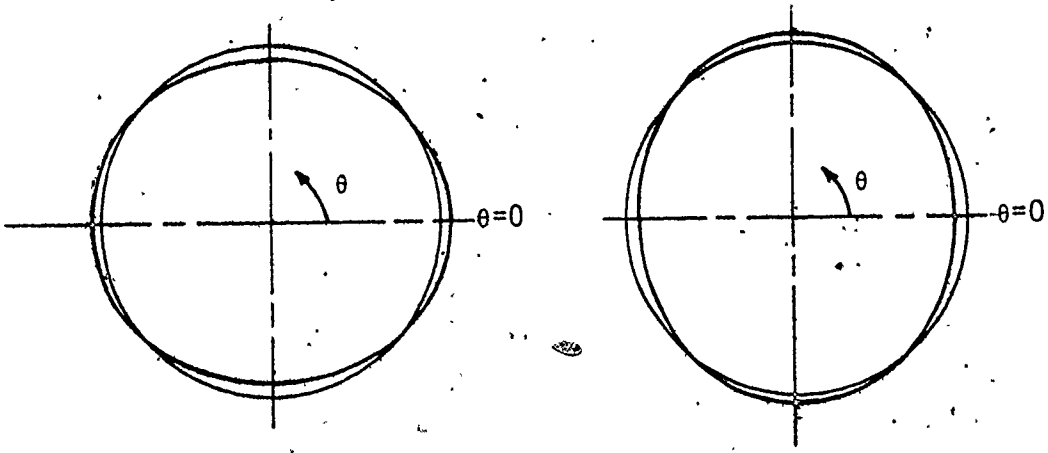

(SYMMETRIC) (ANTISYMMETRIC)

SECOND HARMONIC (n=2)

FIGURE 3.2.2 LOADING IN DIFFERENT HARMONICS

3. Generate the mass matrix for the system.
4. Generate the damping matrix for the system.
5. Solve the resulting equation of motion for the system using a step-by-step approach and obtain the response of the system.
6. Compute stresses and strains from the nodal displacements at the desired time intervals.

3.2.1 STIFFNESS MATRIX FOR THE SYSTEM

If u, v, w are the radial, tangential and axial displacements, they can be expanded into Fourier series as follows (Nair, 1974):

$$\begin{aligned} u &= \sum_{n=0}^{L} u_n \cdot \text{Cos } n\theta + \sum_{m=1}^{L} u_m \cdot \text{Sin } m\theta \\ v &= \sum_{n=1}^{L} v_n \cdot \text{Sin } n\theta + \sum_{m=1}^{L} v_m \cdot \text{Cos } m\theta \\ w &= \sum_{n=0}^{L} w_n \cdot \text{Cos } n\theta + \sum_{m=1}^{L} w_m \cdot \text{Sin } m\theta \end{aligned} \qquad (3.2.1)$$

Similar expressions can be obtained for the forces in these directions. The suffix m or n indicates the m^{th} (for antisymmetric) or n^{th} (for symmetric) harmonic. For each element with a linear displacement field, the relationship between nodal displacements and nine generalized displacement co-ordinates α_{1n} to α_{9n} for the n^{th} (symmetric or antisymmetric) harmonic is given by:

$$\begin{Bmatrix} u_n \\ v_n \\ w_n \end{Bmatrix} = \begin{Bmatrix} \alpha_{1n} + \alpha_{2n} \cdot r + \alpha_{3n} \cdot z \\ \alpha_{4n} + \alpha_{5n} \cdot r + \alpha_{6n} \cdot z \\ \alpha_{7n} + \alpha_{8n} \cdot r + \alpha_{9n} \cdot z \end{Bmatrix} = \begin{bmatrix} \alpha_{1n} & \alpha_{2n} & \alpha_{3n} \\ \alpha_{4n} & \alpha_{5n} & \alpha_{6n} \\ \alpha_{7n} & \alpha_{8n} & \alpha_{9n} \end{bmatrix} \begin{Bmatrix} 1 \\ r \\ z \end{Bmatrix} \qquad (3.2.2)$$

By substituting the nine components of nodal response (three for each node of the triangular element) and the co-ordinates of the nodes, the nine α values can be obtained:

$$\{\alpha\} = [C^{-1}] \cdot \{u_n\} \qquad (3.2.3)$$

where $\{u_n\}$ is the vector of nodal responses and $[C^{-1}]$ is a matrix expressed in terms of nodal co-ordinates of the element, and is given by Equation (3.2.4). Strains are obtained by differentiation of Equation (3.2.3):

$$\begin{aligned} \varepsilon_{rr} &= \frac{\partial u}{\partial r} \\ \varepsilon_{\theta\theta} &= \frac{1}{r}\left(u + \frac{\partial v}{\partial \theta}\right) \\ \varepsilon_{zz} &= \frac{\partial w}{\partial z} \\ \gamma_{rz} &= \frac{\partial u}{\partial z} + \frac{\partial w}{\partial r} \\ \gamma_{r\theta} &= \frac{1}{r}\frac{\partial u}{\partial \theta} + \frac{\partial v}{\partial r} - \frac{v}{r} \\ \gamma_{z\theta} &= \frac{\partial v}{\partial z} + \frac{1}{r} \cdot \frac{\partial w}{\partial \theta} \end{aligned} \qquad (3.2.5)$$

$$\text{or,} \quad \{\varepsilon\} = [B]\{\alpha\} = [B][C^{-1}]\{u_n\} \qquad (3.2.6)$$

where $\{\varepsilon\}$ is the strain matrix, and the [B] matrix is given by Equation (3.2.7). The stresses and strains are related by the constitutive

$$[C]^{-1} = \frac{1}{A}$$

$r_j z_k - r_k z_j$	0	0	$r_k z_i - r_i z_k$	0	0	$r_i z_j - r_j z_i$	0	0
$z_j - z_k$	0	0	$z_k - z_i$	0	0	$z_i - z_j$	0	0
$r_k - r_j$	0	0	$r_i - r_k$	0	0	$r_j - r_i$	0	0
0	$r_j z_k - r_k z_j$	0	0	$r_k z_i - r_i z_k$	0	0	$r_i z_j - r_j z_i$	0
0	$z_j - z_k$	0	0	$z_k - z_i$	0	0	$z_i - z_j$	0
0	$r_k - r_j$	0	0	$r_i - r_k$	0	0	$r_j - r_i$	0
0		$r_j z_k - r_k z_j$	0	0	$r_k z_i - r_i z_k$	0	0	$r_i z_j - r_j z_i$
0		$z_j - z_k$	0	0	$z_k - z_i$	0	0	$z_i - z_j$
0		$r_k - r_j$	0	0	$r_i - r_k$	0	0	$r_j - r_i$

where (3.2.4)

$$2A = \left[r_i(z_j - z_k) + r_j(z_k - z_i) + r_k(z_i - z_j)\right]$$

$$[B] = \begin{bmatrix} 0 & 1 & 0 & 0 & 0 & 0 & 0 & 0 & 0 \\ \frac{1}{r} & 1 & \frac{z}{r} & \frac{n}{r} & n & n\frac{z}{r} & 0 & 0 & 0 \\ 0 & 0 & 0 & 0 & 0 & 0 & 0 & 0 & 1 \\ 0 & 0 & 1 & 0 & 0 & 0 & 0 & 1 & 0 \\ -\frac{n}{r} & -n & -n\frac{z}{r} & -\frac{1}{r} & 0 & -\frac{z}{r} & 0 & 0 & 0 \\ 0 & 0 & 0 & 0 & 0 & 1 & -\frac{n}{r} & -n & -n\frac{z}{r} \end{bmatrix} \qquad (3.2.7)$$

where

r and z are the coordinates

n is the harmonic

For antisymmetric harmonic, terms involving "n" change their sign.

$$[D] = \frac{\nu E}{(1+\nu)(1-2\nu)} \quad \text{(isotropic)}$$

$$\begin{bmatrix} \frac{1-\nu}{\nu} & 1 & 1 & 0 & 0 & 0 \\ 1 & \frac{1-\nu}{\nu} & 1 & 0 & 0 & 0 \\ 1 & 1 & \frac{1-\nu}{\nu} & 0 & 0 & 0 \\ 0 & 0 & 0 & \frac{1-2\nu}{2\nu} & 0 & 0 \\ 0 & 0 & 0 & 0 & \frac{1-2\nu}{2\nu} & 0 \\ 0 & 0 & 0 & 0 & 0 & \frac{1-2\nu}{2\nu} \end{bmatrix} \qquad (3.2.8)$$

matrix $[D]$:

$$\{\sigma\} = [D]\{\varepsilon\}$$

where $[D]$ is given by equation (3.2.8).

The work done by nodal forces is:

$$W = \frac{1}{2} \cdot \{u_n\}^T\{F_n\} \tag{3.2.10}$$

The strain energy stand in the element is:

$$U = \frac{1}{2} \cdot \int_{vol} \{\varepsilon\}^T\{\sigma\} \cdot d_{vol} \tag{3.2.11}$$

From the principle of minimum potential energy, these two quantities are equal, i.e.

$$\{u_n\}^T\{F_N\} = \int_{vol} \{\varepsilon\}^T\{\sigma\} \cdot d_{vol} \tag{3.2.12}$$

or

$$\{F_N\} = [k]_N \cdot \{u_N\} \tag{3.2.13}$$

where $[k]_N$ is the element stiffness matrix given by:

$$[k]_N = [C^{-1}]^T\left(\int_{vol} [B]^T[D][B] \cdot d_{vol}\right) \cdot [C^{-1}] \tag{3.2.14}$$

It should be noted that the element stiffness matrix is different for each harmonic and for symmetric and antisymmetric components of each harmonic. Equation (3.2.15) gives the $[B]^T[D][B]$ matrix.

The strains for different harmonics (symmetric and antisymmetric components) are given by:

$$X =$$

$\frac{m_1+m_2n^2}{r^2}$	$(\frac{1}{\nu}+m_2n^2)\frac{1}{r}$	$(m_1+m_2n^2)\frac{z}{r^2}$	$\frac{(m_1+m_2)n}{r^2}$	$\frac{m_1 n}{r}$	$(m_1+m_2)\frac{nz}{r^2}$	0	0	$\frac{1}{r}$
	$\frac{2}{\nu}+m_2n^2$	$(\frac{1}{\nu}+m_2n^2)\frac{r}{z}$	$(\frac{n}{\nu}+m_2n)\frac{1}{r}$	$\frac{n}{\nu}$	$(\frac{n}{\nu}+m_2n)\frac{z}{r}$	0	0	2
		$m_2+(m_1+m_2n^2)\frac{z^2}{r^2}$	$(m_1+m_2)\frac{nz}{r^2}$	$\frac{m_1 nz}{r}$	$(m_1+m_2)\frac{nz^2}{r^2}$	0	m_2	$\frac{z}{r}$
			$\frac{m_1n^2+m_2}{r^2}$	$\frac{m_1n^2}{r}$	$(m_1n^2+m_2)\frac{z}{r^2}$	0	0	$\frac{n}{r}$
				m_1n^2	$m_1n^2\frac{z}{r}$	0	0	n
					$m_2+(m_1n^2+m_2)\frac{z^2}{r^2}$	$\frac{-m_2n}{r}$	$-m_2n$	$(1-m_2)\frac{nz}{r}$
	(S Y M M E T R I C)					$\frac{m_2n^2}{r^2}$	$\frac{m_2n^2}{r}$	$\frac{m_2n^2z}{r^2}$
For antisymmetric harmonic, terms with first power of n change their sign.							$m_2(1+n^2)$	$\frac{m_2n^2z}{r}$
								$m_1+\frac{m_2n^2z^2}{r^2}$

where $m_1 = \frac{1}{\nu} - 1, \quad m_2 = \frac{1-2\nu}{2\nu}$

$$[B]^T[D][B] = X\nu E/(1+\nu)(1-2\nu) \qquad (3.2.15)$$

$$
\begin{aligned}
\varepsilon_{rr} &= \sum_{n=0}^{L} \varepsilon_{rrn} \cdot \text{Cos } n\theta + \sum_{m=1}^{L} \varepsilon_{rrm} \cdot \text{Sin } m\theta \\
\varepsilon_{\theta\theta} &= \sum_{n=0}^{L} \varepsilon_{\theta\theta n} \cdot \text{Cos } n\theta + \sum_{m=1}^{L} \varepsilon_{\theta\theta m} \cdot \text{Sin } m\theta \\
\varepsilon_{zz} &= \sum_{n=0}^{L} \varepsilon_{zzn} \cdot \text{Cos } n\theta + \sum_{m=1}^{L} \varepsilon_{zzm} \cdot \text{Sin } m\theta \\
\gamma_{rz} &= \sum_{n=0}^{L} \gamma_{rzn} \cdot \text{Cos } n\theta + \sum_{m=1}^{L} \gamma_{rzm} \cdot \text{Sin } m\theta \\
\gamma_{r\theta} &= \sum_{n=1}^{L} \gamma_{r\theta n} \cdot \text{Sin } n\theta + \sum_{m=1}^{L} \gamma_{r\theta m} \cdot \text{Cos } m\theta \\
\gamma_{z\theta} &= \sum_{n=1}^{L} \gamma_{z\theta n} \cdot \text{Sin } n\theta + \sum_{m=1}^{L} \gamma_{z\theta m} \cdot \text{Cos } m\theta
\end{aligned}
\tag{3.2.16}
$$

The formulation of element stiffness matrices involves volume integrals λ_1 to λ_{11}. One point integration about the centroid of these triangular elements often gives reliable estimates of these integrals, especially if the difference between radii of any two nodes is small compared to the radii of the nodes. This simplification does not jeopardize the accuracy of the solution and further, it has been reported (Zienkiewicz, 1979) that often these simplified forms are superior to the exact solutions where large radial distances are involved. The values of λ_1, λ_2, and λ_3 are identical by the two methods, those of λ_4, λ_5 and λ_6 are altered insignificantly. The exact and simplified axisymmetric integrals from Nair (1974) are given in Appendix B.

3.2.2 ASSEMBLING THE STIFFNESS MATRIX FOR REDUCED STORAGE AND EFFICIENT SOLUTION

Present methods suggest that to economize the storage requirement, the nodes of the finite element mesh be numbered in such a way that the difference between any pair of inter-connected displacement freedoms is minimized. If each column of the stiffness matrix contains elements defined by the largest half band width, then the storage is minimized by minimizing this largest half band width for the system. The storage requirement can be further reduced by storing elements in the individual band width for each column by adopting the methods of storage suggested for sparse banded symmetric matrices.

For systems subjected to known boundary displacements and no external forces (other than inertia forces), only those equations which involve unknown (interior) displacements need be solved. Thus, the stiffness matrix can be partitioned into components due to interior and boundary displacement degrees of freedom:

$$[k] = \left[\begin{array}{c|c} k_{11} & k_{12} \\ \hline k_{21} & k_{22} \end{array}\right] \tag{3.2.17}$$

where $[k_{11}]$ is entirely defined for interior displacement freedoms and $[k_{22}]$ is defined for only boundary displacement freedoms. Only $[k_{11}]$ and $[k_{12}]$ need to be stored to solve the problem if the interior and boundary nodes are numbered separately. Separate numbering and partitioning of the stiffness matrix significantly decreases computer storage requirements which is an important feature at both the research

and engineering applications level with available computers.

3.3 PROPOSED METHOD FOR MINIMIZING STORAGE REQUIREMENTS

In addition to numbering the interior nodes in one sequence followed by the boundary nodes, so that the [k] matrix can be partitioned, minimization of the band widths for interior degrees of freedom reduces the band widths for the $[k_{11}]$ matrix. Further, if the displacements, stresses and strains of the central node of any quadrilateral element are not required, then these central nodes can be numbered in one sequence after the boundary nodes. This ensures that the central nodes do not contribute to any increase in band width.

3.4 BOUNDARY ACCELERATIONS OF SYSTEM

Figure 3.2.1 shows the details of a typical ring element for an axisymmetric system. The most general nonsymmetric accelerations along the nodal ring may be expanded in a Fourier series form:

$$\begin{aligned}
\ddot{u}(t) &= \sum_{n=0}^{L} \ddot{u}_n(t) \text{ Cos } n\theta + \sum_{m=1}^{L} \ddot{u}_m(t) \text{ Sin } m\theta \\
\ddot{v}(t) &= \sum_{n=1}^{L} \ddot{v}_n(t) \text{ Sin } n\theta + \sum_{m=1}^{L} \ddot{v}_m(t) \text{ Cos } m\theta \qquad (3.4.1) \\
\ddot{w}(t) &= \sum_{n=0}^{L} \ddot{w}_n(t) \text{ Cos } n\theta + \sum_{m=1}^{L} \ddot{w}_m(t) \text{ Sin } m\theta
\end{aligned}$$

where u, v, w are radial, longitudinal and axial displacements, $u_n(t)$, $v_n(t)$, $w_n(t)$ are the respective quantities for n^{th} harmonic and $u_m(t)$,

$v_m(t)$, $w_m(t)$ are those for m^{th} harmonic. The first summation term is for the symmetric components of the response (symmetric about the $\theta=0$ axis), and the second summation term is for the antisymmetric components of the response. The coefficients $\ddot{u}_n(t)$, $\ddot{u}_m(t)$, etc. may be evaluated by integrating Equation (3.4.1) for the nodal ring under consideration:

$$\ddot{u}_0(t) = \frac{1}{2\pi}\int_{-\pi}^{+\pi} \ddot{u}(t)\cdot d\theta$$

$$\ddot{u}_n(t) = \frac{1}{\pi}\int_{-\pi}^{+\pi} \ddot{u}(t)\cdot \text{Cos } n\theta \cdot d\theta$$

$$\ddot{u}_m(t) = \frac{1}{\pi}\int_{-\pi}^{+\pi} \ddot{u}(t)\cdot \text{Sin } m\theta \cdot d\theta$$

$$\ddot{v}_n(t) = \frac{1}{\pi}\int_{-\pi}^{+\pi} \ddot{v}(t)\cdot \text{Sin } n\theta \cdot d\theta \qquad (3.4.2)$$

$$\ddot{v}_m(t) = \frac{1}{\pi}\int_{-\pi}^{+\pi} \ddot{v}(t)\cdot \text{Cos } m\theta \cdot d\theta$$

$$\ddot{w}_0(t) = \frac{1}{2\pi}\int_{-\pi}^{+\pi} \ddot{w}(t)\cdot d\theta$$

$$\ddot{w}_n(t) = \frac{1}{\pi}\int_{-\pi}^{+\pi} \ddot{w}(t)\cdot \text{Cos } n\theta \cdot d\theta$$

$$\ddot{w}_m(t) = \frac{1}{\pi}\int_{-\pi}^{+\pi} \ddot{w}(t)\cdot \text{Sin } m\theta \cdot d\theta$$

Since it is difficult to develop a general expression for $\ddot{u}(t)$, $\ddot{v}(t)$, $\ddot{w}(t)$ along the ring, the response is computed at regular angular intervals along the ring (say 8 or 12 values depending on required accuracy), and an average value based on the numerical integration over 360 degrees is adopted in the analysis. If the response is computed at 30 degree intervals along the nodal ring, then the component responses in various harmonics by numerical integration are:

$$\ddot{u}_0(t) = \frac{1}{12} \sum_{i=1}^{12} \ddot{u}_i(t)$$

$$\ddot{u}_n(t) = \frac{1}{n\pi} \sum_{i=1}^{12} \ddot{u}_i(t)\{\text{Sin}(30in-15n) - \text{Sin}(30in-45n)\}$$

$$\ddot{u}_m(t) = \frac{1}{m\pi} \sum_{i=1}^{12} \ddot{u}_i(t)\{\text{Cos}(30im-45m) - \text{Cos}(30im-15m)\}$$

$$\ddot{v}_n(t) = \frac{1}{n\pi} \sum_{i=1}^{12} \ddot{v}_i(t)\{\text{Cos}(30in-45n) - \text{Cos}(30in-15n)\}$$

$$\ddot{v}_m(t) = \frac{1}{m\pi} \sum_{i=1}^{12} \ddot{v}_i(t)\{\text{Sin}(30im-15m) - \text{Sin}(30im-45m)\}$$

$$\ddot{w}_0(t) = \frac{1}{12} \sum_{i=1}^{12} \ddot{w}_i(t)$$

$$\ddot{w}_n(t) = \frac{1}{n\pi} \sum_{n=1}^{12} \ddot{w}_i(t)\{\text{Sin}(30in-15n) - \text{Sin}(30in-45n)\} \quad (3.4.3)$$

$$\ddot{w}_m(t) = \frac{1}{m\pi} \sum_{m=1}^{12} \ddot{w}_i(t)\{\text{Cos}(30im-45m) - \text{Cos}(30im-15m)\}$$

Although an infinite number of harmonics exist, only the first few make a significant contribution to the computed response. Nair

(1974) found that the axisymmetric harmonic, the symmetric and antisymmetric components due to the first harmonic, and the symmetric component due to the second harmonic, were adequate to get results accurate enough for engineering purposes. This was adopted for parametric studies. For more detailed analyses, the symmetric component of the second harmonic and the antisymmetric component of the third harmonic were also considered.

3.5 STEP-BY-STEP METHOD OF DYNAMIC ANALYSIS

The step-by-step method of dynamic analysis was first developed by Wilson and Clough (1962). From the known values of displacement, velocity and acceleration at any time $(t-\Delta t)$, it is possible to compute those at time t, where Δt is a small increment in time during which the acceleration may be assumed to vary linearly. The mid-acceleration method proposed by Penzien (1960) may also be used in a similar way. The equations of motion for an interactive system with viscous damping are:

$$[M]\{\ddot{u}\}^t + [C]\{\dot{u}\}^t + [K]\{u\}^t = \{f\}^t \qquad (3.5.1)$$

where $\{f\}^t$ is the vector of external forces acting on the system, $\{u\}^t$, $\{\dot{u}\}^t$, $\{\ddot{u}\}^t$ are displacement, velocity and acceleration vectors, and $[M]$, $[C]$ and $[K]$ are the mass, damping and stiffness matrices of the system. Equation (3.5.1) can be solved by assuming some form of acceleration variations in the time interval Δt. If a linear acceleration variation is assumed, the expressions for velocity and displacement are:

$$\{\dot{u}\}^t = \{\dot{u}\}^{t-\Delta t} + \frac{\Delta t}{2} \cdot \{\ddot{u}\}^{t-\Delta t} + \frac{\Delta t}{2} \cdot \{\ddot{u}\}^t \qquad (3.5.2)$$

$$\{u\}^t = \{u\}^{t-\Delta t} + \Delta t \cdot \{\dot{u}\}^{t-\Delta t} + \frac{\Delta t^2}{3} \cdot \{\ddot{u}\}^{t-\Delta t} + \frac{\Delta T^2}{6} \cdot \{\ddot{u}\}^t \tag{3.5.3}$$

Substituting Equations (3.5.2) and (3.5.3) in Equation (3.5.1), the acceleration vector at time t is:

$$\{\ddot{u}\}^t = [F](\{f\}^t - [C]\{a\} - [K] \cdot \{b\}) \tag{3.5.4}$$

where $$[F] = ([M] + \frac{\Delta t}{2}[C] + \frac{\Delta t}{6}[K])^{-1} \tag{3.5.5}$$

$$\{a\} = \{\dot{u}\}^{t-\Delta t} + \frac{\Delta t}{2}\{\ddot{u}\}^{t-\Delta t} \tag{3.5.6}$$

and $$\{b\} = \{u\}^{t-\Delta t} + \Delta t\{\dot{u}\}^{t-\Delta t} + \frac{\Delta t^2}{3}\{\ddot{u}\}^{t-\Delta t} \tag{3.5.7}$$

From this, the velocity and displacement vectors are:

$$\{\dot{u}\}^t = \{a\} + \frac{\Delta t}{2}\{\ddot{u}\}^t \tag{3.5.8}$$

$$\{u\}^t = \{b\} + \frac{\Delta t^2}{6}\{\ddot{u}\}^t \tag{3.5.9}$$

Through repeated use of Equations (3.5.4) through (3.5.9), the response of the system is found at all time stations.

The standard way to incorporate damping is to assume proportional damping in which the damping matrix is expressed as a linear combination of the mass and stiffness matrices:

$$[C] = \alpha[M] + \beta[K] \tag{3.5.10}$$

where α and β are constants with units of sec^{-1} and sec. Substituting Equation (3.5.10) into Equation (3.5.5) yields:

$$[F] = \left\{(1 + \alpha \cdot \frac{\Delta t}{2})[M] + (\beta \cdot \frac{\Delta t}{2} + \frac{\Delta t^2}{6} \cdot [K]\right\}^{-1} \qquad (3.5.11)$$

The time interval Δt is selected in terms of the dynamic characteristics of the structure. One percent of the smallest significant period is often adopted to ensure numerical stability. If the smallest significant period is not known (i.e. eigen value not solved), a number of trial values may be used and the largest value that gives stable results can be adopted.

In the case of earthquake response problems, the load vector $\{f\}^t$ is due to inertia forces given by:

$$\{f\}^t = -[M]\{\ddot{u}\}^t \qquad (3.5.12)$$

where $\{\ddot{u}\}^t$ are the absolute earthquake accelerations.

Equation (3.5.12) is ideally suited for situations where the spatial distribution of ground motions is available. For small rigid structures where the response at all points can be assumed to be the same at a given time, the forcing vector is:

$$\begin{aligned}\{f\}^t = &- \{\ddot{u}\}_1^t [m_1\ 0\ 0\ \ m_2\ 0\ 0\ \ m_3\ 0\ 0\ \ ---\ \ m_n\ 0\ 0]^T \\ &- \{\ddot{u}\}_2^t [0\ m_1\ 0\ \ 0\ m_2\ 0\ \ 0\ m_3\ 0\ \ ---\ \ 0\ m_n\ 0]^T \\ &- \{\ddot{u}\}_3^t [0\ 0\ m_1\ \ 0\ 0\ m_2\ \ 0\ 0\ m_3\ \ ---\ \ 0\ 0\ m_n]^T\end{aligned} \qquad (3.5.13)$$

where n is the number of degrees of freedoms, and subscripts 1, 2, and 3 stand for two orthogonal horizontal directions and the vertical

direction for the acceleration vectors.

Details for the mid-acceleration method are also available (Nair, 1974; Penzien, 1960). Both methods are quite suitable for any general axisymmetric problem. The mid-acceleration method is deemed to give more accurate results because it uses accelerations at mid-intervals. Another important advantage of this method is that it eliminates the need for storage of the [F] matrix of Equation (3.5.5) for the step-by-step method, which is crucial for large problems. However, it can involve serious numerical problems when dealing with large systems with materials of appreciably different elastic moduli (Nair, 1974). For this reason, the step-by-step method was adopted in this study.

3.6 CURRENT METHODS FOR SOLVING THE EQUATIONS OF MOTION FOR A SYSTEM WITH KNOWN BOUNDARY RESPONSE

The technique for solving the equation of motion under consideration was first proposed by Clough (1971). The equation of motion for the system can be expressed as:

$$[M]\{\ddot{u}^t\} + [C]\{\dot{u}^t\} + [K]\{u^t\} = \{0\} \qquad (3.6.1)$$

where $\{\ddot{u}^t\}$, $\{\dot{u}^t\}$, and $\{u^t\}$ are the absolute acceleration velocity and displacement vectors, and the superscript t denotes the total value of the quantity being referred to, and not time. The time station notation is not included for simplicity, because it remains the same for all the response components. Each of these response vectors can be partitioned into those for the interior displacements $\{\ddot{u}_I^t\}$, $\{\dot{u}_I^t\}$ and $\{u_I^t\}$

and those for boundary displacements $\{\ddot{u}_B^t\}$, $\{\dot{u}_B^t\}$ and $\{u_B^t\}$ which are known. The interior response can be considered to be made up of the pseudo static response $\{\ddot{u}_I^s\}$, $\{\dot{u}_I^s\}$, $\{u_I^s\}$ and the dynamic response $\{\ddot{u}_I^d\}$, $\{\dot{u}_I^d\}$, $\{u_I^d\}$. Thus:

$$\{u_I^t\} = \{u_I^s\} + \{u_I^d\} \tag{3.6.2}$$

The pseudo static response is defined as that set of responses which will keep the system in static equalibrium under the imposed known boundary dynamic response, i.e.:

$$[k_{11} \quad k_{12}] \begin{Bmatrix} u_I^s \\ \hline u_B^t \end{Bmatrix} = 0 \tag{3.6.3}$$

or, $$[k_{11}]\{u_I^s\} + [k_{12}]\{u_B^t\} = 0$$

or, $$[k_{11}]\{u_I^s\} = -[k_{12}]\{u_B^t\}$$

or, $$\{u_I^s\} = -[k_{11}]^{-1}[k_{12}]\{u_B^t\} = [H]\{u_B^t\} \tag{3.6.4}$$

or, $$[H] = -[k_{11}]^{-1}[k_{12}] \tag{3.6.5}$$

or, $$([k_{11}][H] + [k_{12}])\{u_B^t\} = \{0\} \tag{3.6.6}$$

Equation (3.6.1) can be rewritten in the partitioned form:

$$\begin{bmatrix} m_{11} & m_{12} \\ \hline m_{21} & m_{22} \end{bmatrix} \begin{Bmatrix} \ddot{u}_I^t \\ \hline \ddot{u}_B^t \end{Bmatrix} + \begin{bmatrix} c_{11} & c_{12} \\ \hline c_{21} & c_{22} \end{bmatrix} \begin{Bmatrix} \dot{u}_I^t \\ \hline \dot{u}_B^t \end{Bmatrix} + \begin{bmatrix} k_{11} & k_{12} \\ \hline k_{21} & k_{22} \end{bmatrix} \begin{Bmatrix} u_I^t \\ \hline u_B^t \end{Bmatrix} = \begin{Bmatrix} 0 \\ \hline 0 \end{Bmatrix} \tag{3.6.7}$$

Since the boundary response is already known, it is only necessary to solve the equations above the horizontal partition line, i.e.:

$$[m_{11}]\{\ddot{u}_I^t\} + [c_{11}]\{\dot{u}_I^t\} + [k_{11}]\{u_I^t\} + [m_{12}]\{\ddot{u}_B^t\} + [c_{12}]\{\dot{u}_B^t\} + [k_{12}]\{u_B^t\} = \{0\} \tag{3.6.8}$$

i.e.
$$[m_{11}]\{\ddot{u}_I^d\} + [c_{11}]\{\dot{u}_I^d\} + [k_{11}]\{u_I^d\}$$
$$= -[m_{12}]\{\ddot{u}_B^t\} - [m_{11}]\{\ddot{u}_I^s\} - [c_{12}]\{\dot{u}_B^t\} - [c_{11}]\{\dot{u}_I^s\} - [k_{12}]\{u_B^t\} - [k_{11}]\{u_I^s\} \tag{3.6.9}$$

$$= -[m_{11}]\{\ddot{u}_I^s\} - \beta[k_{12}]\{\dot{u}_B^t\} - \alpha[m_{11}]\{\dot{u}_I^s\} - \beta[k_{11}]\{\dot{u}_I^s\} - [k_{11}]\{u_I^s\} - [k_{12}]\{u_B^t\} \tag{3.6.10}$$

$$= -[m_{11}][H]\{\ddot{u}_B^t\} - \alpha[m_{11}][H]\{\dot{u}_B^t\} \tag{3.6.11}$$

The damping terms, in Equation (3.6.11) are insignificant compared to the inertia terms, i.e.:

$$[m_{11}]\{\ddot{u}_I^d\} + [c_{11}]\{\dot{u}_I^d\} + [k_{11}]\{u_I^d\} = -[m_{11}][H]\{\ddot{u}_B^t\} \tag{3.6.12}$$

Equation (3.6.12) is similar in form to Equation (3.6.1) and hence, can be solved for $\{\ddot{u}_I^d\}$. Knowing the dynamic response $\{\ddot{u}_I^d\}$, $\{\dot{u}_I^d\}$ and $\{u_I^d\}$, the net response at any node for any time instant is computed as the sum of the pseudo static and dynamic responses.

3.7 PROPOSED METHOD FOR SOLVING THE EQUATIONS OF MOTION FOR KNOWN BOUNDARY RESPONSE

As discussed in the previous section, since the boundary response is known it is sufficient to solve the equations above the horizontal partition line of Equation (3.6.7). These equations are:

$$[m_{11}]\{\ddot{u}_I^t\} + [c_{11}]\{\dot{u}_I^t\} + [k_{11}]\{u_I^t\} = -[m_{12}]\{\ddot{u}_B^t\} - [c_{12}]\{\dot{u}_B^t\} - [k_{12}]\{u_B^t\} \tag{3.7.1}$$

All terms on the right side of Equation (3.7.1) are known for any instant of time, and are thus similar in form to Equation (3.5.1) which can be solved. This method of course does not give the pseudo static response. However, since this response is not used separately in computing the stresses and strains, it is not always of interest to compute the pseudo static response. There are many advantages of this approach over current methods. The $[k_{12}]$ matrix required is much smaller in size compared to the $[k_{11}]^{-1}[k_{12}]$ matrix required in the method proposed by Clough. It also leads to a considerable savings in computational effort. As shown in the previous section, some of the damping terms of Equation (3.6.11) were neglected since they are not too significant and also because they result in a considerable increase in storage requirements. However, this contribution of damping can be considered in the proposed method with only a marginal increase in storage.

Since the equations of motion are the same for both methods and only the technique of solution is different, the solutions by the two

methods should be identical. A trial problem was solved by these two methods and the results obtained were identical up to six digits.

The finite element mesh idealization of the axisymmetric trial problem is shown in Figure 3.7.1; other details as follows:

Axial length of the system	= 19.5 m (64 ft)
Radial distance for the assumed free field motion boundary	= 24.38 m (80 ft)
Outer radius of the tunnel	= 6.1 m (20 ft)
Thickness of concrete liner	= 0.254 m (10 in)
Number of nodes	= 68
Number of interior nodes	= 55
Number of boundary nodes	= 13
Number of degrees of freedom	= 204
Number of degrees of freedom for interior nodes	= 165
Number of degrees of freedom for boundary nodes	= 39
Half band width of stiffness matrix	
by conventional method	= 51
by proposed method	= 45
Young's Modulus of medium	= 8.04 MPa (168000 psf)
Young's Modulus of concrete	= 20684 MPa (432×10^6 psf)
Number of time stations considered	= 61

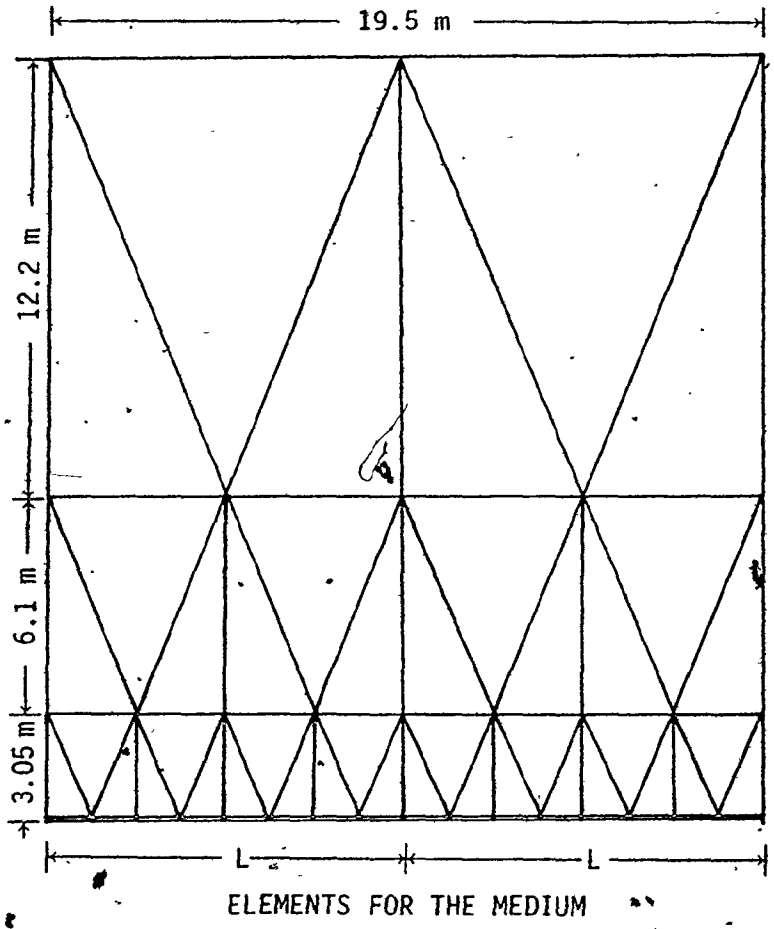

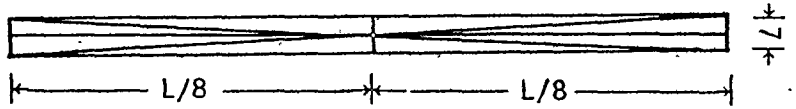

FIGURE 3.7.1 FINITE ELEMENT MESH FOR TUNNEL-SOIL SYSTEM

The stiffness matrix was assembled by the proposed method using the individual band width for each degree of freedom. The dynamic analysis was then completed by:

Method 1. Method proposed by Clough (1971)

Method 2. Method outlined in this chapter.

The size of matrices $[k]$, $[k_{11}]$, $[F]$, $[k_{12}]$ for these two methods, and also for a third method using typical half band width type storage, are given in Table 3.7.1. The table also gives the time of execution for the first two methods and estimated time of execution for the third method. It is clear from these figures that the use of individual band widths results in a considerable saving in storage requirements and time of execution. The use of the proposed method results in a further substantial reduction in both these requirements, and simplifies programming considerably. This is very important for economical analyses of large problems using relatively small computers.

3.8 COMMENTS ON PROPOSED METHOD

In the previous discussion, it was assumed that the response of boundary nodes is known at each time station. If there are time dependent external forces acting at some of the boundary nodes, then the stiffness matrix terms corresponding to the displacement freedoms of these nodes also have to be saved for the analysis. If all of the boundary nodes have such forces, the size of the stiffness matrix by the proposed method will be only marginally smaller than that by the

TABLE 3.7.1

SIZE OF MATRICES AND TIME OF EXECUTION FOR THE TRIAL PROBLEM

ITEM	METHOD 1	METHOD 2	METHOD 3	PERCENTAGE SAVINGS OF (3) WITH RESPECT TO (2)	PERCENTAGE SAVINGS OF (3) WITH RESPECT TO (4)
(1)	(2)	(3)	(4)	(5)	(6)
Half Bandwidth	45	45	51	-	13
$[K_{11}]$ matrix	2,733	2,733	10,404	-	280
[F] matrix	3,777	3,777	10,404	-	175
$[K_{11}]^{-1}[K_{12}]$ matrix	6,435	-	7,956	936	7,856
$[K_{12}]$ matrix	-	621	-		
Total size of the program	24,576	19,570	44,544	26	128
Compilation time	6.33 sec	1.16 sec	-	-	-
Execution time	94.96 sec	57.08 sec	273 sec (estimated)	66.36	378.27

conventional method. But even for this case the size of the $[k_{12}]$ matrix required in the proposed method is considerably smaller than the $[k_{11}]^{-1}[k_{12}]$ matrix required for the method proposed by Clough (1971), and naturally there is a corresponding saving in computational effort.

CHAPTER 4

CONTINUITY OF THE SYSTEM IN AXIAL DIRECTION

4.1 INTRODUCTION

The axial length of buried structures can vary considerably. The entire structure may be included in the analysis if the length is short. However, for structures of considerable length, a dynamic analysis for the entire structure is impracticable. For this case, an analysis for a typical section of the structure is the next best choice, and often adequate for design purposes. However, this does necessitate consideration of system continuity in the axial direction.

The assumption of free field motions at a certain radial distance from the structure (established by trial and error procedures) can be justified. For the transverse end sections, free field motions at these positions do not hold true due to structure-medium interaction. For carrying out the dynamic analysis in the time domain, it is necessary to know the response at these transverse end sections at each time station. As such, this is an indeterminate problem.

In the conventional approach, this limitation is overcome by including additional elements at the ends so that any errors introduced are not significant at the region of interest. This is a reasonable approach if the size of the problem is small. However, the multiple

layers of elements to represent the liner and length of structure makes the size of problem much too large to afford such a proposition. There are some methods available for considering the continuity of the system in the radial direction (Lysmer, J. and Kuhlmeyer, R.L. 1969; Kuhlmeyer, R.L. and Lysmer, J., 1969; Kausel, E. et al, 1975). They are all for dynamic analyses in the frequency domain, and cannot account for continuity in the axial direction.

In this chapter a method for considering the continuity of the system in the axial direction for a time domain dynamic analysis is formulated.

4.2 DETAILS OF THE INTERACTIVE SYSTEM CONSIDERED

For the case of vertical shear wave propagation, the response of all points in a given horizontal plane remains the same. This case is most suitable for evaluating possible methods of handling the end response. A sinusoidal acceleration of 2Hz and maximum amplitude of ± 0.305 m/s^2 was used as the base excitation in the axial and transverse directions. The system is similar to the one shown in Figure 1.7.1 with outside diameter, liner thickness and axial tunnel length of 6 m, 0.254 m and 120 m (195 m for the case discussed in section 4.4), respectively. The axis of symmetry is at a distance of 24.4 m from base rock, and the free field response was assumed to act at a distance of 4D from the axis of symmetry, D being the diameter of the tunnel (shown to be adequate in the next chapter). The bulk density, Poisson's ratio and

Young's modulus of the liner material are 2400 kg/m³, 0.2 and 20,700 MPa, respectively. The bulk density, Poisson's ratio and shear wave velocity of the medium are 1,845 kg/m³, 0.33 and 152.5 m/s; and those of the base rock are 2,325 kg/m³, 0.4 and 1,830 m/s, respectively.

The finite element meshes used in the analysis are shown in Figure 4.2.1. The panels are the same at both ends although details are shown at one end only. The details of the four interior panels are also shown in the Figure. For Case 4, there are no special end panels; instead, the first and last of the four panels serve as the end panels.

4.3 RESPONSE OF THE SYSTEM WITH NODES ON THE TRANSVERSE ENDS SET FREE

Because the response along the transverse ends is not known, a method that localizes the influence of the assumed end conditions would appear reasonable. For this purpose, the nodes along these transverse end sections were set free. Free field motions were assumed along the radial boundary at a distance of 4D from the axis of symmetry. Cases 4, 5 and 7 of Figure 4.2.1 were analyzed, with the axial and radial response of point "P" on the outer periphery of the tunnel, and the corresponding free field response at point P (without the tunnel), shown in Figure 4.3.1 and 4.3.2, respectively. It may be observed that the discrepancies due to the assumed free conditions are largest near the ends. The discrepancies are largest for Case 7 because it has the most ill-conditioned elements. It may also be noted that the axial response of the tunnel is almost identical to the corresponding free field axial response. However, there is some difference between the two in the case

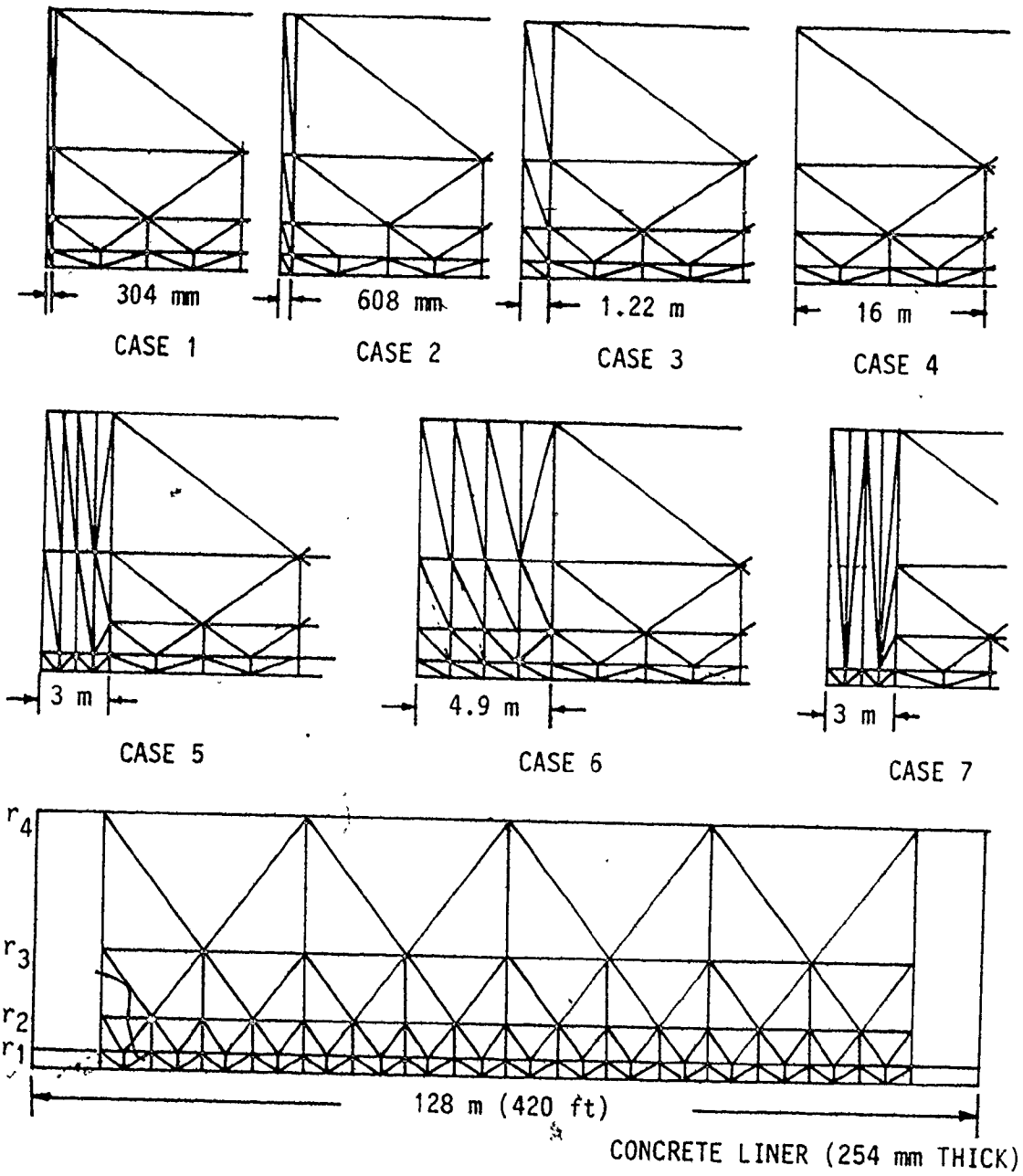

r_1 = 3.05 m, r_2 = 6.1 m, r_3 = 12.2 m, r_4 = 24.4 m

FIGURE 4.2.1 FINITE ELEMENT GRID WITH SPECIAL END PANELS

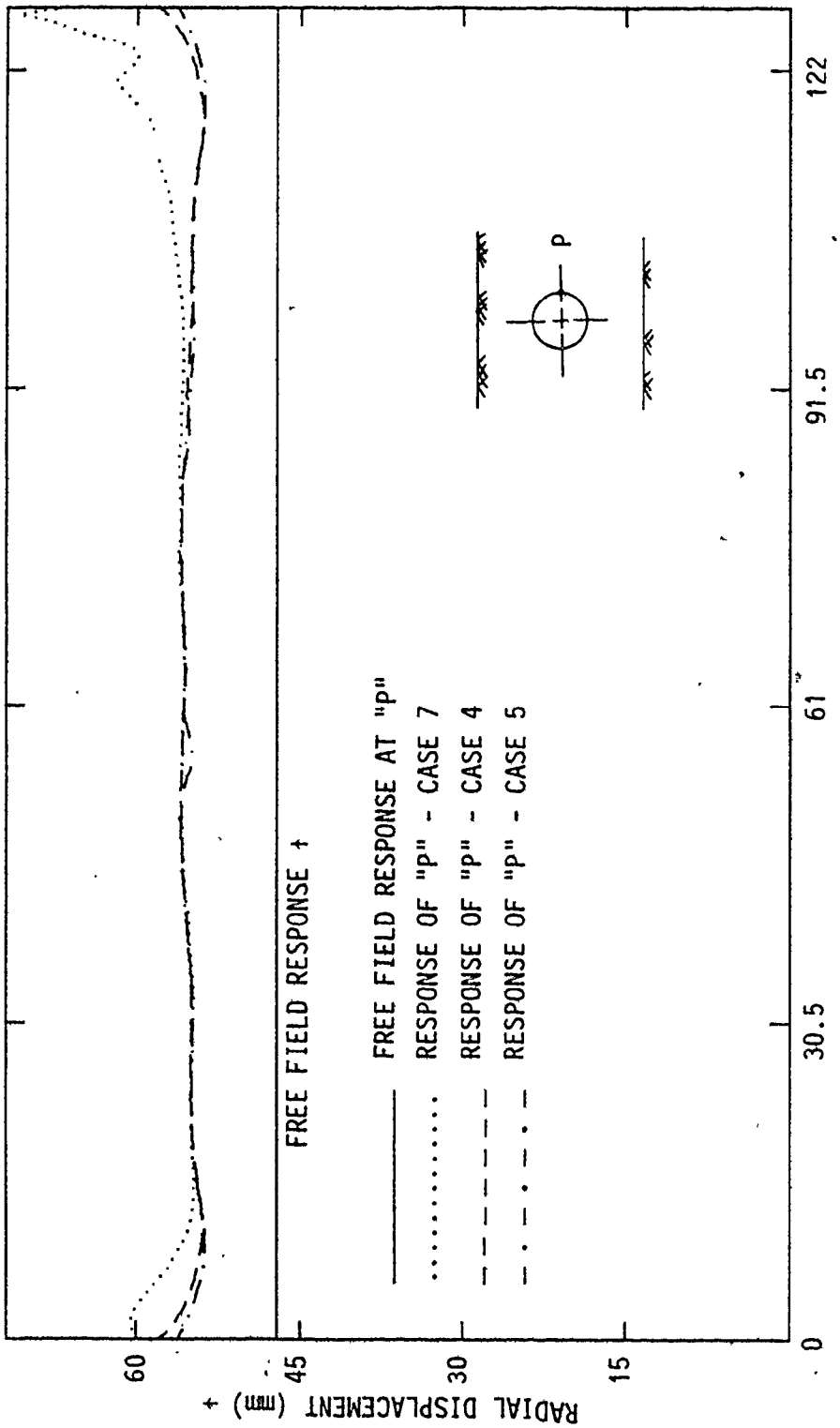

FIGURE 4.3.1 RADIAL DISPLACEMENTS ALONG THE GENERATOR FOR POINT "p" AT TIME 2 SECONDS

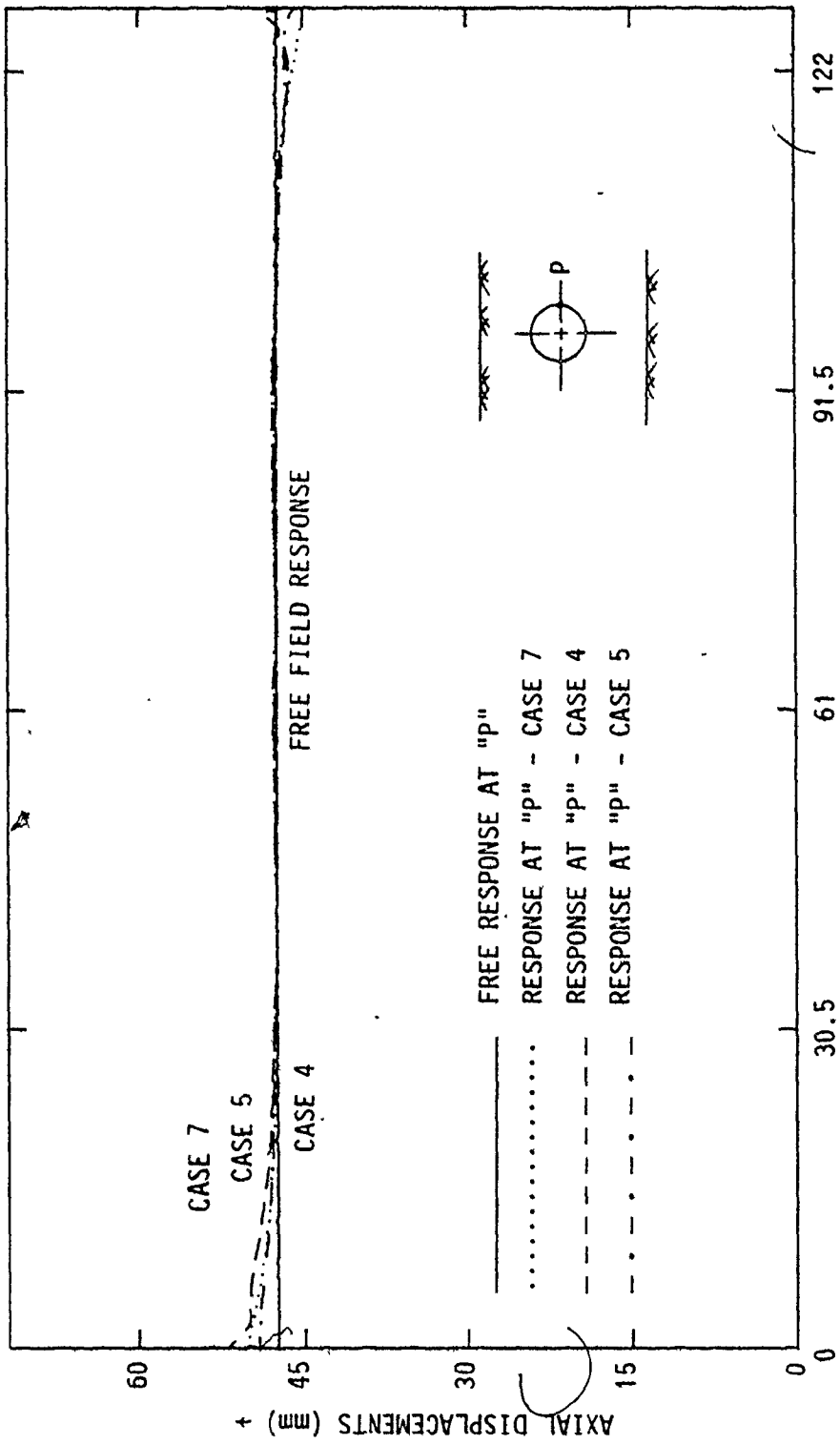

FIGURE 4.3.2 AXIAL DISPLACEMENTS ALONG THE GENERATOR FOR POINT P AT TIME 2 SECONDS

of radial response. This is because the system tends to be weaker in the transverse direction. The figures also indicate that the errors due to the assumed end conditions are negligible at a distance of 30 to 35 m from the transverse end sections.

4.4 RESPONSE OF THE SYSTEM WITH FREE FIELD MOTIONS ASSUMED AT TRANSVERSE ENDS

The study of buried pipe and tunnel behaviour during past earthquakes appears to indicate that the response of such structures closely follows the response of the surrounding medium. For the dynamic analysis in the time domain, it was also proposed to use the free field motions along end boundaries as estimates of the unknown response at these sections. Figures 4.4.1 and 4.4.2 show the resulting response along the generator at the right spring-point "P" of the tunnel. From these figures, it may be seen that the influence of end conditions is negligible at a distance of about 30-35 m from the end sections. It may also be noted that the method given in section 4.3 leads to more desirable results than those by the method in this section. It also highlights the importance of due consideration of the structure-medium interaction. Even though the difference between the actual response of the structure and the corresponding free field response of the medium is small, it is significant enough to cause errors in the computed response of the system near the end sections.

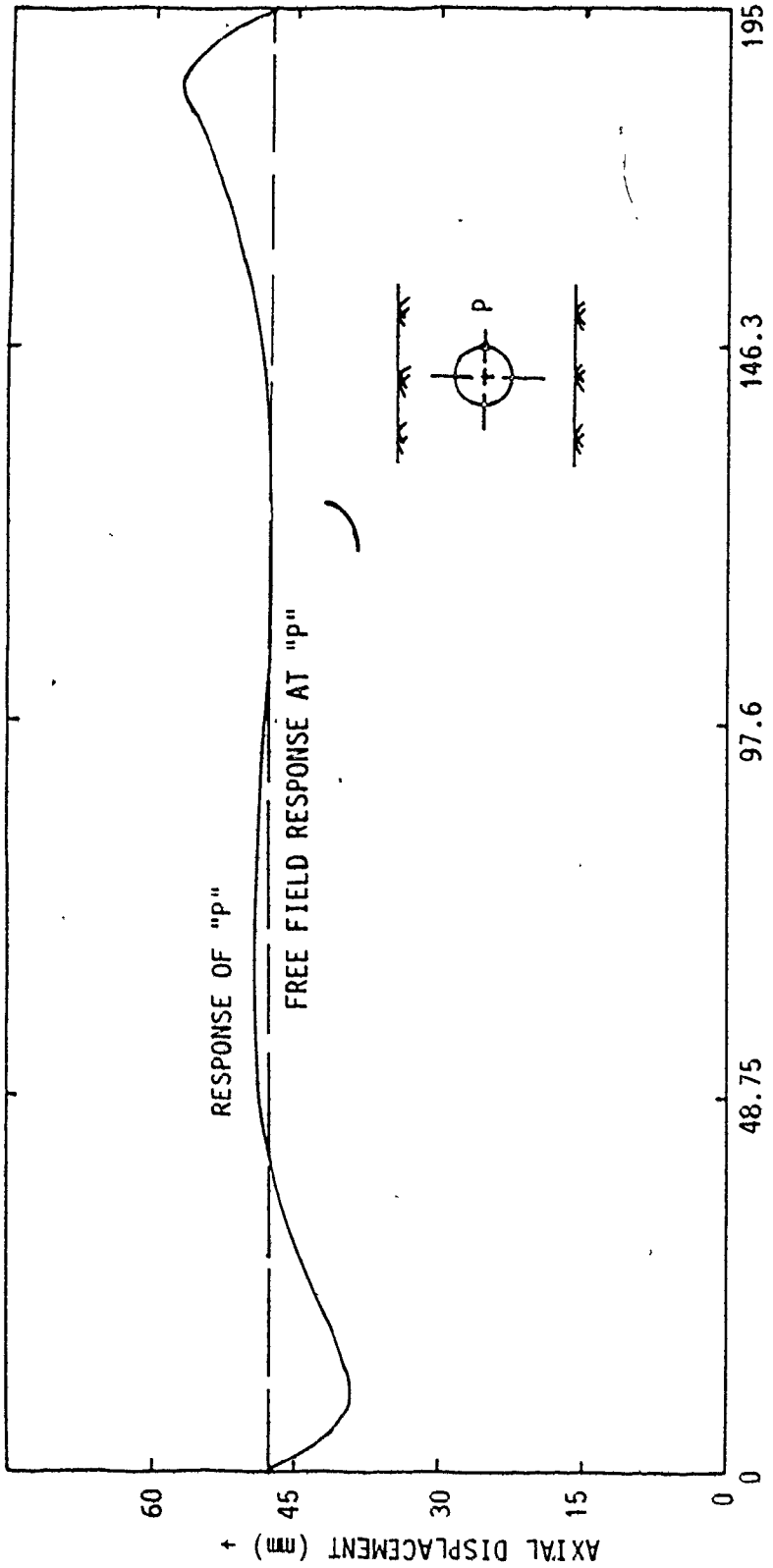

FIGURE 4.4.1 AXIAL RESPONSE OF THE SYSTEM WITH FREE FIELD RESPONSES ASSUMED ALONG THE TRANSVERSE ENDS (TIME = 2 SEC.)

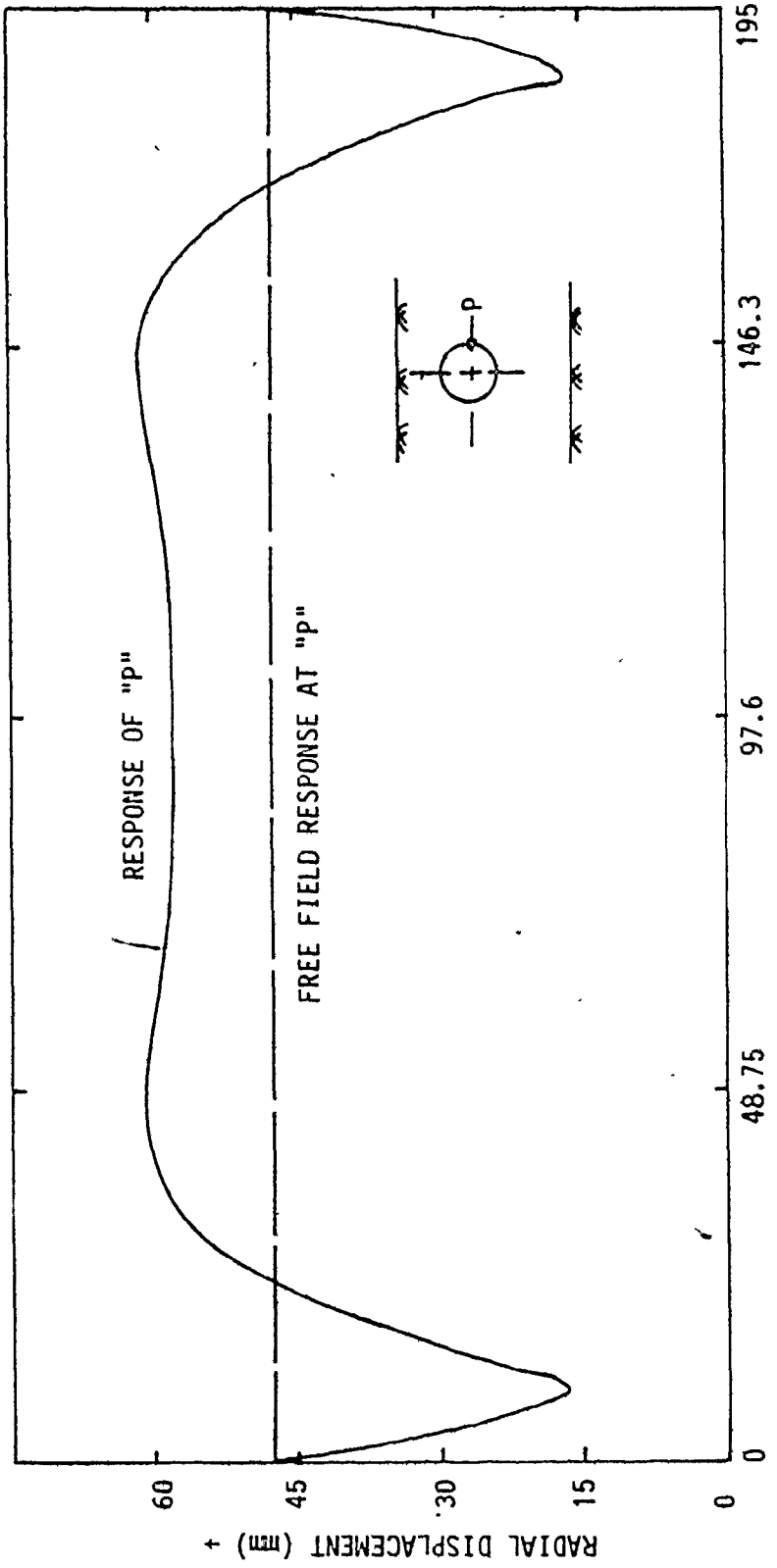

FIGURE 4.4.2 RADIAL RESPONSE OF THE SYSTEM WITH FREE FIELD RESPONSES ASSUMED ALONG THE TRANSVERSE ENDS (TIME = 2 SEC.)

4.5 TIME LAG BETWEEN TWO POINTS ON THE SAME HORIZONTAL GENERATOR

Consider points A and E (Figure 1.7.1) separated by an axial distance z. The response at these points should be identical as z approaches zero (i.e. if z is small enough, the response at E is a good approximation of that at A). The distance z appears in the dynamic analysis as the time lag, the time taken by the shear wave to travel from A to E. Extending this logic to the response for two consecutive time stations at points A and E in the dynamic analysis, if the time interval Δt between the time stations is small enough, the response at E at time $(t-\Delta t)$ may be considered to be a good estimate of the resonse at a time t.

It is quite obvious that a smaller value of Δt will always improve the accuracy of the results obtained. However, the value of z should be such that it leads to a small time lag between the points, but should also be large enough so that the influence of assumed responses at transverse boundaries is acceptably small. Since these requirements conflict with each other, a suitable compromise was to be struck. From the discussions given in sections 4.3 and 4.4 a value of about 6D should be adequate for z, if the corresponding time lag is also acceptable. For the case of vertical propagation of shear waves, there is no problem in adopting this (or even larger) value of z as this does not cause any time lag. In the case of shear wave propagation at an angle θ to the vertical, the time lag δt is given by

$$\delta t = \frac{z.\sin\theta}{\beta} \qquad (4.5.1)$$

where β is the shear wave velocity. It was shown in section 2.7 that the largest value of θ for a surface formation would be about 30°. In most cases, it is much smaller, and gets smaller for formations with lower values of β. Thus, it may be seen that the ratio $(\sin\theta)/\beta$ does not change much for different values of β. For z = 35 m the corresponding time lag would be 0.0083 s if β = 100 m/s; and 0.00828 s if β = 902 m/s.

If somewhat smaller values of z are employed to reduce the corresponding time lag δt, the assumed values of response for the transverse boundaries will contain some error, which will die away at a relatively small distance from the end sections.

To verify the proposed method, Cases 1 to 6 of Figure 4.2.1 were considered. The radial and axial responses at point "P" from the dynamic analyses, and the corresponding free field response, are shown in Figures 4.5.1 and 4.5.2. For cases 1, 2, and 3 the errors due to end conditions are rather large, while for Cases 4 and 5 where 4 small end panels are used at each end (each transverse section separating the end panels "borrowing" the response from the similar section immediately next to it on the inner side), the results are much better. However, with less finite elements, degrees of freedom (and computational effort), Case 4 gives the best (almost ideal) results. For this case, the end panels are identical in layout to the two interior panels.

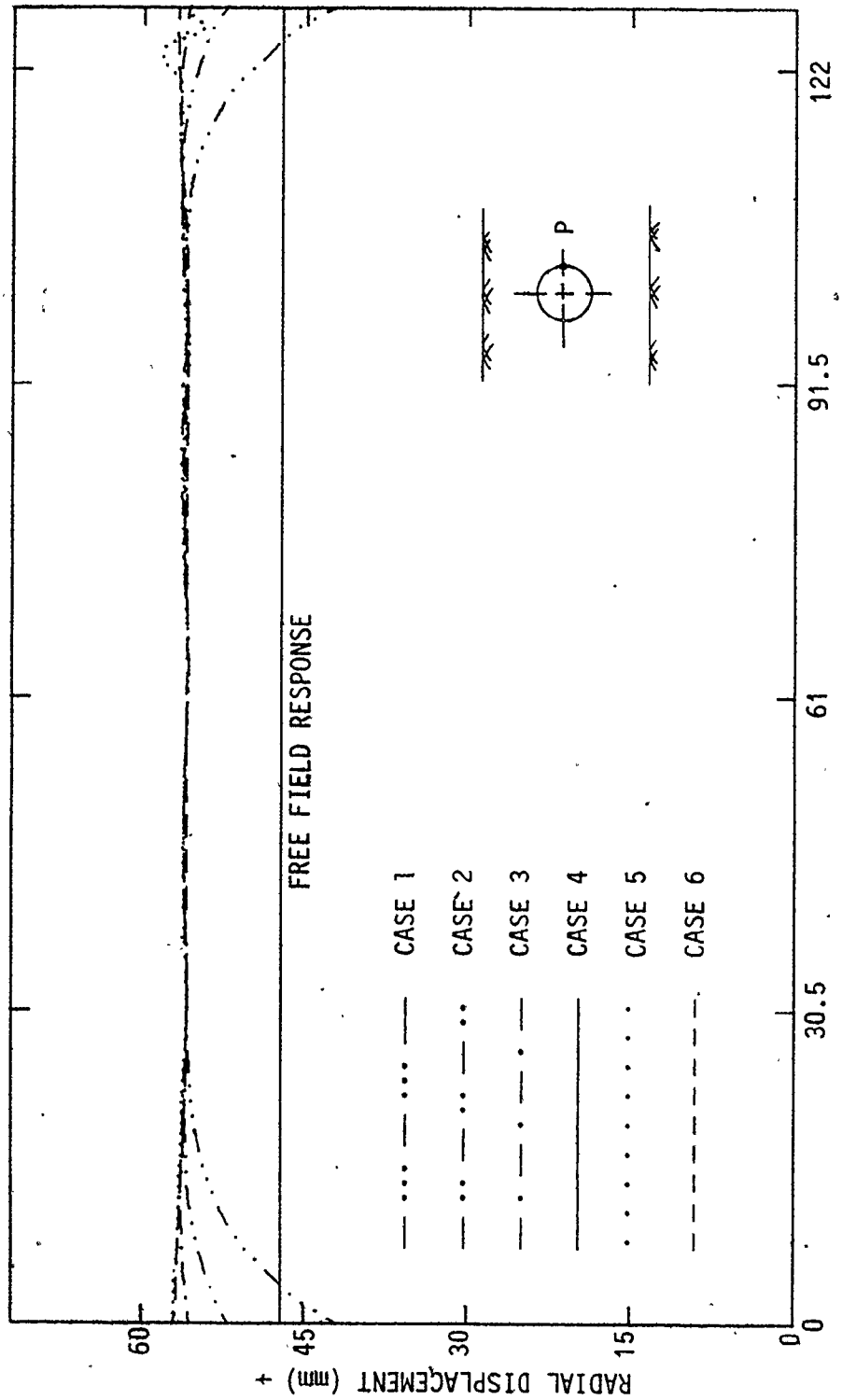

FIGURE 4.5.1 RADIAL DISPLACEMENTS ALONG THE GENERATOR FOR POINT "P" AT TIME 2 SECONDS

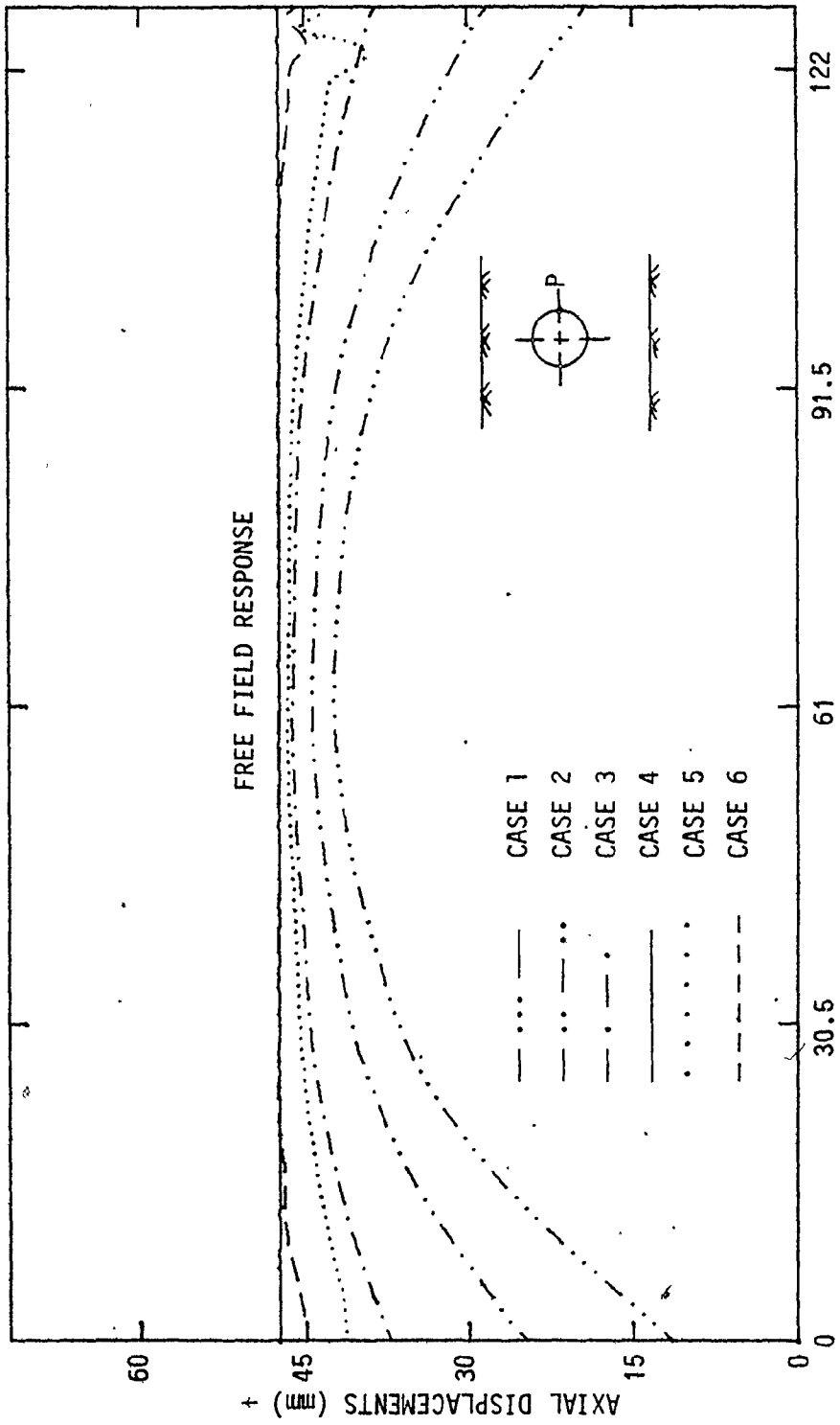

FIGURE 4.5.2 AXIAL DISPLACEMENTS ALONG THE GENERATOR FOR POINT "P" AT TIME 2 SECONDS

4.6 CONCLUSIONS

Because of structure-medium interaction, the response of the system along the transverse boundaries is not known for any time station. Without this knowledge, the dynamic analysis of a finite length system in the time domain cannot really be carried out. There is no remedy for this problem at present, except to provide sufficient extra elements on either side of the portion of the system of interest. This increases the size of the problem for the type of structures under consideration, and the cost of solution.

The influence of the errors due to the assumed boundary conditions appears to be felt up to a distance of 5 to 6D from the ends. Even though the response of the structure is close to the free field response at the same position and same time, the difference is significant enough to cause appreciable deviations from the actual responses near the end zones. This shows the importance of due consideration of the structure-medium interaction.

Very good estimates of these unknown responses along the transverse end sections may be obtained "borrowing" the response at the corresponding node on the same (horizontal) generator at a distance of five or six diameters. As the distance between the "donor" and "receiver" nodes decreases, the distance from the ends up to which the discrepancies in response show up to to assumed end conditions increases.

The largest distance between the donor and receiver nodes that may be allowed in any problem depends on many other details. A smaller time step will always allow a greater distance of separation. Even if the allowable distance of separation is limited to less than 5D, this will result in discrepancies in computed response for a much smaller distance from the end sections, which still makes it a better method than the others described previously.

For most surface formations of practical interest, the largest shear waves propagation angle with respect to vertical is of the order of 30°, and much smaller in most cases. In such cases, horizontal distances of the order of 30 to 35 m result in acceptably small time lags. This further helps to justify the use of this method for cases where the shear wave is propagating at an angle to the vertical.

CHAPTER 5

DYNAMIC ANALYSIS OF TUNNEL-MEDIUM SYSTEMS

5.1 INTRODUCTION

A method for considering finite length sections (i.e. end response boundary conditions) was presented in the previous chapter. In this chapter, results are discussed for a number of parametric studies. For cases where stresses are not used as the basis for comparisons, only displacement responses are considered. The single layer medium was represented by three layers of elements, and the concrete tunnel liner by a single layer of finite elements (Figure 5.2.1). This allows consideration of a longer tunnel length for such a case. A sinusoidal base excitation was considered, with 0.3 m/s^2 peak amplitude and 2 Hz frequency in the axial as well as the transverse directions. The shear wave was considered to propagate in the vertical direction and R-waves were assumed to be absent. A 76 m thick single layer system with a tunnel of outside diameter 6 m and liner thickness of 254 mm was used in these analyses, with the axis of symmetry 27.5 m above base rock level.

In more detailed analyses, where stresses were also considered, the medium was represented by four layers of elements and the tunnel liner by a combination of triangular and quadrilateral elements. The details for this mesh are given in section 5.11.1.

5.2 PARAMETRIC STUDIES WITH A SINGLE LAYER OF ELEMENTS REPRESENTING THE LINER

Figures 5.2.1 and 5.2.2 show the details of the single layer system and finite element mesh employed, respectively. The number of typical panels in the mesh, and the length of these panels, may vary from trial to trial, but the panel pattern remains the same. To facilitate a comparison of the results, the free field motions computed for one set of material properties at a radial distance of 24 m (80 ft) from the axis of symmetry were used as the known response of the system at the free field boundary when different materials were considered. The duration of the analyses was limited to 3 seconds with a time interval of 0.01 seconds. The parameters considered were:

1. Tunnel length;
2. Radial distance of the free field motion boundary;
3. Properties of the liner;
4. Aspect ratio of the liner elements; and
5. Direction of base excitation with respect to the tunnel axis.

5.3 LENGTH OF THE TUNNEL

Free field motions were assumed at the transverse end boundary sections as well as the radial boundary at 24 m (4 D (diameters) from tunnel axis), which is discussed in greater details in section 5.4. Axial lengths of 2, 4, 6, 8 and 10 panels were considered with a panel

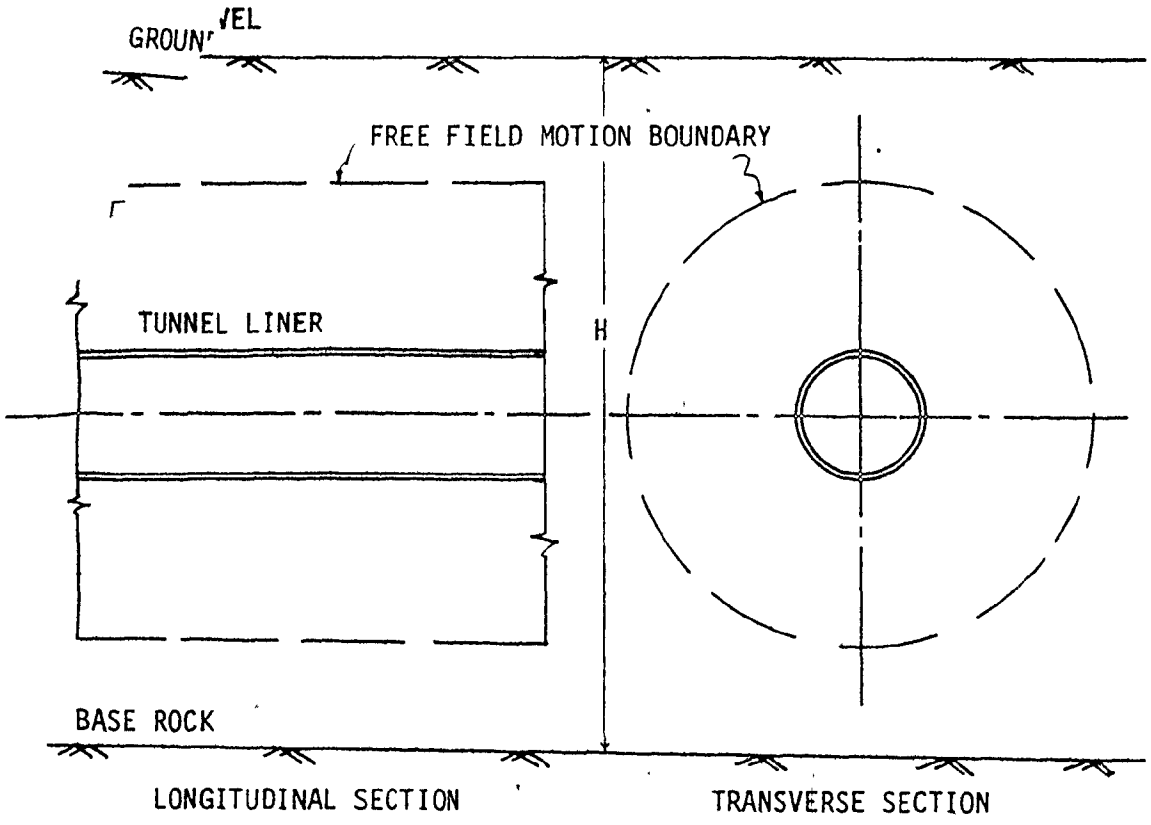

FIGURE 5.2.1 SINGLE LAYER SYSTEM WITH TUNNEL

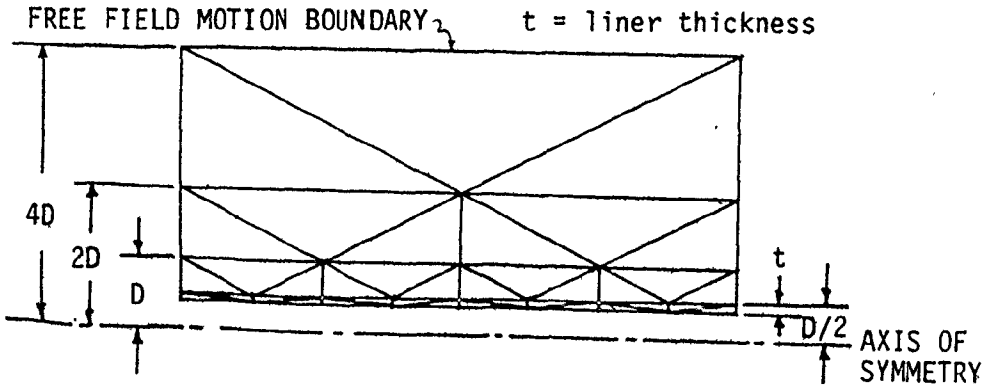

FIGURE 5.2.2 LAYOUT OF A TYPICAL PANEL OF THE INTERACTIVE SYSTEM

length of 19.5 m (64 ft). Figures 5.3.1 and 5.3.2 show the radial and axial displacements of the liner at the right spring point along the axial direction of the tunnel for the base excitation. At a distance of about 36 m (6 D) from the ends, most of the error due to assumed end conditions appears to be eliminated. The discrepancy in the computed response at the end zones is more pronounced for the radial response than for the axial response. This is anticipated since the system is "weaker" in the radial direction due to the tunnel cavity, and in agreement with field observations (Appendix A).

5.4 RADIAL DISTANCE TO THE FREE FIELD MOTION BOUNDARY

The response at the right spring point for the 8 panels axial length tunnel, along the transverse section of its mid-length, is shown in Figure 5.4.1. Over this length, the section is free from the effect of end conditions as shown in Section 5.3. From Figure 5.4.1 it is clear that the response of the system at 2 D from the axis of symmetry is quite close to the free field motions, which in turn indicates that the assumption of free field motions at 4 D in Section 5.3 (and throughout this chpater unless otherwise stated) is both reasonable and adequate.

To check this assumption in more detail, the system was analyzed with the assumed free field motions at a radial distance of 2 D by removing the outer layers of finite elements in Figure 5.2.2. The axial and radial responses obtained are shown in Figures 5.4.2 at

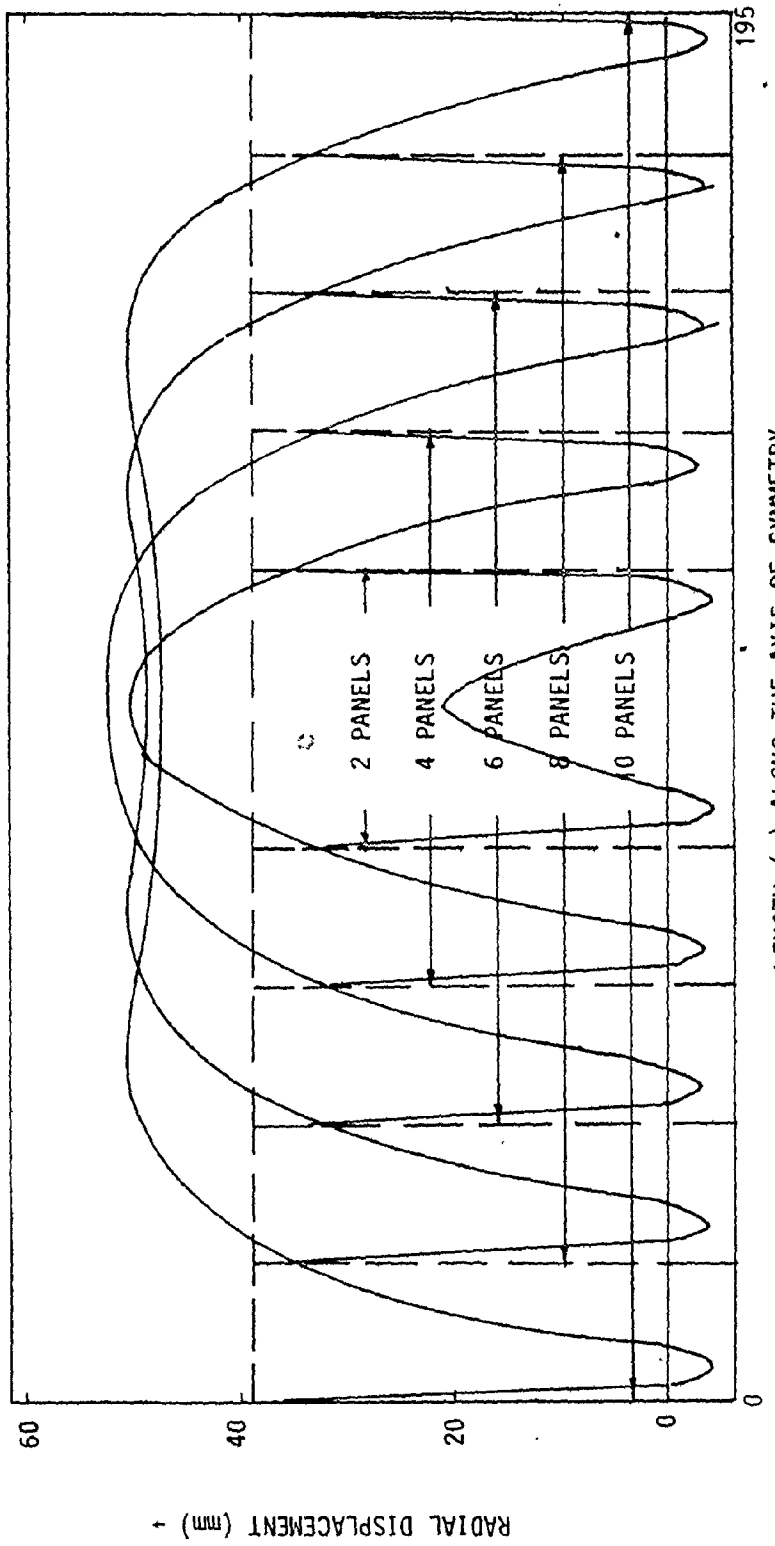

FIGURE 5.3.1 RADIAL RESPONSE OF THE LINER AT RIGHT SPRINGING POINT (TIME = 2 SEC.)

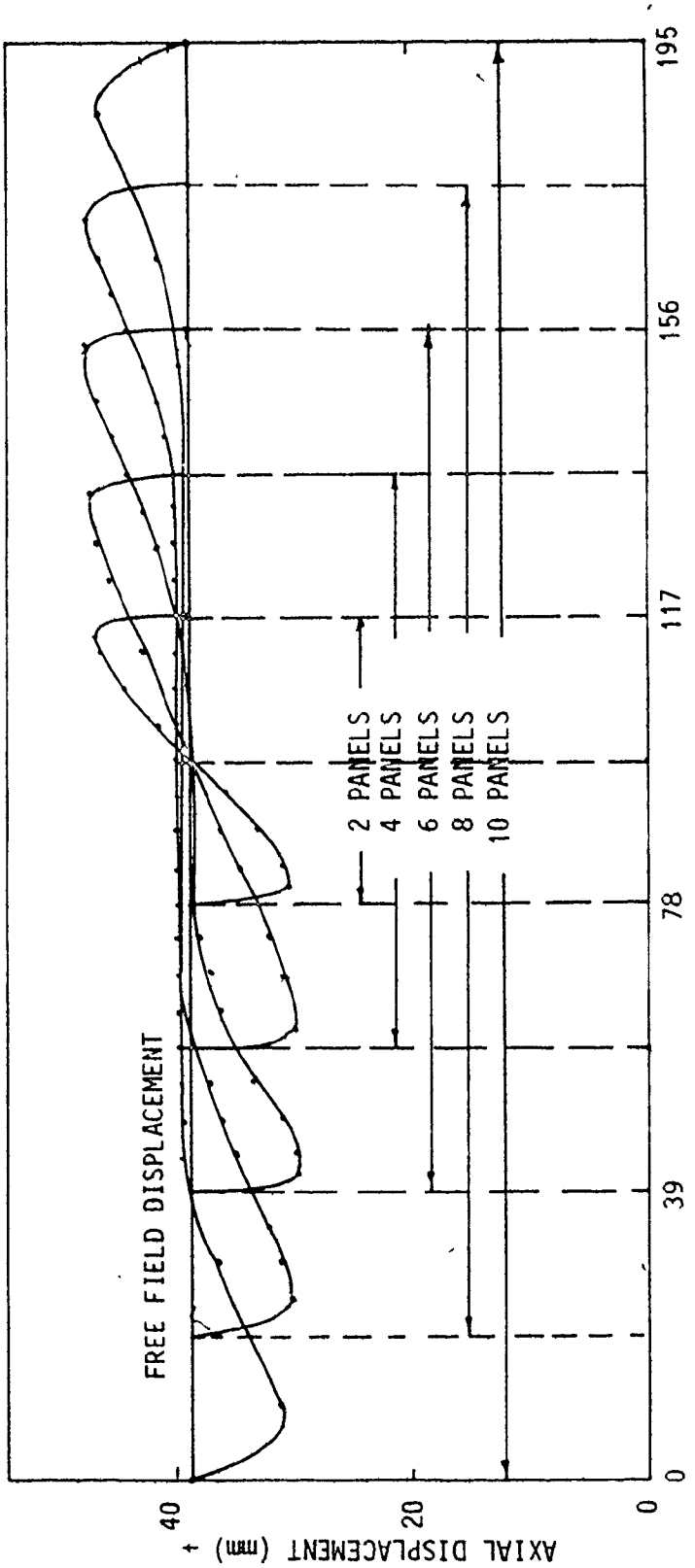

FIGURE 5.3.2 AXIAL RESPONSE OF THE TUNNEL AT RIGHT SPRINGING POINT (TIME = 2 SECONDS)

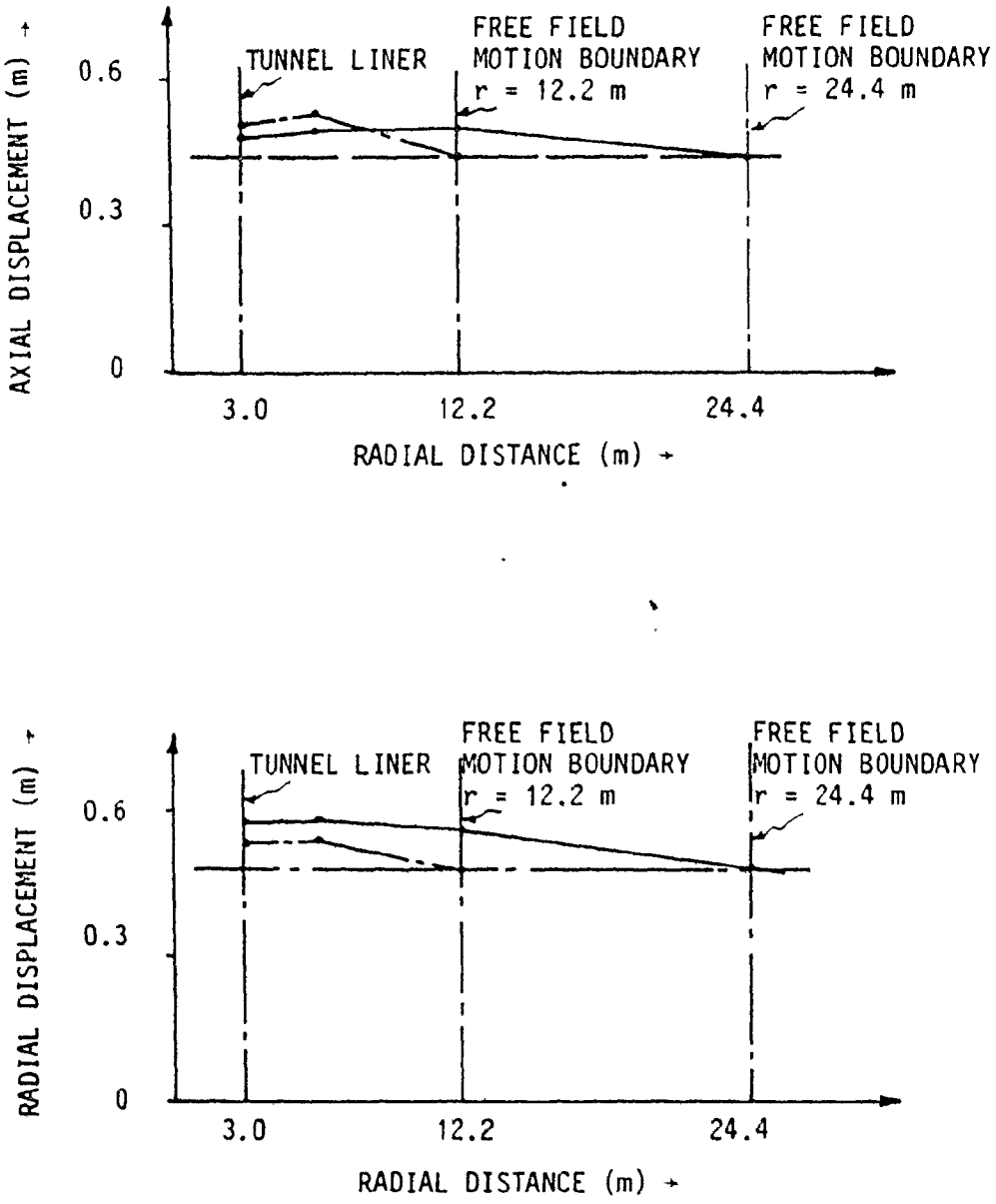

FIGURE 5.4.2 RESPONSE OF THE TUNNEL AT THE RIGHT SPRINGING POINT ON THE TRANSVERSE SECTION AT MID-LENGTH OF THE TUNNEL (TIME = 2 SEC.)

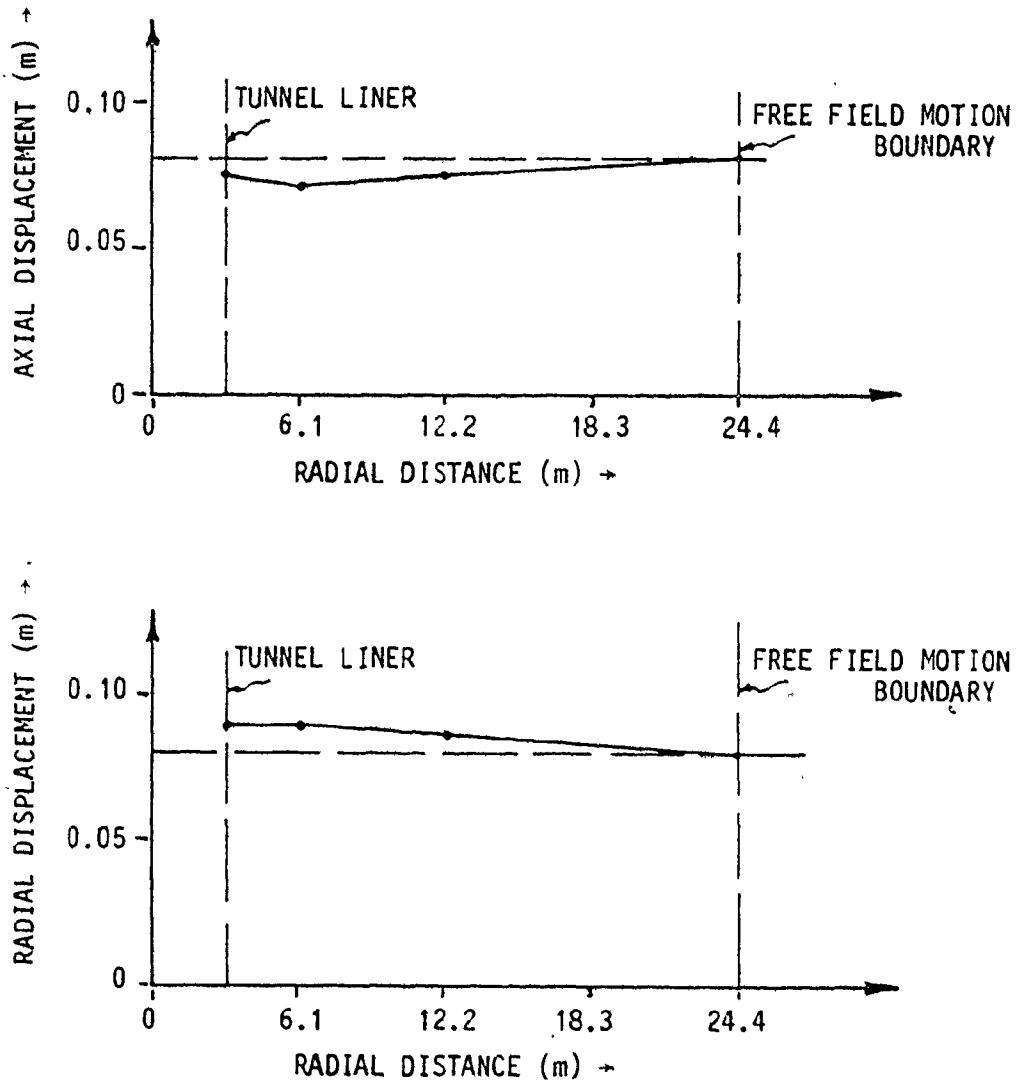

FIGURE 5.4.1 RESPONSE OF THE TUNNEL AT THE RIGHT SPRINGING POINT ON THE TRANSVERSE SECTION AT THE MID-LENGTH OF THE TUNNEL (TIME = 1 SEC.)

2 seconds. The differences in the computed response for this case with respect to the system with free field motions at 4 D are only about 5.5% and 6% for the radial and axial responses, respectively. Part of this discrepancy is due to the small number of elements used to represent the medium. A system with additional layers of elements would be expected to yield more accurate computed responses of the system.

5.5 MATERIAL PROPERTIES OF THE MEDIUM

The material properties used to represent the medium are given in Table 5.5.1. As indicated previously, the free field motions computed for the second set of properties were used in all cases for comparison purposes. The nodes along the transverse end sections were set free for these cases. For these cases the finite elements mesh consists of 8 panels, with end and interior panels 61 m (200 ft) and 30.5 m (100 ft) long, respectively. Figures 5.5.1 and 5.5.2 give the radial and axial response of the liner at the right spring point. The response of the liner does not vary appreciably with medium properties over the representative range considered. For all of these cases, the axial response is close to the free field response of the medium at that point; while the radial response is somewhat different from the corresponding free field motion. The responses are free from end condition influences at a distance of 36 m (6 D) from the transverse boundaries.

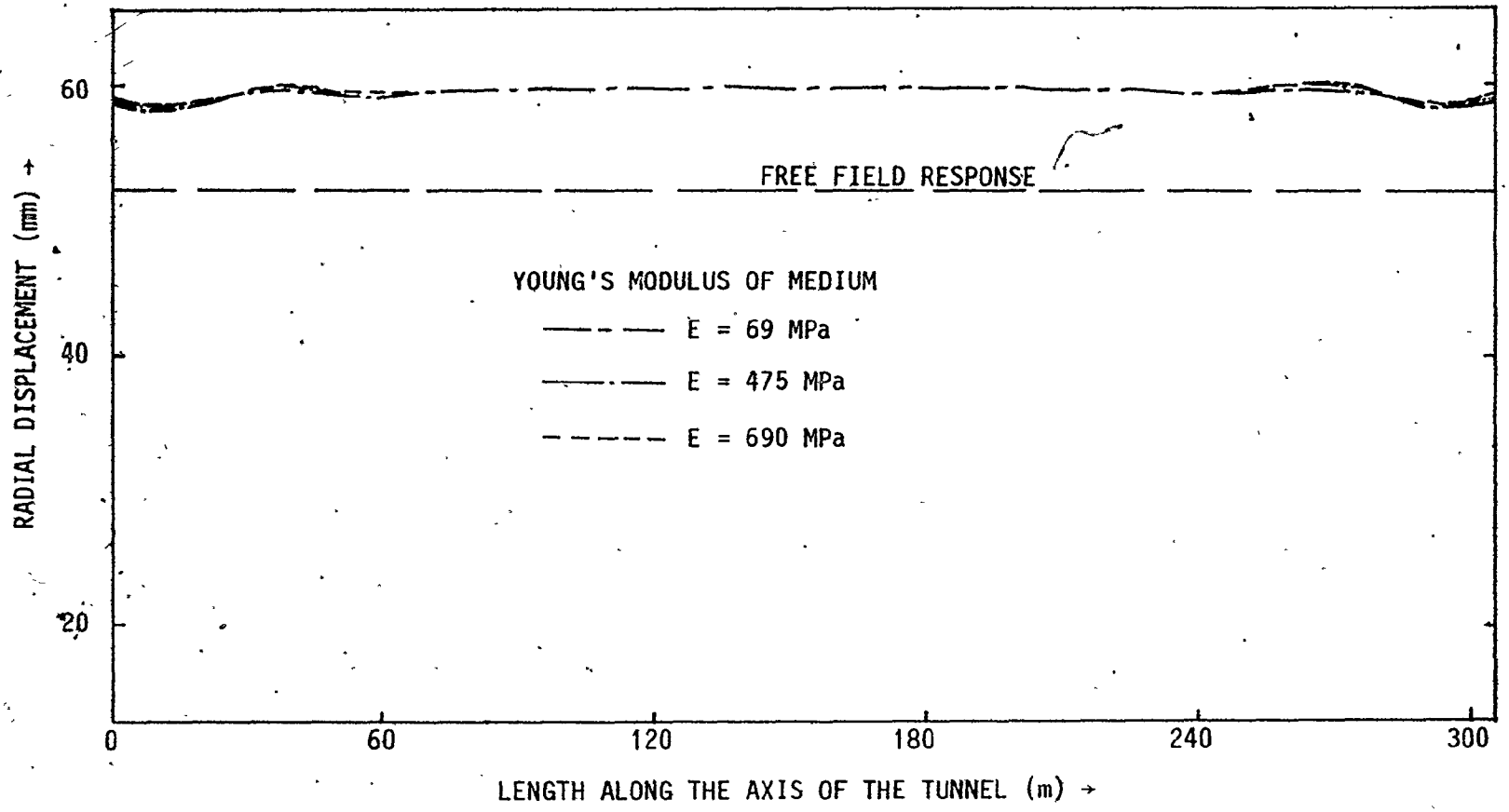

FIGURE 5.5.1 RADIAL RESPONSE OF THE LINER AT RIGHT SPRINGING POINT WITH DIFFERENT MATERIAL PROPERTIES OF THE MEDIUM (TIME = 2 SEC)

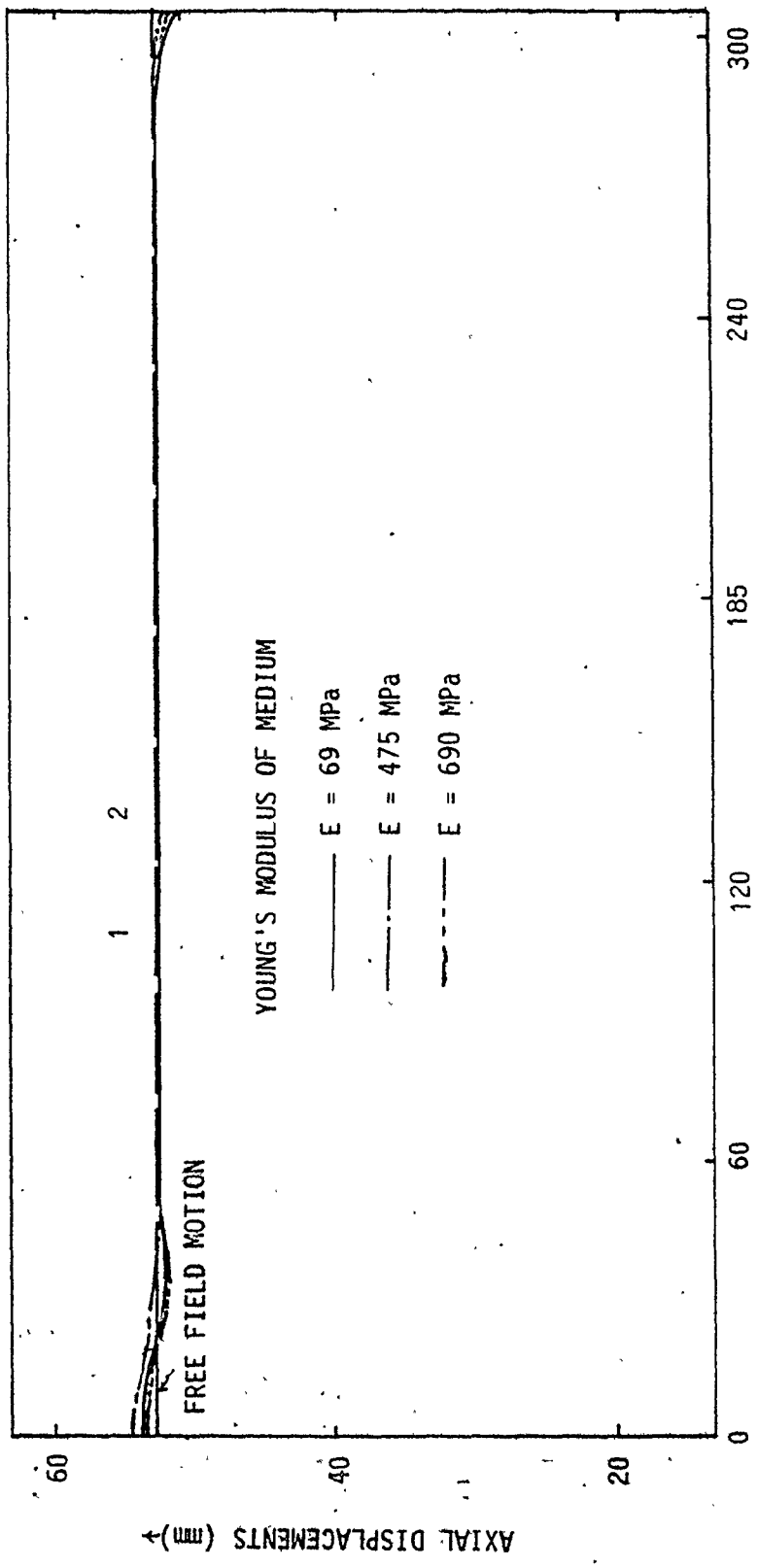

FIGURE 5.5.2 AXIAL RESPONSE OF THE LINER AT THE RIGHT SPRINGING POINT WITH DIFFERENT MATERIAL PROPERTIES OF THE MEDIUM (TIME = 2 SEC).

TABLE 5.5.1 MATERIAL PROPERTIES OF THE MEDIUM

NO.	YOUNG'S MODULUS (MPa)	MASS DENSITY (kg/m^3)	POISSON'S RATIO
1	69	1867	0.33
2	470	1867	0.33
3	690	1867	0.33

5.6 PROPERTIES OF THE LINER

The stiffness of the liner is a function of both the different material properties and thicknesses given in Table 5.6.1 Free field motions were again assumed at the nodes along the transverse end sections for these cases. For these cases, end and interior panels were 39 m (128 ft) and 19.5 m (64 ft) long, respectively. The responses obtained are given in Figures 5.6.1 and 5.6.2 for the liner right spring point. The computed response for the liner does not change much with the stiffness of the liner over the representative range considered. For all cases, the axial response at the mid-length transverse section remains close to the corresponding free field motion.

TABLE 5.6.1 PROPERTIES OF THE TUNNEL LINER

NO.	YOUNG'S MODULUS (MPa)	MASS DENSITY (kg/m^3)	POISSON'S RATIO	LINER THICKNESS (mm)
1	2981	2435	0.2	254
2	3974	2435	0.2	305
3	4968	2435	0.2	305

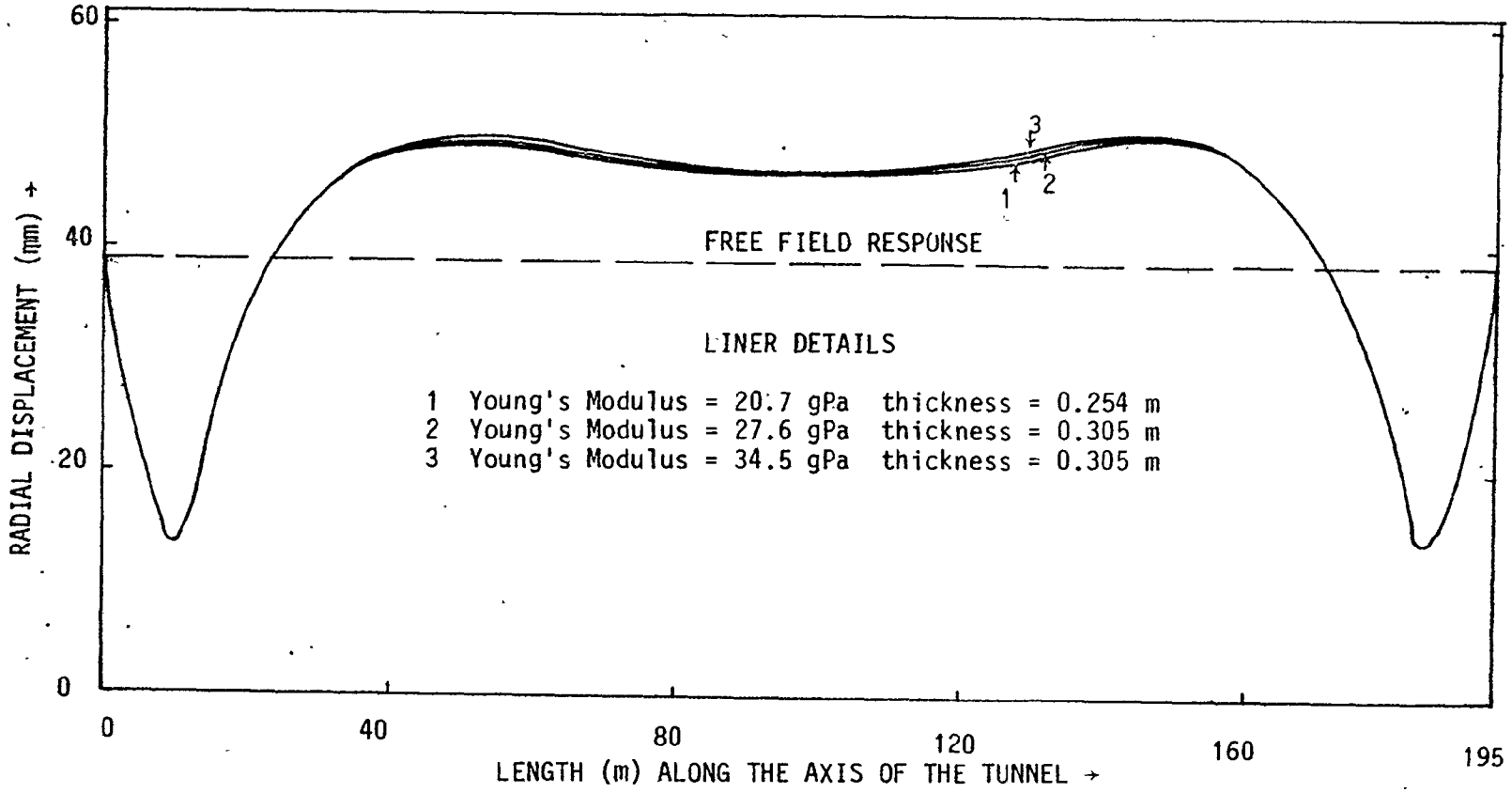

FIGURE 5.6 1 RADIAL RESPONSE OF THE LINER AT RIGHT SPRINGING POINT FOR DIFFERENT LINERS (TIME = 2 SEC)

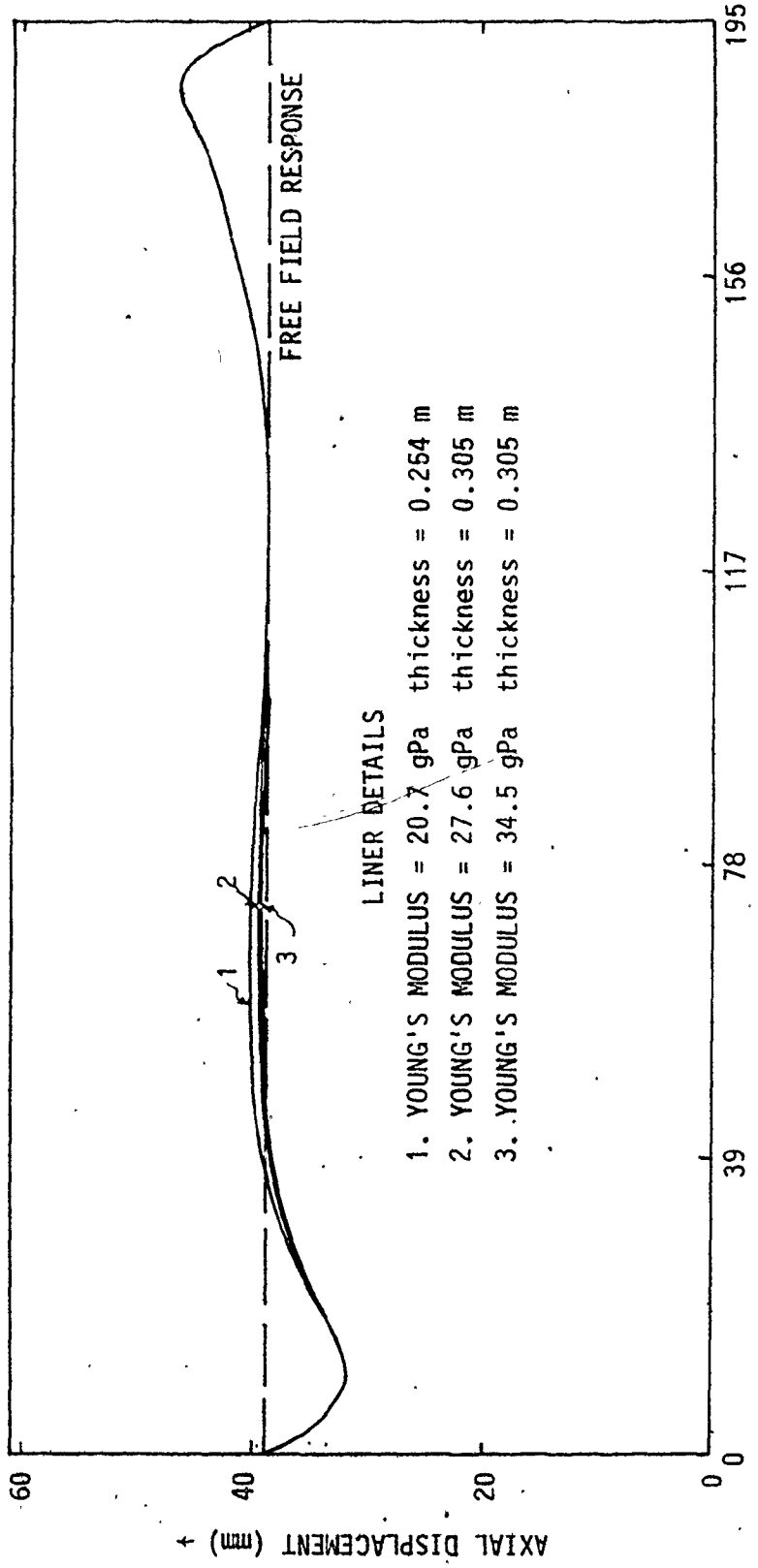

FIGURE 5.6.2 AXIAL RESPONSE OF THE TUNNEL AT THE RIGHT SPRINGING POINT WITH DIFFERENT LINERS (TIME = 2 SEC).

5.7 ASPECT RATIO OF LINER ELEMENTS

For the triangular elements involved, the aspect ratio is the ratio of the long side to its shorter adjacent side. As the liner thickness is quite small compared to the radial thickness of the medium included in the analyses, large aspect ratio elements are required to represent the long tunnel systems. However, larger aspect ratios (ill-conditioned elements) can often result in computing errors. While limiting aspect ratios of about 1:10 are often suggested, with the CDC 60 bit word, it should be possible in many cases to use larger aspect ratios.

Figures 5.3.1 and 5.3.2 show results obtained using elements of aspect ratio 1:9.6; while Figures 5.5.1 and 5.5.2 give those for an aspect ratio of 1:15. These results do not show any significant effect of aspect ratio on the response for the cases considered. It should be noted here that the dynamic analyses were limited to 3 seconds only, and the time step used was 0.01 seconds. Since the type of errors being considered would build up progressively with time, smaller time steps might be required (i.e. more expensive analysis) to limit such errors to acceptable limits if the duration of the analyses is long.

5.8 DIRECTION OF THE EXCITATION WITH RESPECT TO THE TUNNEL AXIS

The seismic motion is a vector varying in the time domain, and may have any general orientation with respect to the tunnel axis. For convenience, the vector may be resolved into components in the axial

and transverse directions; with the vertical component associated with these two components defined by the product of the tangent of the angle of propagation of the shear wave with the vertical and the horizontal response vector in that direction. To study the effect of the direction of propagation, the problem was analyzed with only the axial component of the base excitation for the previous cases. Then the analysis was repeated by using the transverse component only as the base excitation. The results showed that when the transverse component of base excitation was absent, the response of the tunnel in the transverse direction was negligible. The axial response was the same as the axial response when both axial and transverse components of the base excitation were present. Similarly, when the axial component of the base excitation was absent, the axial response was negligible, and the transverse response was the same as that when the same excitation was used in both directions. This indicates that the plane wave basically causes displacements mainly in the plane of propagation.

5.9 RESPONSE OF THE SYSTEM WITH SINUSOIDAL ACCELERATIONS AT THE FREE FIELD BOUNDARY

The single layer system under consideration, with a tunnel lining of 5 m outer diameter and horizontal axis, was analyzed for a sinusoidal acceleration of frequency 1 Hz and amplitude $\pm$ 1 m/s^2 at the free field boundary 20 m from the axis. At rest initial conditions were assumed, i.e. initial acceleration, velocity and displacement of zero. The computed response at the outer right spring point is shown

in Figure 5.9.1. The accelerations are of course sinusoidal, but the displacements keep increasing with time. This is as anticipated since the velocity curve obtained by integration of the specified acceleration function always has positive (or zero) ordinates. The displacement function obtained by integration of this velocity curve then always has positive ordinates and keeps increasing with time. These results can be substantiated by analytical means as well.

The displacements will be periodic for this case if the initial conditions corresponding to steady state vibrations are specified, i.e. at time t = 0, the acceleration and displacement are both zero while the initial velocity is at its negative maximum. Alternatively, a transient component may be introduced, which 'dies' out after a certain period of time. An acceleration function in which the transient component dies out in one cycle was adopted (Figure 5.9.2). The computed responses at the outer right spring point are shown in Figure 5.9.3.

In following sections, whenever sinusoidal excitations are referred to, the acceleration function is the one shown in Figure 5.9.2.

5.10.1 MORE DETAILED DYNAMIC ANALYSIS OF THE INTERACTIVE SYSTEM

A more detailed analysis of the system was carried out using the much finer mesh shown in Figure 5.10.1 (not to scale). The tunnel had an outer diameter of 5 m with horizontal axis of symmetry 35 m above the base rock. The depth of the single layer was 75 m. Free field motions were assumed at a radial distance of 20 m from the tunnel axis. Two sets

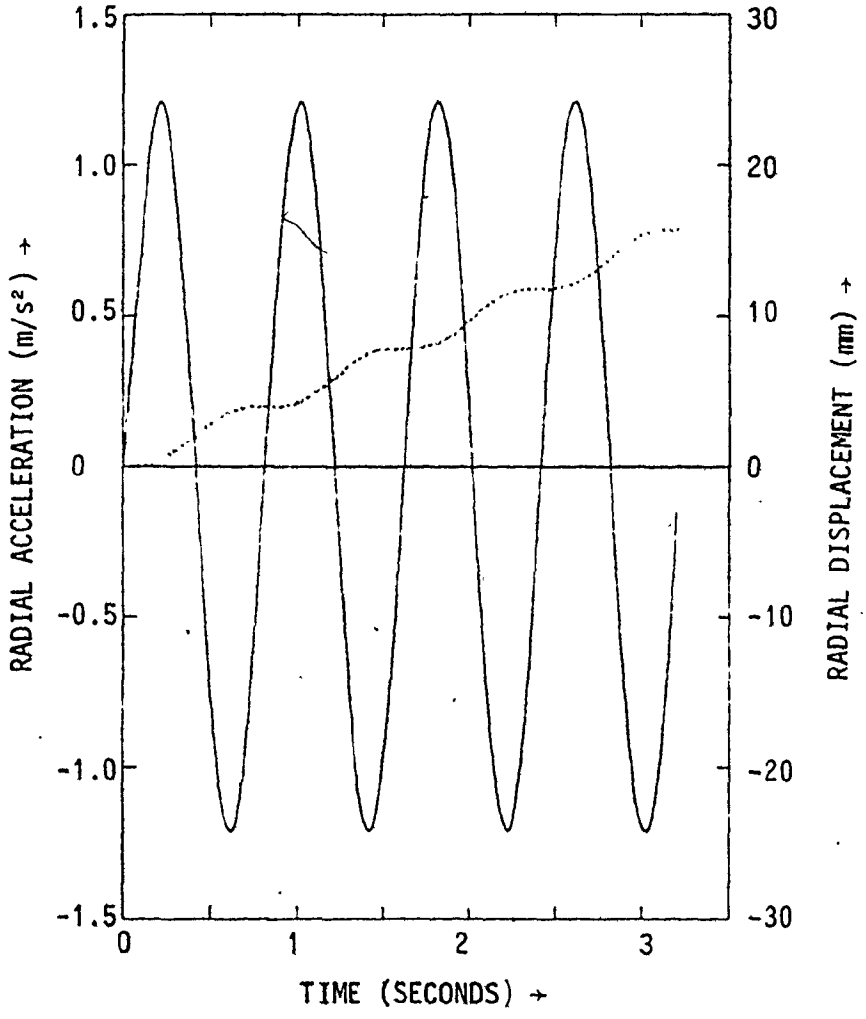

FIGURE 5.9.1 RADIAL RESPONSE OF RIGHT SPRING POINT OF THE LINER FOR SINUSOIDAL FREE FIELD ACCELERATION

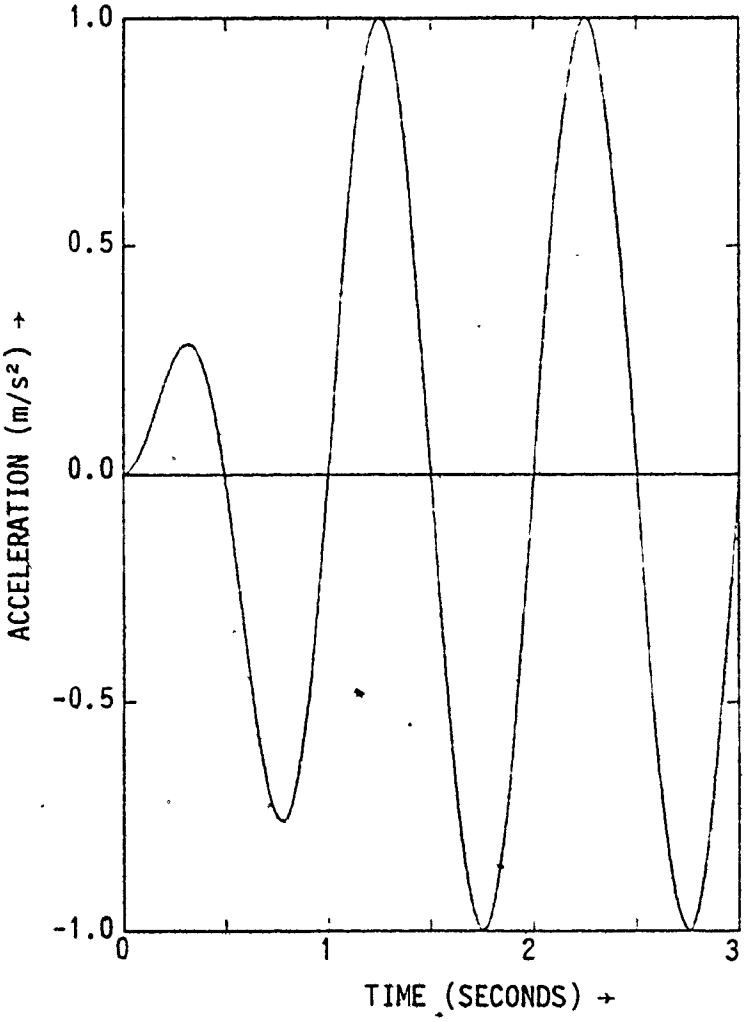

FIGURE 5.9.2 ACCELERATION FUNCTION AT THE FREE FIELD BOUNDARY OF THE SYSTEM

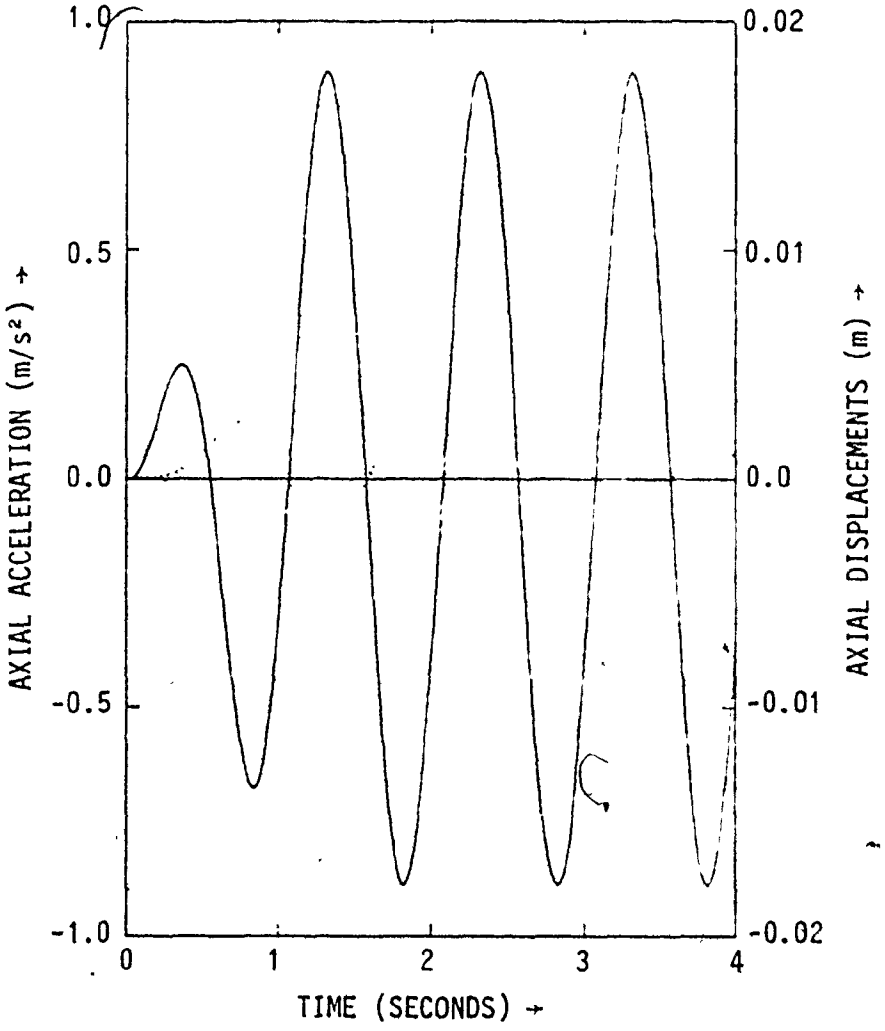

FIGURE 5.9.3 AXIAL RESPONSE OF THE RIGHT SPRING POINT OF THE LINER FOR SINUSOIDAL FREE FIELD MOTION WITH TRANSIENT COMPONENT

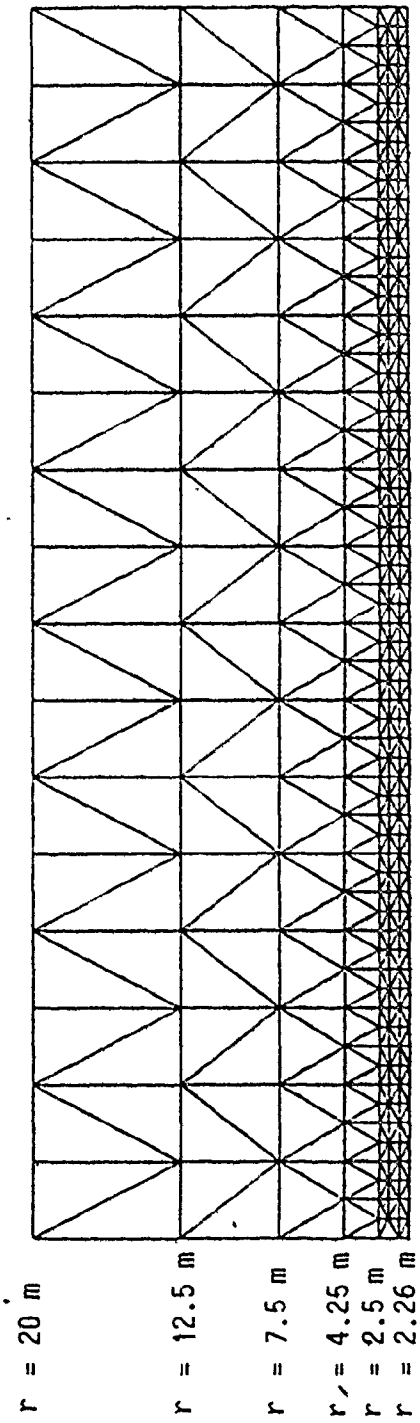

FIGURE 5.10.1 FINITE ELEMENT GRID REPRESENTING THE TUNNEL - MEDIUM SYSTEM (NOT TO SCALE).

TABLE 5.10.1 MATERIAL PROPERTIES

Details	TOP LAYER OF THE SYSTEM		BASE ROCK	TUNNEL LINER
	SYSTEM E1	SYSTEM E2		
Shear Wave Velocity (m/s)	100.125	902.2	2124	-
Poisson's Ratio	0.33	0.35	0.4	0.2
Mass Density (kg/m^3)	1875	2275	2375	2400
Young's Modulus (MPa)	50	5000	-	31000

of material properties were used for the medium as given in Table 5.10.1. The axial length of the tunnel was 61.44 m for system E1 and 76.8 m for system E2. The aspect ratios of triangular liner elements were 12 and 15 for the two systems, respectively.

Each system was analyzed for three cases. For case 1, the sinusoidal acceleration function of frequency 1 Hz and peak amplitude ± 1.0 m/s^2 given in Figure 5.9.2 was employed as the excitation at base rock level in the axial and transverse directions. Vertical propagation of shear waves was assumed, and as such, Rayleigh waves were not accounted for. For case 2, the base excitation was the same as for case 1, except that the shear wave was assumed to propagate at an angle to the vertical and the Rayleigh waves were accounted for. For case 3, the N-S component of the 1941 El-Centro Earthquake, modified to a peak value of 1 m/s^2, was used as the base excitation in the axial direction. No base excitation was assumed in the transverse direction for this case, however the R-waves were accounted for. The angle of propagation of shear waves was obtained by the procedure given in Section 2.7. For systems E1 and E2 these were 12.3° and 1.368°, respectively.

The dynamic analysis was carried out at time intervals of 0.005 seconds. The constants α and β used to compute the Rayleigh Damping matrix from the mass and stiffness matrices were 0.0 and 0.05, respectively. The axisymmetric harmonic, symmetric and antisymmetric components of the first and second harmonics, and the symmetric component of the third harmonic were included in the analysis.

5.10.2 RESPONSE OF THE SYSTEMS

The responses obtained for the two systems of each case are presented in Figures 5.10.2 through 5.10.38. In these figures: labels 1, 2, 3 and 4 represent the response of the tunnel at its outer right spring point, crown, left spring point and invert, respectively; labels 5, 6, 7 and 8 represent the free field responses (i.e. as if no tunnel was present) at the four positions; and 9, 10, 11 and 12 represent the free field responses at the corresponding positions on the free field response boundary (r = 20 m). The free field responses at the tunnel periphery locations without the tunnel were obtained for case 1 and case 3 using system E1, and case 3 using system E2. In all of these figures, the response for the first 4 seconds is given.

The axial responses for the three cases (system E2, stiff medium) indicate that the response of the tunnel is very close to the corresponding free field response at the same positions (Figures 5.10.2 through 5.10.7). For a shear wave velocity of 902.2 m/s and angle of propagation of 12.3°, a horizontal distance of 17.5 m (between the periphery of tunnel and the free field boundary) causes a very small time

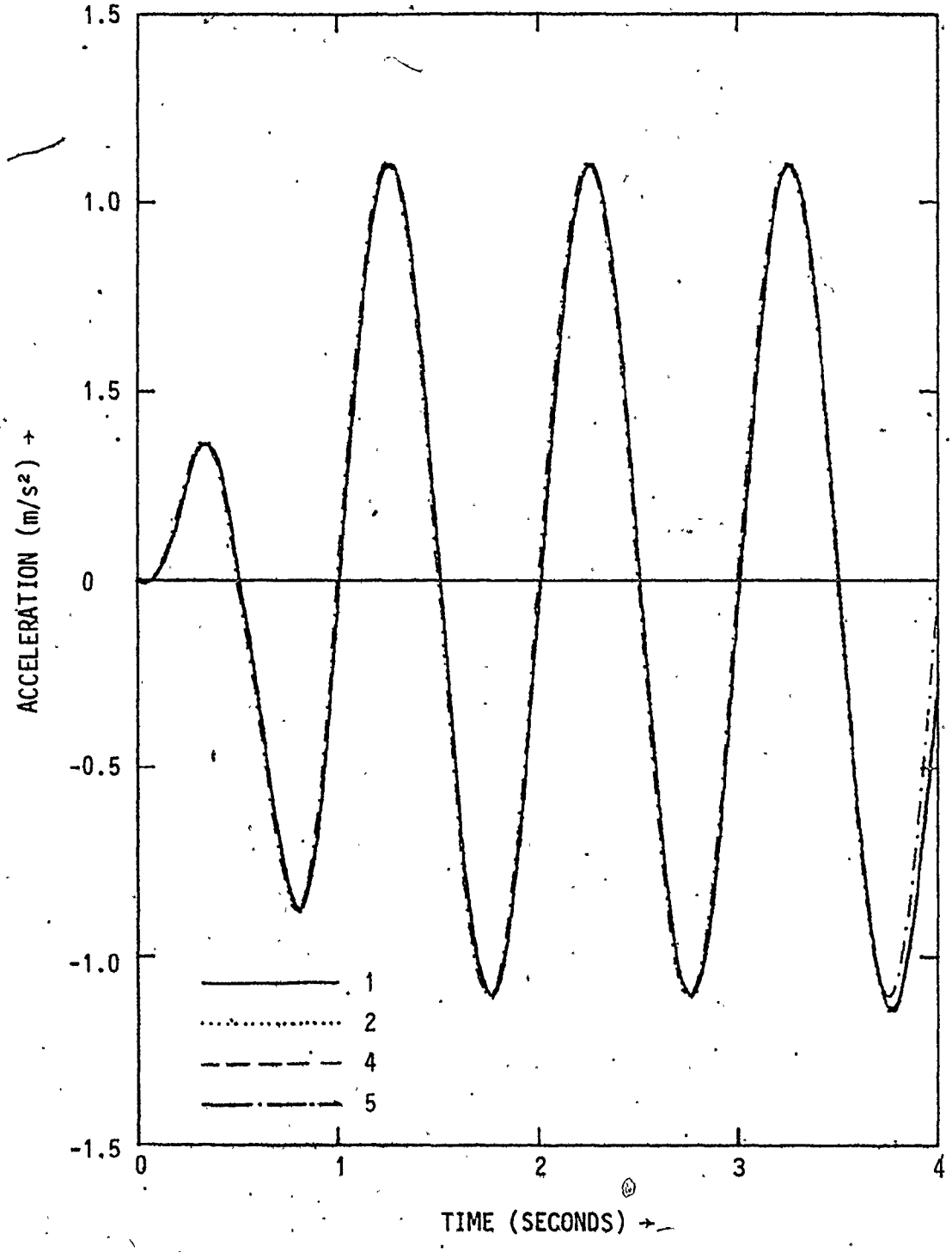

FIGURE 5.10.2 AXIAL ACCELERATIONS FOR SYSTEM E2, CASE-1

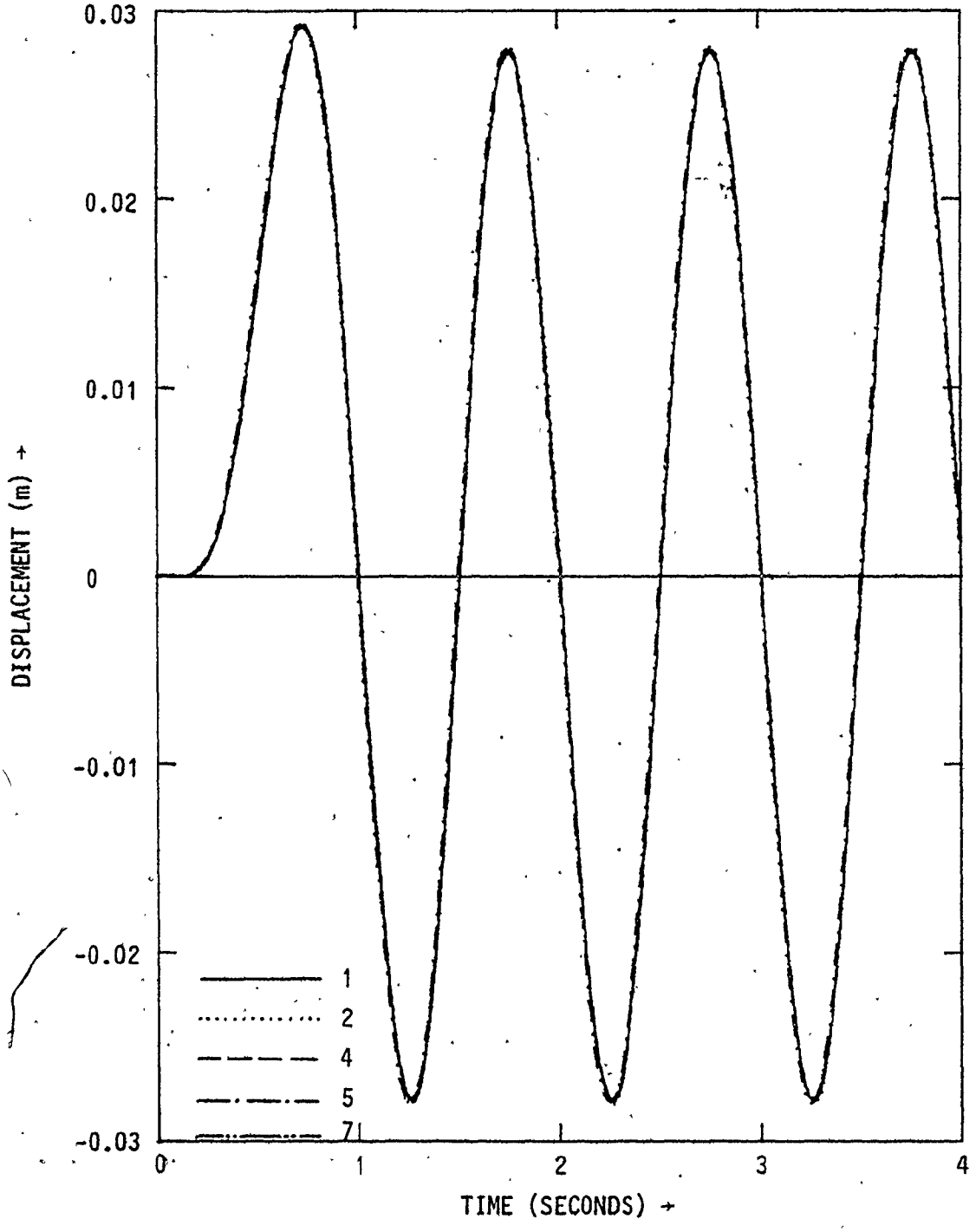

FIGURE 5.10.3 AXIAL DISPLACEMENTS FOR SYSTEM E2, CASE-1

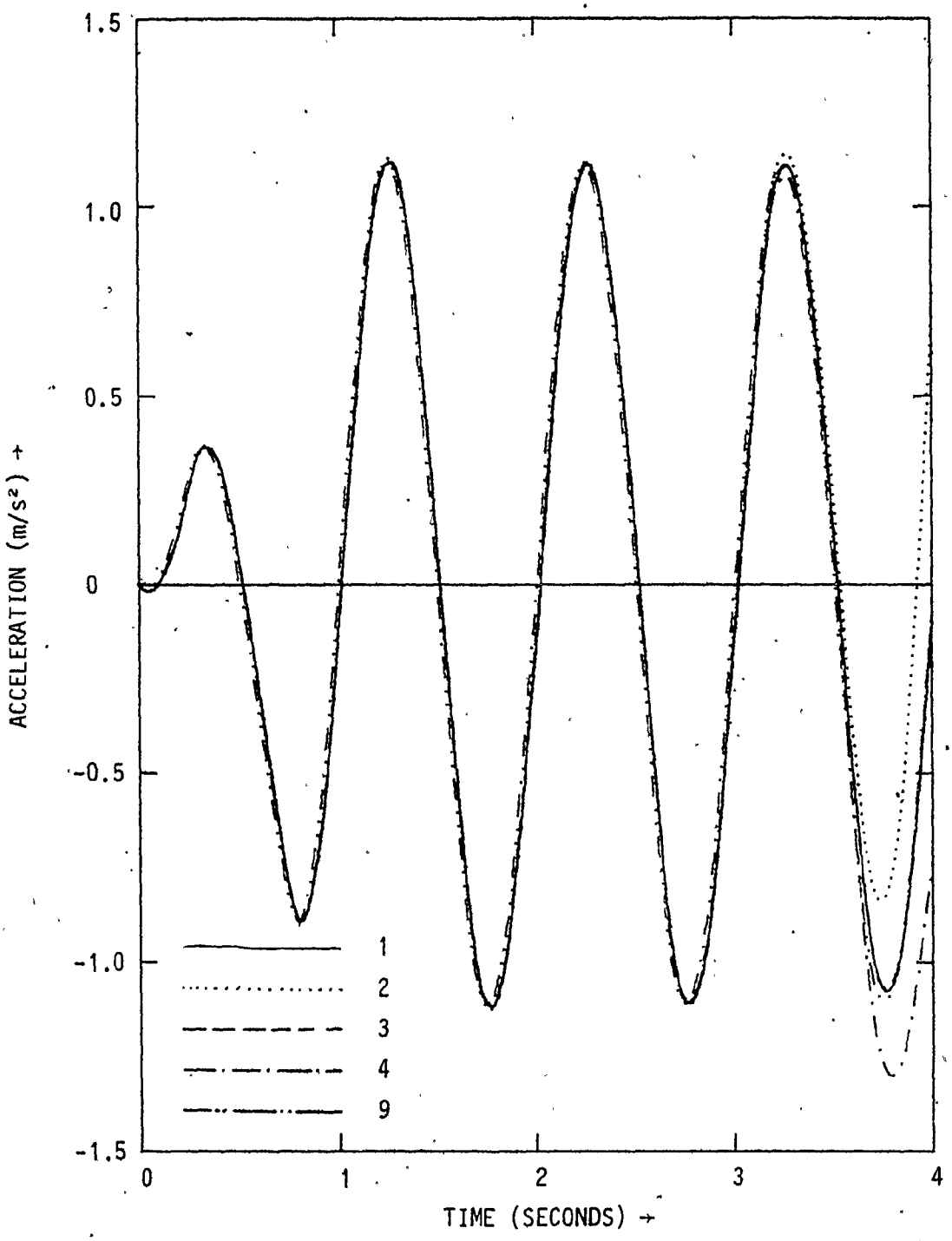

FIGURE 5.10.4 AXIAL ACCELERATIONS FOR THE SYSTEM E2, CASE-2

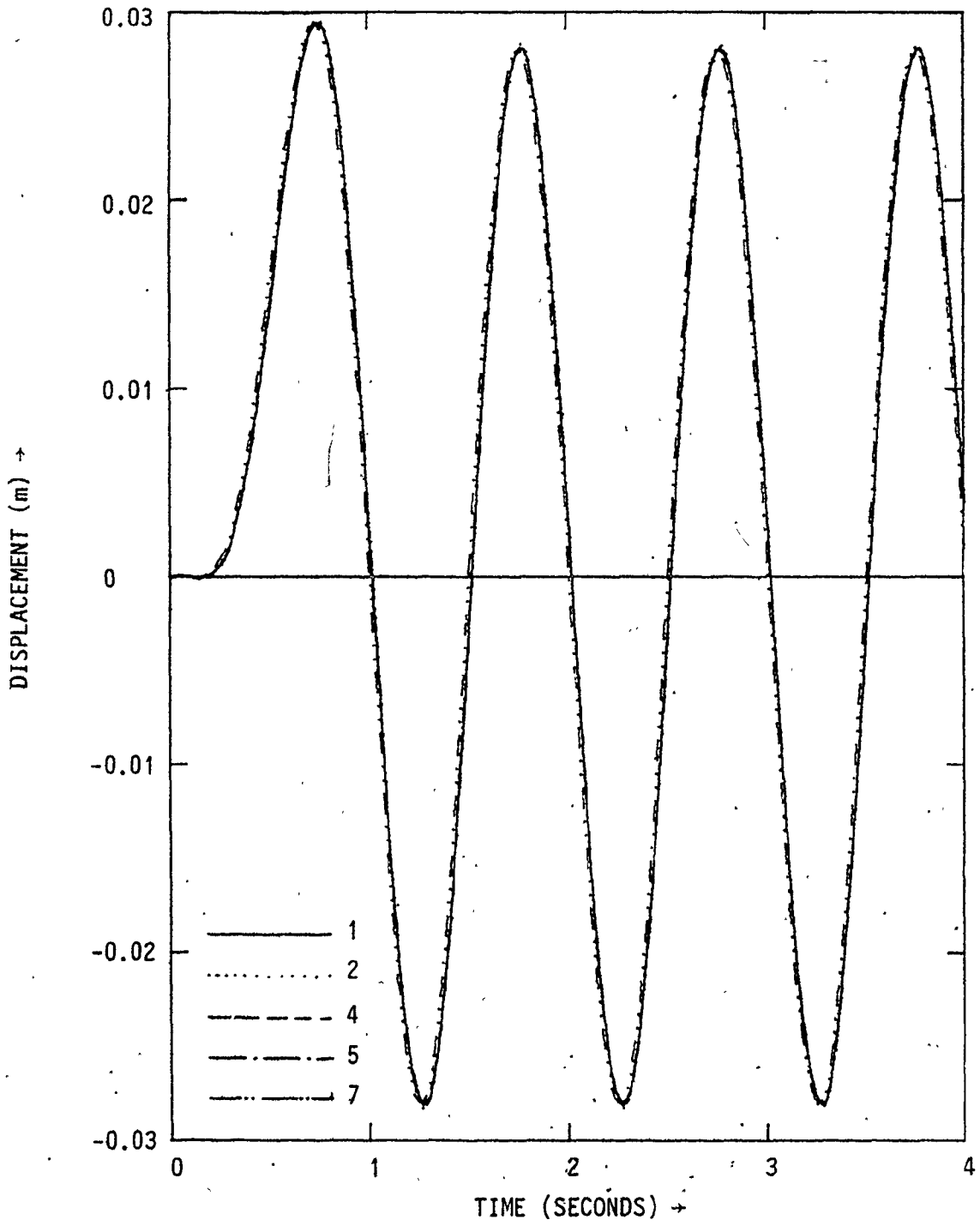

FIGURE 5.10.5 AXIAL DISPLACEMENTS FOR THE SYSTEM E2, CASE-2

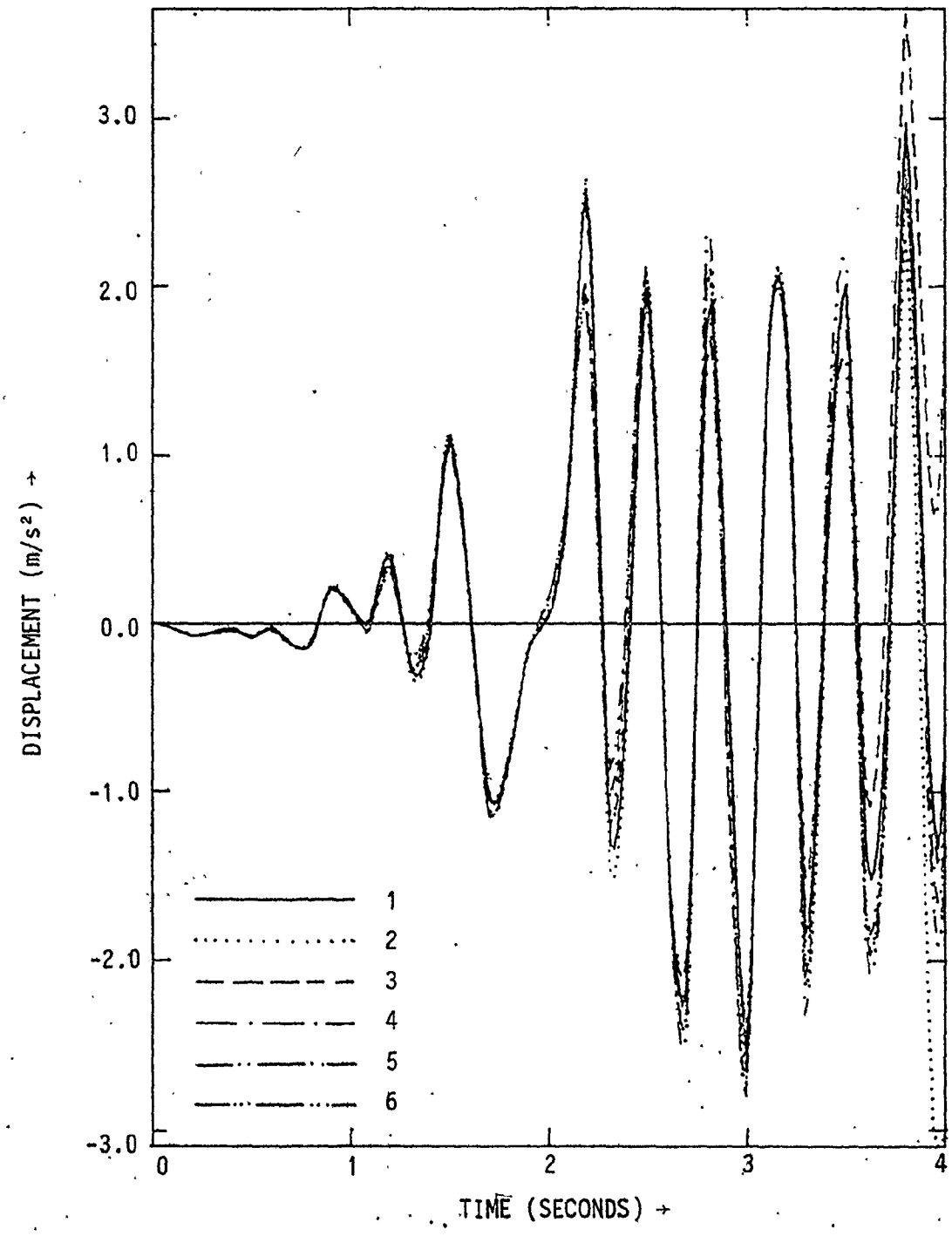

FIGURE 5.10.6 AXIAL ACCELERATION FOR THE SYSTEM E2, CASE-3

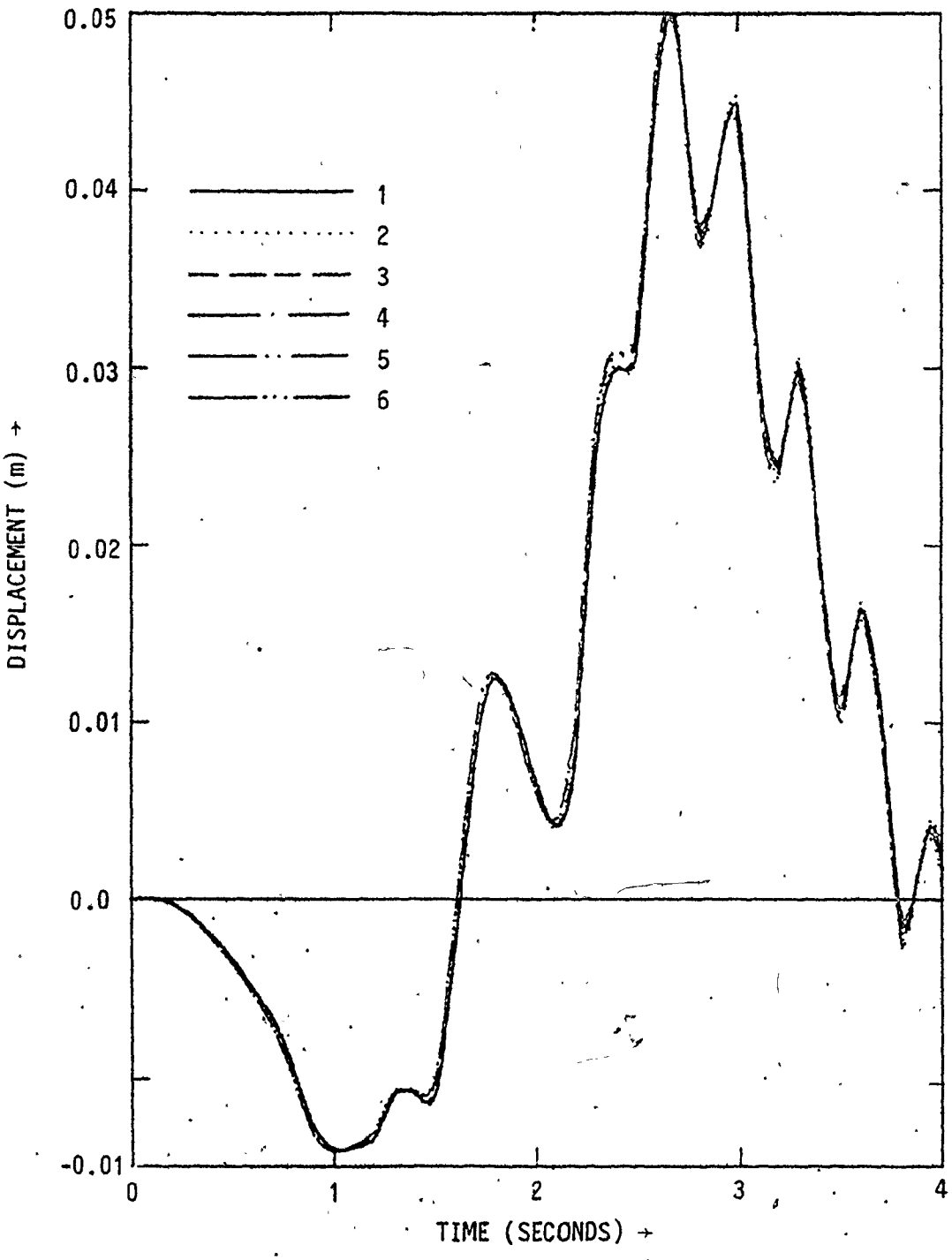

FIGURE 5.10.7 . AXIAL DISPLACEMENTS FOR THE SYSTEM E2, CASE-3

lag of 0.00413 seconds. As such, for case 2 (system E2), the free field motions at positions 9 and 11 may be considered (for the purpose of comparison) to be the same as the free field responses at the outer right and left spring points. The extremely small phase difference between the tunnel response and the corresponding free field response shows that the medium structure interaction has a relatively small influence on the axial displacements for a relatively stiffer medium.

The axial responses for the three cases (system E1, soft medium) indicate that the medium structure interaction has a greater influence on the axial response of the structure (Figures 5.10.8 through 5.10.13). For case 1, the response of the tunnel at the right spring point, crown and invert are practically identical, and appreciably different from the free field responses at these positions. The free field responses at these positions differ appreciably from one another too. The 'phase difference' between the response of the structure and the corresponding free field response is also quite evident. The response of the structure lags behind the corresponding free field response, which is in accordance with reported observations (Appendix A). For case 3, where there are sharp peaks in the earthquake record free field accelerations at the tunnel periphery, the structure-medium interaction smooths these peaks considerably. This can be observed for axial displacements also, but to a lesser extent.

The transverse responses for case 1 (system E2) indicate that there are noticeable differences between the response of the structure at the right spring point, crown and invert positions; and all of them

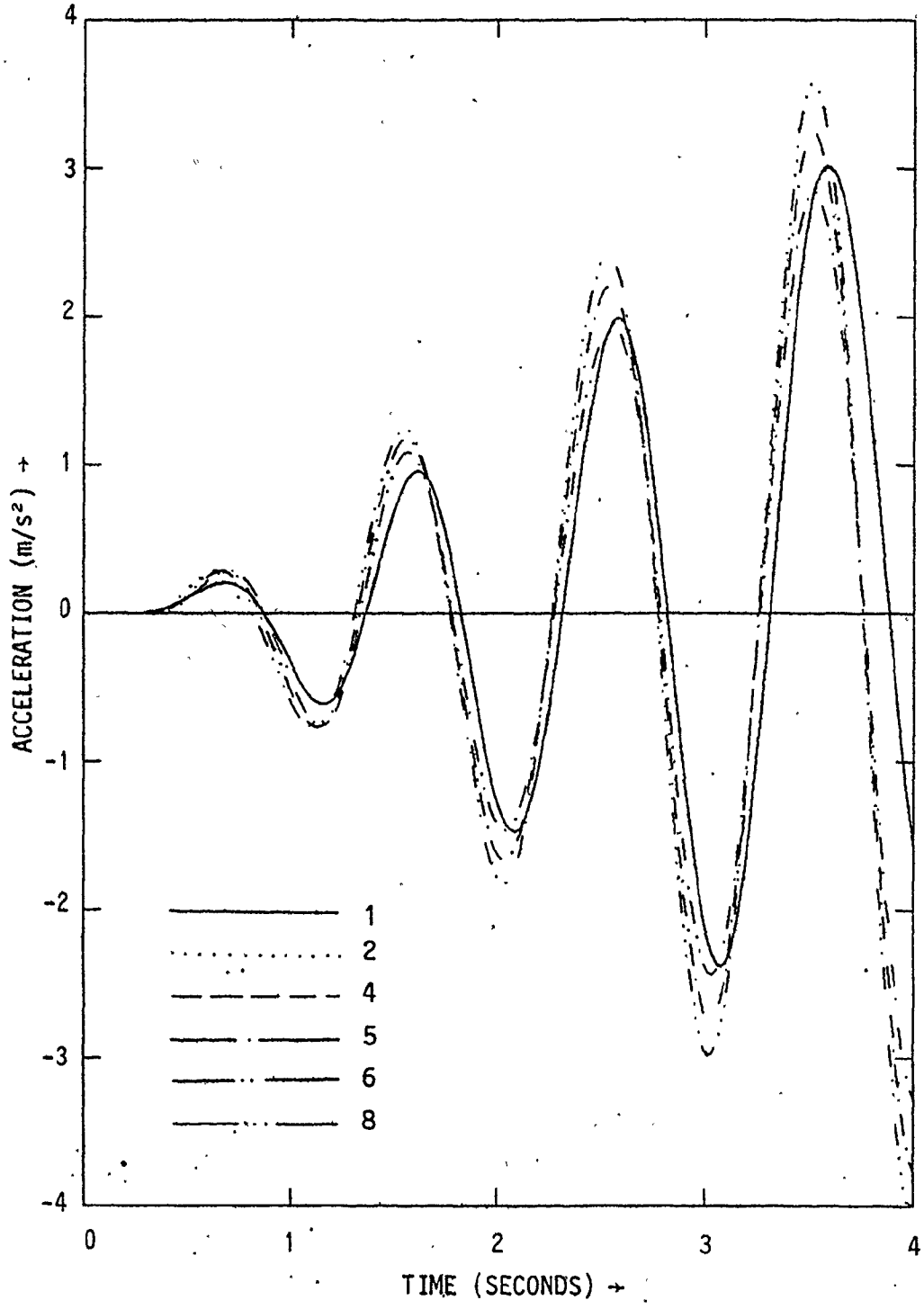

FIGURE 5.10.8 AXIAL ACCELERATIONS FOR SYSTEM E1, CASE-1

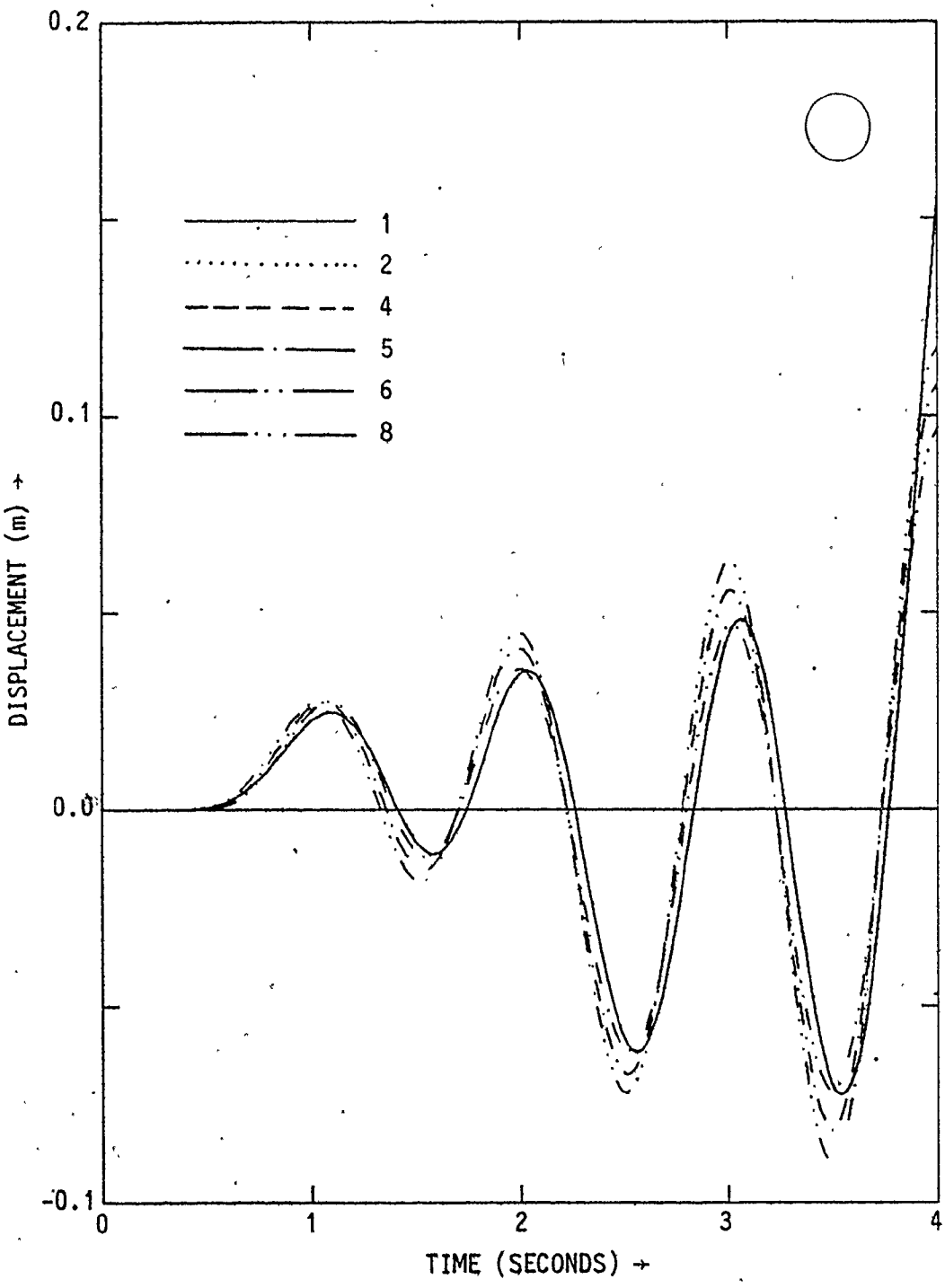

FIGURE 5.10.9 AXIAL DISPLACEMENTS FOR SYSTEM E1, CASE-1

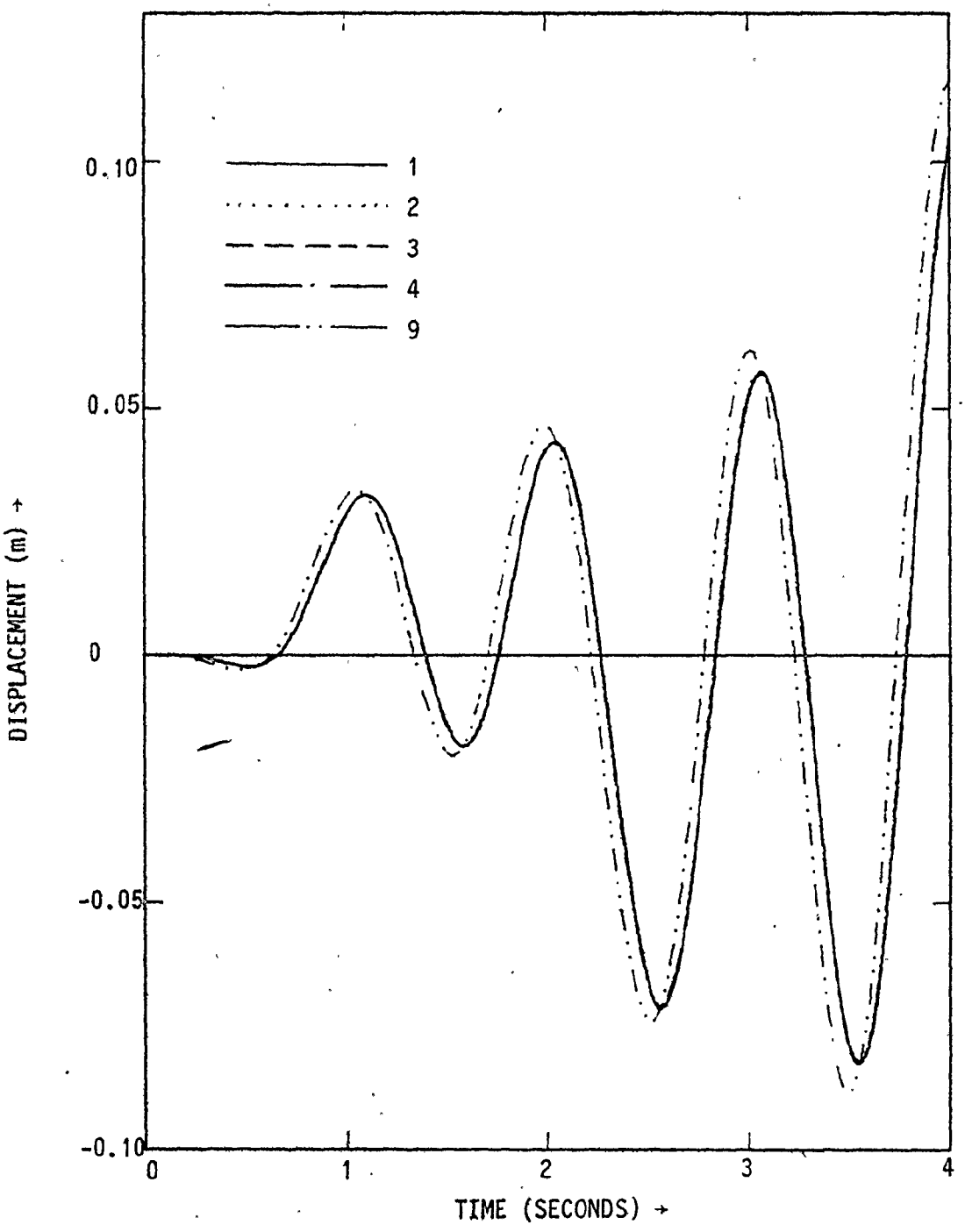

FIGURE 5.10.10 AXIAL DISPLACEMENTS FOR THE SYSTEM E1, CASE-2

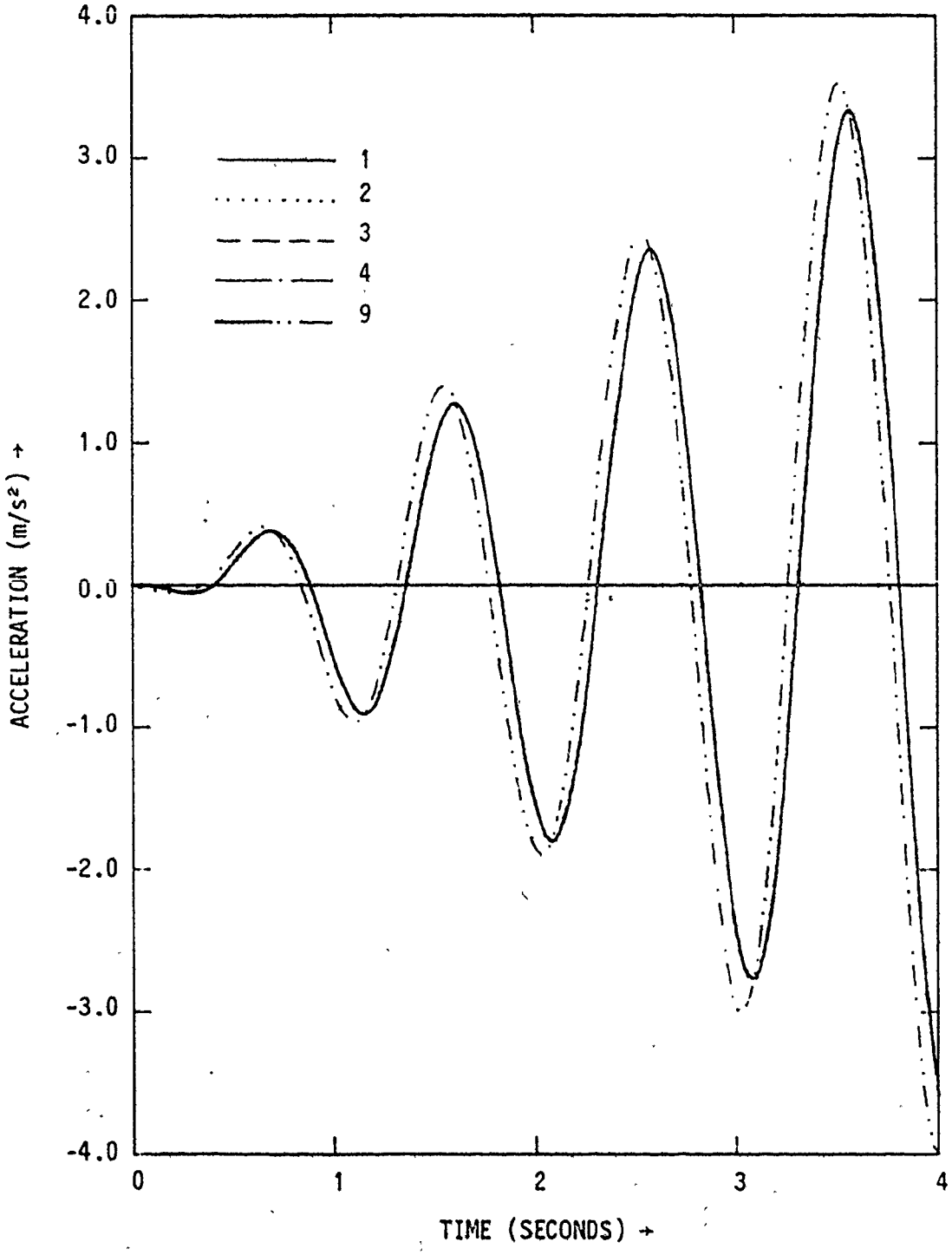

FIGURE 5.10.11 AXIAL ACCELERATION FOR THE SYSTEM E1, CASE-2

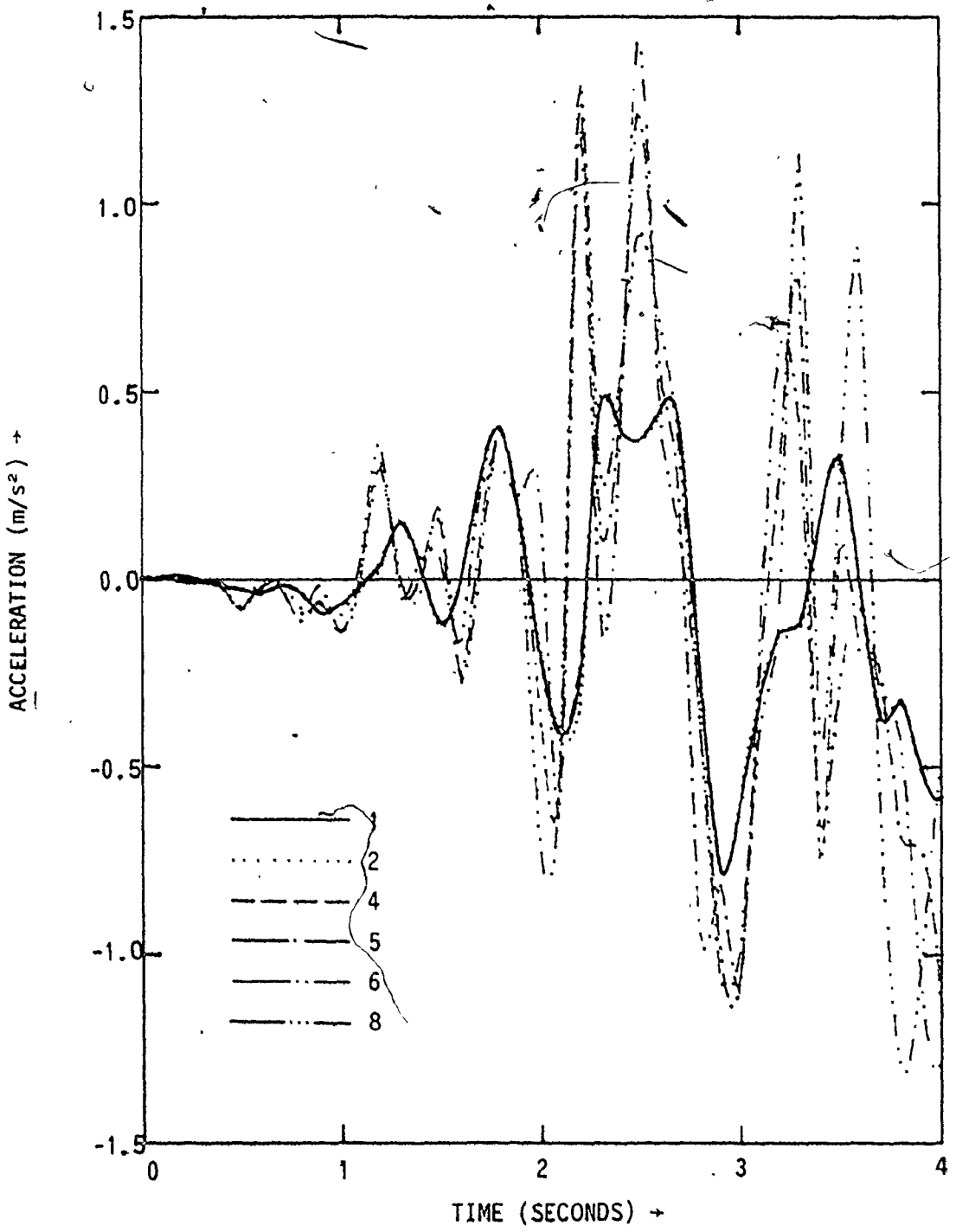

FIGURE 5.10.12 AXIAL ACCELERATIONS FOR THE SYSTEM E1, CASE-3

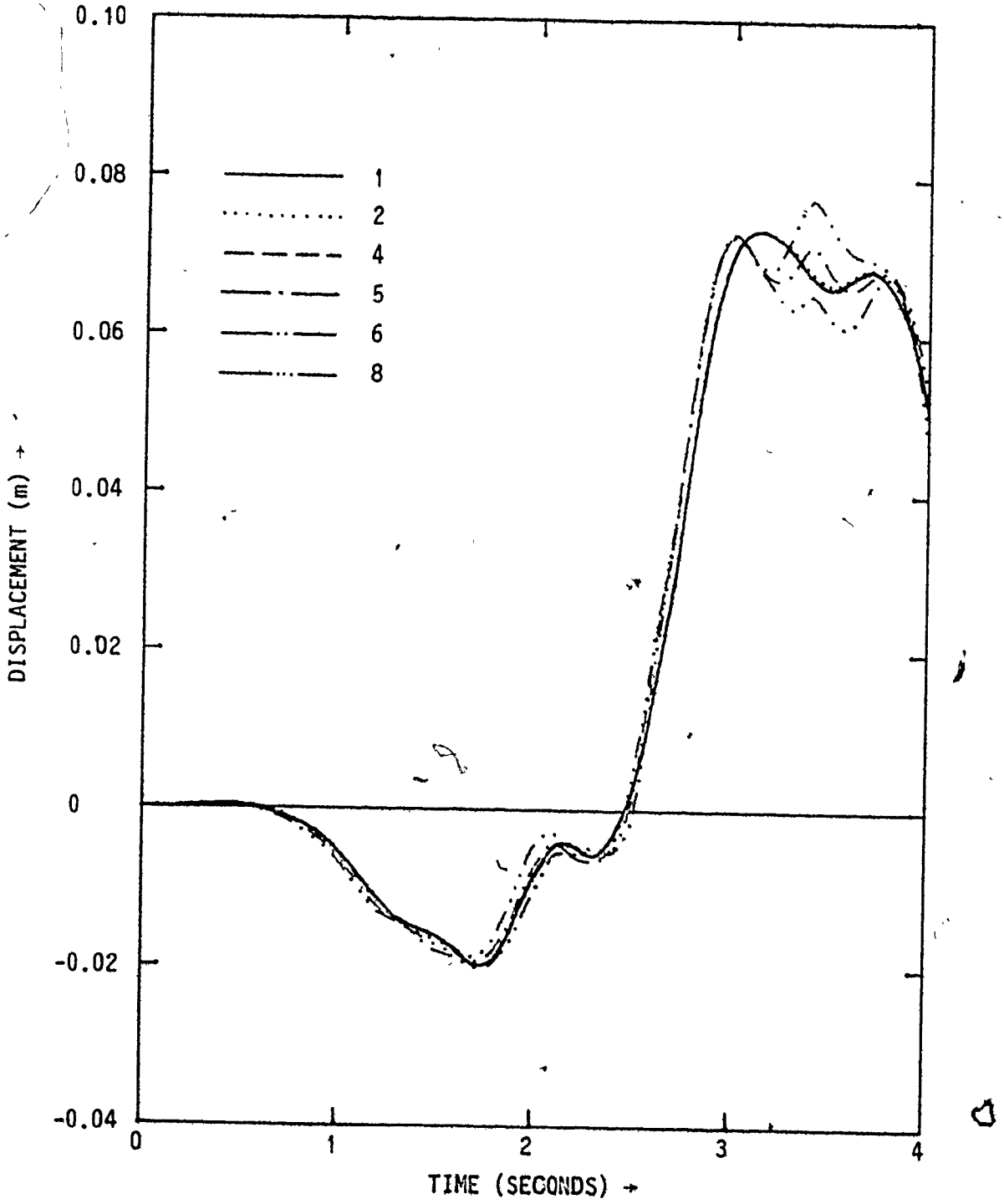

FIGURE 5.10.13 AXIAL DISPLACEMENTS FOR THE SYSTEM E1, CASE-3

are noticeably different from the free field response at the spring points (Figures 5.10.14 and 5.10.15). This is anticipated since the system is more flexible in the transverse direction than in the axial direction, and also because the stiffness of the structure in the transverse directions at the spring points is less than that at the crown or invert positions due to the tunnel cavity. There is little or no evidence of a phase difference between the response of the structure and the free field response at the corresponding positions. For case 1 (system E1), the transverse response of the tunnel is somewhat larger than the free field response at the same point (Figures 5.10.19 and 5.10.20). For case 2 (system E1), it is marginally smaller than the corresponding free field response (Figures 5.10.21 and 5.10.22). The presence of a vertical component of response for this case modifies the response of the structure which causes this change. For case 3, there is no excitation in the transverse direction. As such, the transverse response of the system should be zero at all times. However, as only a finite number of harmonics are considered in the analysis, some small values may be obtained for the transverse response from the dynamic analysis. Figure 5.10.18 shows transverse displacements for case 3 (system E2), which indicate that they are quite small compared to axial or vertical responses.

The vertical responses for case 1 are very small as anticipated, and are not given in the form of figures for system E2. Figures 5.10.25 and 5.10.26 show these responses for system E1. For case 2, the free field responses at the tunnel boundary were not obtained. For comparison

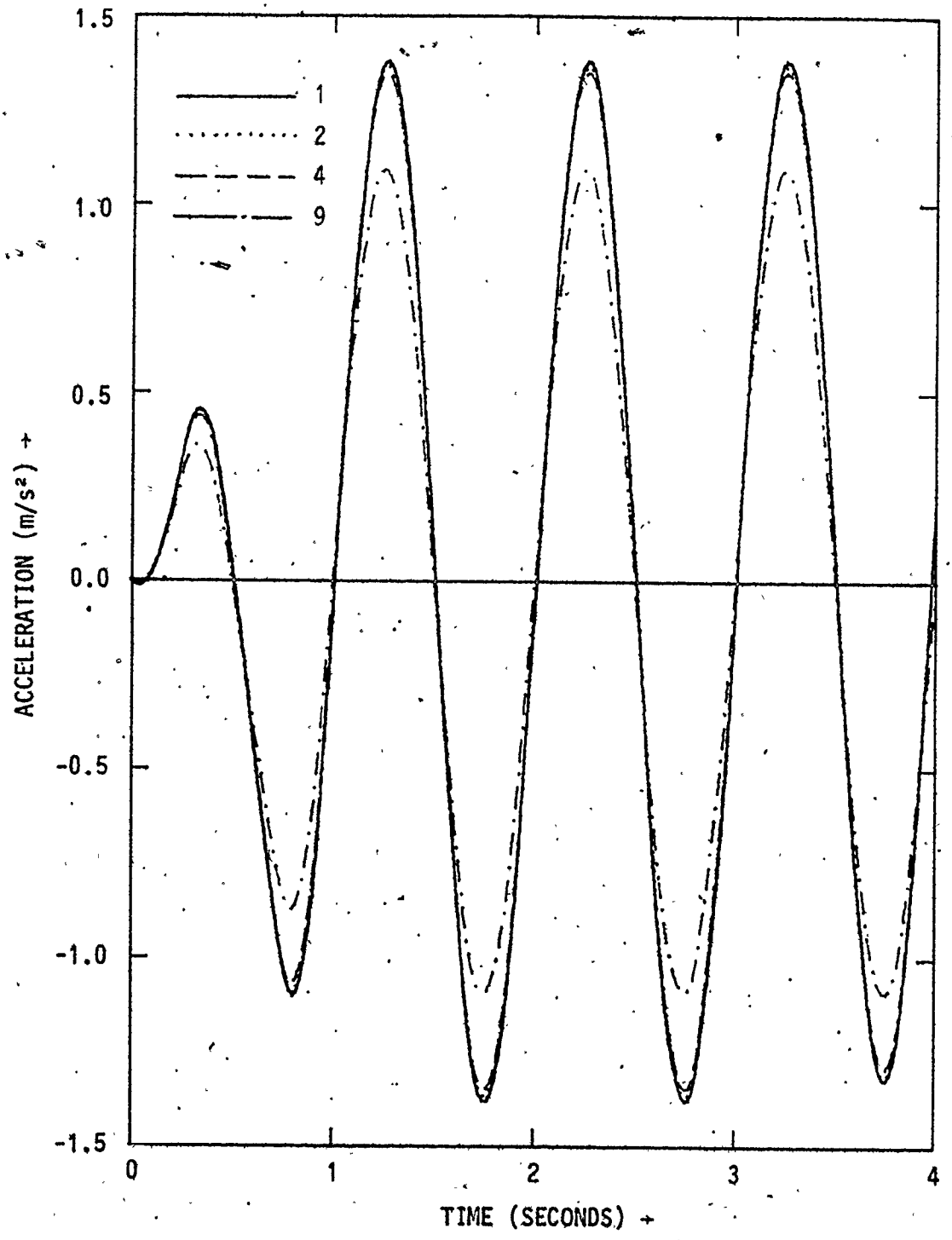

FIGURE 5.10.14 TRANSVERSE ACCELERATIONS FOR SYSTEM E2, CASE-1

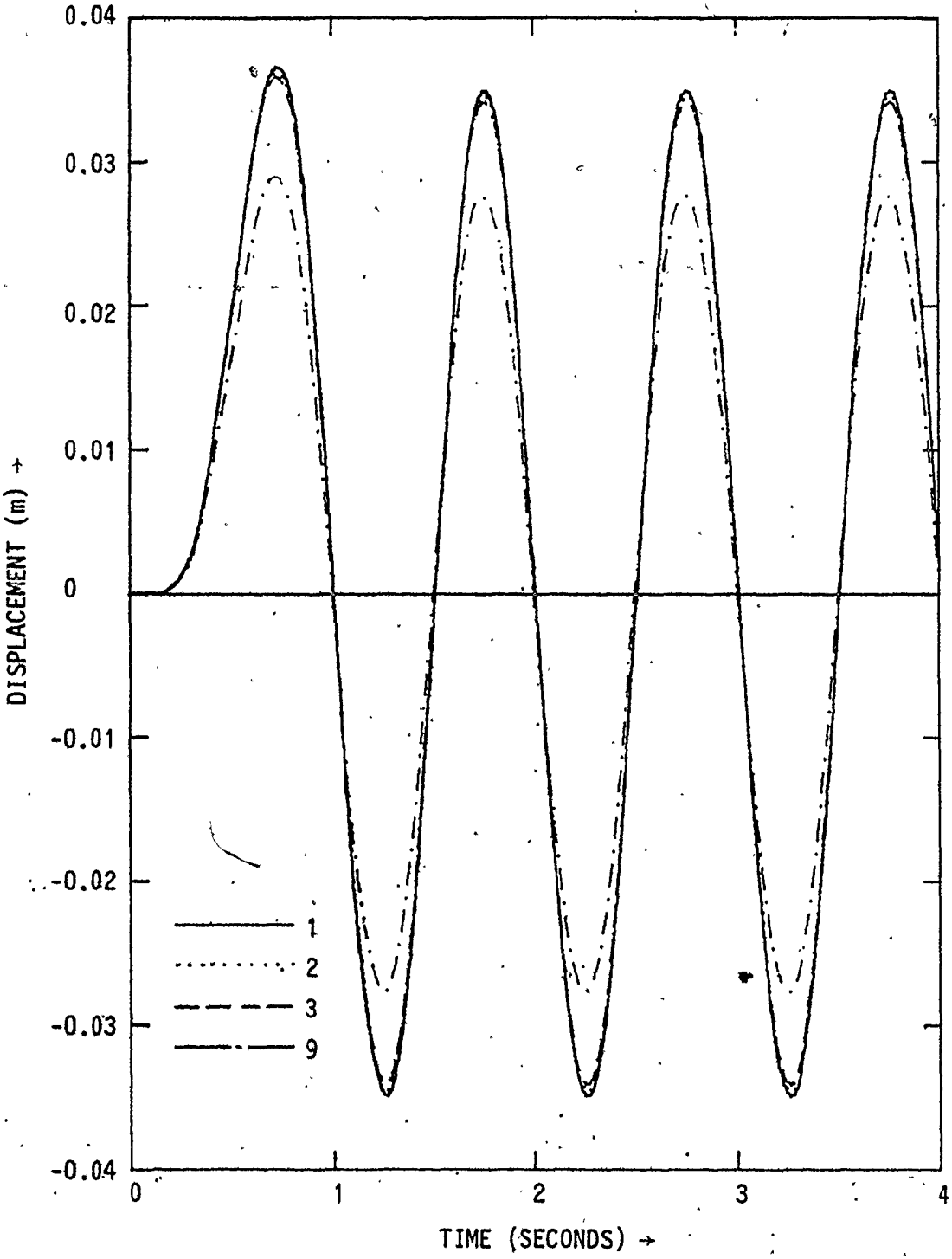

FIGURE 5.10.15 TRANSVERSE DISPLACEMENTS FOR SYSTEM E2, CASE 1

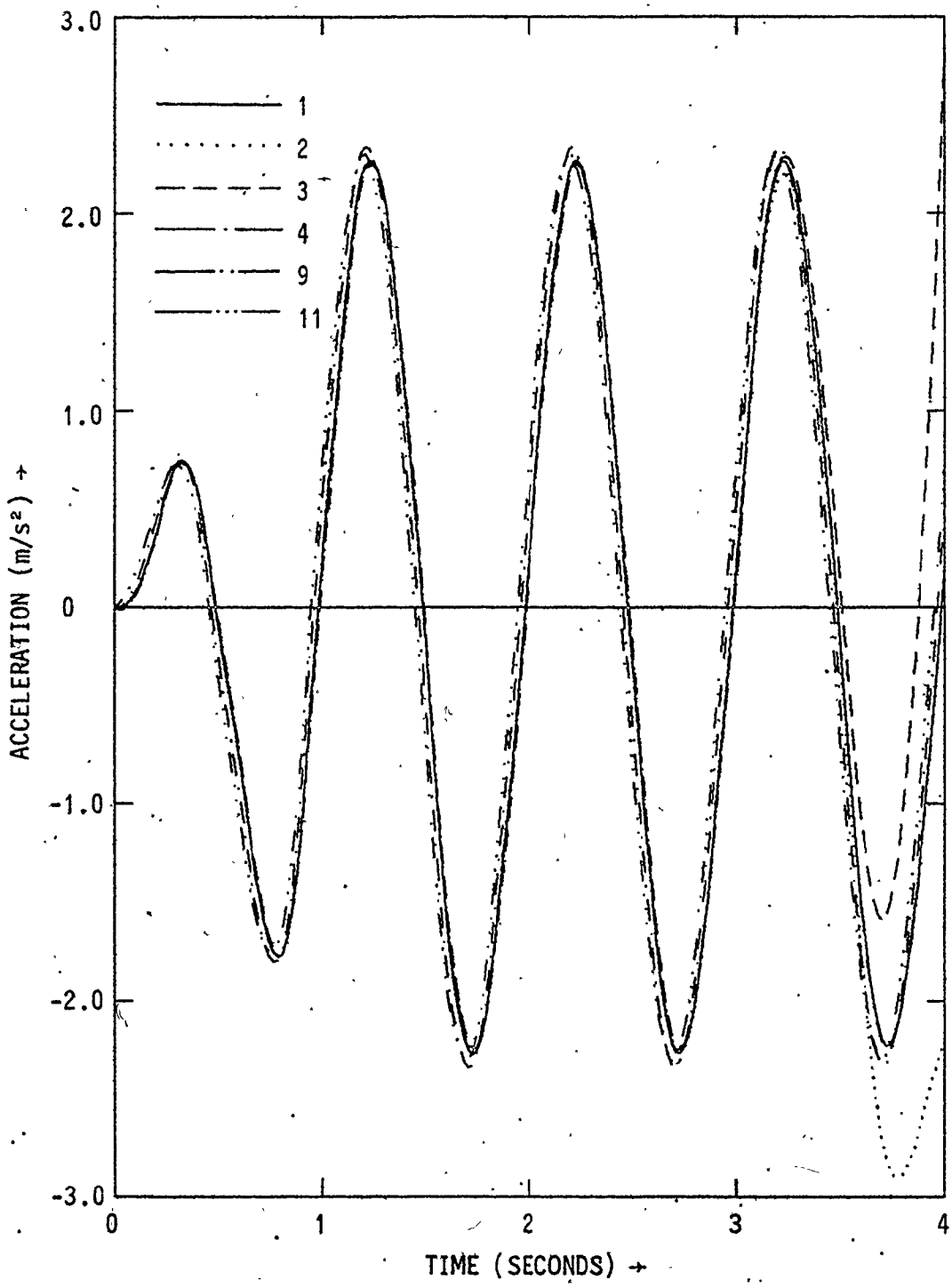

FIGURE 5.10.16 TRANSVERSE ACCELERATIONS FOR THE SYSTEM E2, CASE-2

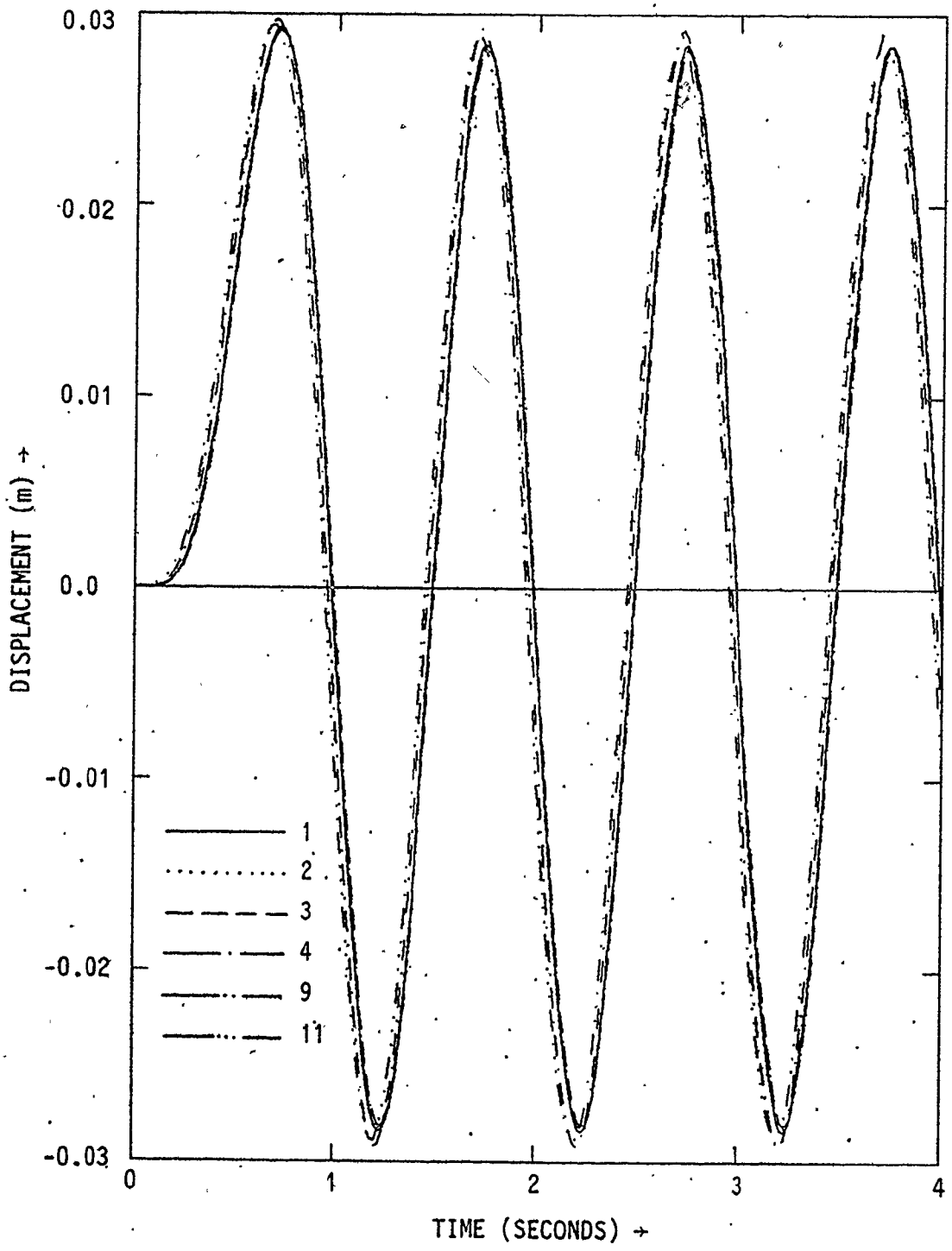

FIGURE 5.10.17 TRANSVERSE DISPLACEMENTS OF THE SYSTEM E2, CASE 2

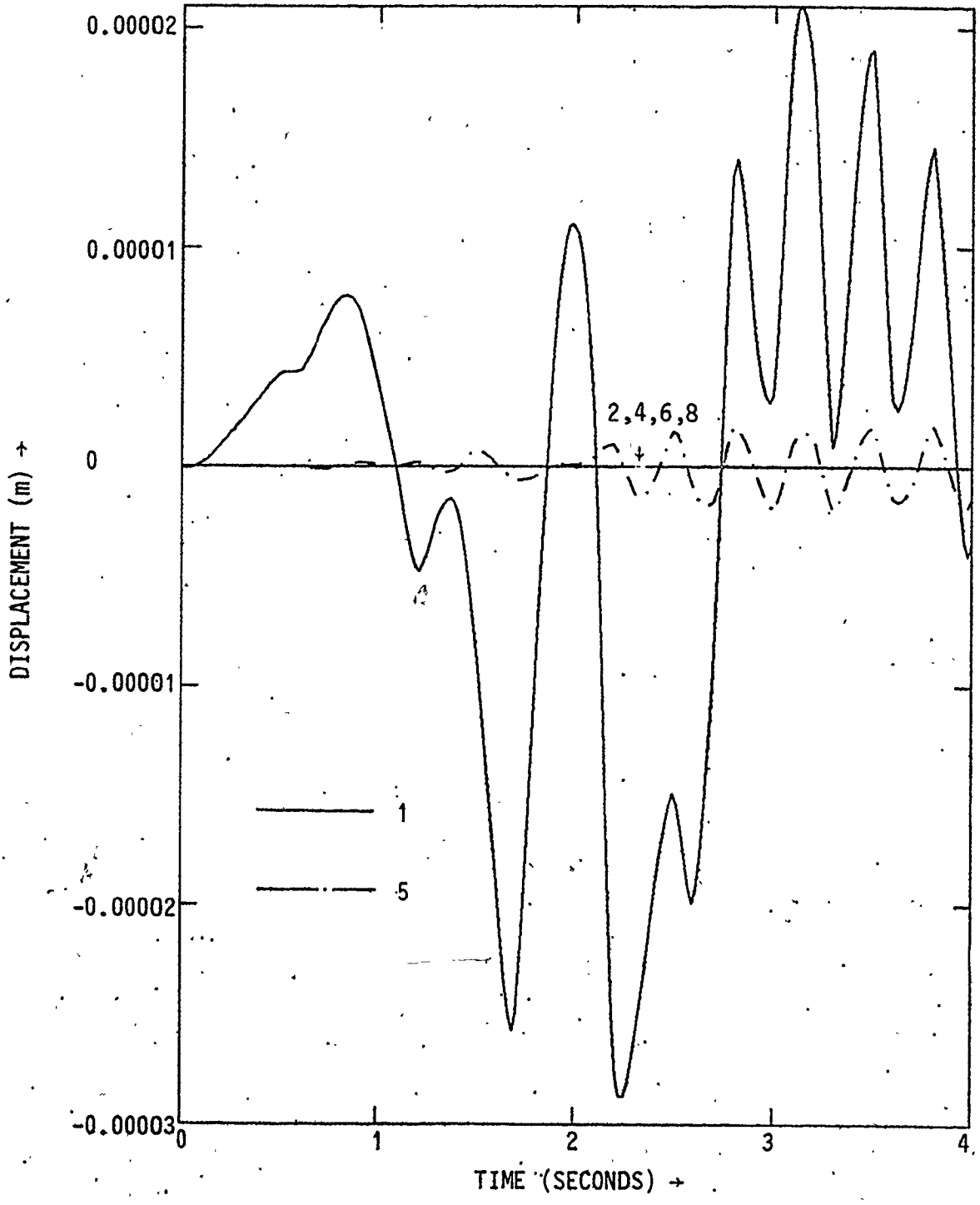

FIGURE 5.10.18 TRANSVERSE DISPLACEMENTS FOR SYSTEM E2, CASE-3

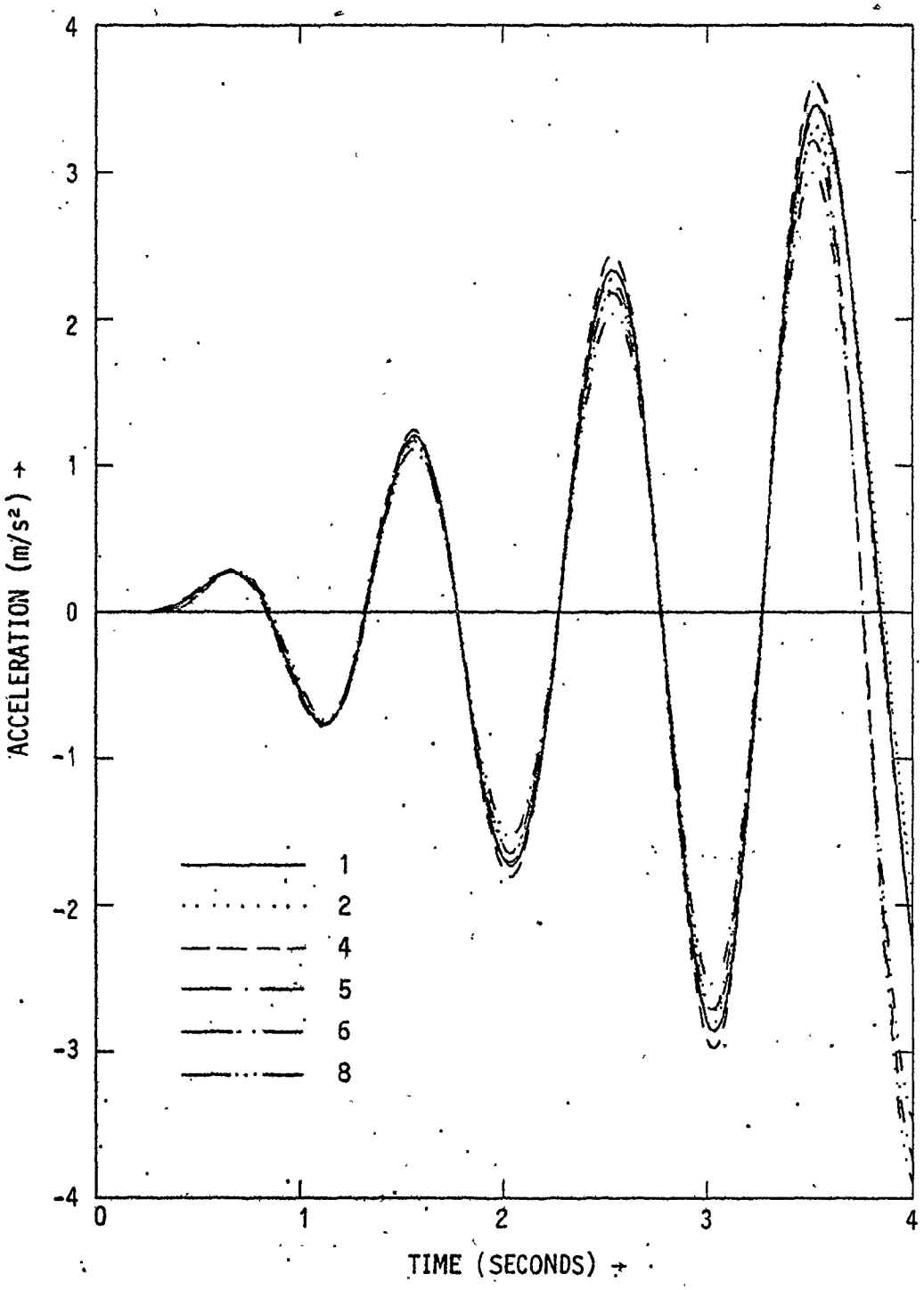

FIGURE 5.10.19 TRANSVERSE ACCELERATIONS FOR THE SYSTEM E1, CASE-1

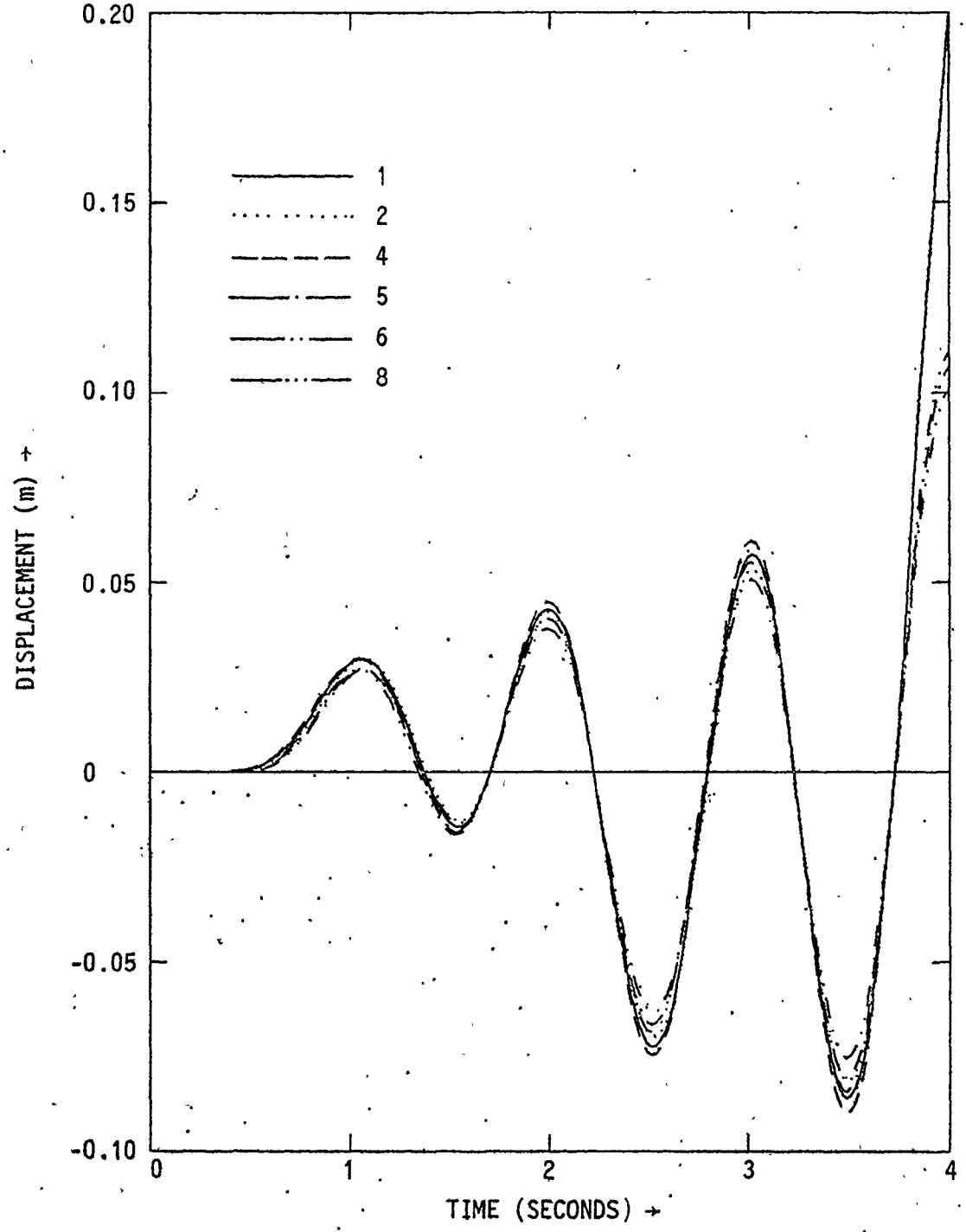

FIGURE 5.10.20 TRANSVERSE DISPLACEMENTS FOR SYSTEM E1, CASE 1

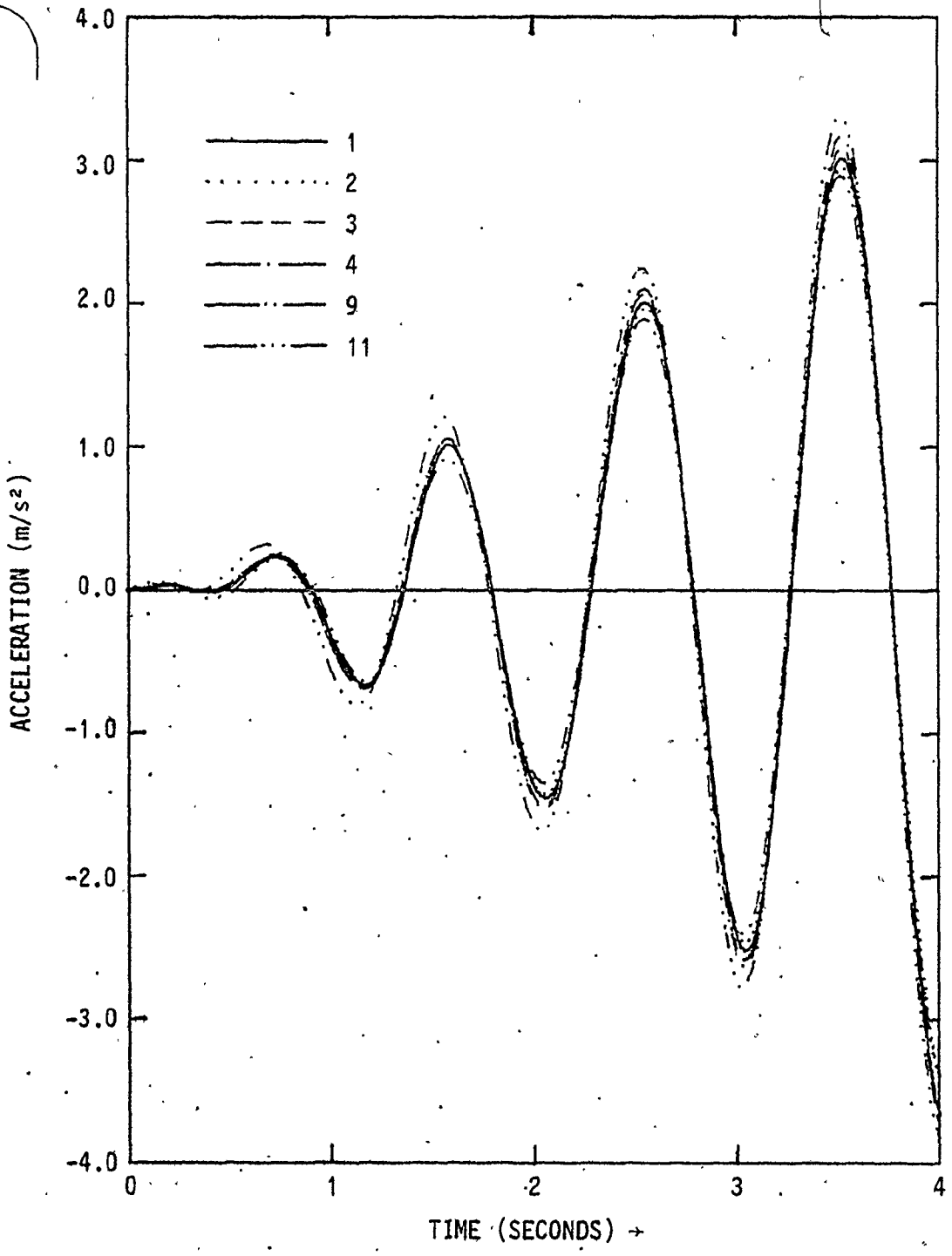

FIGURE 5.10.21 TRANSVERSE ACCELERATIONS FOR SYSTEM E1, CASE 2

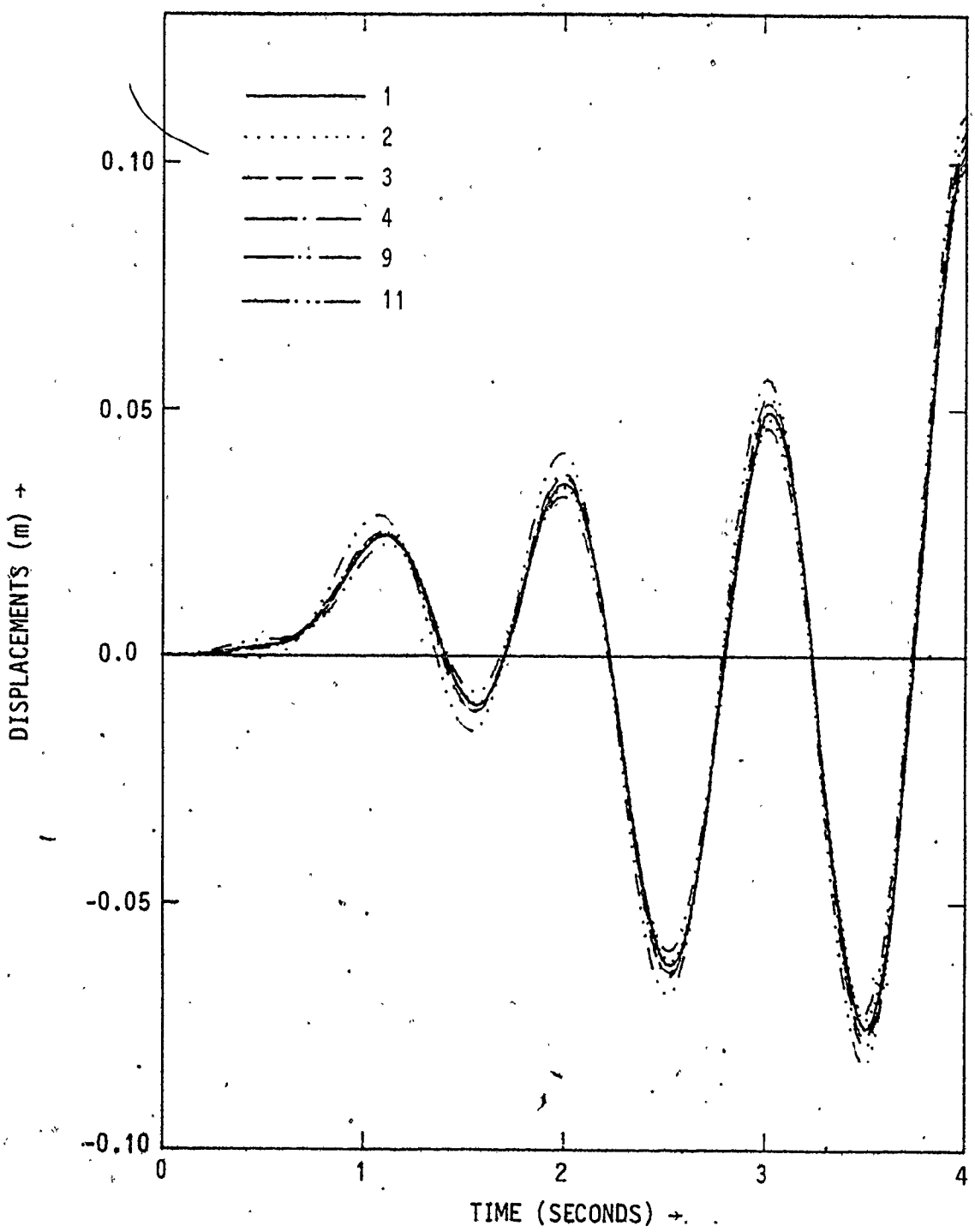

FIGURE 5.10.22 TRANSVERSE DISPLACEMENTS FOR SYSTEM E1, CASE-2

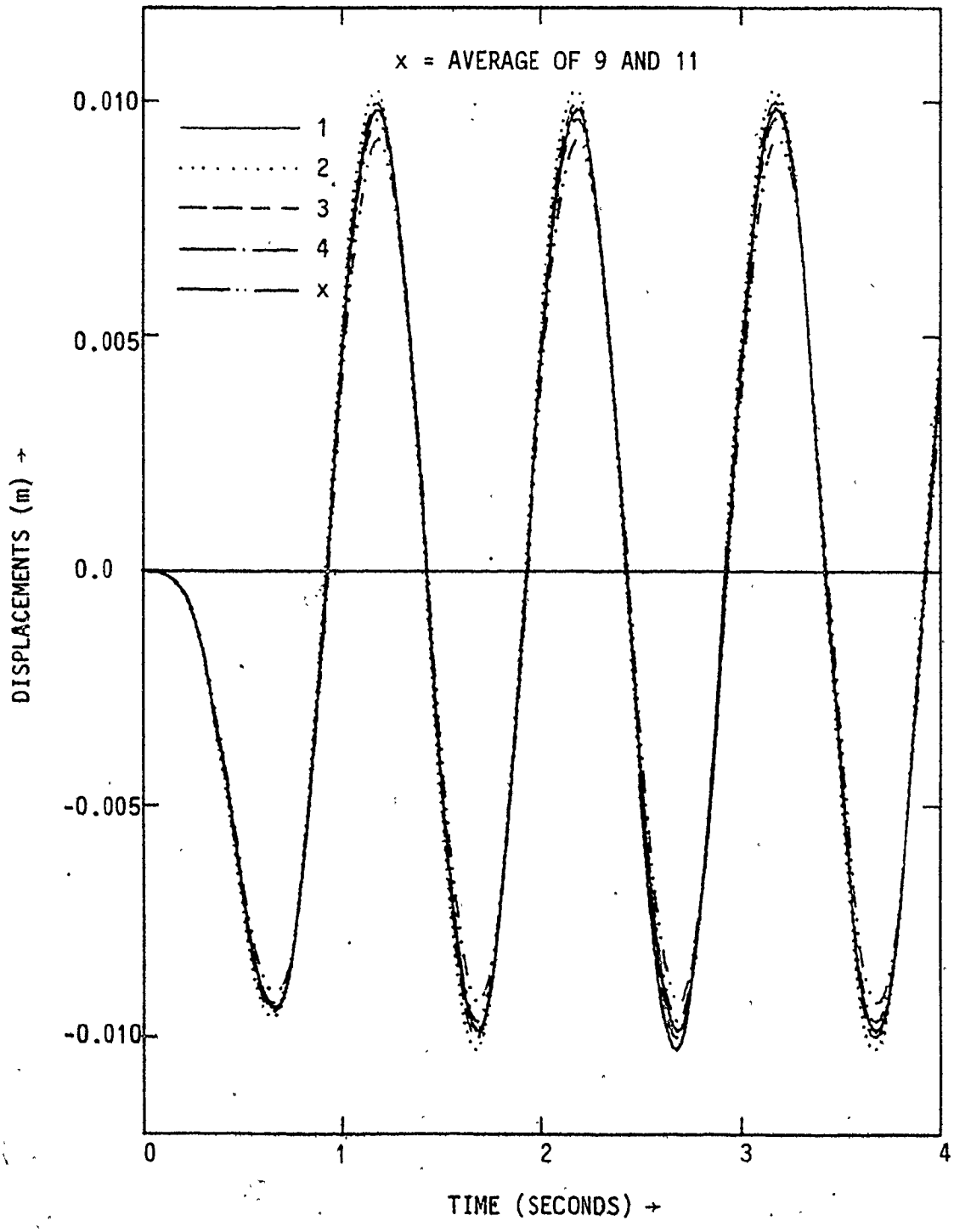

FIGURE 5.10.23 VERTICAL DISPLACEMENTS FOR SYSTEM E2, CASE-2

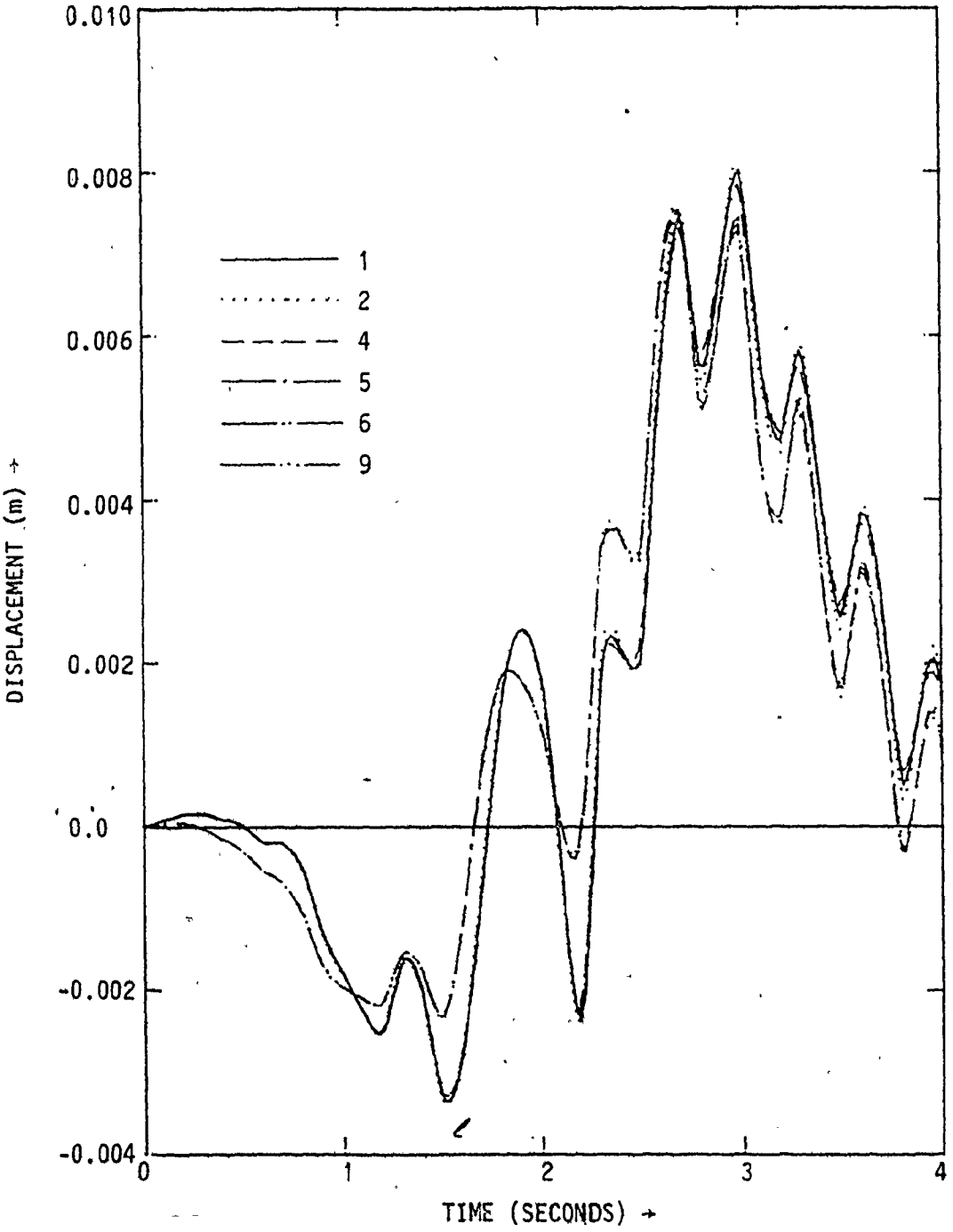

FIGURE 5.10.24 VERTICAL DISPLACEMENTS FOR THE SYSTEM E2, CASE-3

purposes, the mean of the vertical responses at the free field boundary (r = 20 m) on its horizontal diameter are considered to be a good estimate of the free field vertical response at the spring points. (The horizontal distances involved result in very small time lags for system E1 and E2.) The vertical displacements at the four positions for case 2 (system E1) show noticeable differences, which indicate the distortion that the structure undergoes in the vertical (transverse) plane (Figure 5.10.27). From the same figure, it may also be noted that these responses at the tunnel periphery differ noticeably from the (averaged) free field vertical response. Similar observations can be made for case 2 (system E2), although the differences are much smaller (Figure 5.10.23). The vertical displacements for case 3 for both systems also highlight similar observations showing the influence of the medium structure interaction on vertical resonses (Figures 5.10.24 and 5.10.29).

In Chapter 4, a method was suggested for considering continuity of the system in the axial direction. In that discussion, the analyses included only the vertical propagation of shear waves. A further consideration of this method is summarized here. Figure 5.10.30 gives the displacements of the right spring point positions along the length of the tunnel for case 1 (system E1). The distance between the donor (interior) nodes and the receiver (boundary) nodes in this case is 30.72 m. The suggested method has kept the difference between the response at the mid-span cross section and that at the end section to under 1.2% for axial displacements, and under 2.5% for radial displacements. For vertical displacements there is hardly any noticeable variation. For case 2 (system E1 - inclined shear wave propagation), it may be

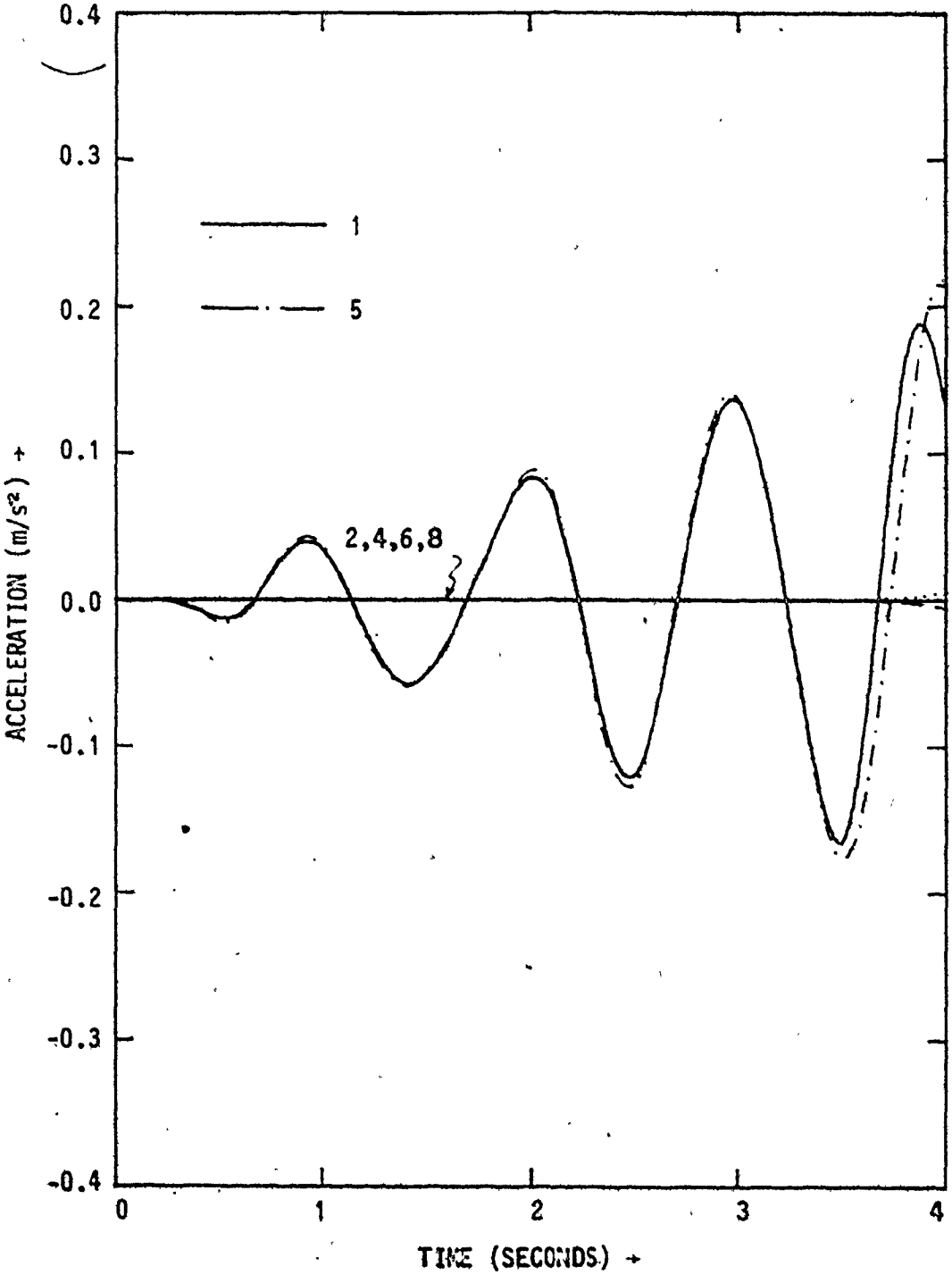

FIGURE 5.10.25 VERTICAL ACCELERATIONS FOR SYSTEM E1, CASE-1

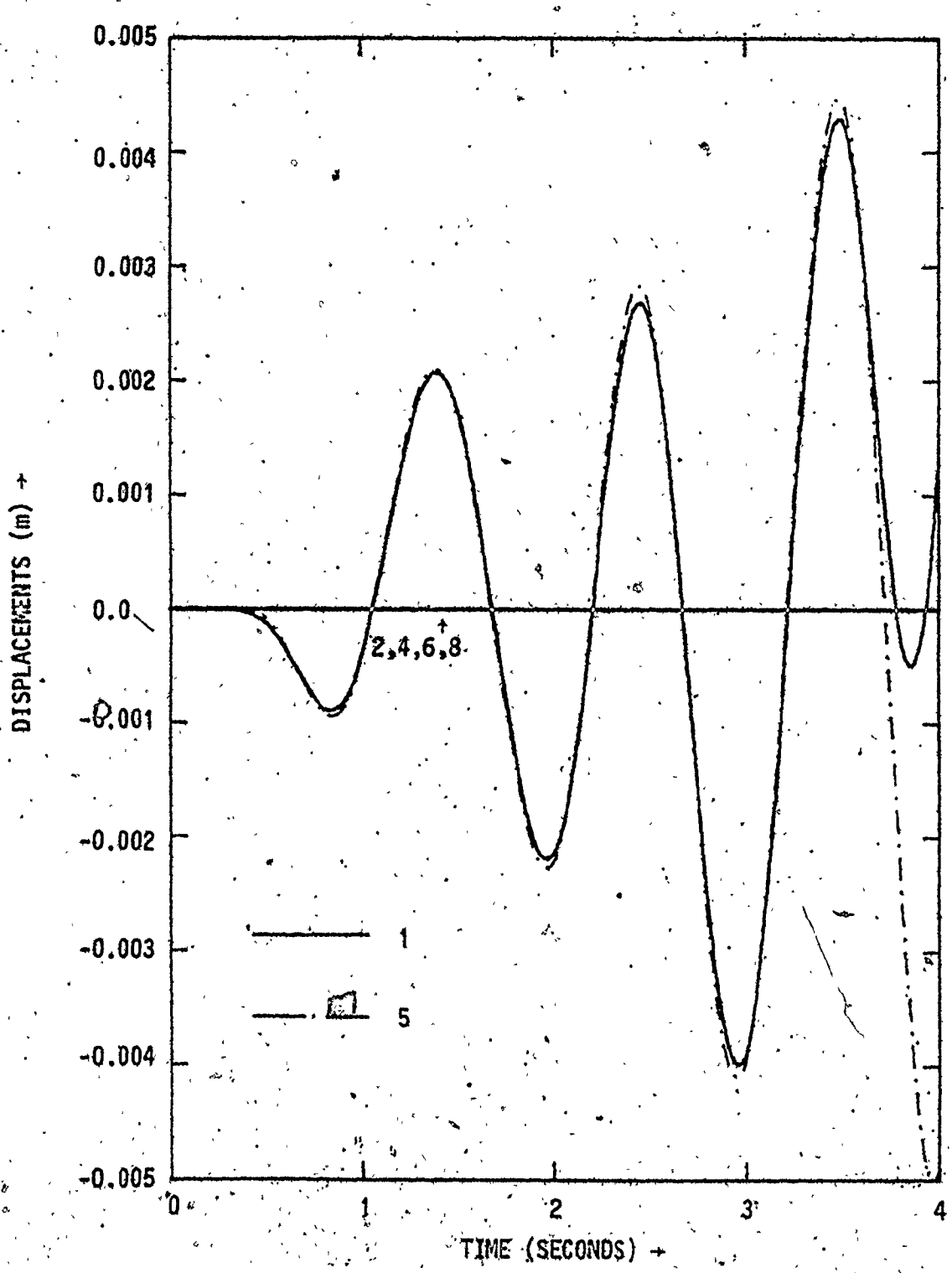

FIGURE 5.10.26 VERTICAL DISPLACEMENTS FOR SYSTEM E1, CASE-1

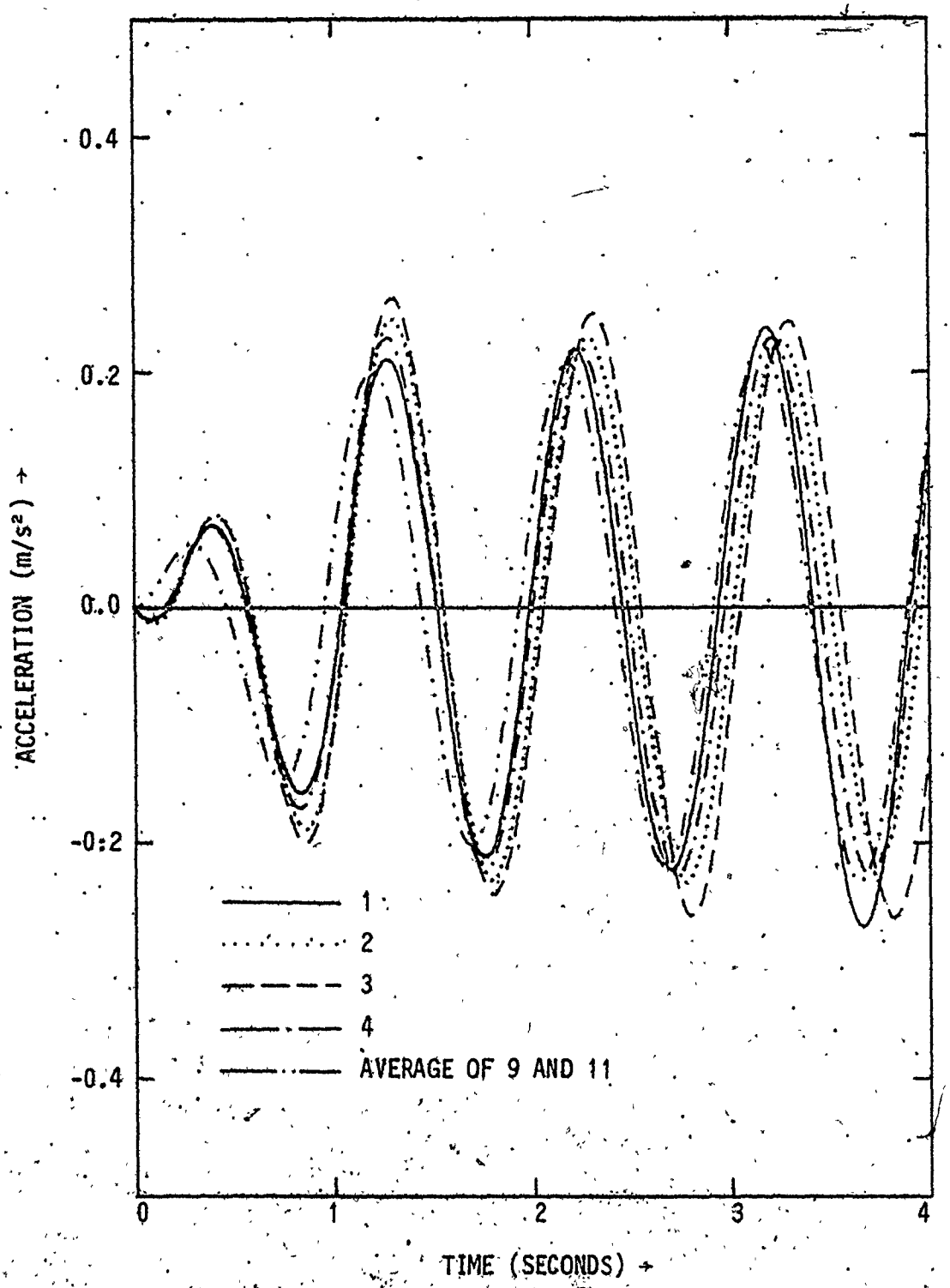

FIGURE 5.10.27 VERTICAL ACCELERATION FOR SYSTEM E1, CASE-2

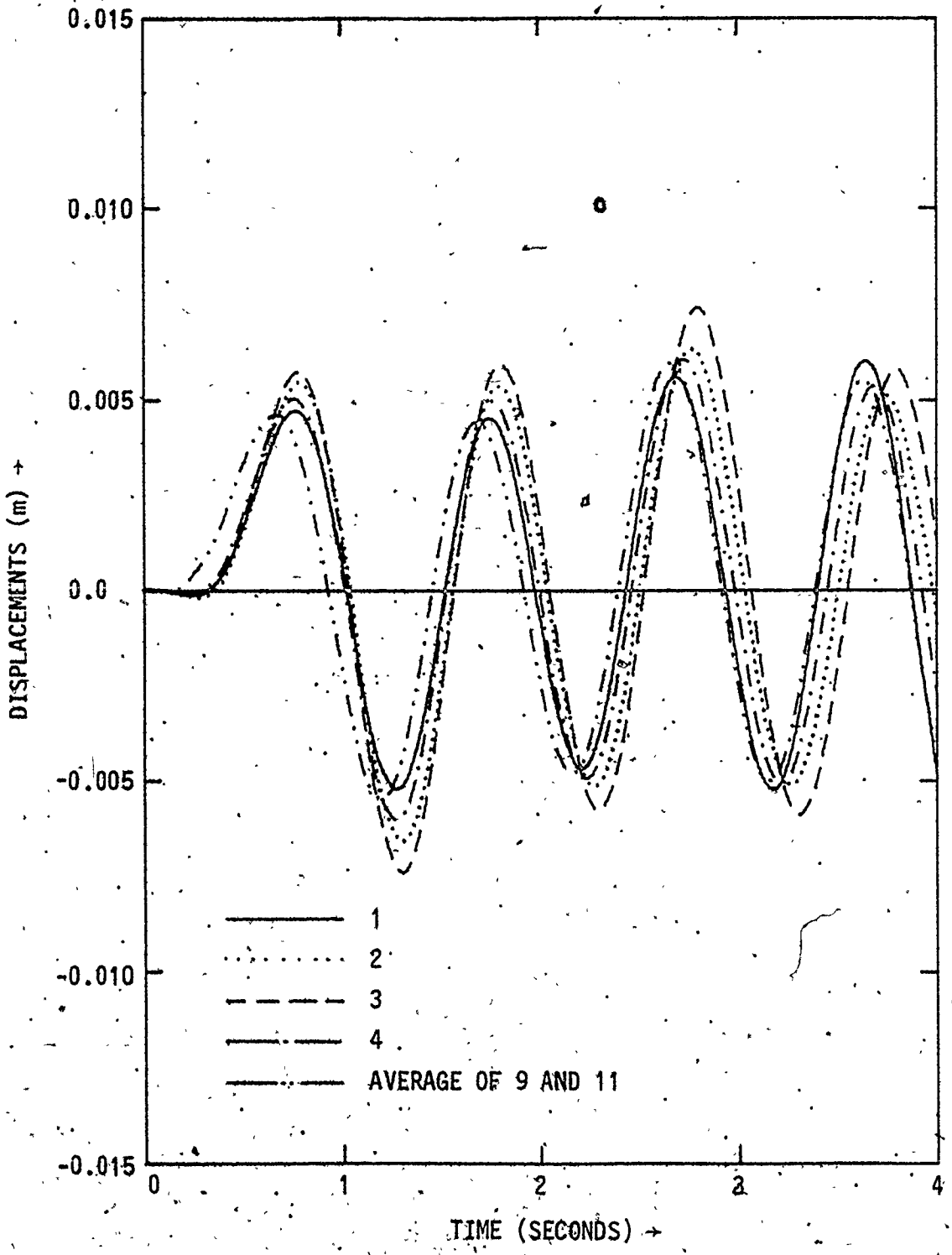

FIGURE 5.10.28 VERTICAL DISPLACEMENTS FOR SYSTEM E1, CASE-2

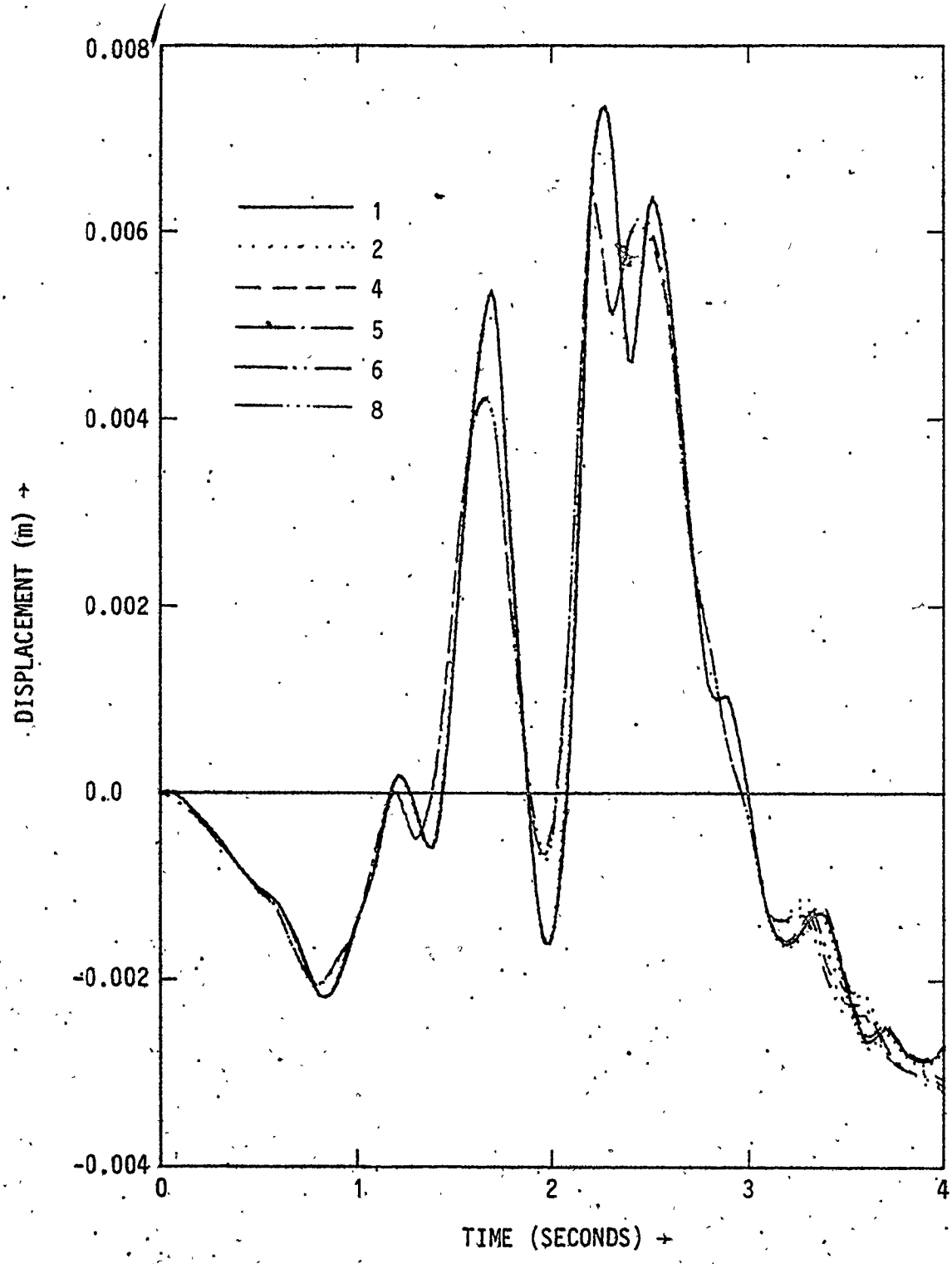

FIGURE 5.10.29 VERTICAL DISPLACEMENTS FOR SYSTEM E1, CASE-3

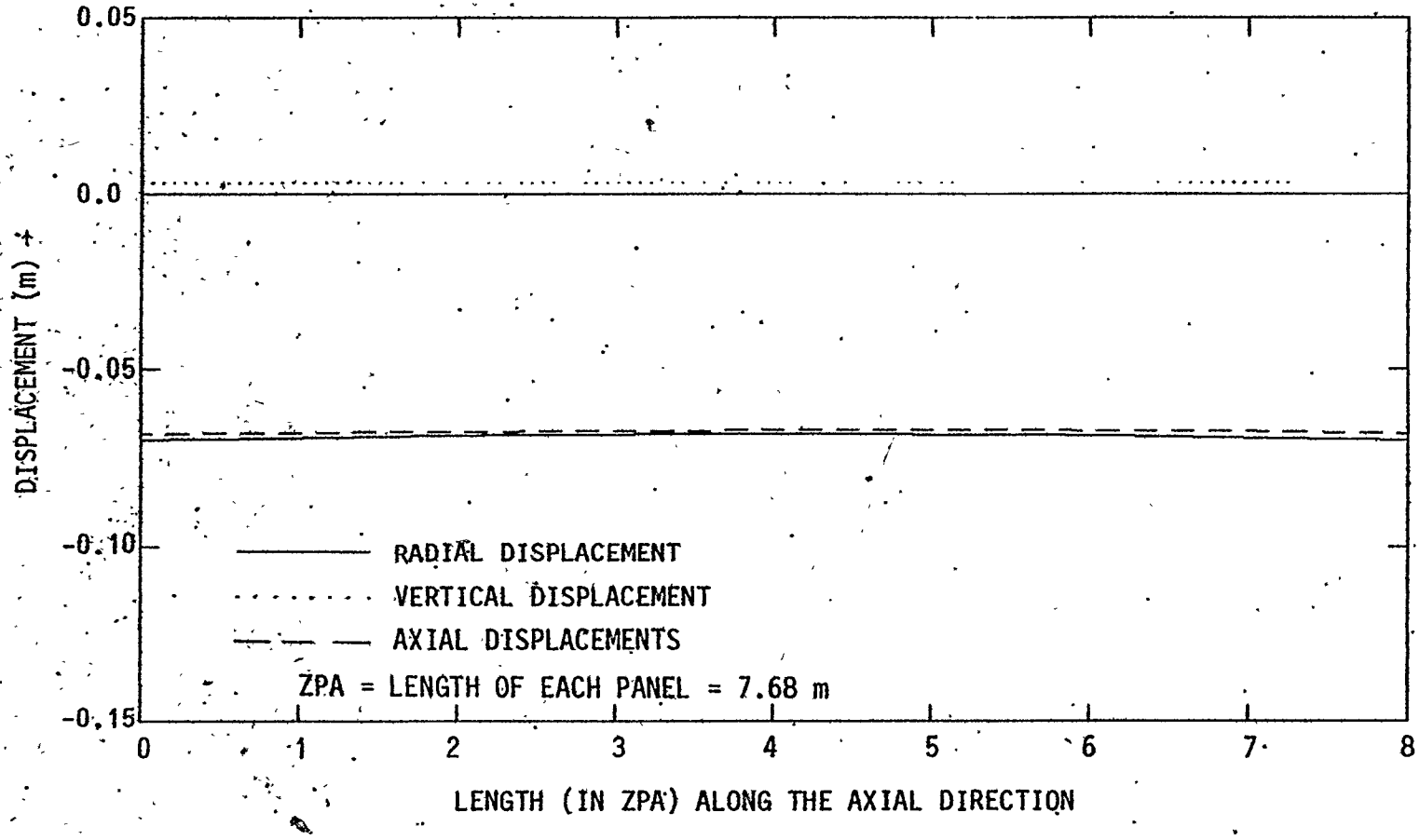

FIGURE 5.10.30 DISPLACEMENTS AT RIGHT SPRINGPOINT ALONG THE LENGTH OF THE TUNNEL FOR SYSTEM E1, CASE-1

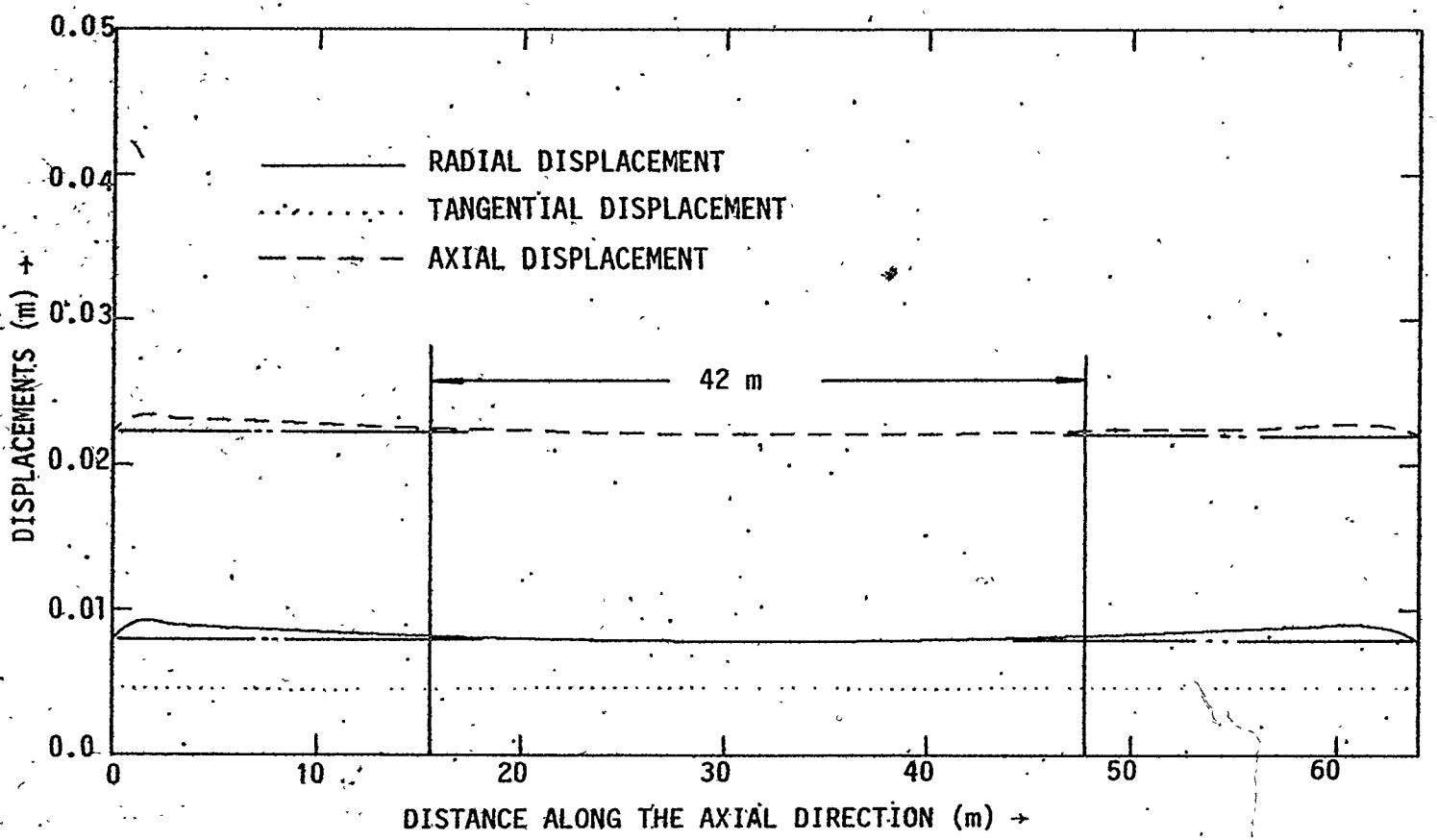

FIGURE 5.10.31 DISPLACEMENTS ALONG THE LENGTH OF THE TUNNEL AT THE RIGHT SPRING POINT POSITIONS FOR SYSTEM E1, CASE 2.

noted that some influence of the assumed responses at the transverse ends is present, as anticipated. As suggested in Chapter 4, the basic idea is to strike a balance between the extra length of the system to reduce such errors, and the distance between donor and receiver nodes. From Figure 5.10.31, there is hardly any variation in the computed response in the middle 42 m span of the tunnel, which shows that the suggested method has worked the way it was intended. Case 2 (system E1) has one advantage in this matter as the angle of shear wave propagation is very small (1.3°). A similar plot for case 3 (system E2) is given in Figure 5.10.32. The radial (or transverse) displacements are close to zero as anticipated. It is difficult to assess the amount of error introduced by the assumed end responses, because the angle of shear wave propagation is large, resulting in a noticeable variation in response along the tunnel length. The variation of the response at the free field boundary gives some indication, but does not quantify it. This is considered again in the next section on stresses.

5.10.3 STRESSES OBTAINED FROM THE DYNAMIC ANALYSES

The simplest of the three cases to consider for stresses is case 3, where the displacements in the transverse direction are zero. Since the shear wave propagates at an angle, vertical displacements are present, with values changing along the tunnel length. These differential vertical displacements give rise to shear in the z-θ plane at the spring points, and normal stresses in the axial direction at the

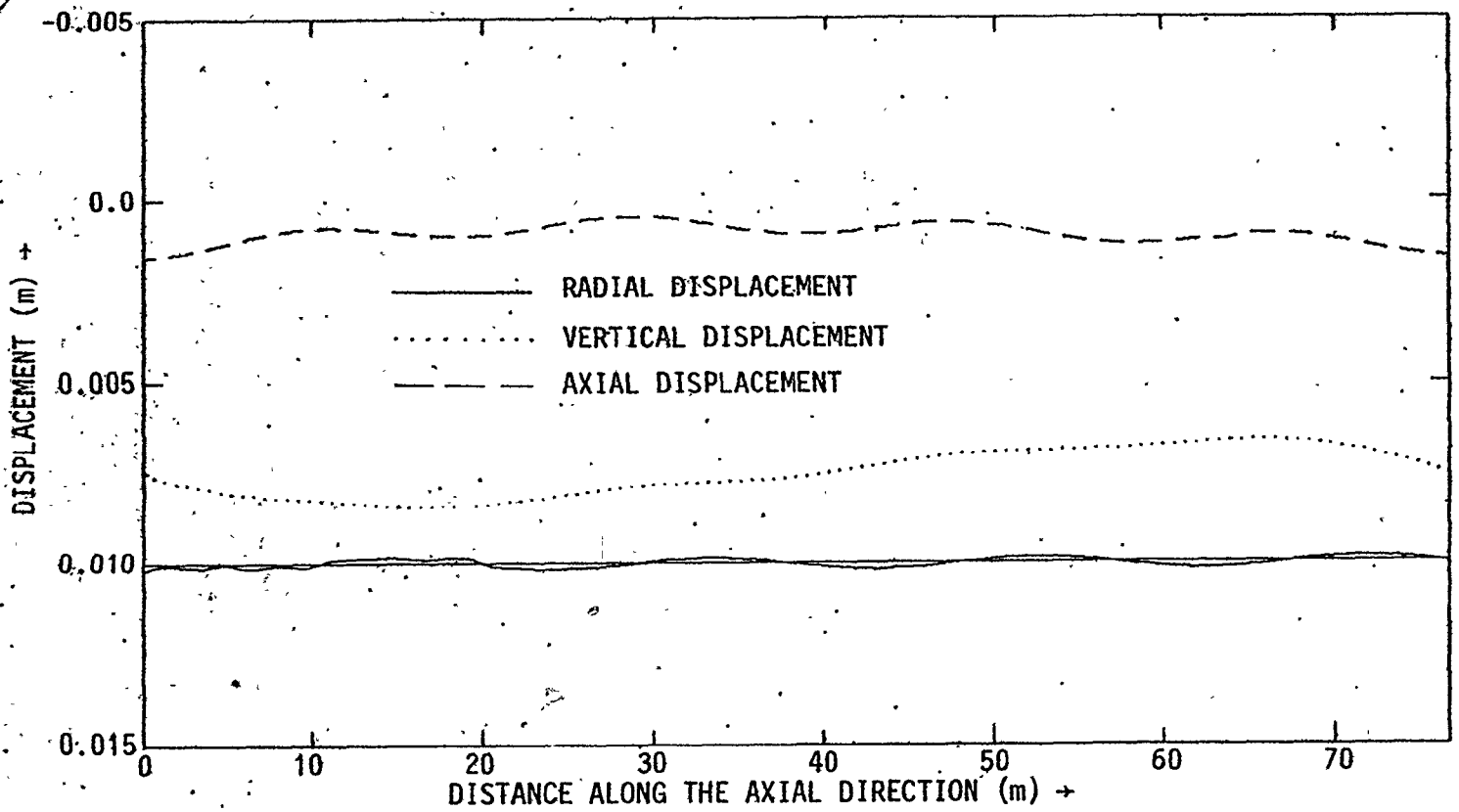

FIGURE 5.10.32 DISPLACEMENTS AT THE RIGHT SPRING POINT POSITIONS ALONG THE LENGTH OF TUNNEL FOR SYSTEM E1, CASE 2.

crown and invert positions (Figure 5.10.33). Since the excitation is in the axial direction, the axial response predominates. This also leads to significant differential axial displacements between points at different depths, which contribute to shear in the z-θ plane. Thus, axial stresses and z-θ shear stresses are expected to be significant at the spring point. At the crown and invert positions, these displacements cause significant axial stresses and some shear in the r-z plane. For this case, stresses at the left spring point are identical to those at the right spring point , and are not presented. The stresses at the outer right spring point, a point mid-way between this point and the crown, the crown and the invert are shown in Figures 5.10.34 to 5.10.37 for system E2 and in Figures 5.10.38 to 5.10.41 for system E1. These figures substantiate the observations discussed previously. The peaks in the axial stresses for the crown and invert positions closely follow the significant peaks of the vertical displacements, thus indicating the relative importance of the differential vertical displacements. This is more explicit for system E1. Between 2 to 2.25 s, the vertical displacement curve shows a sharp gradient. If this gradient is used as the basis for calculating the differential vertical displacement between two consecutive nodes at the right spring point, the resulting shear stress in the z-θ plane works out to be 0.14 MPa. Considering the errors and approximations involved in obtaining this stress, and considering the presence of much sharper gradients at some points, this is in good agreement with the peak value of 0.4 MPa observed from Figure 5.10.38. The stresses appear to be reasonable

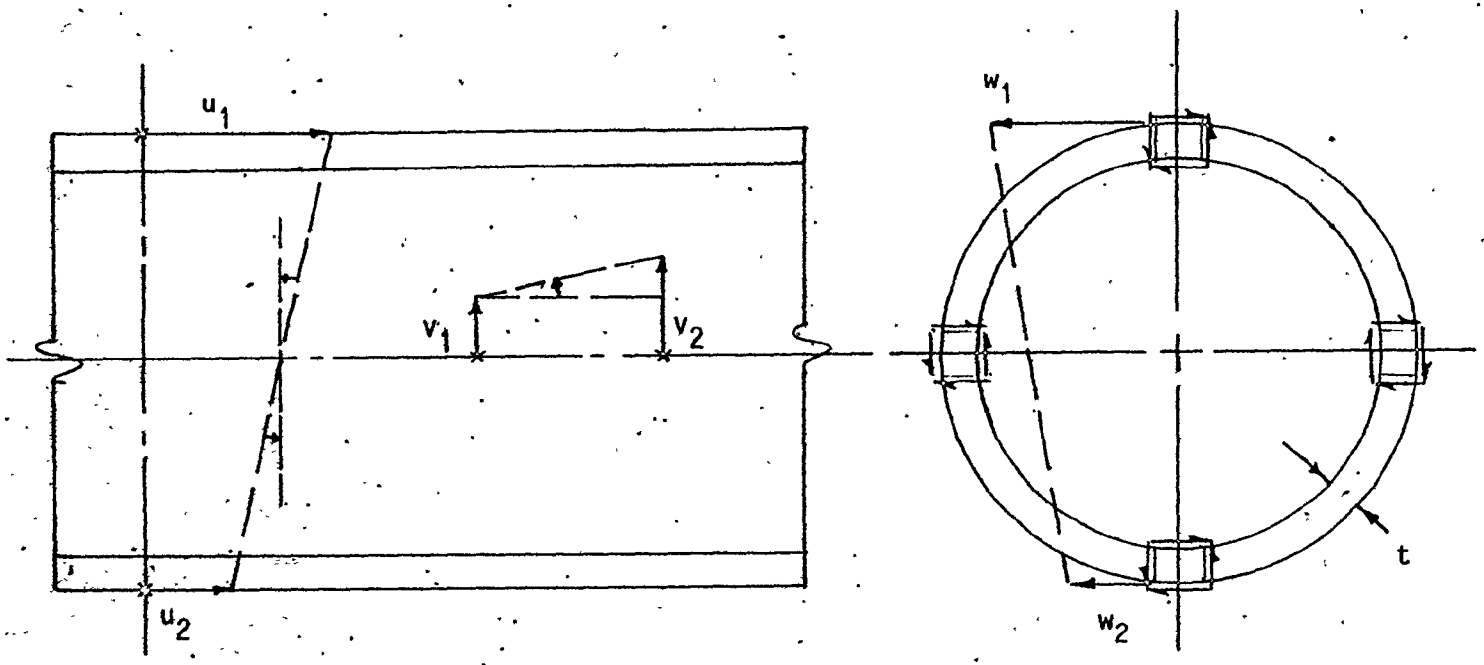

LONGITUDINAL SECTION

TRANSVERSE CROSS SECTION

u_1, u_2: AXIAL DISPLACEMENTS
v_1, v_2: VERTICAL DISPLACEMENTS
w_1, w_2: TRANSVERSE DISPLACEMENTS
t: LINER THICKNESS

FIGURE 5.10.33 SHEAR STRESSES ON r-θ AND z-θ PLANES DUE TO VARIOUS RELATIVE DISPLACEMENTS

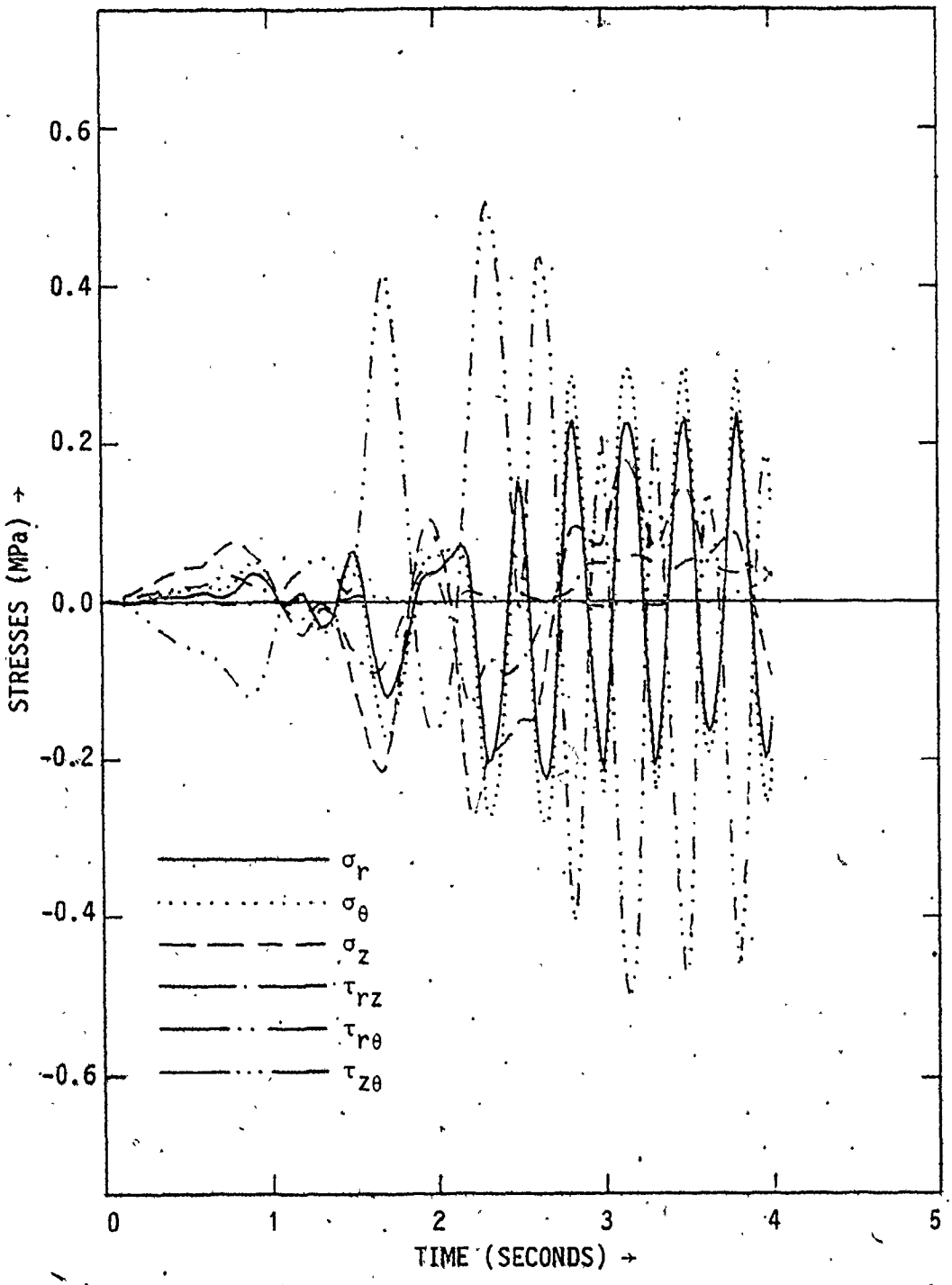

FIGURE 5.10.34 STRESSES IN THE LINER AT RIGHT SPRING POINT, SYSTEM E2, CASE 3.

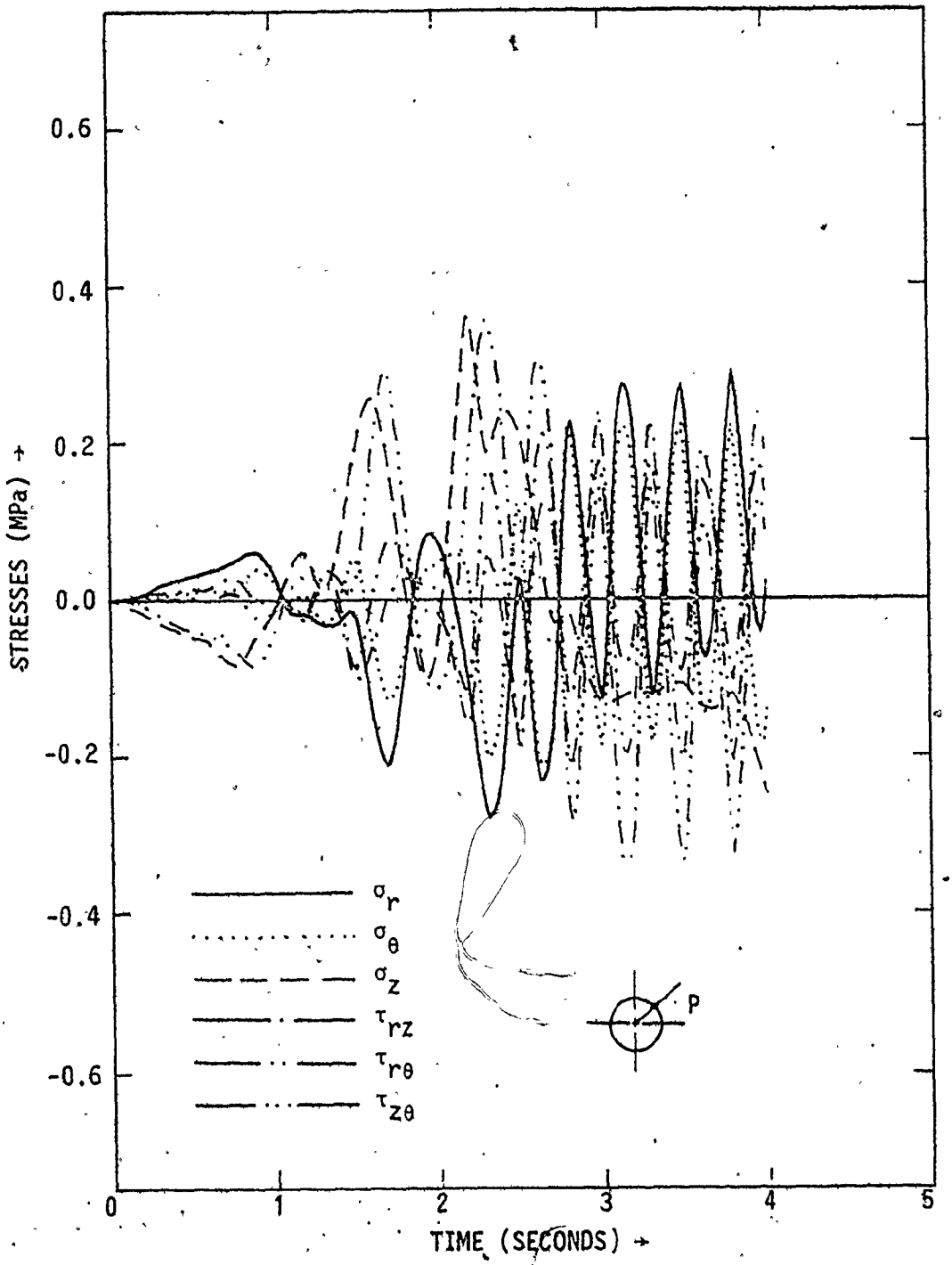

FIGURE 5.10.35 STRESSES AT THE POINT P IN THE TUNNEL LINER FOR SYSTEM E2, CASE 3.

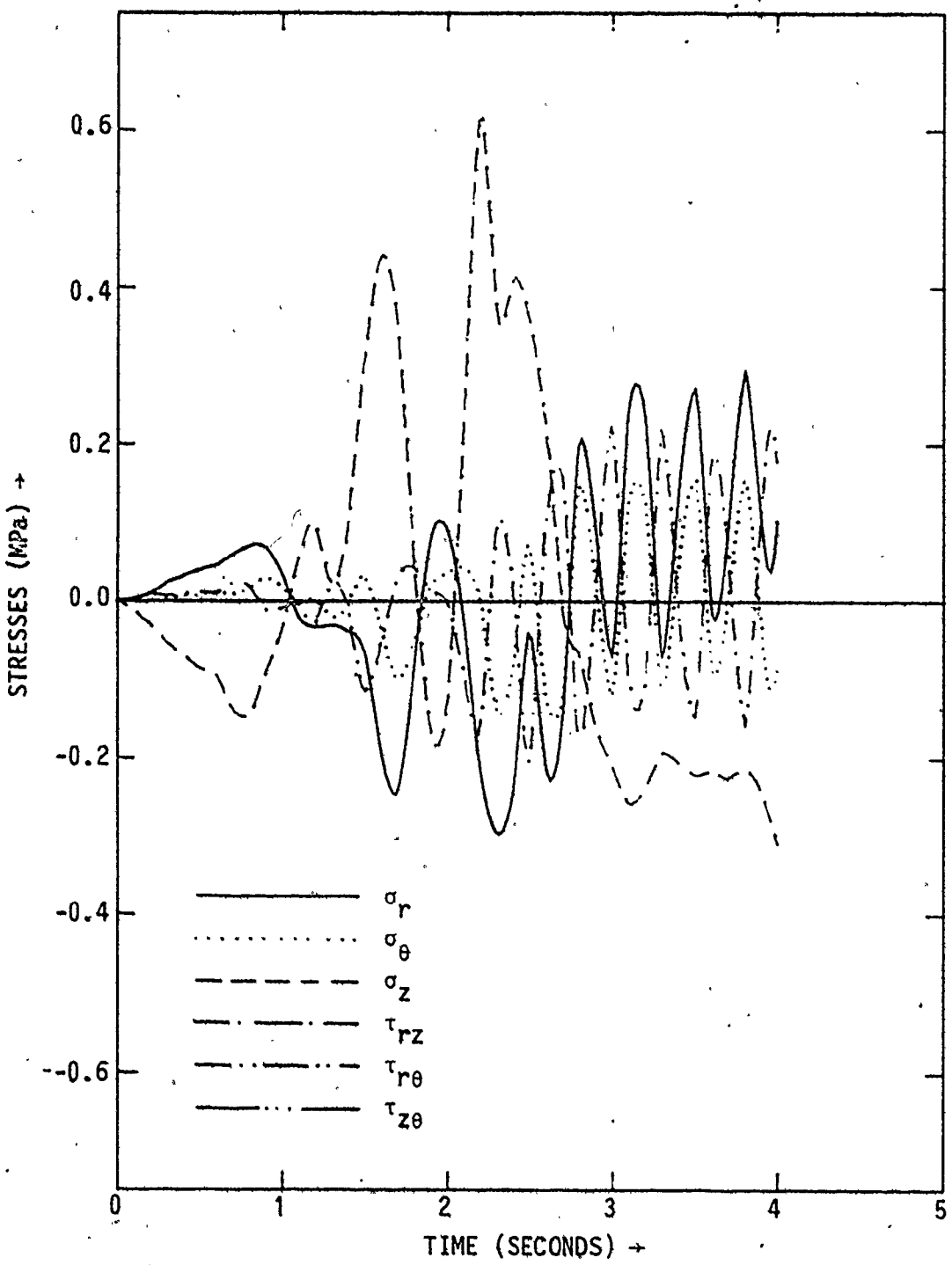

FIGURE 5.10.36 STRESSES IN THE LINER AT THE CROWN FOR SYSTEM E2, CASE 3

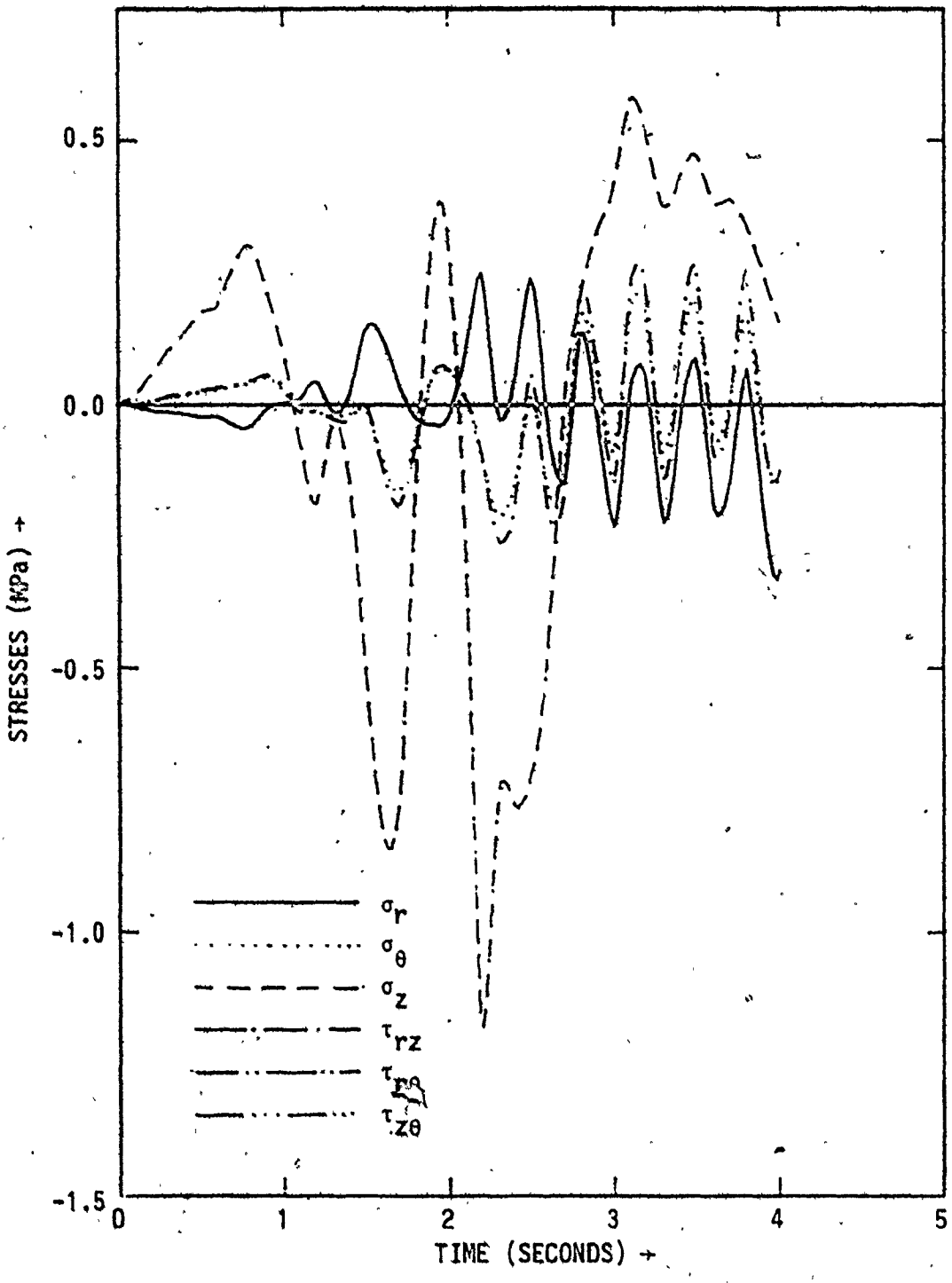

FIGURE 5.10.37 STRESSES IN THE LINER AT THE INVERT FOR SYSTEM E2, CASE 3

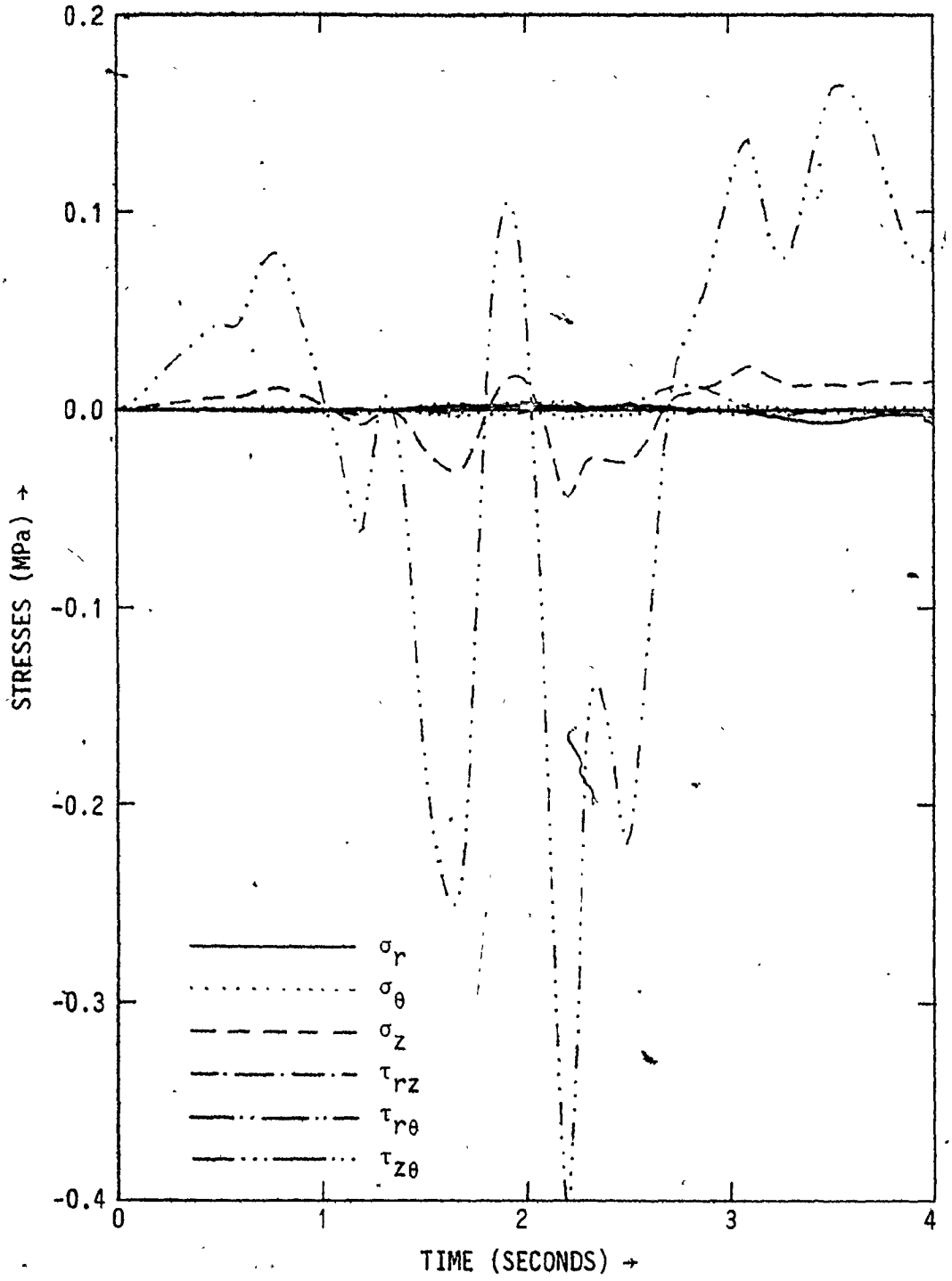

FIGURE 5.10.38 STRESSES IN THE LINER AT RIGHT SPRING POINT FOR SYSTEM E1, CASE 3

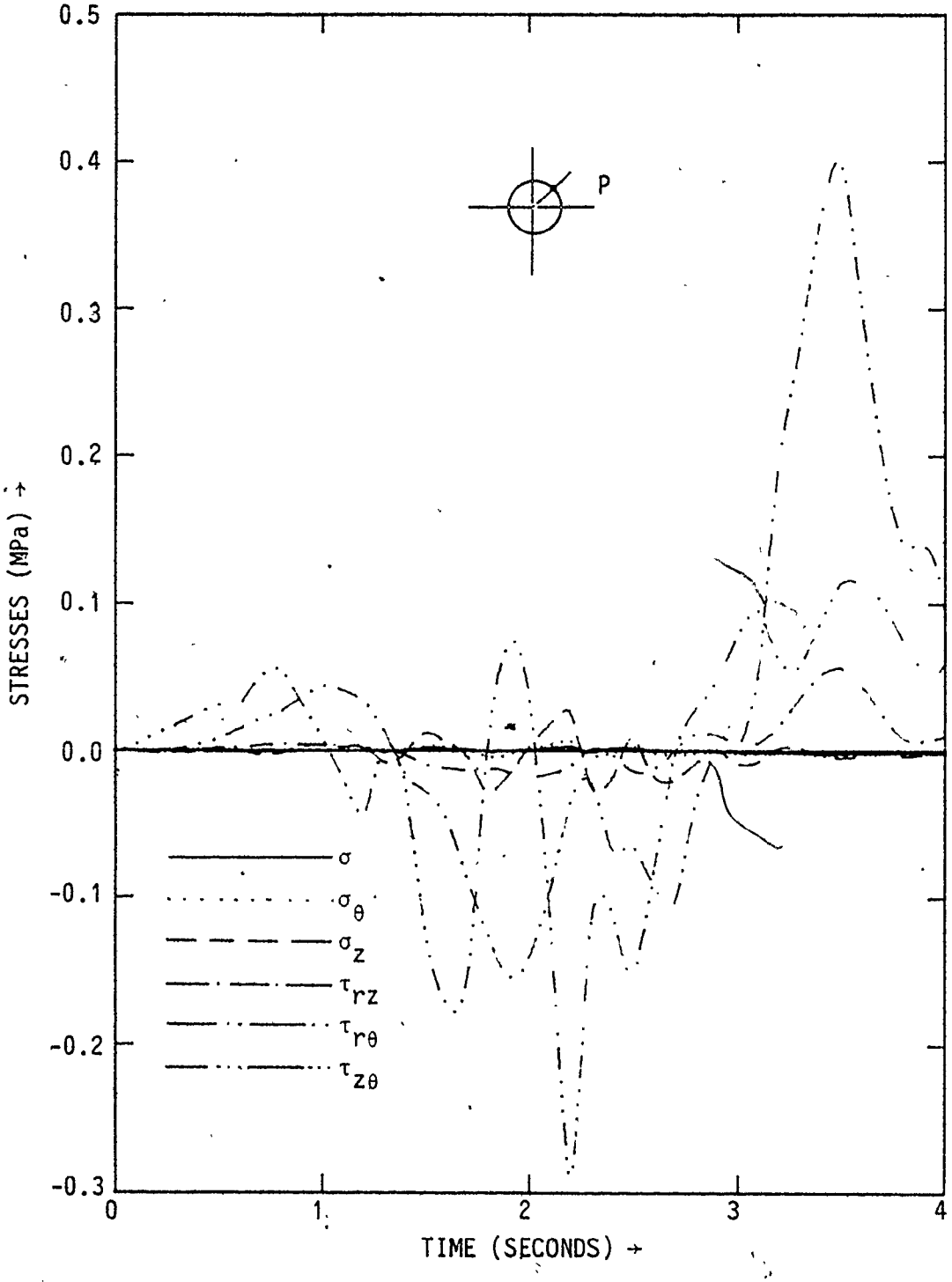

FIGURE 5.10.39 STRESSES IN LINER AT POINT "P" FOR SYSTEM E1, CASE 3

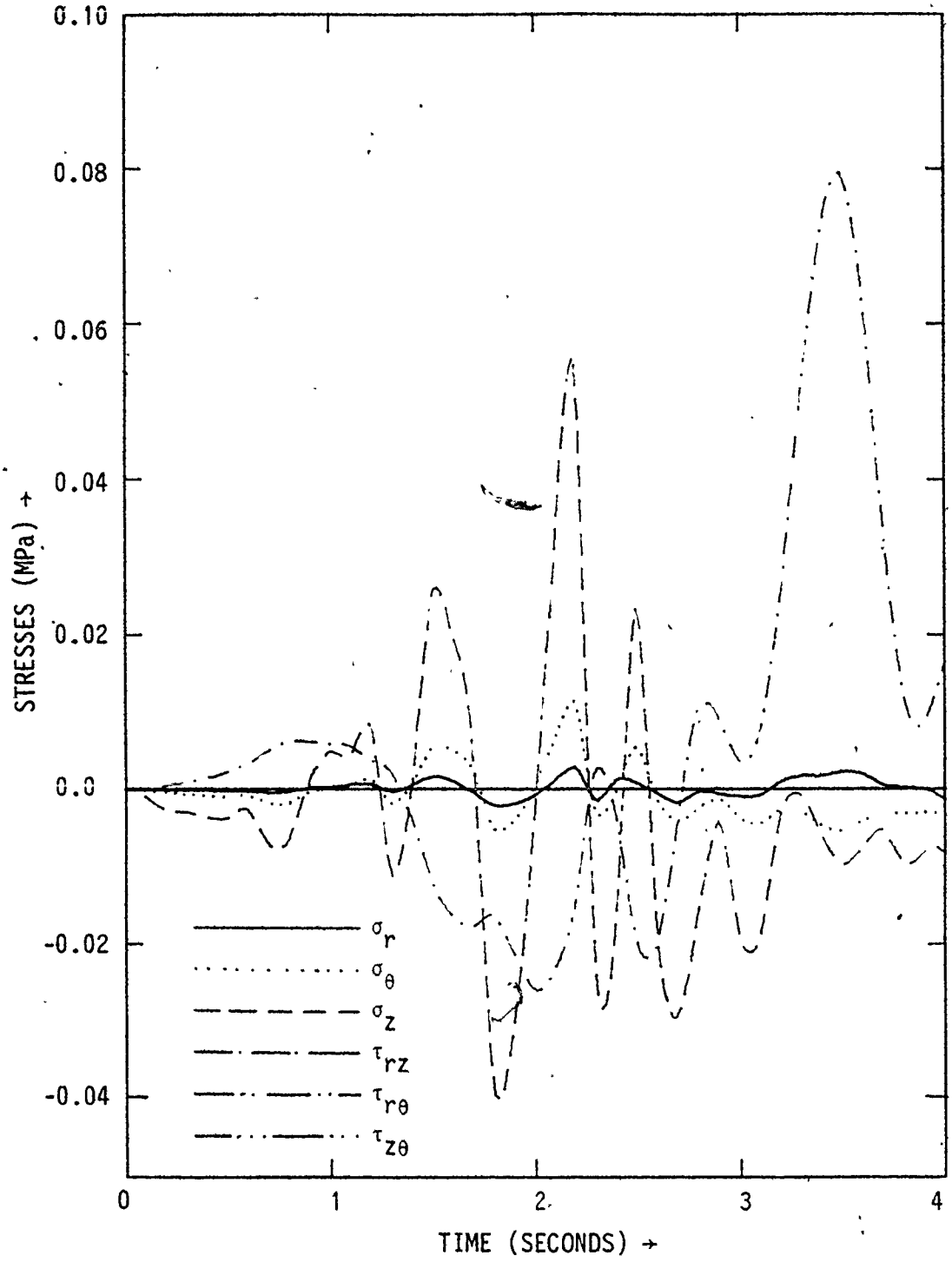

FIGURE 5.10.40 STRESSES IN THE LINER AT THE CROWN, SYSTEM E1, CASE 3

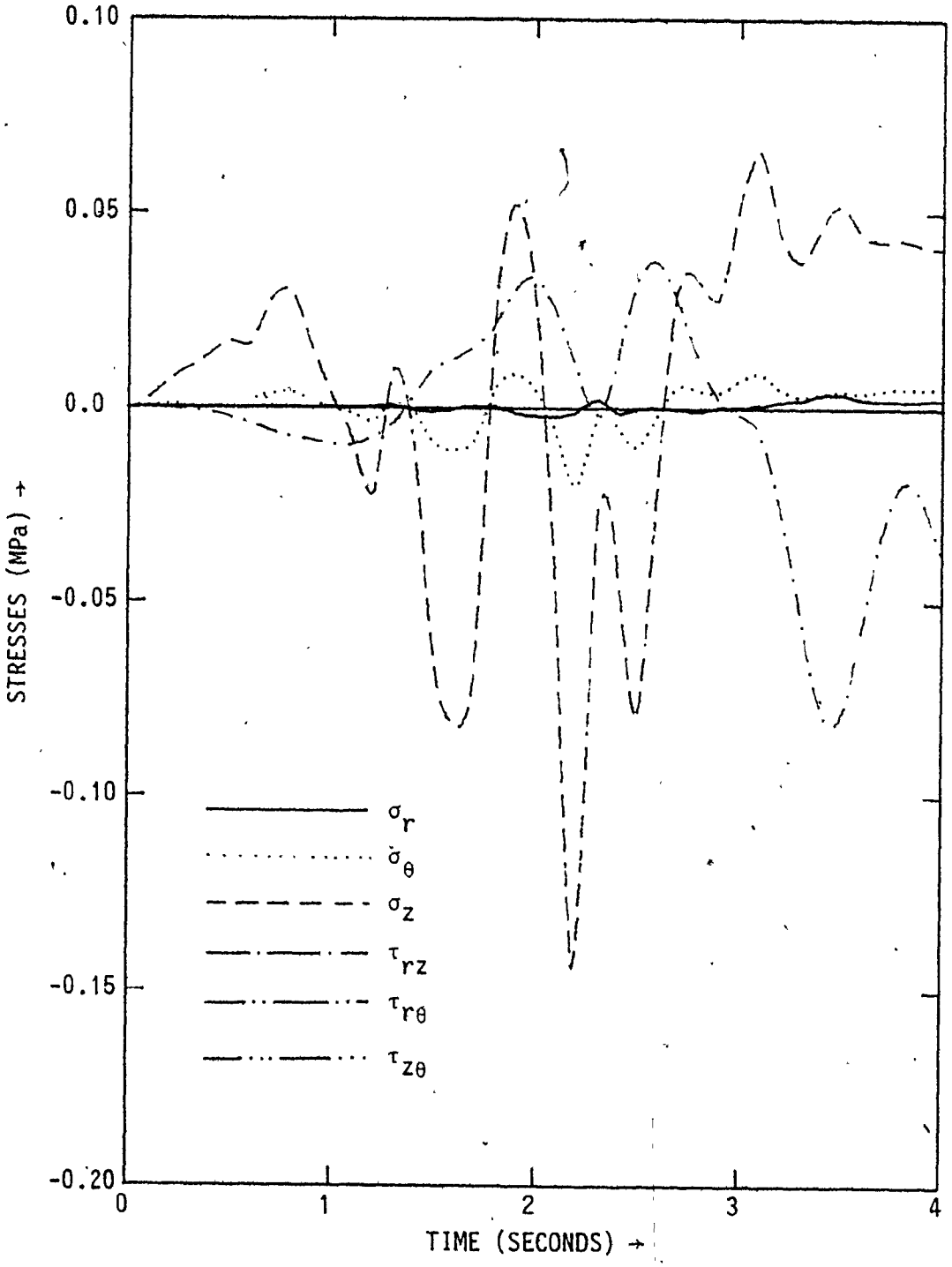

FIGURE 5.10.41 STRESSES IN THE LINER AT THE INVERT FOR SYSTEM E1, CASE 3

for the computed responses, and are well within the allowable values for the liner material.

When the excitation in the transverse direction is present, the differential transverse displacements between points at different horizontal levels lead to shear forces in the transverse directions. The resulting shear stresses and the accompanying complementary shear stresses cause distortions in the r-θ plane. These shear forces in the r-θ plane act on a relatively small cross section of the liner (Figure 5.10.33). As such, a differential transverse displacement between the crown and invert positions is likely to cause more severe stresses compared to an equal differential displacement in the axial direction between the same two points. Since identical acceleration functions were employed as base excitations in the axial and transverse directions, the responses in the axial and transverse directions will be comparable. For this reason, the shear stresses in the r-θ plane may be expected to dominate. Because of the vertical shear wave propagation, the vertical displacements are close to zero. This leads to negligible shear stresses in the z-θ plane at the spring points. Figures 5.10.42 through 5.10.45 show the results for case 1 (system 1). These results confirm the observations made above. In fact, the shear stresses in the r-θ plane are so dominant that this stress has to be plotted to a different scale to make the other curves clearer. The shear stress in the r-θ plane dominates in all of these figures.

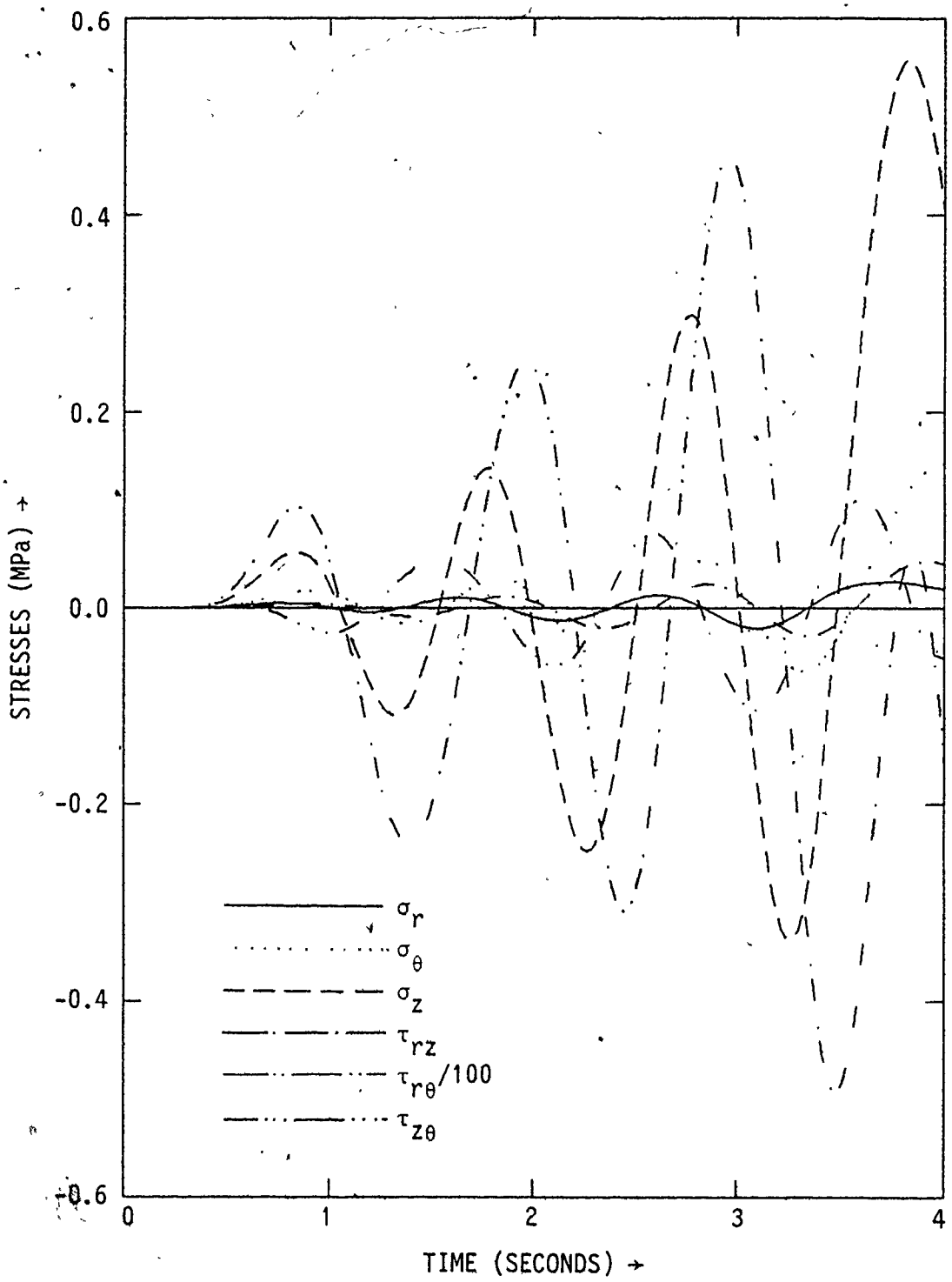

FIGURE 5.10.42 STRESSES IN THE LINER AT RIGHT SPRING POINT FOR SYSTEM E1, CASE 1

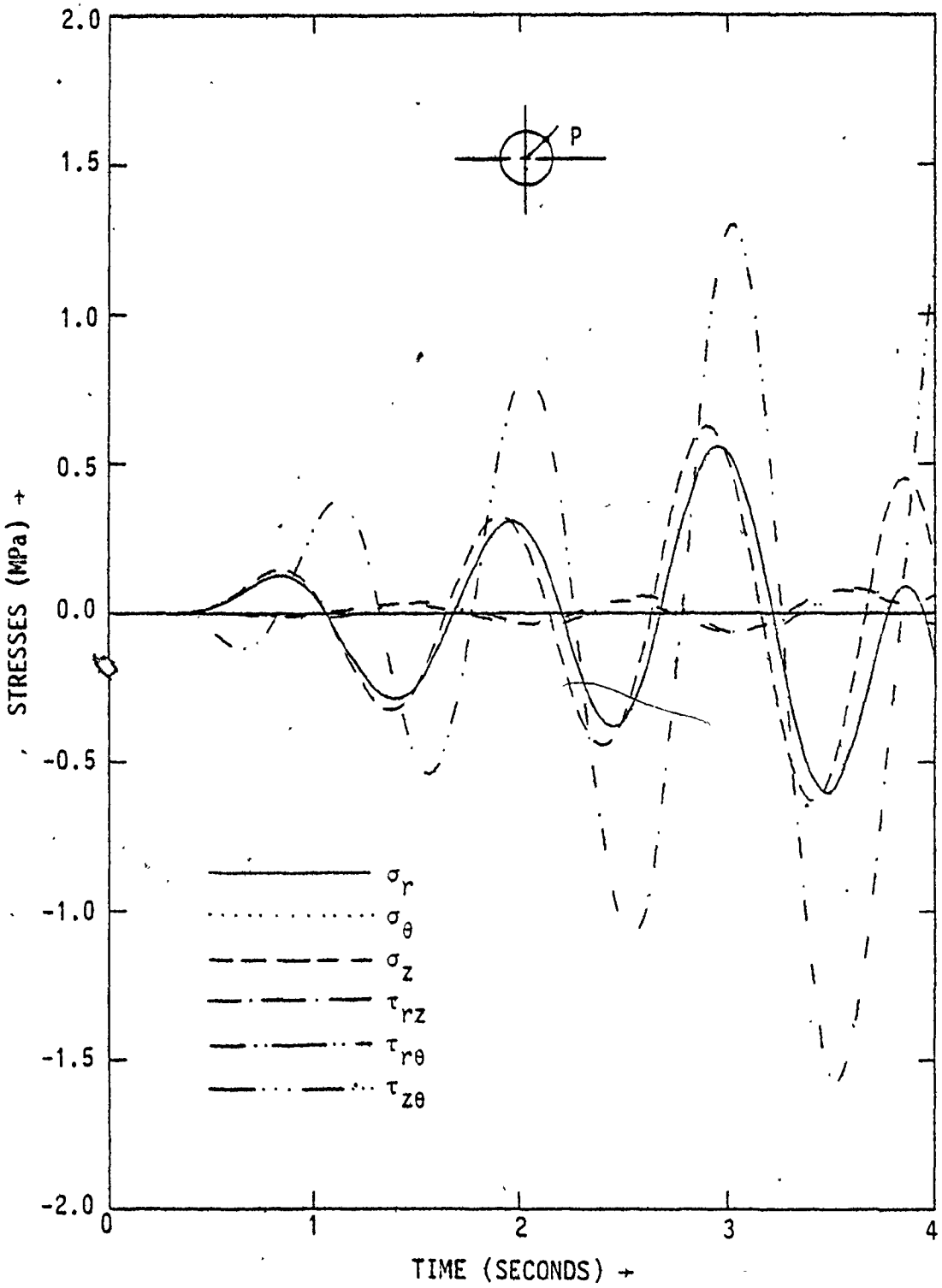

FIGURE 5.10.43 STRESSES IN THE LINER AT POINT "P" FOR SYSTEM E1, CASE 1.

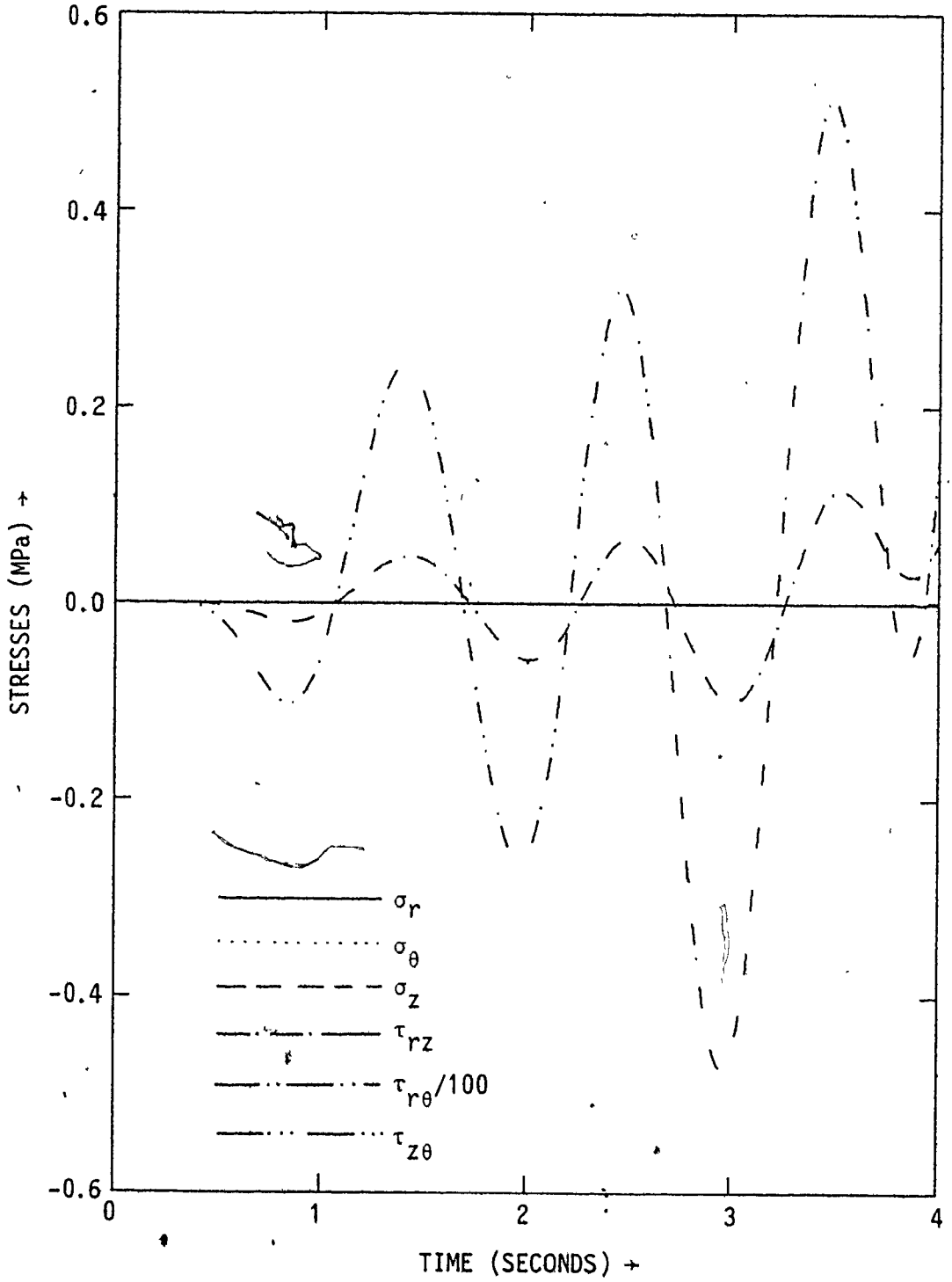

FIGURE 5.10.44 STRESSES IN LINER AT THE CROWN FOR SYSTEM E1, CASE 1

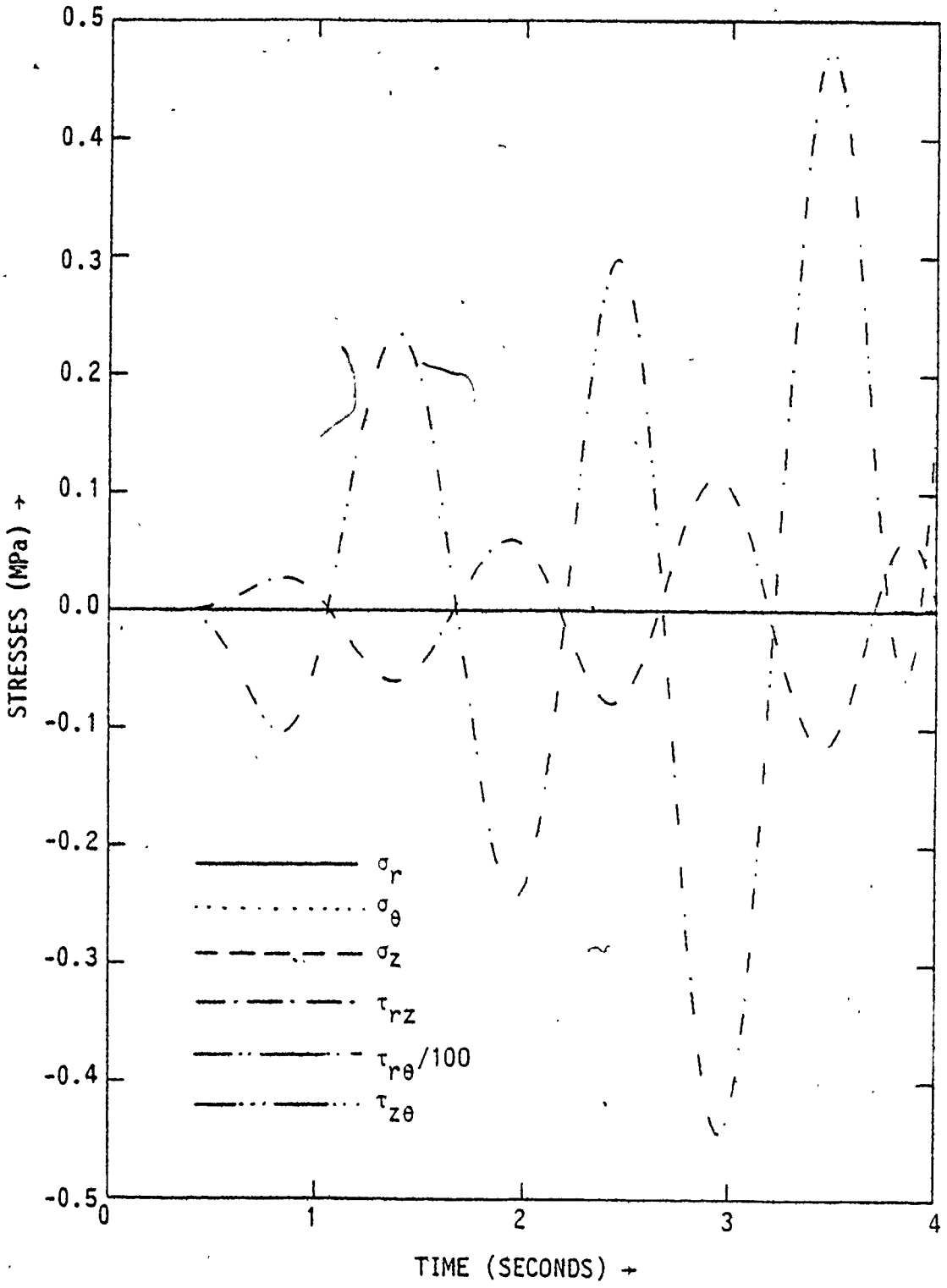

FIGURE 5.10.45 STRESSES IN THE LINER AT THE INVERT FOR SYSTEM E1, CASE 1

For case 2, the vertical displacements are present. For this reason, the shear stresses in the z-θ plane should be significant at the spring points and axial stresses at the crown and invert positions. Because the relative transverse displacements between different positions on the tunnel are influenced by the presence of the vertical displacements, the magnitudes of the resultant shear stresses in the r-θ plane also change from case 1 to case 2. Figures 5.10.46 through 5.10.50 give the stresses for case 2 (system E1). As mentioned previously, there are significant shear stresses in the r-θ and z-θ planes at the spring points. At the crown and invert position the shear stress in the r-θ plane remains significant, but the shear stress in the z-θ plane is not. Instead, the axial stresses assume significant proportions. The results for cases 1 and 2 (system E1) clearly indicate the important changes in stresses due to the angle of earthquake propagation.

Similar results were obtained for cases 1 and 2 for system E2. However, the shear stresses are of the order of 35.5 MPa and clearly beyond the allowable limits for typical liner materials. This means that the material slippage takes place between the medium and structure. For this reason, the results for system E2 are not presented in detail. These results also show that the direction of propagation of seismic waves with respect to the axis of the tunnel is a very important parameter.

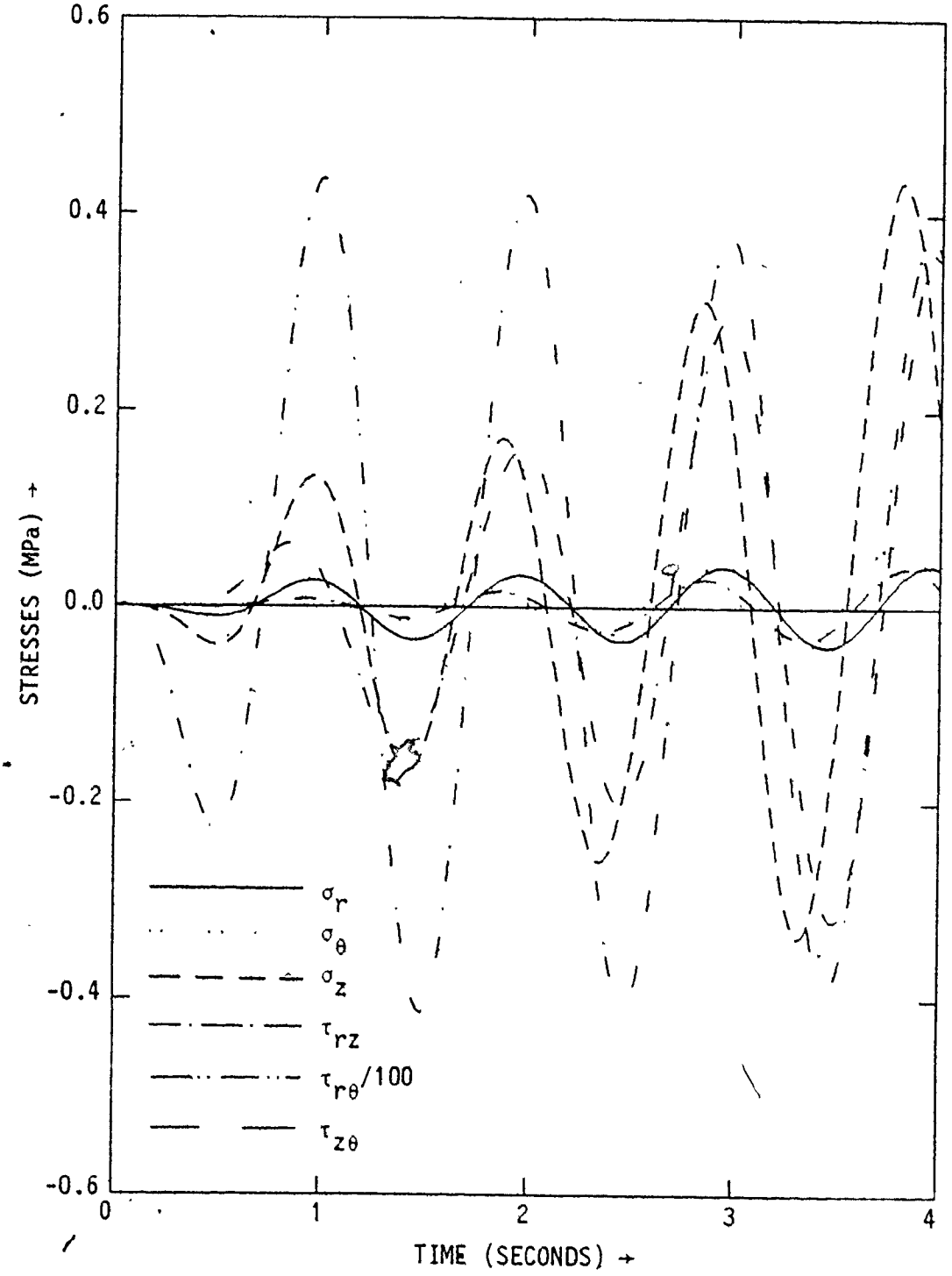

FIGURE 5.10.46 STRESSES IN THE LINER AT RIGHT SPRING POINT FOR SYSTEM E1, CASE 2.

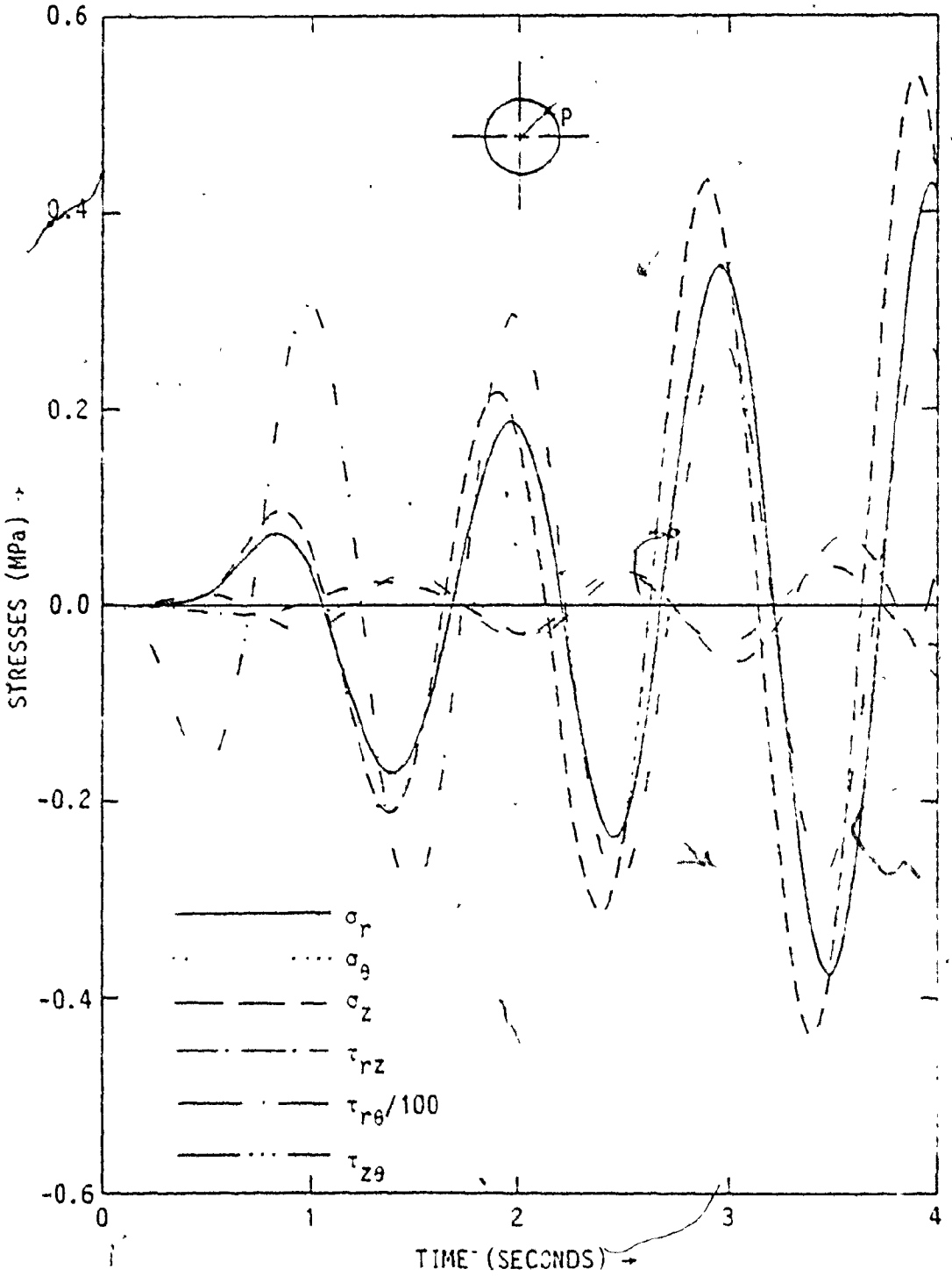

FIGURE 5.10.47 STRESSES IN THE LINER AT THE POINT "P" FOR SYSTEM E1, CASE 2

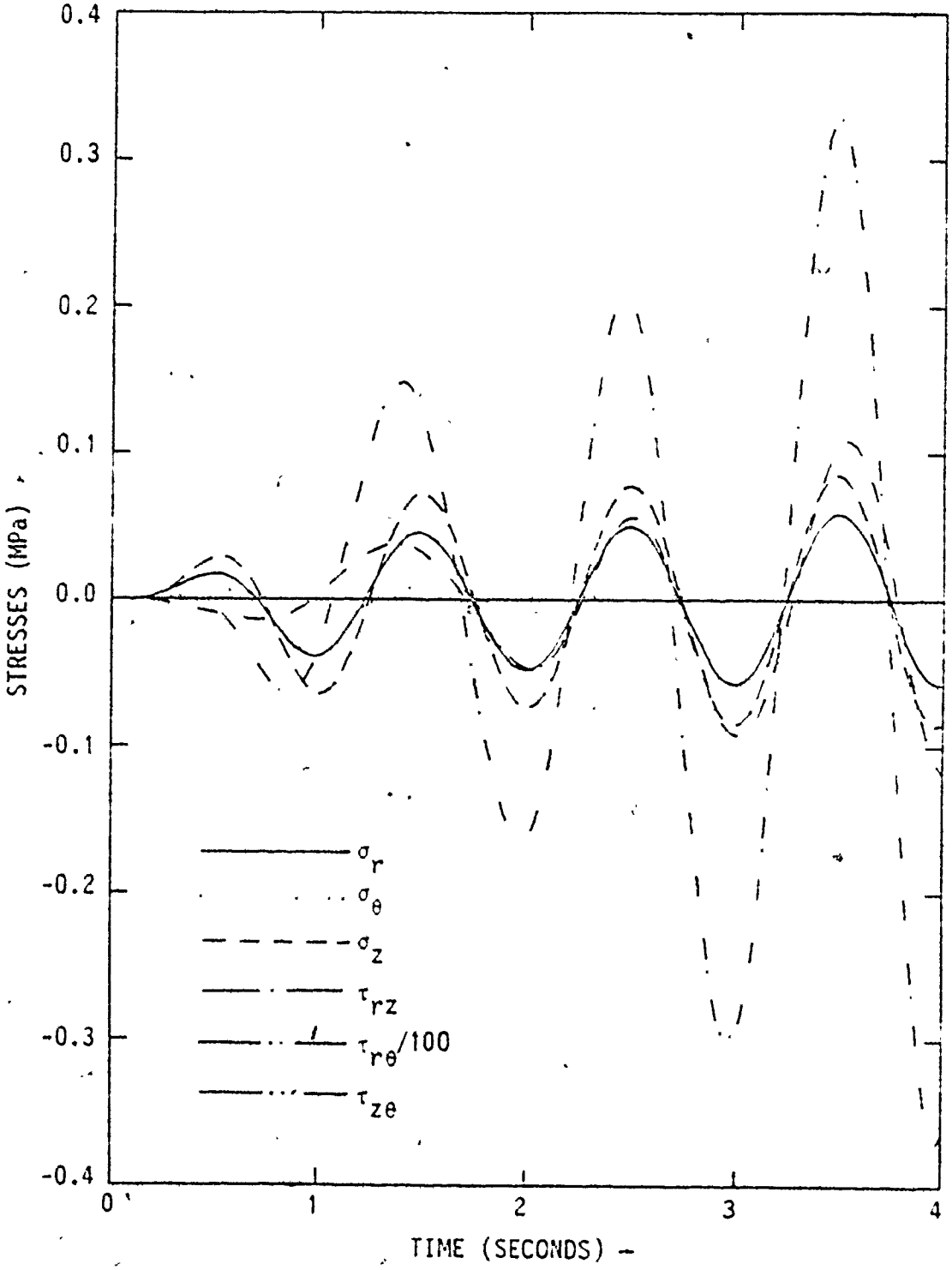

FIGURE 5.10.48 STRESSES IN THE LINER AT THE CROWN FOR SYSTEM E1, CASE 2

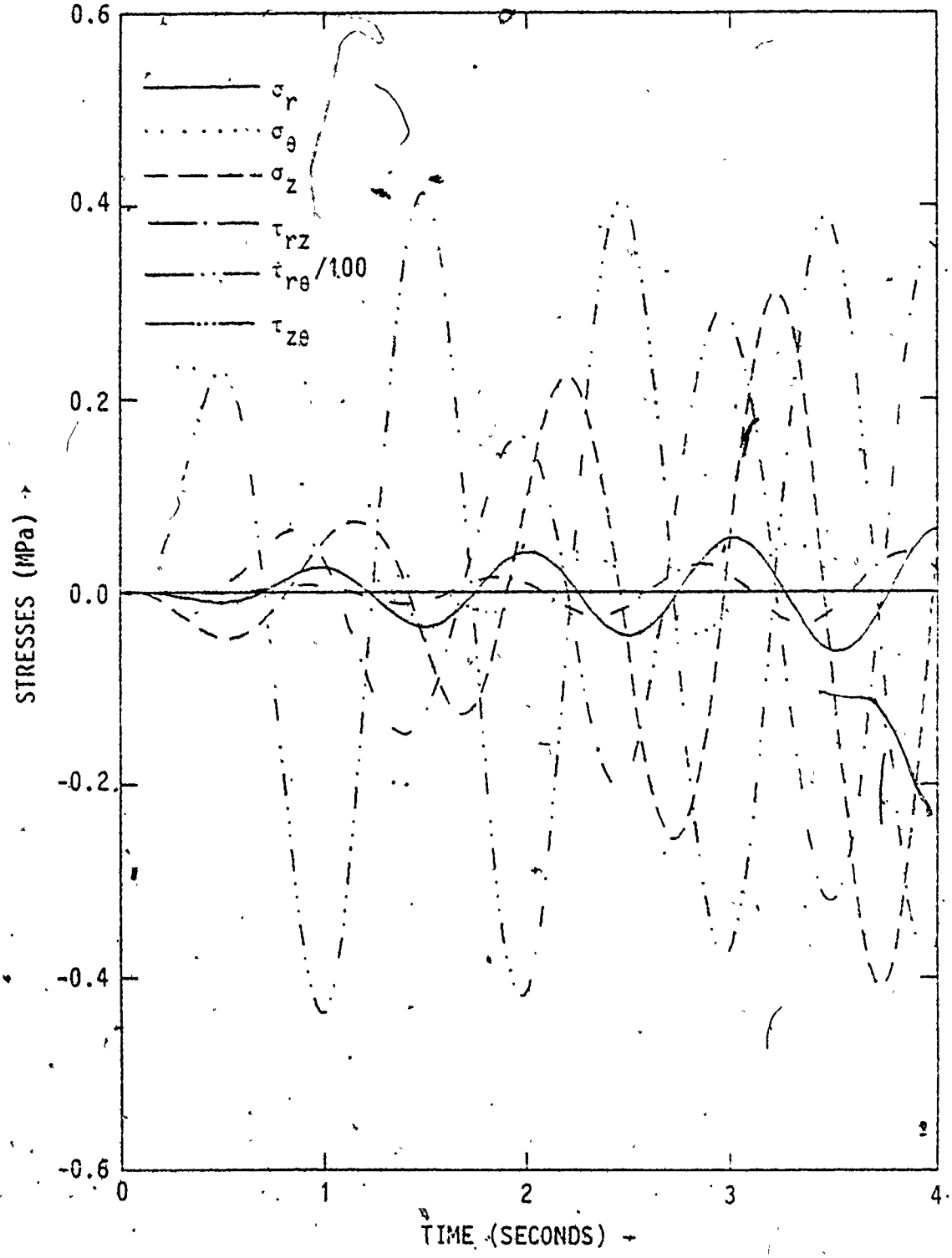

FIGURE 5.10.49 STRESSES IN THE LINER AT THE LEFT SPRING POINT FOR SYSTEM E1, CASE 2

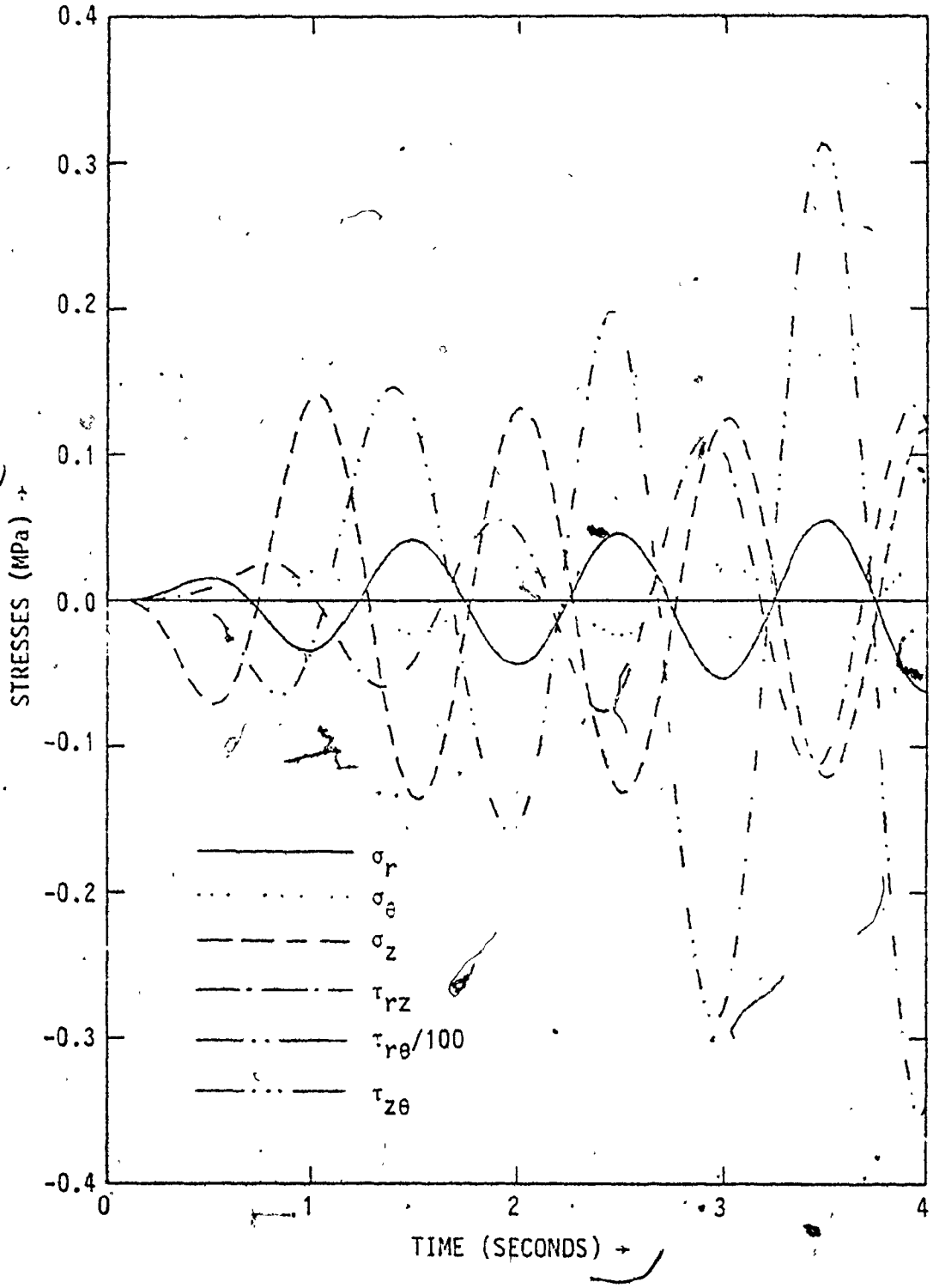

FIGURE 5.10.50 STRESSES IN THE LINER AT THE INVERT FOR SYSTEM E1, CASE 2

To verify the results of the analysis for system E1, the shear strain and shear stress in the r-θ plane at the right spring point were calculated using the displacements of the tunnel at the right spring point and the invert position. The liner was treated as a free-standing, circular sector, being fixed at its invert and free at its spring point (Timoshenko, 1970). Using this approximate method, the shear strain and stress at the right spring point in the r-θ plane at time 3.6 s are 0.0060187 and 77.64 MPa, respectively; and those obtained from the dynamic analysis are 0.0041 and 15.9 MPa, respectively. These two sets of results are not in close agreement because of the simplifications involved in the hand calculations. However, the order of the strain and stress values are comparable. Shear strain and shear stress for time 2.5 s are, -0.003416 and -44.07 MPa by hand calculations; and -0.001305 and 11.212 MPa from the computer output.

The results given in this chapter help to understand the importance of structure-medium interaction on the response of the structure. When the medium is quite soft compared to the structure (system E1, for instance), the interaction leads to significant differences between the response of the structure and the free field motion at corresponding positions. Figure 5.10.13 shows how different these two responses can be. Design of the structure assuming free field motions at the periphery could be very uneconomical. Here, the interaction tends to reduce the axial stresses in the structure. For a stiffer medium (system E2 for instance), the influence of interaction is considerably reduced and the structure's response is closer to the corresponding

free field response. When the medium is very stiff (competent rock, for instance), the free field response and the response of the structure may be expected to be almost identical.

5.10.4 DYNAMIC ANALYSIS USING WILSON'S θ METHOD

As indicated earlier in section 5.10.1, the program was noticeably unstable after 4 seconds when the linear acceleration method was employed. To study the influence of the instability, if any, on the results obtained by this method, the analysis was repeated for case 2 and case 3 (system E1) using the unconditionally stable Wilson's θ method algorithm for dynamic analysis (Bathe and Wilson, 1976). The value of θ used in these analyses was 1.4. In this section, the linear acceleration method and the Wilson's θ method will be referred to as the first and second methods, respectively, for convenience.

As expected, the instability is not observed in the analyses using the second method for the entire duration of 5 s. For case 3, figures for the transverse response are not presented, because this response is insignificant (as expected). Figure 5.10.51 shows the axial accelerations at the spring points, crown and invert of the tunnel by the two methods. At 4.5 s the values of accelerations become unstable for the first method. For the first 4.5 s duration the accelerations obtained by the two methods are very nearly the same (Figure 5.10.51). The corresponding axial displacements by the two methods are also very nearly the same, and do not show any sign of instability (Figure 5.10.52).

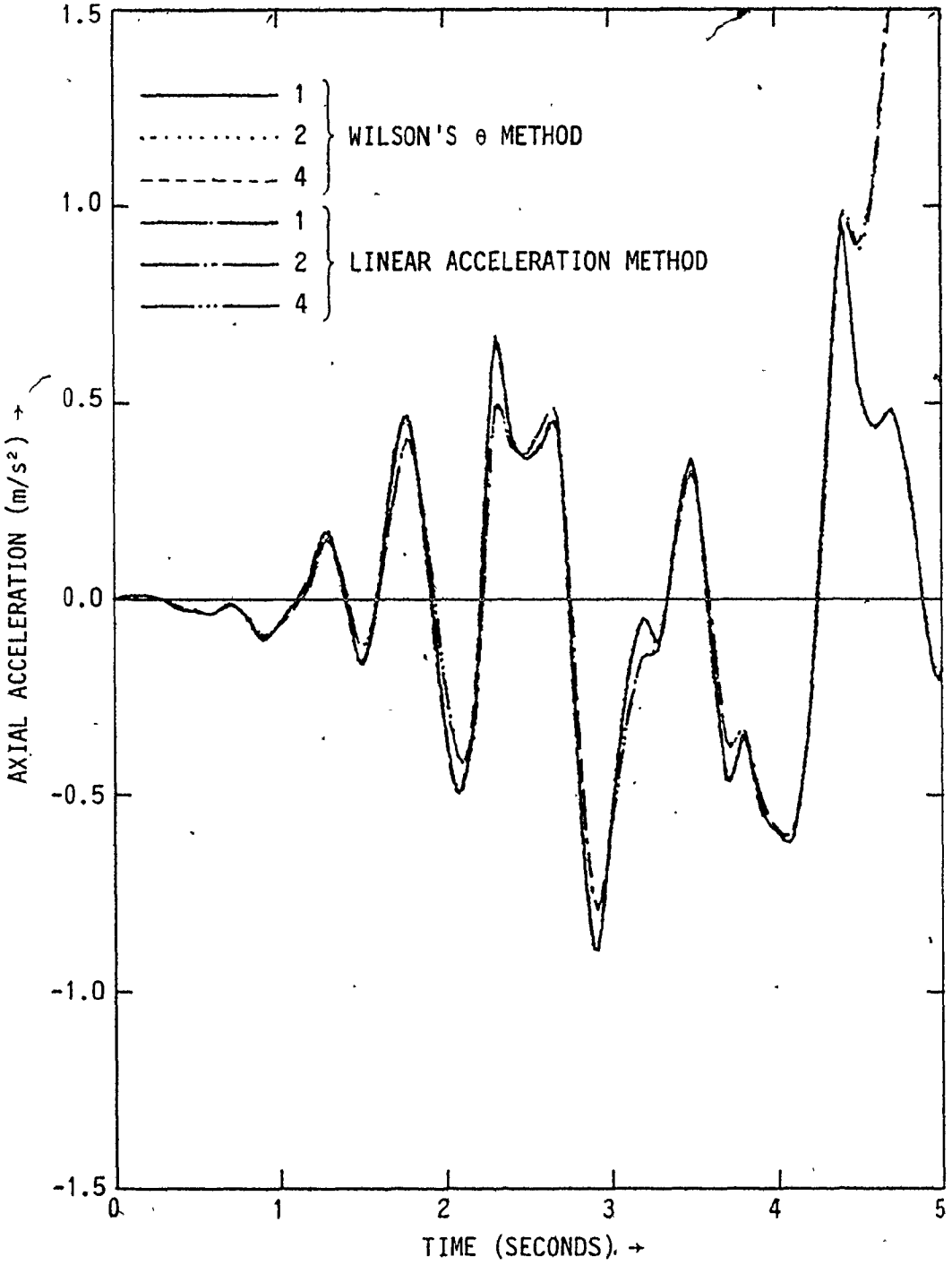

FIGURE 5.10.51 AXIAL ACCELERATIONS OF THE TUNNEL FOR SYSTEM E1, CASE 3

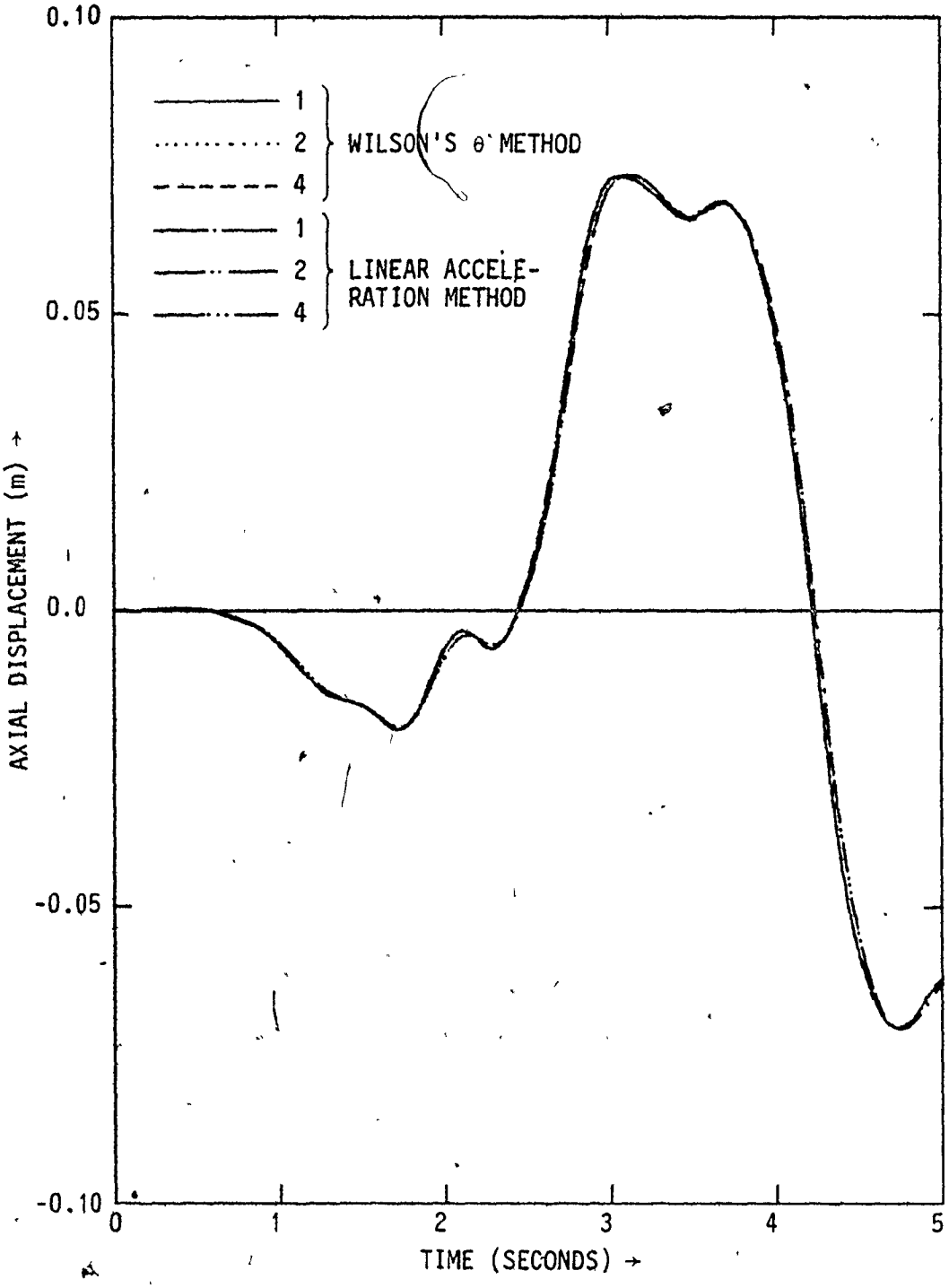

FIGURE 5.10.52 AXIAL DISPLACEMENTS OF TUNNEL FOR SYSTEM E1, CASE 3

As such, the accompanying stresses may also be expected to be free from the undesirable influence of any instability. The vertical displacements by the second method and the free field motions for the corresponding positions are shown in Figure 5.10.54. This figure is practically identical to Figure 5.10.29 for the first method. Here again, instability is not indicated at all. The stresses at various positions on the tunnel liner obtained by the second method are presented in Figures 5.10.55 through 5.10.58. It may be noted that the stresses obtained by the two methods are comparable. Differences observed for some stresses at some points are not significant.

For case 2, the accelerations and displacements at these positions on the tunnel liner in the axial, transverse and vertical directions by the two methods are given in Figures 5.10.59 through 5.10.64. The results are presented for the first 4 seconds only (which is the duration of analysis using the first method). Here again, there is no sign of instability by either method and the responses obtained by the two methods are practically the same. The stresses at various points on the tunnel liner obtained by the Wilson's θ method are presented in Figures 5.10.65 through 5.10.68. They are very comparable to those obtained by the first method (Figures 5.10.46 through 5.10.50).

Based on these results, and as indicated in sections 5.10.2 and 5.10.3, the results of the analysis obtained from the first method for cases 2 and 3 (system E1) are practically the same as those by the second method for the first 4 seconds for practical engineering purposes. It is reasonable to presume the same for the results obtained

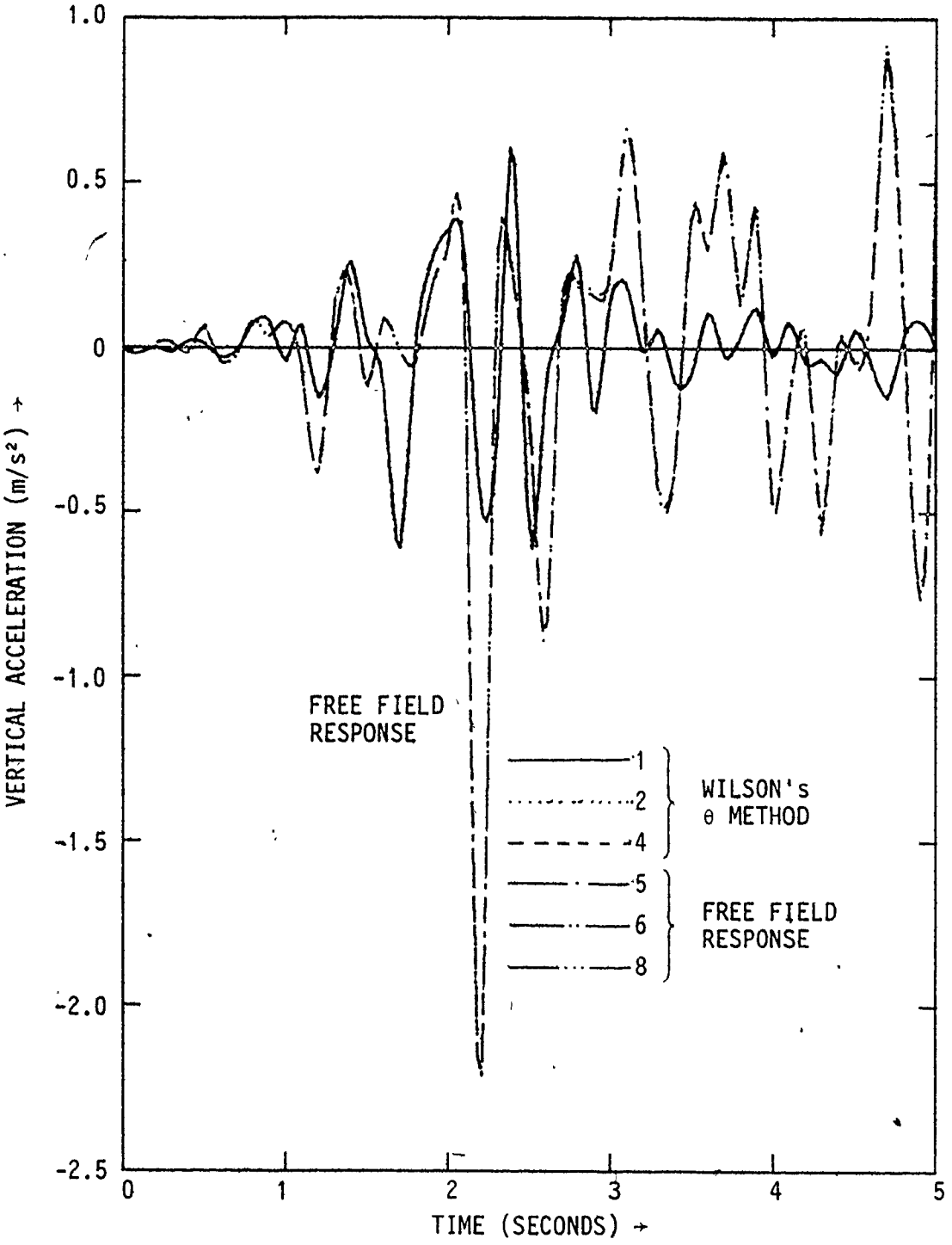

FIGURE 5.10.53 VERTICAL ACCELERATIONS OF TUNNEL FOR SYSTEM E1, CASE 3

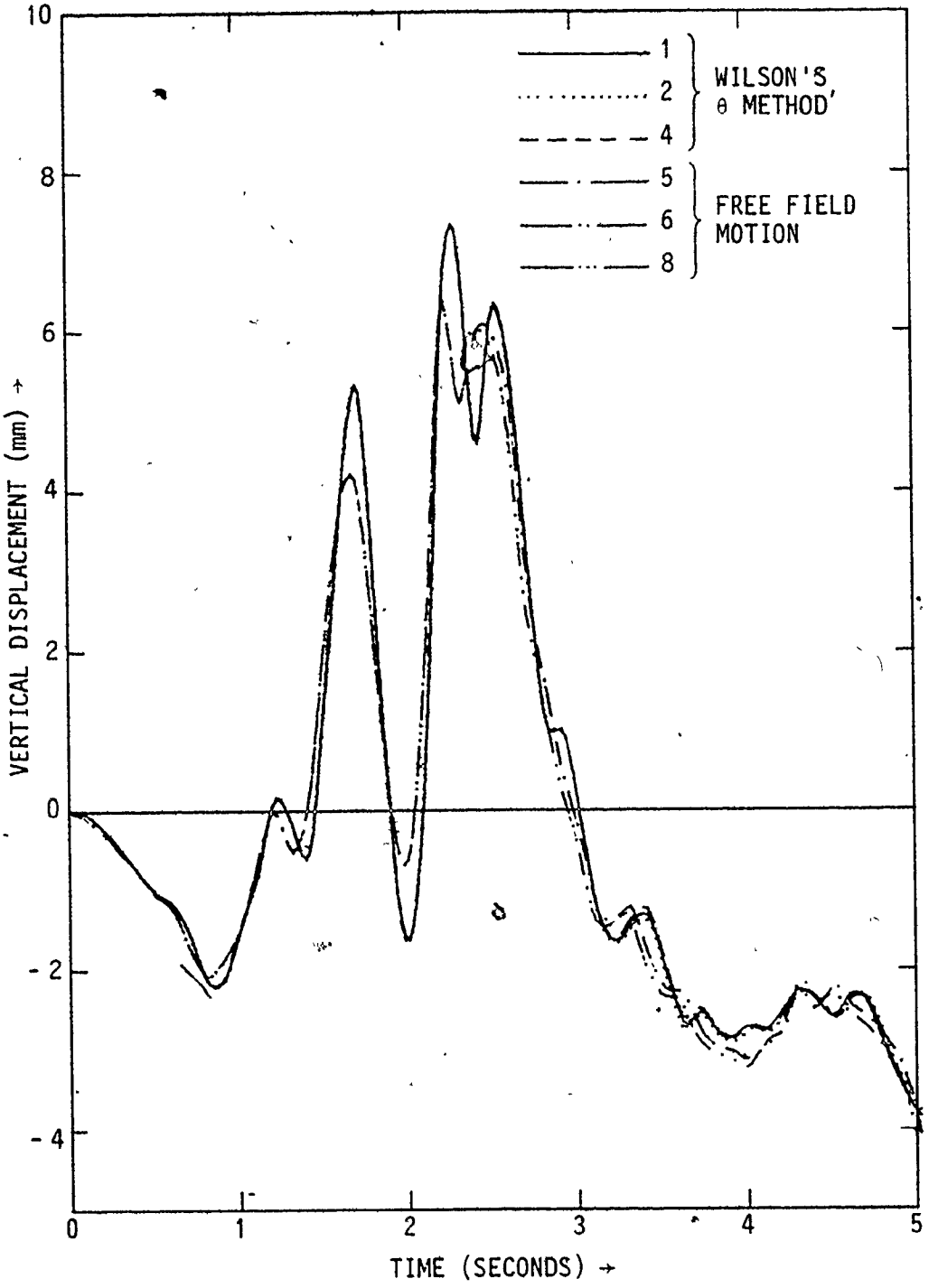

FIGURE 5.10.54 VERTICAL DISPLACEMENTS OF THE TUNNEL FOR SYSTEM E1, CASE 3

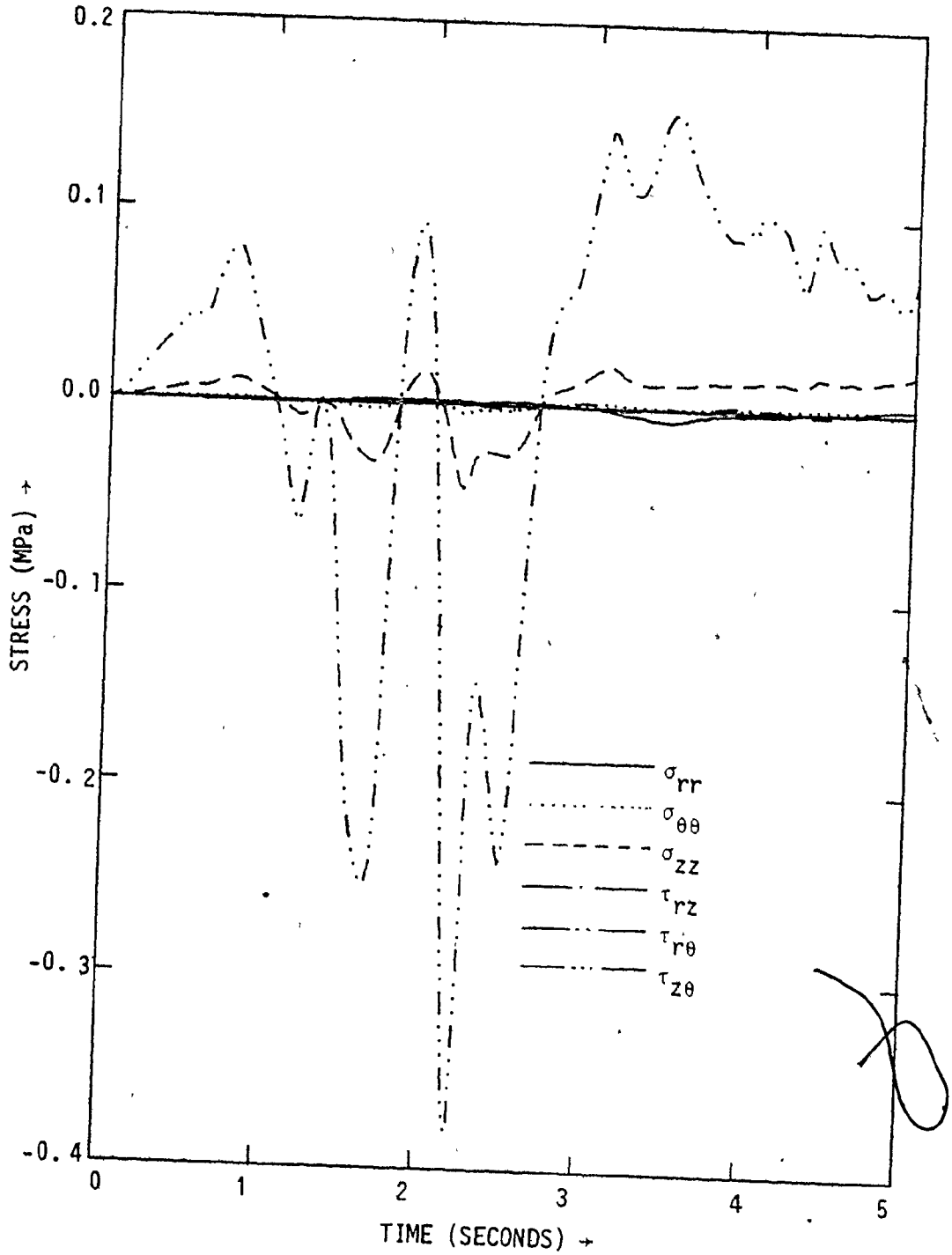

FIGURE 5.10.55 STRESSES IN THE LINER AT THE RIGHT SPRING POINT FOR SYSTEM E1, CASE 3 (WILSON'S θ METHOD)

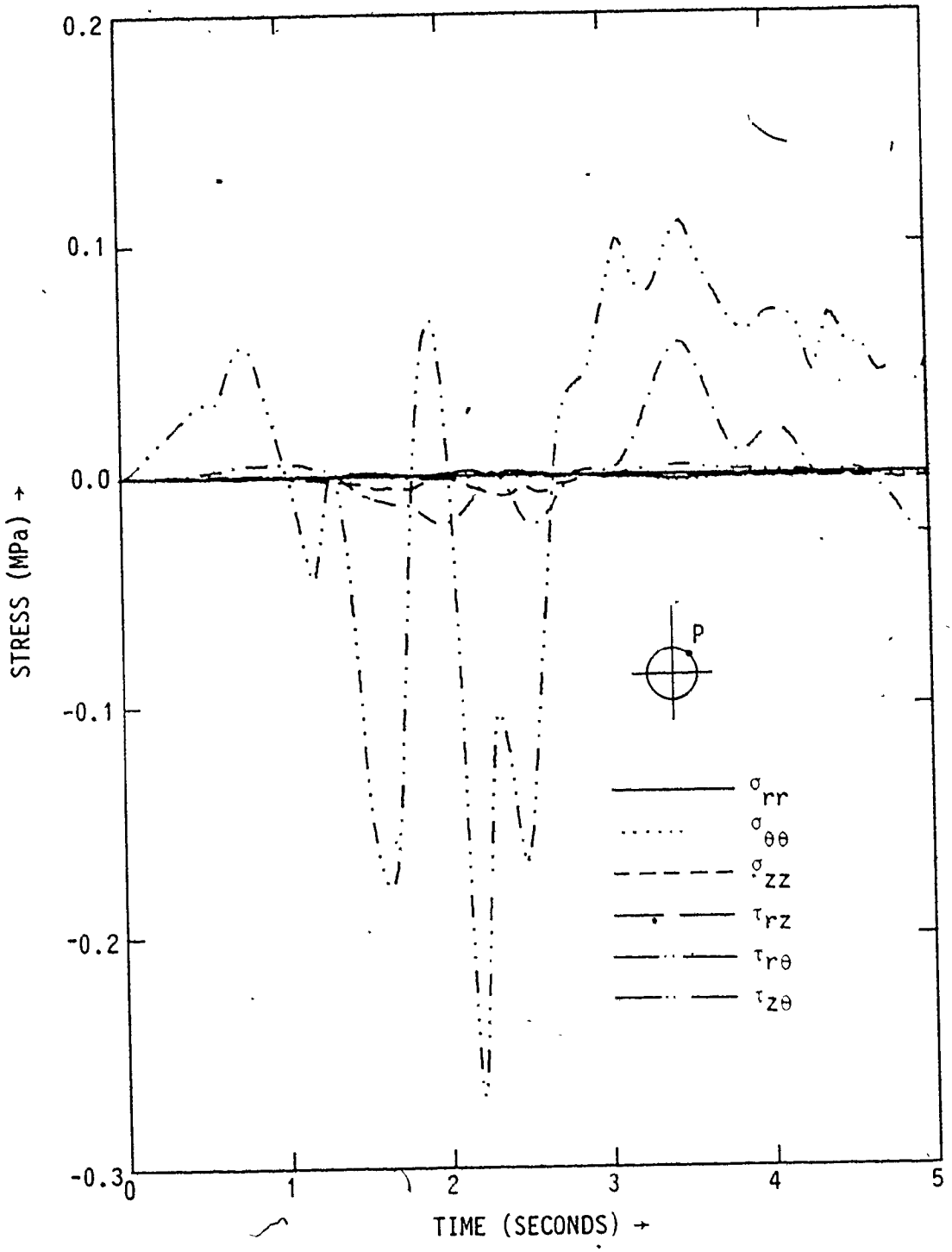

FIGURE 5.10.56 STRESSES AT POINT "P" OF THE LINER FOR SYSTEM E1, CASE 3 (WILSON'S θ METHOD)

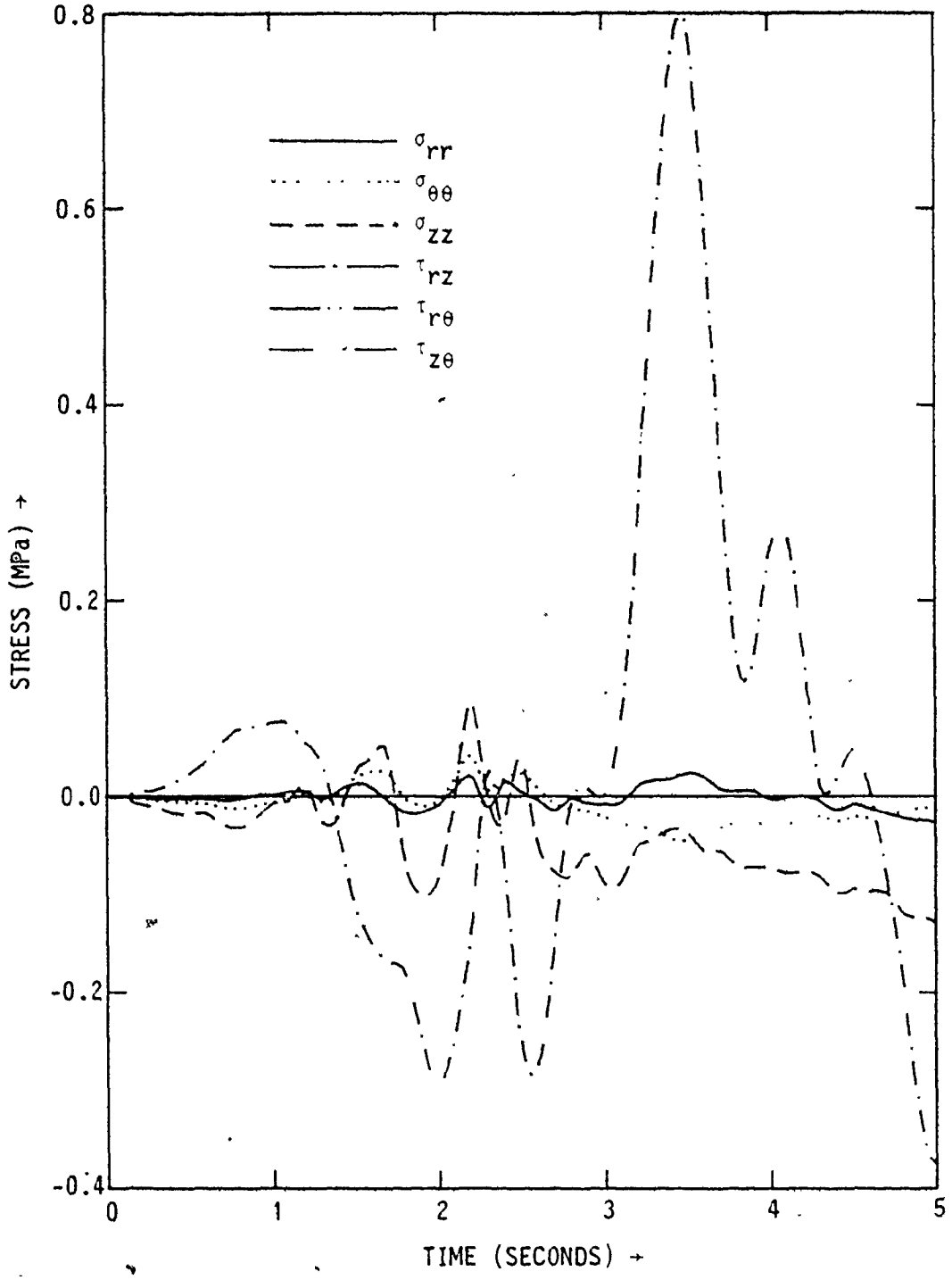

FIGURE 5.10.57 STRESSES IN THE LINER AT THE CROWN FOR SYSTEM E1, CASE 2 (WILSON'S θ METHOD)

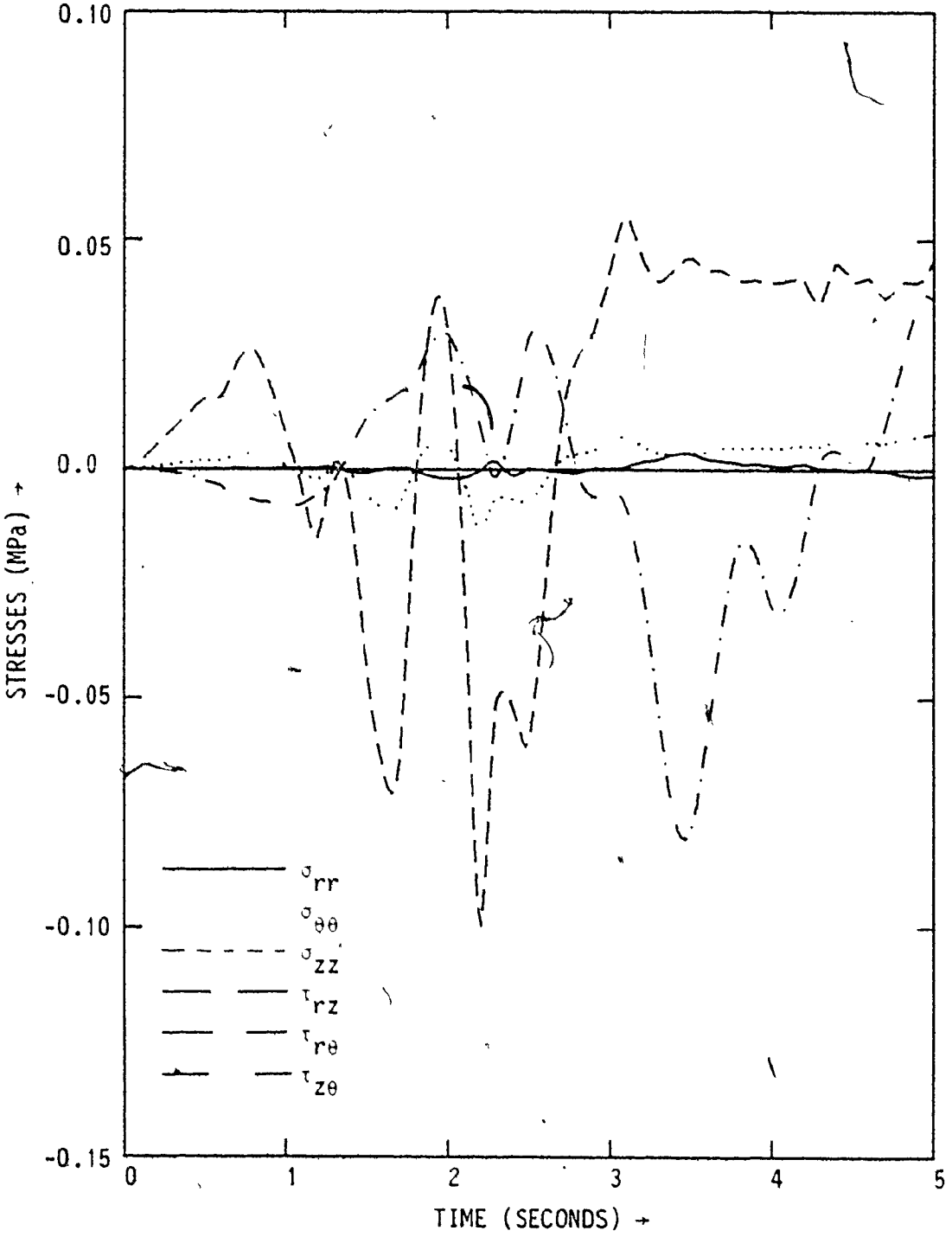

FIGURE 5.10.58 STRESSES IN THE LINER AT THE INVERT FOR SYSTEM E1, CASE 3 (WILSON'S θ METHOD)

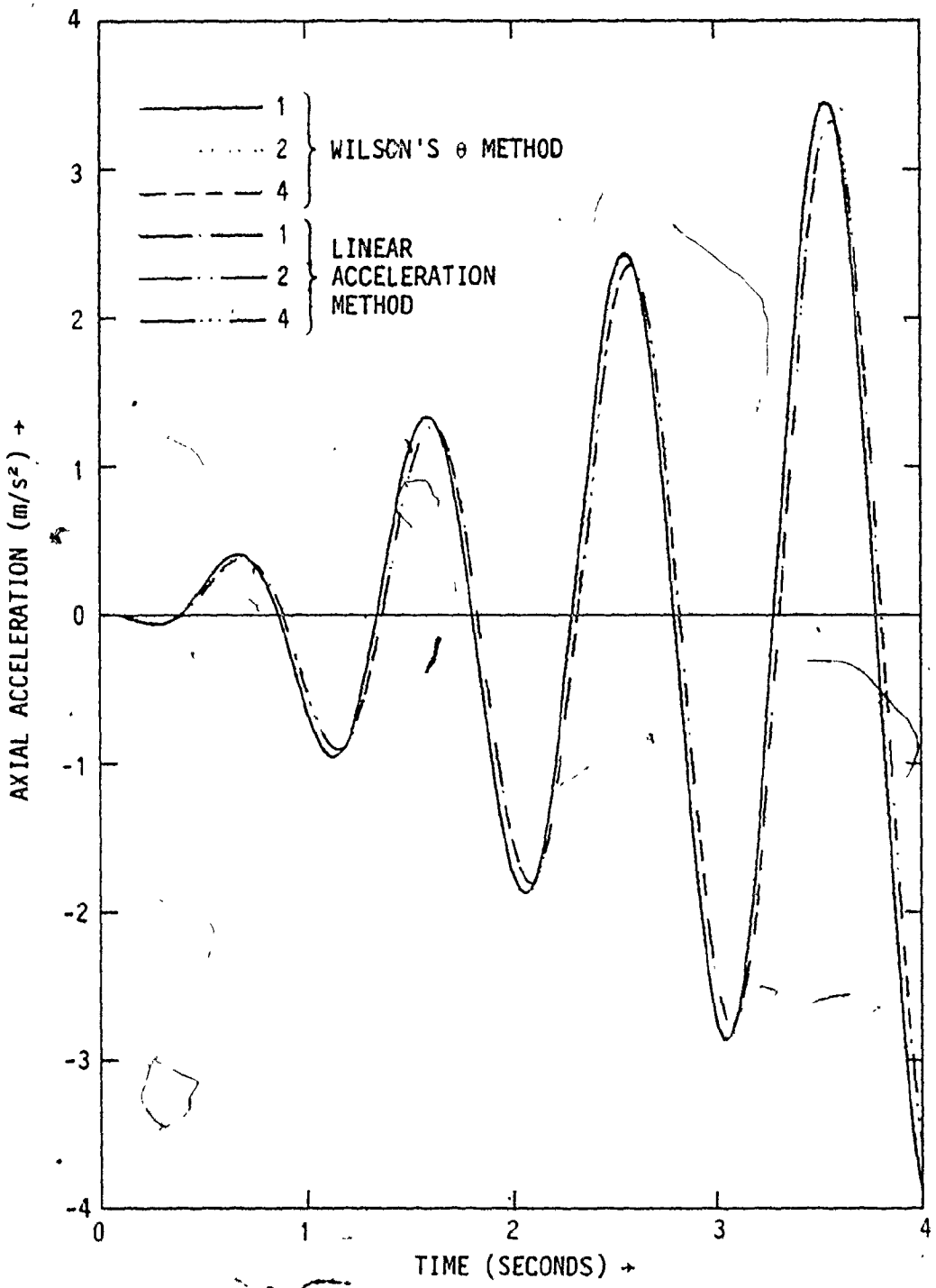

FIGURE 5.10.59 AXIAL ACCELERATIONS OF THE TUNNEL FOR SYSTEM E1, CASE 2

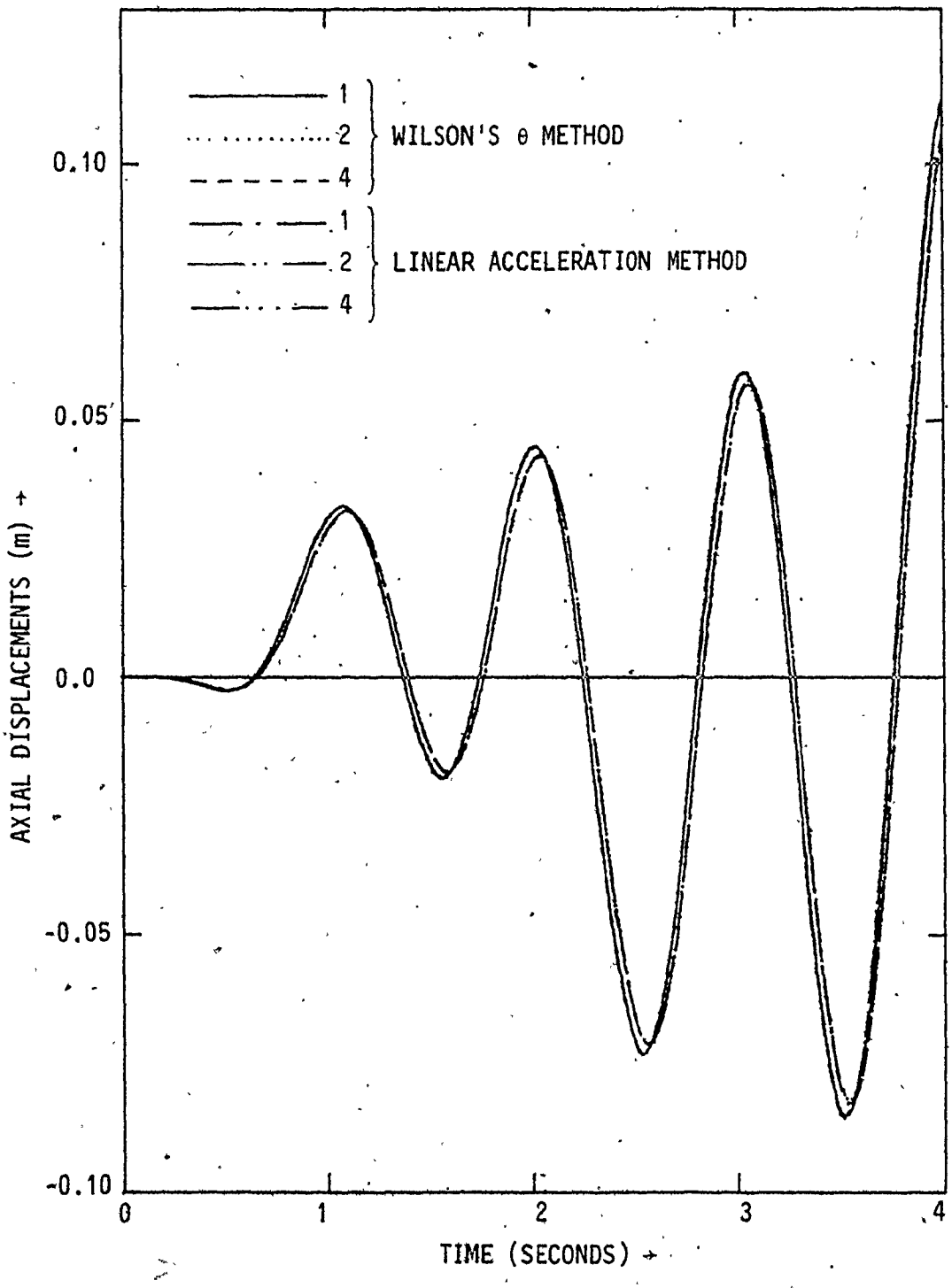

FIGURE 5.10.60 AXIAL DISPLACEMENTS OF THE TUNNEL LINER FOR SYSTEM E1, CASE 2

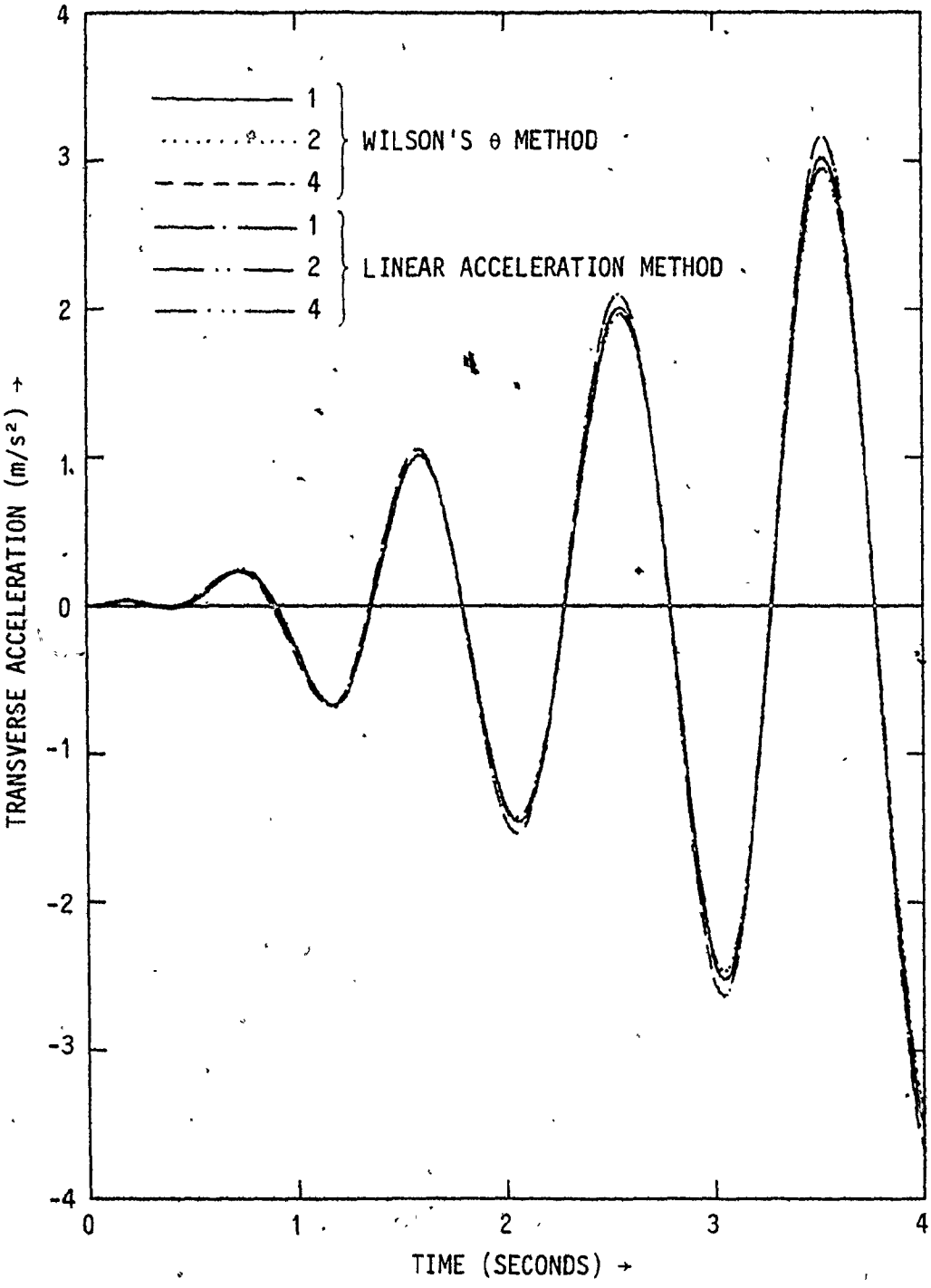

FIGURE 5.10.61 TRANSVERSE ACCELERATIONS OF THE TUNNEL FOR SYSTEM E1, CASE 2

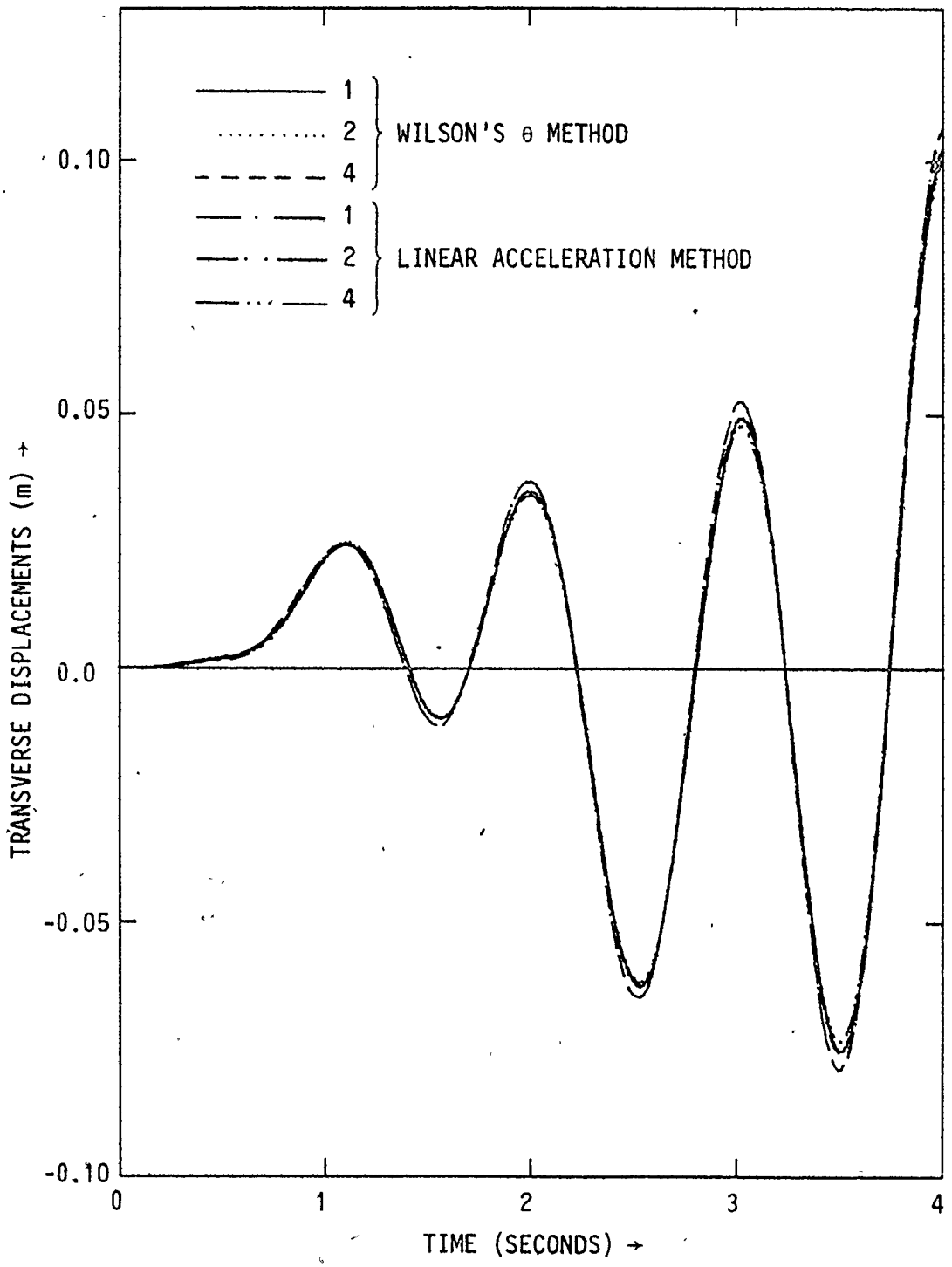

FIGURE 5.10.62 TRANSVERSE DISPLACEMENTS OF THE TUNNEL FOR SYSTEM E1, CASE 2

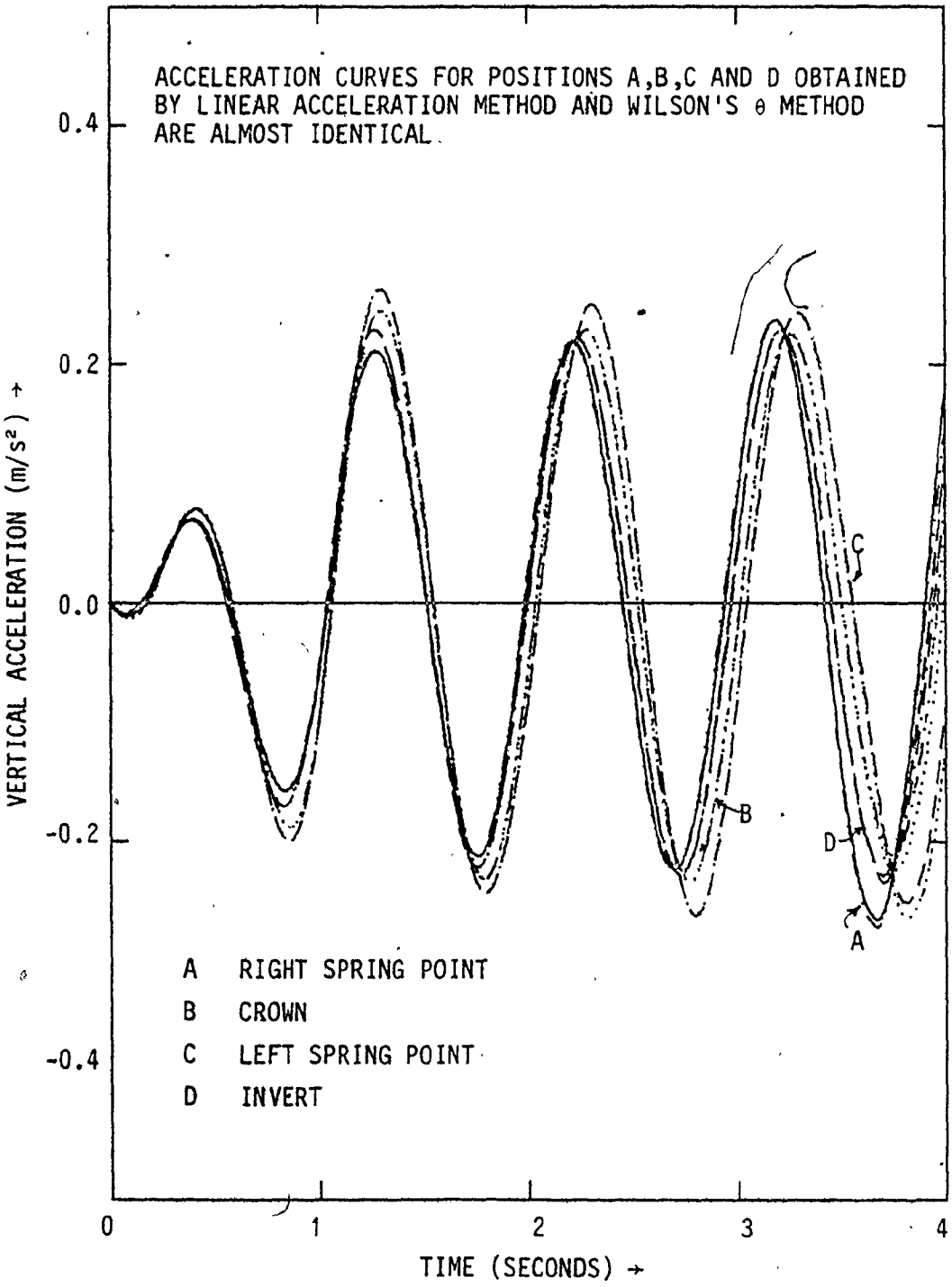

FIGURE 5.10.63 VERTICAL ACCELERATION OF TUNNEL FOR SYSTEM E1, CASE 2

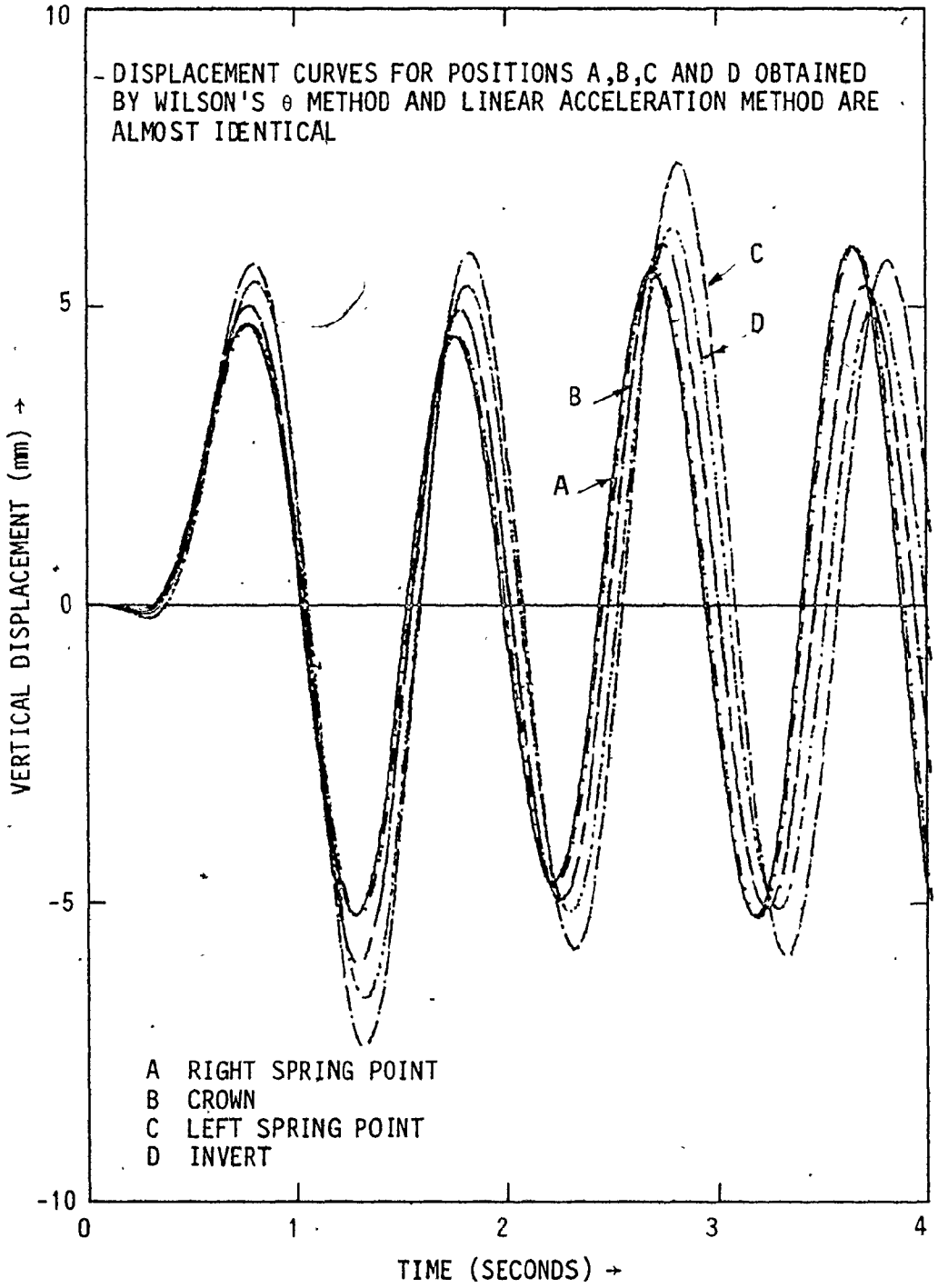

FIGURE 5.10.64 VERTICAL DISPLACEMENTS OF TUNNEL FOR SYSTEM E1, CASE 2

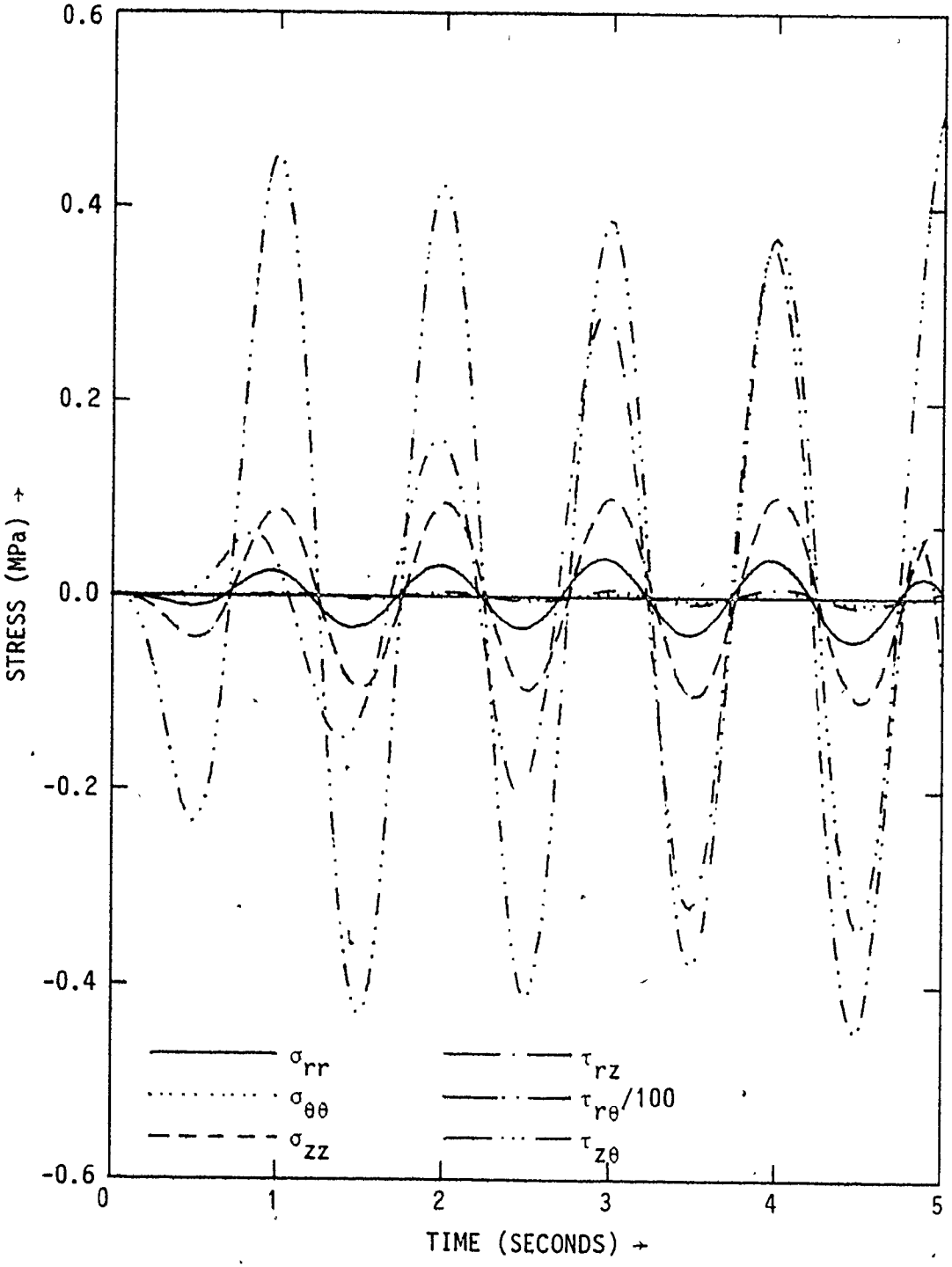

FIGURE 5.10.65 STRESSES AT THE RIGHT SPRING POINT OF THE TUNNEL LINER FOR SYSTEM E1, CASE 2 (WILSON'S θ METHOD)

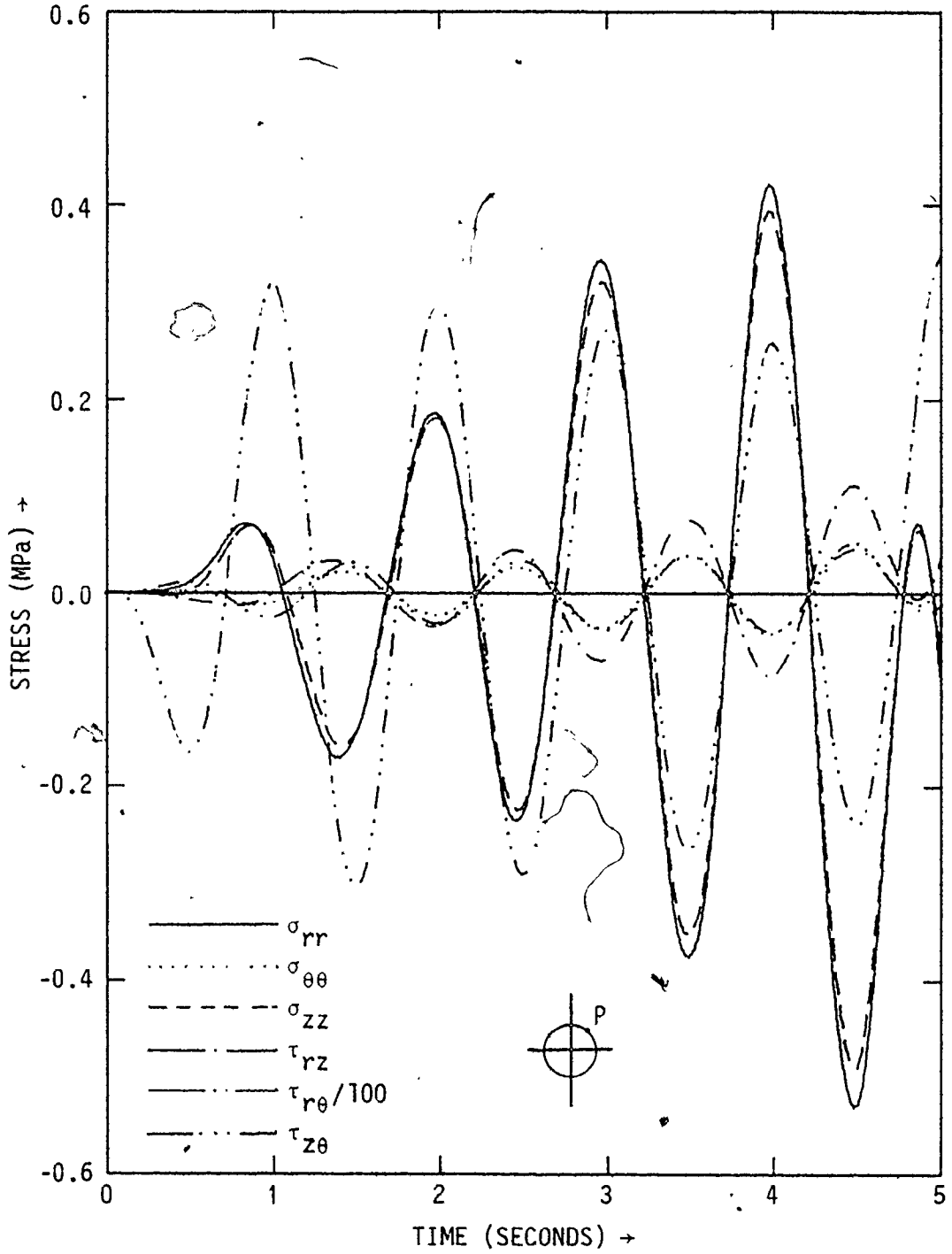

FIGURE 5.10.66 STRESSES AT THE POINT P OF THE TUNNEL LINER FOR SYSTEM E1, CASE 2 (WILSON'S θ METHOD)

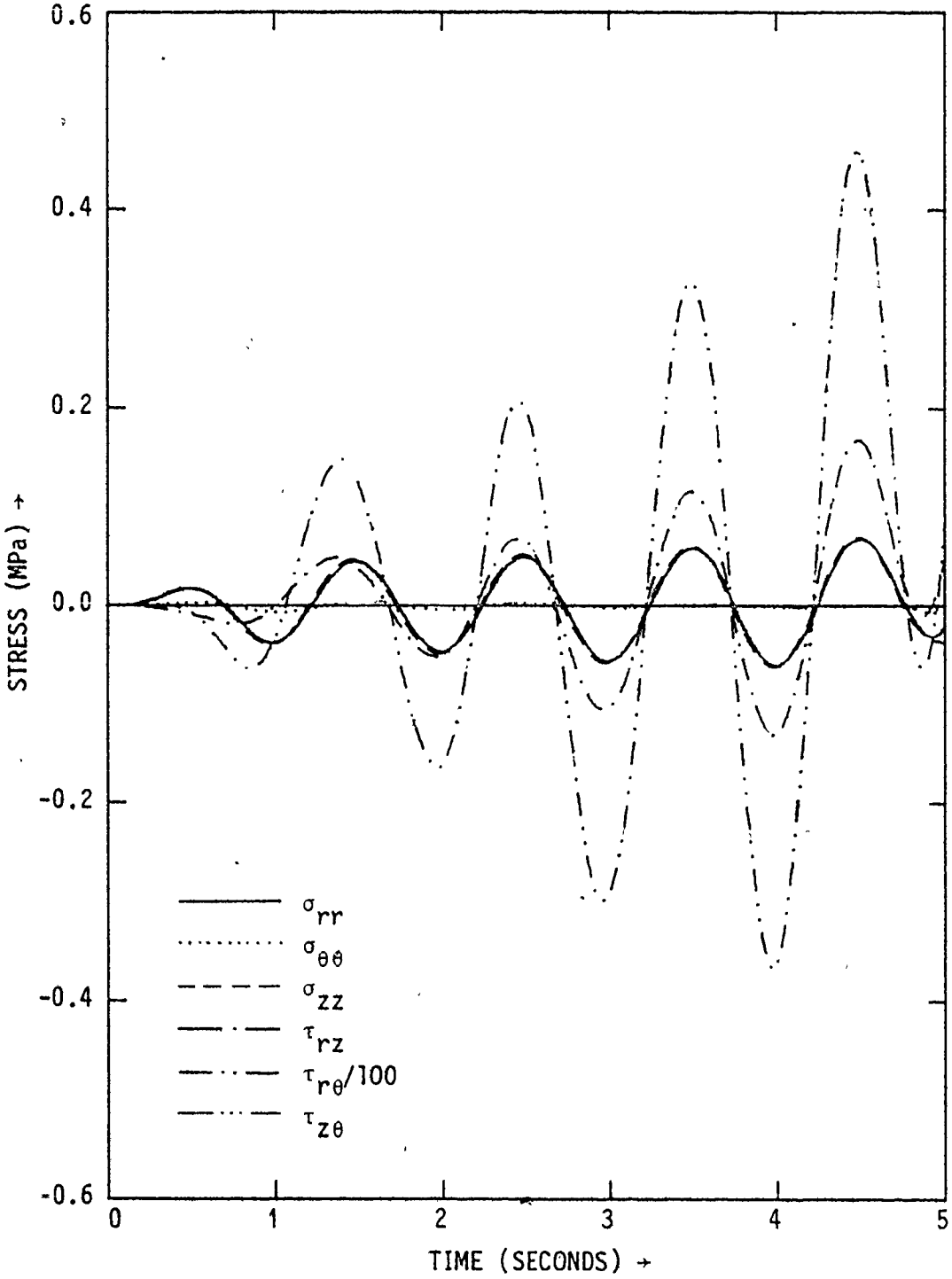

FIGURE 5.10.67 STRESSES AT THE CROWN OF THE TUNNEL LINER FOR SYSTEM E1, CASE 2 (WILSON'S θ METHOD)

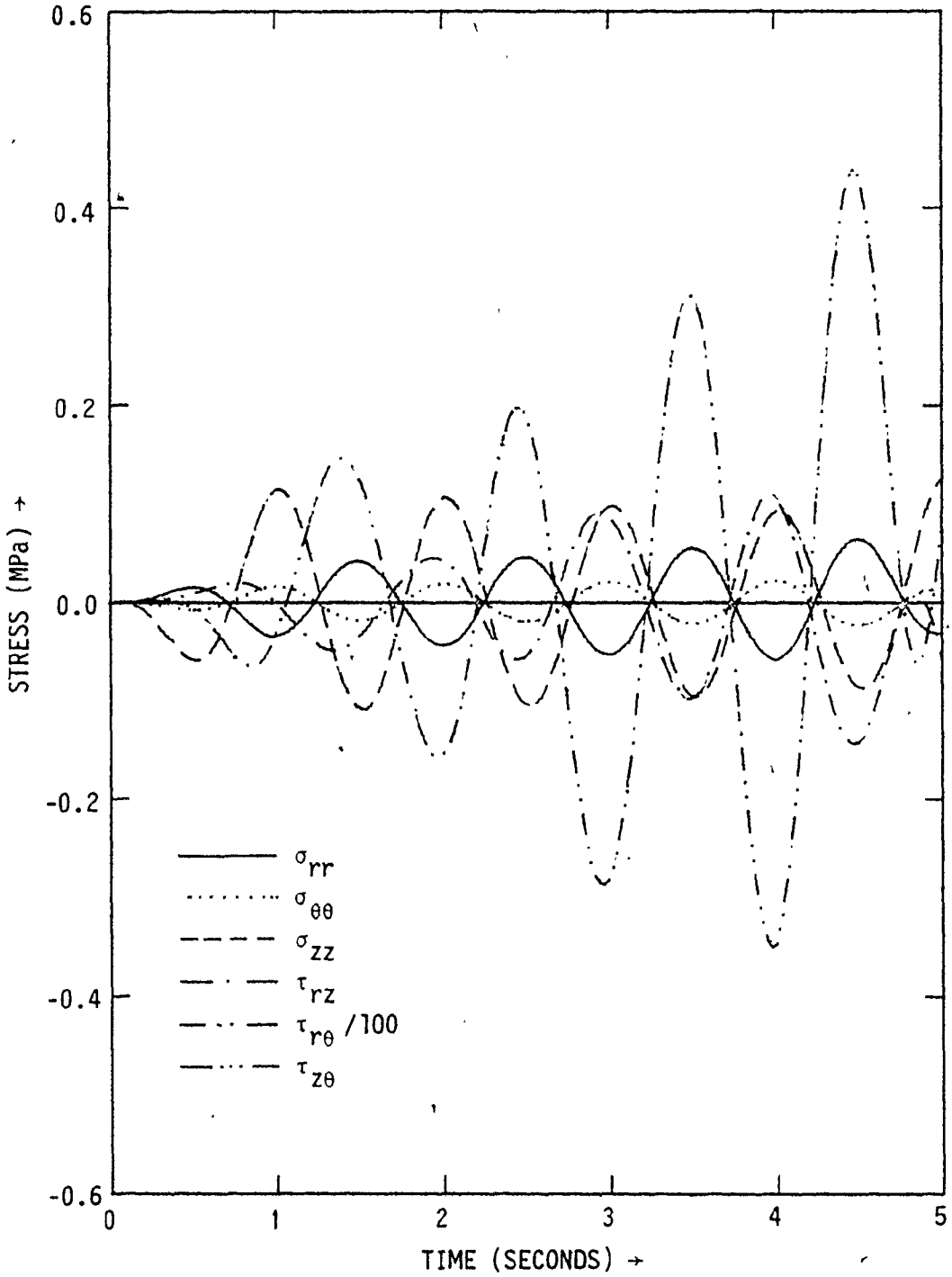

FIGURE 5.10.68 STRESSES AT THE INVERT OF THE TUNNEL LINER FOR SYSTEM E1, CASE 2 (WILSON'S θ METHOD)

by the first method for the other cases discussed in sections 5.10.2 and 5.10.3.

Of course, for future analyses, the Wilson's θ method should be adopted as it is unconditionally stable and permits longer acceleration records to be considered.

5.10.5 NUMBER OF HARMONICS TO BE CONSIDERED IN DYNAMIC ANALYSES.

The response of the system along any nodal ring in any coordinate direction may be expressed in the form of Fourier series. Although there are infinite terms in the series, to limit the cost of analysis, only a finite number of harmonics are included in any engineering analysis.

To study the adequacy of the number of harmonics required to represent a given distribution of responses along a nodal ring, different response distributions were assumed and analyzed with the zero harmonic and symmetric and antisymmetric components of the next nine harmonics. The quantitative results are not of significance here because of the numerous patterns of distributions involved. However, some general observations may be made. Generally the contribution of a higher harmonic is smaller. If the distribution is symmetric about a diameter of the ring, the zero harmonic, symmetric and antisymmetric components of the first harmonic, and symmetric component of the second harmonic are adequate enough to represent the response distribution. If the distribution is not symmetric about any diameter of the ring, more harmonics

need to be considered for adequate representation. The need for more harmonics increases as the degree of nonuniformity of response distribution along the ring increases.

From these observations, it is clear that it is hard to provide simplistic rules for choosing the number of harmonics, especially for a random phenomenon like an earthquake response. Nevertheless, if the earthquake propagation is in the axial direction only, the zero harmonic, symmetric and antisymmetric components of the first harmonic, and the symmetric component of the second harmonic are adequate. The response components of the system for the antisymmetric component for the second harmonic and symmetric component of the third harmonic were of the order of 10^{-19} m to 10^{-20} m for system E2 and 10^{-17} m to 10^{-19} m for system E1 for case 3, which are quite small compared to the response components in the lower harmonics.

For cases 1 and 2, the excitation is present in the axial as well as transverse directions. For such cases, a larger number of harmonics is important in the analyses. However, the dynamic analysis had to be limited by computer resources to the zero harmonic, symmetric and antisymmetric components of the first and second harmonics, and the symmetric component of the third harmonic. (This was dictated by the largest size of the permanent data file that could be allowed in the available computing facilities at the McMaster Computing Centre.) The component responses for the symmetric component of the third harmonic for cases 1 and 2 of system E1 for most time stations are under 10%

(and generally much less) of the component responses for the lower harmonics. It is believed that this is an acceptable level of accuracy for most engineering purposes.

5.10.6 LIMITATIONS OF THE ANALYSIS

The following limitations should be kept in mind when evaluating the results discussed in this section.

1. Adequacy of the model suggested in Chapter 4.

The model has worked the way it was intended to. However, in the case of inclined shear wave propagation, the borrowed responses for the boundary nodes of the end transverse sections are somewhat different from the actual responses at those positions. For this reason, the responses and stresses obtained in the end zones should not be considered. Since the seismic response varies along the length of the structure, it is difficult to quantify the associated error. In the absence of a better approach, it is still considered the best approach, and also helps to reduce the extra length needed to eliminate the errors due to assumed end section responses in the zone of interest.

The analysis used for obtaining the results discussed in sections 5.10.2 and 5.10.3 did not employ any extrapolation functions in predicting the response at the present time station from the responses at previous time stations. In the dynamic analysis using Wilson's θ method, a cubic function was used to extrapolate the response at the present time station from the responses at the preceeding four time

stations. This feature should prove to be helpful in reducing the chances of instability, even with the linear acceleration method. The comparison of results for case 1 (system E1) by these two methods appears to indicate that this factor does not have a significant effect on the computed results.

2. Instability in the analysis.

The acceleration values reach unusually large values for some cases at some time after 4 seconds for analyses with the linear acceleration method. The magnitudes of the displacements of the structure in this time range (i.e. up to 4 s) compare well with the corresponding free field motions, which is a good check against the occurrence of instability in the analysis. As a further check, the analysis was repeated for case 1 (system E1) using Wilson's θ method (with $\theta = 1.4$) which confirmed that the first four seconds of the analysis are not influenced by the instability for engineering purposes.

However, it is clear that as far as possible, an unconditionally stable algorithm like Wilson's θ method should be used in such analyses.

3. Number of harmonics used in the analysis

This item was discussed in greater detail in section 5.10.5. It is believed that the number of harmonics considered was adequate enough for engineering purposes, although inclusion of the antisymmetric component of the third harmonic (and both components of the fourth harmonic, if possible) would be desirable. This would of course increase the cost of computation.

4. Linear elastic analysis

Soils and rocks are actually nonlinear materials. For this reason, the simplifying assumption of linear elastic behaviour is reasonable only when the strains and stresses are at fairly low levels. Certain stresses for cases 1 and 2 are clearly beyond such limits, suggesting that yield and/or slippage has occurred. The analysis for these cases should employ linkage elements between the structure and the medium, which would lead to an increased number of degrees of freedoms and higher cost of analysis.

5.11 CONCLUSIONS

The results of various parametric studies were given in this chapter. The results indicate that free field motions may be expected to occur as a radial distance of 4 to 6 diameters from the axis. The properties of the liner material do not appear to significantly alter the response of the structure, but will of course have a significant influence on the computed stresses. Elements of aspect ratio 1:15 appear to be adequate with the CDC computer. The results also indicate that a plane wave basically induces displacements only in its plane of propagation.

For a tunnel of considerable axial length, analysis of a typical length is the problem of interest. The response at the transverse boundaries for this case are actually unknown. However, satisfactory analyses in the time domain can be carried out if these boundaries

'borrow' the responses from another cross section at a distance of 5 to 6 diameters from the end. This method can be improved by using more refined interpolation functions. For the case of inclined shear wave propagation, this method still causes some error in the assumed (borrowed) boundary response. The best results are obtained by making a compromise between the distance to the 'donor' cross section and the extra length of the structure included to eliminate the errors due to assumed end conditions.

The system is stiffer in the axial direction than in the vertical or transverse directions. This is reflected in the pattern of displacements produced in these directions. The structure-medium interaction can have a strong influence on the response of the structure. However, as the stiffness of the medium increases in comparison to that of the structure, the interaction appears to have little influence on the response of the structure. The response in the vertical direction depends on the angle of shear wave propagation.

The stresses are important in any engineering analysis, and are quite sensitive to small changes in the relative displacements between different positions in the tunnel lining. The vertical displacement variations along the length of the tunnel causes shear stresses in the z-θ plane at the two spring points, and axial stresses at the crown and invert position. Variation of axial displacements over a given transverse section also cause this type of shear. Variations in transverse (horizontal) displacements over a given cross-section cause shear

stresses in the r-θ plane. This shear acts over the thickness of the liner, which is relatively small. For this reason, the structure has greater resistance against relative displacements in the axial direction than in the transverse direction, unless a low tensile strength material such as concrete is involved. This indicates that the direction of seismic wave propagation with respect to the tunnel axis is important. Similarly, the angle of seismic wave propagation with respect to the vertical is very important.

The stresses and displacements obtained from the analysis using the linear acceleration method for system E1 (cases 2 and 3) compare well with those obtained by use of Wilson's θ method. It is believed that this is also true for the other analyses up to 4 seconds, or so, discussed in this chapter based on the linear acceleration method. As such, meaningful observations of engineering importance have also been made for these examples in previous sections.

CHAPTER 6

CONCLUSIONS

The spatial variation of seismic ground motions is a critical factor in the dynamic analyses of structure-medium interactive systems. Present practices do not generally account for the principles of shear-wave propagation at base rock level, which may lead to errors of the order of 30 to 50 per cent in the computed ground response. The method developed to account for reflected, as well as refracted, components of the upward and downward propagating shear waves is a very important improvement over current practices.

R-wave contributions to the seismic ground response are significant in many situations. Considerable information is available regarding the propagation of R-waves through layered media. However, there is no method available that can quantitatively estimate their contribution in a rational way based on the available data. The proposed method for this is in accord with principles of R-wave propagation; and uses parameters that are required in such analyses, and can be obtained with reasonable accuracy. This enables a more rational and meaningful consideration of R-waves in the aseismic analysis. Further, it provides a better understanding of the R-waves.

Current practices consider the entire range of R-wave phase velocities at regular intervals, with trial and error methods to

determine the period and wave number for each phase velocity. This is costly and laborious. Moreover, only a narrow range of phase velocites enable the R-waves to reach the site together with shear waves which are of interest in the engineering analysis. The method proposed for obtaining the phase velocity and period of R-waves for a given site is based on the observations from many available seismic records. This rationalizes the method for dealing with the R-waves and eliminates the need for trial and error approaches. The transfer functions obtained by this procedure are relatively insensitive to errors in the periods of R-waves.

There are methods available to determine the angle of propagation of shear waves in any layer with respect to the vertical. However, they do not indicate for which layer it should be computed. If this basic quantity is computed for the surface layer, the computed angle in the base rock could lead to absurd values. A more rational approach is to obtain the basic quantity for the base rock first. The velocity of shear wave for rocks at about 30 km below the ground level is reported by many investigators; from this the largest angles of incidence at the base rock level may be obtained. This further enables the largest values of angles of propagation for other formations to be determined. This will be of great help in avoiding the use of higher estimates of the angle that may otherwise appear to be reasonable. This is rather important because the stresses computed for the structures being considered are quite sensitive to the angle of shear wave propagation with the vertical.

For the structures under investigation, the liner thickness is quite small compared to the overall dimensions of the problem included in the finite element analysis. This leads to a large number of displacement degrees of freedom, which in turn demand increased central memory storage and a higher cost of computation. Improvements to the numbering of the mesh nodes (together with a technique for storing the sparse banded matrices), and the proposed method of solving the equation of motion can often significantly reduce the size of such problems.

For structures of large axial length, the results of the analysis for a typical portion of finite length are often adequate. This also helps in keeping down the size of the problem. However, because of structure-medium interaction, the response along the transverse end sections is unknown; without which the dynamic analysis in the time domain cannot be carried out for boundary value problems. A method has been developed for the reasonable estimation of these unknown responses for vertical or inclined propagation of shear waves with a horizontal axis of symmetry. Current practices suggest the inclusion of an additional length of structure at either transverse end so that the errors due to assumed end conditions are negligible in the zone of interest. Since these errors are felt to a considerable length from the transverse ends, this leads to a considerable increase in size of the problem and cost of analysis. The proposed method is a definite improvement in reducing the size as well as the cost of analysis. Further, it also rationalizes the analysis for a range of problems.

A rigorous three-dimensional analysis is possible, but the size of the problem and analysis cost would often be prohibitively high. Fortunately, satisfactory three-dimensional analyses may be carried out using an axisymmetric approach. In many situations this is quite appropriate. In situations where it is not, in the absence of better alternatives, it is still the best proposition available. However, the results in such cases should be interpreted in the light of the simplifying assumptions made.

Many conclusions can be made from the results of the parametric studies. The ground responses at distances of three to four diameters from the axis of symmetry differ from the free field motions by less than 10 per cent. The propagation of plane waves mainly cause resonses in the plane of propagation. This is helpful in studying the responses and stresses induced by the axial and transverse components of the excitation acting separately. For a given intensity of excitation, the transverse exciation induces greater stress levels than those for the same excitation in the axial direction. This is because the shear due to the relative response between points on the structure in the same vertical plane has to be transferred through a relatively small thickness of liner. The vertical response and the stresses are quite sensitive to the angle of shear wave propagation with the vertical. The structure medium interaction is very important, because even for small changes in relative displacements, the corresponding changes in stress can be large depending upon the stiffness of the system in that direction. This is more so for a softer medium where it helps to reduce the relative

displacements in comparison to the differential free field response at the same points. As the elastic modulii of the medium grow closer to those of the liner material, the influence of the structure-medium interaction on the response of the system also decreases. The interaction has a greater influence on the transverse response than the axial response because the system has greater stiffness in the axial direction than in the transverse direction. This indicates that the use of free field responses at the periphery of the structure is not always a reasonable approach in such analyses, especially for softer media with axial excitations. The approach leads to very conservative designs since interaction leads to a significant reduction in the relative displacements of the structure in the axial direction. The relative transverse responses are not influenced in a similar way for the softer medium because the stiffness of the system is comparable to that of the medium without the structure. But significant relative displacements can occur between the spring point and the crown (or invert) because the stiffness in the transverse direction may be different because of the cavity of the structure.

The investigation has employed somewhat idealized conditions in assuming an homogeneous single layer system and linear elastic material properties. Numerical errors appear after 4.5 s in the analyses using the linear acceleration method, but the results are good enough for the first 4 seconds to make observations of engineering importance. This is substantiated by the results obtained using the unconditionally stable algorithm of Wilson's θ method. The results are in good agreement

with the behaviour of structures observed during past earthquakes. The results clearly contribute to a further understanding of medium structure interaction for such problems during earthquakes.

The response of the liner was very close to the free field response at the corresponding position (without the tunnel) even when the Young's modulus of the medium is about one sixth of that of the liner. The results also indicate that as the Young's modulus of the medium becomes larger, the liner response becomes closer to the free field response. This suggests that for media with Young's modulus comparable to that of the liner, the liner response would be almost identical to the free field response at that position. This will enable the design engineer to compute the response of the liner once and for all and to use the same response to test different liner designs. This will eliminate the need to run repeatedly the entire dynamic analysis, thus economizing on the cost of design and analysis.

FUTURE RESEARCH

Based on the results of this investigation, the following suggestions for future research are made. Because of the large size of the problem, special care should be taken to reduce truncation and rounding errors. To assure unconditional stability, Newmark's β method or Wilson's θ method should be used. Quadratic or cubic function may be used in extrapolating the response of the node at the present time from a knowledge of the response at the previous time stations when obtaining the estimates of the response of the nodes on the transverse boundaries of the structure. This should help in improving numerical stability.

The parametric analysis should be extended to include special features such as changes in cross-section and/or stiffness of the structure; the presence of interfaces of media across the structure; analysis of the system with multiple formations of different elastic moduli; and depth of cover and its variation along the axial length. A wider range of medium modulii should be considered to study the importance (or the lack of importance) of the medium-structure interaction on the response of the structure and the resulting stresses and strains.

The response of the structure does not appear to be very sensitive to changes in the liner properties. This needs to be substantiated by further studies. This would be of great help in simplifying the design procedures if the response of the system is not very sensitive to changes in the liner properties. In the range of interest for design, similar studies may be carried out with respect to the influence of

special features like pipeline flanges and anchor blocks, etc., since stress concentrations that are observed to occur near such features are of great interest to the design engineer.

In future research, liquefaction of the medium and nonlinear behaviour of the medium should be studied. Recent advances in the methods of computation of pore pressures as a function of the strain levels, confining pressures, etc., make it possible to incorporate the pore pressures in such studies. The nonlinearity of the materials can be readily incorporated in such analyses by an incremental approach. The extent of nonlinearity in the liner material should be very limited in many situations since relatively conservative criteria are adopted for lifeline structures.

BIBLIOGRAPHY

Akoi, Y. and Hayashi, S. "Spectra for Earthquake Resistive Design of Underground Long Structures", Proc. 5th World Conf. On Earthquake Engineering. Rome, 1973. pp. 558.

Bathe, K.J. and Wilson, E.C. Numerical Methods in Finite Element Analysis. Prentice Hall, Inc., Englewood Cliffs, New Jersey, 1976.

Chandra, U. "Angle of Incidence of S-Waves", Bull. of Seism. Soc. of America, Vol. 62, No. 4, Augusut 1972, pp. 903-915.

Clough, R.W. "Analysis of Structural Vibrations and Dynamic Response", Recent Advances in Matrix Methods of Structural Analysis and Design. Univ. of Alabama Press, Huntsville, 1971. pp. 441-486.

Clough, R.W. and Penzien, J. Dynamics of Structures. McGraw Book Co., New York, 1975.

Clough, R.W. and Rashid, Y. "Finite Element Analysis of Axisymmetric Solids", Journal of ASCE, Eng. Mech. Div. Vol. 91, EM-1, February 1965, pp. 71-85.

Dahlquist, G. and Bjorck, A. (Translator Ned Anderson) Numerical Methods. Prentice Hall Inc., Englewood Cliffs, New Jersey, 1974.

Desai, C.S. and Abel, J.F. Introduction to the Finite Element Method. Van Nostrand Reinhold Co., New York, 1972.

Dibaj, M. and Penzien, J. "Response of Earth Dams to Travelling Seismic Waves", Journal of ASCE, Soil Mech. and Found. Div., Vol. 95, SM-2, March 1969, pp. 541-560.

Duke, C.M. and Moran, D.F. "Guidelines for Evolution of Lifeline Earthquake Engineering", Proc. of U.S. National Conf. on Earthquake Engineering, Ann Arbor, 1975, pp. 367.

Emery, J.J. and Joshi, V.H. "Seismic Response of Underground Openings", Thirteenth Canadian Rock Mechanics Symposium, University of Toronto, May 1980.

Faddev, D.K. and Faddeeva, V.N. Computational Methods of Linear Algebra. Freeman and Co., San Francisco, 1963.

Goodman, R.E., Taylor, R. and Brekke, T.L. "A Model for Jointed Rock", Journal of ASCE, Soil Mech. and Found. Div., Vol. 94, SM-3, May 1968, pp. 637-659.

Goto, Y., Ota, J. and Sato, T. "On the Earthquake Response of Submerged Tunnels", Proc. 5th World Conf. on Earthquake Engineering, Rome, 1973, pp. 579.

Hamada, M., Akimoto, T. and Izumi, H. "Dynamic Stress of a Submerged Tunnel During Earthquake", Sixth World Conf. on Earthquake Engineering, New Delhi, 1977, pp. 4-55.

Hardin, B.O. and Drenvich, V.P. "Shear Modulus and Damping in Soils: Measurements and Parameter Effects", Journal of ASCE, Soil. Mech. and Found. Div., Vol. 98, SM-6, June 1972, pp. 603-624.

Hardin, B.O. and Drenvich, V.P. "Shear Modulus and Damping in Soils: Design Equations and Curves", Journal of ASCE, Soil Mech. and Found. Div., Vol. 98, SM-7, July 1972, pp. 667-692.

Haskell, N.A. "The Dispersion of Surface Waves in Multilayered Media", Bulletin of Seism. Soc. of America, Vol. 58, No. 4, August 1968, pp. 1193-1241.

Hindy, A. and Novac, M. "Earthquake Response of Underground Pipelines", Journal of Earthquake Engineering and Structural Dynamics, Vol. 7, 1979, pp. 451-476.

Housner, G.W. "Intensity of Earthquake Ground Shaking Near the Causative Fault", Proc. Third World Conf. on Earthquake Engineering, New Zealand, 1965, Vol. 3, pp. 94-115.

Idris, I.M. and Seed, H.B. "An Analysis of Ground Motions During the San Francisco Earthquake", Bull. of Seism. Soc. of America, Vol. 58, No. 6, December 1968, pp. 2013-2032.

Iwan, W.D. "Earthquake Resistance of Public Utility Systems - A Report on Findings of the California Governor's Inter-Agency Earthquake Committee", Proc. of U.S. National Conf. on Earthquake Engineering, Ann Arbor, 1975, pp. 387.

Iwasaki, T. and Tatsuoua, F. "Dynamic Soil Properties with Emphasis on Comparison of Laboratory Tests and Field Measurements", Sixth World Conf. on Earthquake Engineering, New Delhi, 1977, pp. 6-153.

Joshi, V.H. and Emery, J.J. "Seismic Response of Tunnels", Second Conf. on Ground Movements and Structures, Department of Civil Eng. and Building Tech., UWIST, Cardiff, April 1980.

Kanai, K. "On the Predominant Periods of Earthquake Motion", Bull. of Engineering Research Institute, Univ. of Tokyo, Vol. 40, 1962.

Katayama, T., Kubo, K. and Sato, N. "Earthquake Damage to Water and Gas Distribution Systems", Proc. of U.S. National Conf. on Earthquake Engineering, Ann Arbor, 1975, pp. 396.

Kaussel, E., Roseet, J.M. and Waas, G. "Dynamic Analysis of Footings on Layered Media", Journal of ASCE, Eng. Mech. Div., EM-5, October 1975.

Kobayashi, H. and Kagami, H. "A Method for Local Seismic Intensity Zoning Maps", Proc. of the International Conference on Microzonation for Safer Construction Research and Application, Vol. 2, Seattle, Washington, October - November 1972, pp. 513-528.

Kubo, K. "Behaviour of Underground Water Pipes During an Earthquake", Proc. of World Conf. on Earthquake Engineering, Rome, 1973, pp. 569.

Kuhlmeyer, R.L. and Lysmer, J. "Finite Element Accuracy for Wave Propagation Analysis", Journal of ASCE, Soil Mech. and Found. Div., SM-5, May 1973, pp. 421.

Lysmer, J. and Kuhlmeyer, R.L. "Finite Dynamic Model for Infinite Media", Journal of ASCE, Eng. Mech. Div., EM-4, August 1969, pp. 859-877.

Matsuo, M. and Horiuchi, T. "Earthquake Damage and Methodology of Design of Small Diameter Pipelines", Soils and Foundations, Vol. 19, No. 1, March 1979, pp. 23-38.

Nair, G.P. "Response of Soil-Pile Systems to Seismic Waves", Ph.D. Thesis, McMaster University, Hamilton, January 1974.

Nasu, N., Kazama, S., Morioka, T. and Tamura, T., "Vibration Test of the Underground Pipe with a Comparatively Large Cross Section", Proc. of Fifth World Conf. on Earthquake Engineering, Rome, 1973, pp. 579.

Newmark, N.M. "A Method of Computation for Structural Dynamics", Journal of ASCE, Eng. Mech. Div., EM-3, July 1959, pp. 67-94.

Newmark, N.M. and Hall, W.J. "Pipeline Design to Resist Large Displacements", Proc. of U.S. National Conf. on Earthquake Engineering, Ann Arbor, 1975, pp. 416.

Newmark, N.M. and Rosenblueth, E. Fundamentals of Earthquake Engineering. Prentice-Hall Inc., Englewood Cliffs, New Jersey, 1971.

Novac, M, and Fakhry, A.E. "Impedence Functions for Piles in Layered Media", Journal of ASCE, Eng. Mech. Div., EM-3, 1978, pp. 643-659.

Okamoto, S. Introduction to Earthquake Engineering. John Wiley and Sons, New York, 1973.

Okamoto, S., Tamura, C., Kato, K. and Hamada, M. "Behaviours of Submerged Tunnels During Earthquakes", Proc. of Fifth World Conf. on Earthquake Engineering, Rome, 1973, pp. 544.

Oliver, J. and Ewing, M. "Higher Modes of Continental Rayleigh Waves", Bull. of Seism. Soc. of America, Vol. 47, No. 3, July 1957, pp. 187-203.

Parmalee, R.A. "Investigation of Soil-Structure Interaction of Buried Concrete Pipe", Highway Research Record, No. 443, 1973, pp. 1-32-39.

Pipes, L.A. Applied Mathematics for Engineers and Physicists, McGraw Hill Book Co., 1958.

Penzien, J. "Elasto-Plastic Response of Idealized Multistorey Structures Subjected to Strong Motion of Earthquakes", Proc. of the Second World Conf. on Earthquake Engineering, Tokyo, 1960, Vol. 2, pp. 739-760.

Poulos, H.G. and Davis, E.H. Elastic Solutions for Soil and Rock Mechanics. John Wiley and Sons, Inc., New York, 1974.

Richart, F.E., Woods, R.D. and Hall, J.R. Vibrations of Soils and Foundations. Prentice-Hall Inc., Englewood Cliffs, New Jersey, 1970.

Richart, F.E., Anderson, D.G. and Stolle, K.H. "Predicting Insitu Strain Dependent Shear Modulus of Soils", Sixth World Conf. on Earthquake Engineering, New Delhi, 1977, pp. 6-159.

Sakurai, A. and Takahashi, T. "Dynamic Stresses in Underground Pipeline During Earthquakes", Proc. of Fourth World Conf. on Earthquake Engineering, Santiago, Chile, 1969, pp. B-4, 81.

Seed, H.B., Idris, I.M. and Kiefer, F.W. "Characteristics of Rock Motions During Earthquakes", EERC Report No. 68-5, Earthquake Engineering Research Centre, University of California, Berkeley, Calif., September 1968.

Sezawa, K. "Dispersion of Elastic Waves Propagated on the Surface of Stratified Bodies and Curved Surfaces", Bull. of the Earthquake Eng. Research Institute, Univ. of Tokyo, Vol. 3, 1927, pp. 1-18.

Suzuki, T. "On the Angle of Incidence of the Initial Motion Observed at Hongo and Mitaka", Bull. of Earthquake Eng. Research Institute, Univ. of Tokyo, Vol. 10, 1932, pp. 517-535.

Szechy, K. The Art of Tunnelling. Akademi Kiado, Budapest, 1966.

Thompson, W.T. "Transmission of Elastic Waves Through a Stratified Solid Medium", Journal of Applied Physics, Vol. 21, February 1950, pp. 89-93.

Timoshenko, S. and Goodier, J.N. Theory of Elasticity. McGraw Hill Book Co., Inc., New York, 1951.

Trifunac, M.D. "Response Evelope Spectrum and Interpretation of Strong Earthquake Ground Motion", Bull. of Seism. Soc. of America, Vol. 61, No. 2, April 1971, pp. 343-356.

Trifunac, M.D. and Brune, J.N. "Complexity of Energy Release During the Imperial Valley, California Earthquake of 1940", Bull. of Seism. Soc. of America, Vol. 60, No. 1, February 1970, pp. 137-160.

Tsai, N.C. "Influence of Local Geology on Earthquake Ground Motion", Ph.D. Thesis, California Institute of Tech., Pasadena, California, 1969.

U.S. Dept. of Commerce. San Fernando California Earthquake of February 1971, Vol. II, Utilities Transportation and Sociological Aspects.

White, J.E. Seismic Waves: Radiation, Transmission and Attenuation, McGraw Hill Book Co., Inc., New York, 1965.

Whitman, R.V., Cornel, C.A. and Ghiath, T.A. "Analysis of Earthquake Risk for Lifeline Systems", Proc. of U.S. National Conf. on Earthquake Engineering, Ann Arbor, 1975, pp. 377.

Wiegel, R.L., ed. Earthquake Engineering, Prentice-Hall, Inc., Englewood Cliffs, New Jersey, 1970.

Wilson, E.L. "Finite Element Analysis of Two-Dimensional Structures", Ph.D. Thesis, Univ. of California, 1963.

Wilson, E.L. "Structural Analysis of Axisymmetric Solids", IAAA Journal, 1965, pp. 2269-2274.

Wilson, E.L. and Clough, R.W. "Dynamic Response by Step-by-Step Analysis", Proc. Symposium on the Use of Computers in Civil Engeering, Lisbon, October 1962, pp. 45.1-45.14.

Wolf, J.P. "Seismic Response due to Travelling Shear Wave Including Soil-Structure Interaction with Base-Mat Uplift", Journal of Earthauake Eng. and Structural Dynamics, Vol. 5, 1977, pp. 337-363.

Yamahara, H. "Ground Motions During Earthquakes and the Input Loss of Earthquake Power to an Excitation of Buidlings", Soils and Foundations, Vol. 10, No. 2, June 1970, pp. 145-161.

Zienkiewicz, O.C. The Finite Element Method. McGraw-Hill Book Co. Inc., 1977.

APPENDIX A

EARTHQUAKE CONSIDERATIONS FOR LIFELINE SYSTEMS

A1 INTRODUCTION

Public utilities such as water supply, sewage disposal systems, gas and power supply, etc. are termed lifeline facilities which are essential for day-to-day living. They are also of crucial importance in providing post disaster relief to people affected by possible earthquake damage. The facilities coming under the lifeline category are listed in Table A-1. Although the potential for loss of life due to failure of lifelines is quite high, past earthquake experience shows very little evidence of this nature compared to that due to failure of buildings, earth dams, landslides and liquefaction, although the 1971 San Fernando Earthquake came very close to reversing this trend.

There have been some attempts made to catalogue the essential services that must be maintained even when an earthquake occurs. Table A-1 gives the recommendations made by Duke and Moran (1975). The recommendations of the Earthquake Council appointed by the Governor of California regarding the basic elements of a program for earthquake resistance of public utility systems are given in Tables A-3 to A-5 (Iwan, 1975).

A2 EARTHQUAKE DAMAGE TO BURIED PIPES

Earthquake damage to buried pipes can be described in terms of a number of items.

1. Pipe material.
2. Joint type.
3. Location of the joints, valves, manholes, etc.
4. Diameter or the size of the pipe.
5. Intensity of the earthquake.
6. Nature of the ground.
7. Direction of the pipeline with respect to the incident seismic waves.
8. Direction of any land movement.

1. Pipe Material

It appears that if the pipe material has at least 1 to 2% ductility, then the pipeline has a much better chance of resisting earthquake damage than if the pipe is brittle.

2. Joint Type

Available information indicates that the strength of the joints plays a major role in resisting damage to pipes. Cast iron and asbestos cement pipes suffer relatively more damage partly because their jointing material is either too weak to resist pulling apart or too brittle to withstand reasonably large displacements. Tearing of pipelines with welded or bolted joints indicates a joint strength comparable

to that of the pipe itself. It is possible to incorporate slip joints in areas of anticipated seismic activity that permit the necessary axial deformations to resist damage.

3. Location of joints, manholes, and bends.

As explained in a following section, since the pipe has practically the same displacements and accelerations as the surrounding soil, inertia forces have little role to play in causing pipeline damage. However, as indicated in a following section, the direction of the seismic waves will have some effect on the stresses induced in the pipe and joints, manholes, bends, etc. can act as stress raisers, particularly in the axial direction.

4. Diameter or size.

Smaller diameter pipes appear to sustain greater damage than larger pipes. However, this may be partly because of a lack of attention to the design, construction and maintenance of such lines compared to important pipelines of larger diameter. Moreover, the material properties and stiffness of the pipe with respect to the surrounding medium is more important than the diameter alone.

5. Intensity of the Earthquake.

The damage to pipe lines in Los Angeles during the 1971 San Fernando Earthquake decreased sharply with epicentral distance, i.e. with decreasing intensity of earthquake. In general, it would appear that damage does not occur for shaking below 0.3 g as a qualitative guide.

6. Nature of the ground.

It is difficult to outline the influence of the ground on earthquake damage because there are many soil types with diverse soil properties. However, some useful qualitative observations can be made. Damage to pipes during the Kanto, Fukui, Niigata and San Fernando Earthquakes indicate that differences in dynamic properties of horizontally adjacent layers is one of the main causes of shaking damage. Even with large displacements in softer soils, the displacements can be much smaller than the relative displacements that occur at the junction between stiffer and softer soils resulting in damage in the junction area.

Damage to pipe lines in the city of Niigata due to the Niigata Earthquake are of interest as liquefaction was involved. The whole area under consideration can be divided into three parts, firm ground (A), medium firm ground (B), and soft reclaimed ground (C). The damage in soil (A) was less than that in soil (B). The damage was heaviest in soil (C) because it suffered liquefaction, causing very large settlements. Since the movements of buried pipes are nearly the same as those of the surrounding soil, they too suffered large deformations from the liquefaction resulting in heavy damage. Pipe lines passing through soil strata with a potential for liquefaction must be considered carefully during seismic designs.

7. Direction of the pipeline with respect to the incident seismic waves.

Although field data are not well classified with respect to this variable, the results of theoretical and model studies tend to indicate that for a given intensity of ground shaking and type of soil, the stresses induced in the pipe due to seismic waves parallel to the axis of the pipe line are approximately twice those due to waves at right angles to the axis.

8. Direction of land movement.

For pipelines in areas of gross land movements due to liquefaction or sliding, the damage will be greatest in the direction of the land movements.

A3 FIELD TESTS ON BURIED PIPE

A full-scale testing of a buried pipe 84 m long, 1.219 m in diameter and 0.117 m thick was conducted at the Fukuyama Iron Foundry in Japan (Nasu et al, 1973). This is the largest size of pipe tested for which reports are available. The length of the pipe was chosen equal to the wave length of the seismic wave as indicated by theoretical investigations. The pipe was made up of six pieces of 12 m length joined by welding.

The top 3.4 m of the soil was a recent fill, followed by a 14.5 m thick silty clay layer, which had a great influence on the

response of the pipe. The instrumentation consisted of seismometers at various depths and at the ground level along the length of the pipe. Vibrations were induced by explosions, as air gun in water filled bore holes and by an iron ingot of 15 t weight hit by a pendulum of 1.5 t weight.

Several observations can be made from the tests:

1. For the entire duration of the vibrations, the pipe vibrates almost in phase with the ground, and with the same displacement amplitudes as that of the surrounding soil medium.
2. The axial strains closely follow the displacements of the ground in the axial direction.
3. The bending strains closely follow the ground displacements in the vertical direction.
4. The ratio of the maximum axial strain to maximum bending strain observed was 3.1, which tallies well with the calculated value of 3.0 using maximum amplitudes of axial and bending deformations and wavelengths of shear and compressive waves.

A4 MONITORING DURING MATSUSHIRO EARTHQUAKES

Between August 1965 and February 1967 there were a series of earthquakes in Japan with the epicentre near the town of Matsushiro. They were so frequent that it was possible to make some actual field

tests for buried pipes.

Out of the several earthquakes recorded for three types of pipes, the maximum acceleration was 0.2 g. The following observations were made:

1. There was no difference between the dynamic displacements of the pipes and the surrounding soil.
2. At the ground level the deformations in the axial direction were equal to those in transverse direction.
3. At the straight part of the pipes the axial strains predominated.
4. Maximum strains in the pipes did not appear at the time when the acceleration at the ground level was a maximum, but occurred at a later instant.
5. Strains at the connecting part of the pipes and the manholes were much larger compared to those at other parts in steel pipes. Bending strain at the connections was predominant, but at a short distance away from the connection, axial strains predominated again. After seismic waves died out, axial strains predominate near the connections also.

A5 DAMAGE TO TUNNELS DUE TO EARTHQUAKES

There are few published reports about earthquake damage to tunnels. This is quite understandable since tunnels are very important and costly structures, and constructed only after detailed

investigations and careful design. They are seldom designed to run accross a potentially active fault line. However, since they are essentially similar to buried pipe lines most of the observations made for pipes should in general hold true for tunnels.

Behaviour of Railway Tunnel in Tokyo During Earthquake

The tunnel across the Tama river in Tokyo is 80 m long; 13 m wide and 7.35 m high. It is made up of six segments. The second and fourth segments were instrumented with accelerometers and strain meters which measure strains over a length of 1 m (Okamoto et al, 1973). The geological studies of the site revealed mudstone base rock overlain with alluvium, which varies in thickness from 30 m at segment 4 to 4 m at segment 2.

The tunnel experienced an earthquake of magnitude 6, focal depth 10 km and epicentral distance 270 on August 31, 1972. The performance of the tunnel can be summarized as:

1. Axial strains predominate, though bending strains are also present.
2. Fairly low frequencies dominate the strain records and they coincide with the natural frequencies of the soil system as indicated by microtremor records.
3. Low frequency shocks have more effect on the strain records, while high frequency shocks have very little effect.
4. Increasing accelerations result in increasing strains, and

there appears to be an upper bound for the strains when expressed as a function of maximum accelerations which may be approximated by a linear relationship. This tallies well with the findings of theoretical investigations.

A6 EXPERIMENTS WITH MODELS OF TUNNELS

Model studies of a submerged tunnel at a scale of 1:250 were conducted by Okamoto et al (1973). The ground was simulated by gelatine and the tunnel by silicone rubber. Four different types of ground conditions were considered. The findings of these model studies were:

1. The thickness and rigidity of the surface layer have a great influence on the vibration characteristics of the soil-tunnel system.
2. The tunnel deformations are mainly influenced by the fundamental vibrations of the ground.
3. Deformations of the tunnel are severe where the material properties of the supporting ground change abruptly.
4. The natural frequency of the ground is not much affected by the presence of the tunnel.
5. Relative displacements between the tunnel and the surrounding medium are a maximum at places where the dynamic characteristics of the ground change abruptly. Consequently these are the places where the tunnel is likely to sustain maximum damage.

6. Hinges reduce the moments, but their influence is more or less localized.

One more experimental study was reported by Goto et al (1973). Random vibrations were induced by using a laboratory shake table. Materials similar to those used by Okamoto were used to simulate the soil and tunnel. These studies also indicated that the fundamental mode of ground vibrations mainly influences the response of the soil-tunnel system.

TABLE A-1

SUGGESTED RELIABILITY LEVELS FOR LIFELINES

LIFELINE		RELIABILITY WITHIN INTENSITY AREAS	
		HIGH INTENSITY GROUND MOTION - (MMI IX-X WITH SURFACE FAULTING)	MODERATE INTENSITY GROUND MOTION - (MMI VI-VII)
Water Supply System	Storage Reservoirs*	No failure that will endanger lives	Fully functional
	For fire fighting	Level A - Adequate storage available	Fully functional
	Treatment facilities*	Level A	Fully functional
	Distribution	Level B - Tank trucks available for potable water	Fully functional
Sewage System	Collection*	Level C	Level A
	Treatment facilities*	Level B	Fully functional
Electrical Power System	Generating Plants (Except Nuclear)*	Level A	Fully functional
	Transmission*	Level A	Fully functional
	Terminals	Level B	Fully functional
	Distribution*	Level B	Level A
Natural Gas System	Transmission*	Level A	Fully functional
	Storage (above grade)*	Level A	Fully functional
	Distribution	Level B	Level A
Highway Freeway & Railroad	Bridges*	Level A - no collapses	Fully functional
	Roadways	Level B	Fully functional
Airports	Control facilities	Level A	Fully functional
	Runways and Taxiways*	Level A	Fully functional
Port Facilities		Level B	Level A
Radio and TV		Level A	Fully functional
Telephone		Level A	Fully functional

NOTES:

Reliability level A: 5% or less of intensity area without service for one day; fully restored in 1 week.

Reliability level B: 20% or less of intensity area without service for 1 week; fully restored in 1 month.

Reliability level C: 50% or less of intensity area without service for 1 week; 20% or less without service for 1 month; and fully restored in 3 months.

Asterisk* : Hazard of loss of life and private property.

(Duke and Moran (1975))

TABLE A-2

BASIC ELEMENTS OF A PROGRAM FOR EARTHQUAKE RESISTANCE
OF PUBLIC UTILITY SYSTEMS
(Iwan, 1975)

1. SEISMIC RISK IDENTIFICATION AND INDOCTRINATION PROGRAM
   - STRONG MOTION INSTRUMENTATION
   - FAULT MAPPING AND SEISMIC RISK INVESTIGATIONS
   - SOILS INVESTIGATIONS
   - ESTABLISHMENT OF DESIGN SPECTRA AND/OR EARTHQUAKES
   - INDOCTRINATION AND TRAINING OF KEY PERSONNEL

2. DISASTER RESPONSE PLAN
   - AVAILABILITY OF TRAINED PERSONNEL
   - AVAILABILITY AND SURVIVABILITY OF ALTERNATE ENERGY/MATERIAL SOURCES
   - AGILITY AND MOBILITY
   - HIGHLY PROTECTED COMMUNICATIONS/DISASTER CENTERS
   - MUTUAL ASSISTANCE AGREEMENTS

3. SYSTEM SEISMIC DESIGN PROGRAM
   - ABILITY TO ISOLATE DAMAGED AREAS
   - ROUTE PLANNING TO AVOID HIGHLY SEISMIC AREAS
   - SPECIAL CRITERIA FOR UNAVOIDABLE HIGHLY SEISMIC AREAS
   - INTERCONNECTION WITH OTHER UTILITIES
   - AUTOMATIC SHUT DOWN/REROUTE DEVICES
   - PROVISION FOR EMERGENCY ACCESS

4. STRUCTURAL SEISMIC DESIGN PROGRAM
   - COMPLIANCE WITH OR SURPASSING OF EXISTING CODES
   - DESIGN REVIEW PROGRAM
   - REPLACEMENT OR UPGRADING OF OLDER STRUCTURES
   - DEVELOPMENT OF SPECIALIZED DESIGN CRITERIA
   - DEVELOPMENT OF SPECIFICATIONS FOR VENDORS

5. TESTING AND MONITORING PROGRAM
   - SYSTEMATIC TESTING OF CRITICAL OR SPECIAL COMPONENTS
   - MONITORING OF SYSTEM RESPONSE - SHORT TERM AND LONG TERM

TABLE A-3

CURRENT RESEARCH ON EARTHQUAKE RESISTANCE
OF PUBLIC UTILITY SYSTEMS
(Iwan, 1975)

ALL SEGMENTS

- POST EARTHQUAKE INSPECTION TEAMS
- PARTICIPATION ON SEISMIC DESIGN AND CODE COMMITTEES
- PARTICIPATION IN DISASTER PREPAREDNESS STUDIES
- SUPPORT OF UNIVERSITY RESEARCH AND SPECIAL PROJECTS

ELECTRIC

- INSTALLATION OF STRONG MOTION ACCELEROGRAPHS AT SELECTED SITES
- SEISMIC RISK/ZONING STUDIES
- TESTING PROGRAM FOR CRITICAL SYSTEM COMPONENTS
- DEVELOPMENT OF ALARM REPORTING SYSTEMS
- REDESIGN OF CIRCUIT BREAKERS FOR 0.5 g GROUND ACCELERATION
- DESIGN AND TESTING OF ANCHORAGE SYSTEMS
- TRAINING PROGRAMS FOR CRITICAL PERSONNEL

WATER

- INSTALLATION OF STRONG MOTION RECORDERS AT SELECTED SITES
- DEVELOPMENT OF EMERGENCY RESERVOIR DRAIN SYSTEMS
- PREPARATION OF DAM FAILURE FLOOD MAPS
- DYNAMIC ANALYSIS OF OLDER DAM STRUCTURES
- RESPONSE OF EARTH EMBANKMENTS/LIQUEFACTION
- DEVELOPMENT OF IMPROVED FAULT CROSSING TECHNIQUES
- MEASUREMENT OF FAULT MOVEMENT AT SELECTED SITES
- RESPONSE OF THIN-WALLED STORAGE TANKS

NATURAL GAS

- SEISMIC RISK/ZONING STUDIES
- MONITORING OF STRAIN ON BURIED GAS MAINS
- COMPUTER STUDIES OF SELECTED STRUCTURES
- RESPONSE OF PIPING SYSTEMS

SANITATION

- DEVELOPMENT OF FLEXIBLE PIPE JOINTS

TELEPHONE

- INSTALLATION OF STRONG MOTION ACCELEROGRAPHS AT SELECTED SITES
- SEISMIC RISK/ZONING STUDIES
- TESTING OF CRITICAL EQUIPMENT COMPONENTS
- STRUCTURAL RESPONSE STUDIES

TRANSPORTATION

- INSTALLATION OF STRONG MOTION ACCELEROGRAPHS AT SELECTED SITES
- COMPUTER AND MODEL STUDIES OF RESPONSE OF BRIDGES
- SOIL-STRUCTURE INTERACTION COMPUTER STUDIES

TABLE A-4

RECOMMENDATIONS FOR RESEARCH ON EARTHQUAKE RESISTANCE
OF PUBLIC UTILITY SYSTEMS
(Iwan, 1975)

1. RESEARCH ON SITE CONDITIONS

HIGHEST PRIORITY

- PREPARATION OF A COMPREHENSIVE SEISMIC RISK MAP OF ENTIRE STATE
- DEVELOPMENT OF METHODS FOR DETERMINING THE EFFECTS OF LOCAL GEOLOGY ON EARTHQUAKE GROUND MOTION

MIDDLE PRIORITY

- PREPARATION OF A COMPREHENSIVE GEOLOGIC HAZARDS MAP OF STATE
- PREPARATION OF GEOLOGIC AND FAULT MICROREGIONALIZATION MAPS OF URBAN AREAS
- COLLECTION, ANALYSIS AND DISTRIBUTION OF STRONG MOTION RECORDS
- DETERMINATION OF BASE ROCK AMPLIFICATION/ATTENUATION FOR TUNNEL DESIGN

LOWER PRIORITY

- COLLECTION AND COMPILATION OF ACCURATE SOIL CONDITION AND GEOLOGIC FEATURES DATA FOR URBAN AREAS
- DEVELOPMENT OF DESIGN SPECTRA FOR BEDROCK, DENSE SOILS AND MUD FILLS
- DEVELOPMENT OF METHODS OF JUDGING SEISMIC RISK/COST TRADEOFFS

2. RESEARCH ON EARTHQUAKE RESPONSE OF EQUIPMENT

HIGHEST PRIORITY

- DETERMINATION OF EQUIPMENT RESPONSE CHARACTERISTICS FOR USE IN ANCHORAGE SYSTEMS
- DETERMINATION OF THE DAMPING FACTORS TO BE USED IN DYNAMIC ANALYSIS OF EQUIPMENT

MIDDLE PRIORITY

- DEVELOPMENT OF IMPROVED ANCHORAGE SYSTEMS FOR:
  - FUEL BURNING APPLIANCES
  - ISOLATOR MOUNTED EQUIPMENT
  - PIPING SYSTEMS
  - SPECIALIZED EQUIPMENT

LOWER PRIORITY

- UPGRADING OF INDUSTRY STANDARDS FOR GENERATORS, COMPRESSORS, ETC.
- DEVELOPMENT OF IMPROVED SEISMIC DESIGN CRITERIA FOR ELECTRICAL AND MECHANICAL EQUIPMENT
- INVESTIGATION OF AIR RELEASE AND AIR INLET VALVES ON LARGE TRANSMISSION LINES

TABLE A-4 - CONTINUED

3. RESEARCH ON EARTHQUAKE RESPONSE OF STRUCTURES

HIGHEST PRIORITY

- DEVELOPMENT OF FAST, INEXPENSIVE METHODS FOR ELASTIC AND INELASTIC STRUCTURES
  - IDENTIFICATION OF MAXIMUM ALLOWABLE EXCITATION
  - SIMPLIFICATION OF DESIGN SPECTRA SELECTION
- INVESTIGATION OF EFFECTS OF LARGE SOIL MOVEMENT ON STRUCTURES, WALLS, PIPE SYSTEMS, ETC.
- DEVELOPMENT OF DESIGN ALTERNATIVES TO MASSIVE FOUNDATIONS
- DEVELOPMENT OF FAST, INEXPENSIVE METHODS FOR ANALYSIS OF EARTH STRUCTURES
- DEVELOPMENT OF BETTER TECHNIQUES FOR ESTIMATING/MEASURING DAMPING
- DEVELOPMENT OF LOCAL DESIGN EARTHQUAKES

MIDDLE PRIORITY

- ACQUISITION OF DATA ON EFFECTS OF EARTHQUAKES ON UNDERGROUND STRUCTURES
- INVESTIGATION OF EFFECT OF RELATIVE MOTION OF STRUCTURAL ELEMENTS FOR ALL OR PARTIALLY UNDERGROUND STRUCTURES
- INVESTIGATION OF THE EFFECTS OF VERTICAL EARTHQUAKE MOTIONS
- DEVELOPMENT OF DESIGN CRITERIA FOR FREE-STANDING RESERVOIR TOWERS
- DETERMINATION OF RESPONSE OF PIPING AND CABLE SYSTEMS
- INVESTIGATION OF BEHAVIOR OF LARGE PIPELINES NEAR FAULTING ZONE
- DEVELOPMENT OF ECONOMICAL FLEXIBLE JOINTS FOR RIGID PIPES

LOWER PRIORITY

- DETERMINATION OF EFFECTIVENESS OF VARIOUS ANCHORING TECHNIQUES FOR EQUIPMENT AND LARGE STORAGE TANKS

4. RESEARCH ON MATERIALS

MIDDLE PRIORITY

- STUDY OF EFFECTS OF AGING AND CYCLIC LOADING ON PORCELAIN, SEALS AND GASKETS
- STUDY OF SEISMIC RESISTANCE OF ALTERNATE INSULATOR MATERIALS

APPENDIX B

AXISYMMETRIC INTEGRALS
(Nair, 1974)

There are eleven axisymmetric integrals λ_1 to λ_{11} which are often used in the analysis of axisymmetric structures. Only the first six are needed in the static program, while all of them are required in the dynamic analysis. The absolute forms of these integrals are evaluated using Green's Lemma and these are lengthy expressions. However, there are simplified expressions for these integrals which are approximate in the case of λ_4, λ_5, λ_6 and λ_9 to λ_{11}. These approximations are valid under the assumption that the dimension of the cross section of the element is small compared to its radius of revolution. The simplified forms are:

$$\lambda_1 = A\,\bar{r}$$

$$\lambda_2 = A$$

$$\lambda_3 = A\,\bar{z}$$

$$\lambda_4 = A/\bar{r}$$

$$\lambda_5 = A\,\bar{z}/\bar{r}$$

$$\lambda_6 = \frac{A}{12\,\bar{r}}\left[(z_i + z_j)^2 + (z_j + z_k)^2 + (z_k + z_i)^2\right]$$

$$\lambda_7 = \frac{A}{12}\left[(r_i + r_j)^2 + (r_j + r_k)^2 + (r_k + r_i)^2\right]$$

$$\lambda_8 = A\bar{z}\bar{r}$$

$$\lambda_9 = \frac{A}{24}\left[(r_i + r_j)^3 + (r_j + r_k)^3 + (r_k + r_i)^3\right]$$

$$\lambda_{10} = \frac{A\bar{z}}{12}\left[(r_i + r_j)^2 + (r_j + r_k)^2 + (r_k + r_i)^2\right], \text{ and,}$$

$$\lambda_{11} = \frac{A\bar{r}}{12}\left[(z_i + \dot{z}_j)^2 + (z_j + z_k)^2 + (z_k + z_i)^2\right]$$

where

$$2A = r_i\,(z_j - z_k) + r_j(z_k - z_i) + r_k(z_i - z_j)$$

$$\bar{r} = \frac{1}{3}(r_i + r_j + r_k)$$

and

$$\bar{z} = \frac{1}{3}(z_i + z_j + z_k)$$

The exact integrals are:

$$\lambda_1 = \iint r\,dr\,dz = -\oint rz\,dr = -\left[\frac{a_1}{2}(r_j^2 - r_i^2) + \frac{b_1}{3}(r_j^3 - r_i^3) + \frac{a_2}{2}(r_k^2 - r_j^2)\right.$$

$$\left. + \frac{b_2}{3}(r_k^3 - r_j^3) + \frac{a_3}{2}(r_i^2 - r_k^2) + \frac{b_3}{3}(r_i^3 - r_k^3)\right]$$

$$\lambda_2 = \iint dr\,dz = -\oint z\,dr = -\left[a_1(r_j - r_i) + \frac{b_1}{2}(r_j^2 - r_i^2) + a_2(r_k - r_j)\right.$$

$$\left. + \frac{b_2}{2}(r_k^2 - r_j^2) + a_3(r_i - r_k) + \frac{b_3}{2}(r_i^2 - r_k^2)\right]$$

$$\lambda_3 = \iint z\,dr\,dz = -\oint \frac{z^2}{2}\,dr = -\left[\frac{a_1^2}{2}(r_j-r_i) + \frac{a_1 b_1}{2}(r_j^2 - r_i^2)\right.$$

$$+ \frac{b_1^2}{6}(r_j^3-r_i^3) + \frac{a_2^2}{2}(r_k-r_j) + \frac{a_2 b_2}{2}(r_k^2-r_j^2)$$

$$+ \frac{b_2^2}{6}(r_k^3-r_j^3) + \frac{a_3^2}{2}(r_i-r_k) + \frac{a_3 b_3}{2}(r_i^2-r_k^2)$$

$$\left. + \frac{b_3^2}{6}(r_i^3-r_k^3)\right]$$

$$\lambda_4 = \iint \frac{1}{r}\,dr\,dz = -\oint \frac{z}{r}\,dr = -\left[a_1 \ln\left(\frac{r_j}{r_i}\right) + b_1(r_j-r_i) + a_2 \ln\left(\frac{r_k}{r_j}\right)\right.$$

$$\left. + b_2(r_k-r_j) + a_3 \ln\left(\frac{r_i}{r_k}\right) + b_3(r_i-r_k)\right]$$

$$\lambda_5 = \iint \frac{z}{r}\,dr\,dz = -\oint \frac{z^2}{2r}\,dr = -\left[\frac{a_1^2}{2}\ln\left(\frac{r_j}{r_i}\right) + a_1 b_1(r_j-r_i) + \frac{b_1^2}{4}(r_j^2-r_i^2)\right.$$

$$+ \frac{a_2^2}{2}\ln\left(\frac{r_k}{r_j}\right) + a_2 b_2(r_k-r_j) + \frac{b_2^2}{4}(r_k^2-r_j^2)$$

$$\left. + \frac{a_3^2}{2}\ln\left(\frac{r_i}{r_i}\right) + a_3 b_3(r_i-r_k) + \frac{b_3^2}{4}(r_i^2-r_k^2)\right]$$

$$\lambda_6 = \iint \frac{z^2}{r}\,drdz = -\oint \frac{z^3}{3r}\,dr = -\left[\frac{a_1^3}{3}\ln\left(\frac{r_j}{r_i}\right) + a_1^2 b_1\,(r_j - r_i)\right.$$
$$+ \frac{a_1 b_1^2}{2}(r_j^2 - r_i^2) + \frac{b_1^3}{9}(r_j^3 - r_i^3)$$
$$+ \frac{a_2^3}{3}\ln\left(\frac{r_k}{r_j}\right) + a_2^2 b_2\,(r_k - r_j) + \frac{a_2 b_2^2}{2}$$
$$(r_k^2 - r_j^2) + \frac{b_2^3}{9}(r_k^3 - r_j^3) + \frac{a_3^3}{3}\ln$$
$$\left(\frac{r_i}{r_k}\right) + a_3^2 b_3\,(r_i - r_k) + \frac{a_3 b_3^2}{2}(r_i^2 - r_k^2)$$
$$\left. + \frac{b_3^3}{9}(r_i^3 - r_k^3)\right]$$

$$\lambda_7 = \iint r^2\,drdz = -\oint r^2\,z\,dr = -\left[\frac{a_1}{3}(r_j^3 - r_i^3) + \frac{b_1}{4}(r_j^4 - r_i^4) + \frac{a_2}{3}(r_k^3 - r_j^3)\right.$$
$$\left. + \frac{b_2}{4}(r_k^4 - r_j^4) + \frac{a_3}{3}(r_i^3 - r_k^3) + \frac{b_3}{4}(r_i^4 - r_k^4)\right]$$

$$\lambda_8 = \iint z\,dr\,dz = -\oint \frac{r z^2}{2}\,dr = -\left[\frac{a_1^2}{4}(r_j^2 - r_i^2) + \frac{a_1 b_1}{3}(r_j^3 - r_i^3)\right.$$
$$+ \frac{b_1^2}{8}(r_j^4 - r_i^4) + \frac{a_2^2}{4}(r_k^2 - r_j^2) + \frac{a_2 b_2}{3}(r_k^3 - r_j^3)$$
$$+ \frac{b_2^2}{8}(r_k^4 - r_j^4) + \frac{a_3^2}{4}(r_i^2 - r_k^2) + \frac{a_3 b_3}{3}(r_i^3 - r_k^3)$$
$$\left. + \frac{b_3^2}{8}(r_i^4 - r_k^4)\right]$$

$$\lambda_9 = \iint r^3 \, drdz = -\oint r^3 z \, dr = -\left[\frac{a_1}{4}(r_j^4-r_i^4)+\frac{b_1}{5}(r_j^5-r_i^5)+\frac{a_2}{4}(r_k^4-r_j^4)\right.$$

$$\left.+\frac{b_2}{5}(r_k^5-r_j^5)+\frac{a_3}{4}(r_i^4-r_k^4)+\frac{b_3}{5}(r_i^5-r_k^5)\right]$$

$$\lambda_{10} = \iint r^2 z \, drdz = -\oint \frac{r^2 z^2}{2} \, dr = -\left[\frac{a_1^2}{6}(r_j^3-r_i^3)+\frac{a_1 b_1}{4}(r_j^4-r_i^4)+\frac{b_1^2}{10}(r_j^5-r_i^5)\right.$$

$$+\frac{a_2^2}{6}(r_k^3-r_j^3)+\frac{a_2 b_2}{4}(r_k^4-r_j^4)+\frac{b_2^2}{10}(r_k^5-r_j^5)$$

$$\left.+\frac{a_3^2}{6}(r_i^3-r_k^3)+\frac{a_3 b_3}{4}(r_i^4-r_k^4)+\frac{b_3^2}{10}(r_i^5-r_k^5)\right]$$

and,

$$\lambda_{11} = \iint r z^2 \, drdz = -\oint \frac{r z^3}{3} \, dr = -\left[\frac{a_1^3}{6}(r_j^2-r_i^2)+\frac{a_1^2 b_1}{3}(r_j^3-r_i^3)+\frac{a_1 b_1^2}{4}(r_j^4-r_i^4)\right.$$

$$+\frac{b_1^3}{15}(r_j^5-r_i^5)+\frac{a_2^3}{6}(r_k^2-r_j^2)+\frac{a_2^2 b_2}{3}(r_k^3-r_j^3)$$

$$+\frac{a_2 b_2^2}{4}(r_k^4-r_j^4)+\frac{b_2^3}{15}(r_k^5-r_j^5)+\frac{a_3^3}{6}(r_i^2-r_k^2)$$

$$\left.+\frac{a_3^2 b_3}{3}(r_i^3-r_k^3)+\frac{a_3 b_3^2}{4}(r_i^4-r_k^4)+\frac{b_3^3}{15}(r_i^5-r_k^5)\right]$$

where

$$a_1 = z_i - b_1 r_i \qquad b_1 = \frac{z_j - z_i}{r_j - r_i}$$

$$a_2 = z_j - b_2 r_j \qquad b_2 = \frac{z_k - z_j}{r_k - r_j}$$

$$a_3 = z_k - b_3 r_k \qquad b_3 = \frac{z_i - z_k}{r_i - r_k}$$

When any radius is zero, the corresponding logarithm becomes infinite; however, the limit of such terms as determined using L'Hospital's rule is zero. Whenever a radius is zero, the corresponding logarithmic term should be deleted. When two radial coordinates of an element are equal, apparently a and b constants become infinite. In these cases, the line integration is not required and the constants should be set to zero.

For the triangular ring element with coordinates (2,1), (7,3) and (4,7), the values of these integrals were obtained using both the lengthy expressions as wellas the simplified forms. These are given in Table B-1 for comparison purposes.

TABLE B-1

COMPARISON BETWEEN THE EXACT AXISYMMETRIC INTEGRALS AND THEIR SIMPLIFIED FORMS

Element	Integral	Exact Value	Value Obtained Using The Simplified Expressions
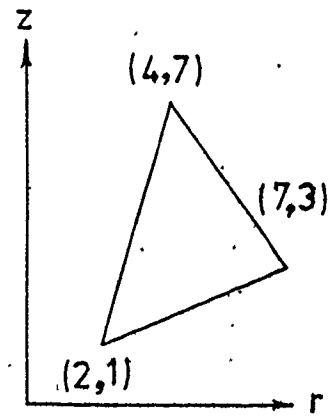	λ_1	56.33	56.33
	λ_2	13.00	13.00
	λ_3	47.68	47.68
	λ_4	3.1	3.00
	λ_5	11.12	11.00
	λ_6	45.45	45.00
	λ_7	257.83	257.83
	λ_8	210.67	210.67
	λ_9	1237.02	1232.83
	λ_{10}	968.40	945.39
	λ_{11}	863.10	845.00

APPENDIX C

LIST OF SYMBOLS

(As used in each Chapter)

Chapter 2

Ru_k	upward reflection coefficient at interface of layers k and k + 1.
Rd_k	downward reflection coefficient at interface of layers k and k + 1.
Tu_k	upward transmission coefficient at interface of layers k and k + 1.
Td_k	downward transmission coefficient at interface of layers k and k + 1.
t	time coordinate
t_k	time of travel for shear wave through layer k.
X	horizontal coordinate, horizontal response.
Xu	horizontal response due to upward propagating shear wave.
Xd	horizontal response due to downward propagating shear wave.
X_t	total response.
Xub_k	response due to upward propagating shear wave at the bottom of the layer k.
Xut_k	response due to upward propagating shear wave at the top of the layer k.
Xdt_k	response due to downward propagating shear wave at the top of the layer k.
Xdb_k	response due to downward propagating shear wave at the bottom of the layer k.
β_k	shear wave velocity in layer k.

β_r	shear wave velocity in base rock.
β_1	shear wave velocity in surface layer.

Section 2.5

G_T	magnification factor suggested by Kanai.
T	period of component vibration of seismic wave.
T_G	natural period of horizontal vibrations of ground.
h	depth of the single layer.

Section 2.9, 2.10 and 2.11

Tgv	natural period of compression vibrations of the top mantle.
μ_0	shear modulus for the surface formation.
μ_1	shear modulus for the lower formation.

Section 2.12

c	phase velocity of the R-wave.
H	depth of the surface layer.
L	wave length of the R-wave.
L/H	dimensionless wave length.
c/β_0	dimensionless phase velocity.
β_0	shear wave velocity of base rock.

Section 2.17

U_r	total horizontal response.
U_{rr}	horizontal response due to R-wave only.
U_{rs}	horizontal response due to S-wave only.
V_r	total vertical response.

V_{rr}	vertical response due to R-wave only.
V_{rs}	vertical response due to S-wave only.
θ	angle between the direction of propagation of shear wave and the vertical.

Chapter 3

$\{a\}$	vector used in the step-by-step method.
$[B]$	matrix relating the strains and displacements.
$\{b\}$	vector used in the step-by-step method.
$[C]$	damping matrix.
$[C^{-1}]$	transformation matrix relating the generalized displacement coordinates and nodal displacements.
$[D]$	constitutive matrix for stress-strain relations.
E	Young's modulus.
$[F]$	matrix used in step-by-step method.
$\{f\}_t$	exciting force vector.
$[H]$	matrix relating the dynamic (balancing) displacements to the boundary displacements.
$[K]$	stiffness matrix.
r	radial coordinate.
t	time coordinate.
U	strain energy.
u	radial displacement.
$\{u_I^s\}$, $\{\dot{u}_I^s\}$, $\{\ddot{u}_I^s\}$	pseudostatic response vectors for the interior displacement freedoms,
$\{u_I^d\}$, $\{\dot{u}_I^d\}$, $\{\ddot{u}_I^d\}$	dynamic (balancing) response vector for the interior displacement freedoms.
$\{u_I^t\}$, $\{\dot{u}_I^t\}$, $\{\ddot{u}_I^t\}$	total response vectors for the interior displacement freedoms.

$\{u_B\}, \{\dot{u}_B\}, \{\ddot{u}_B\}$	response vectors for the boundary displacements.
v	tangential displacement.
W	work done.
w	axial displacement.
z	axial coordinate.
α	empirical constant in proportional damping.
$\{\alpha\}$	generalized displacement coordinate matrix.
β	empirical constant in the proportional damping.
γ	shear strain.
ε	normal strain.
$\{\varepsilon\}$	strain matrix.
θ	angular coordinate.
ν	poisson's ratio.
σ	normal stress.
$\{\sigma\}$	stress matrix.
τ	shear stress.
Δt	time interval used in the step-by-step method.

Chapter 4

t	time coordinate.
z	horizontal (axial) distance.
β	shear wave velocity.
Δt	time interval used in the step-by-step method.
δt	time lag due to horizontal distance z.
θ	angle of propagation of the shear wave with respect to vertical.

Chapter 5

D	diameter of the tunnel.
r	radial coordinate.
z	axial coordinate.
θ	angular coordinate.

Superscripts

·	first derivative with respect to time.
··	second derivative with respect to time.
T	transpose of a matrix or vector.
-1	inverse of a matrix.
t	total response, also time coordinate.
s	pseudostatic component.
d	dynamic (balancing) component.